2019

SUPPRESSION AND ACTIVATION OF LIPID SIGNALLING IN CANCER: TUMOUR SUPPRESSOR PTEN AND ONCOGENIC SPHINGOSINE KINASE

A thesis submitted in fulfilment of the requirements of the degree of Doctor of Philosophy

Submitted by

Nahal Haddadi

(BSc, MSc (MedBiotech))

School of Life Sciences, Faculty of Science

University of Technology Sydney, Australia

2019

CERTIFICATE OF ORIGINAL AUTHORSHIP

I, Nahal Haddadi declare that this thesis, is submitted in fulfilment of the requirements for the award of Doctor of Philosophy, in the Faculty of Science at the University of Technology Sydney.

This thesis is wholly my own work unless otherwise reference or acknowledged. In addition, I certify that all information sources and literature used are indicated in the thesis.

This document has not been submitted for qualifications at any other academic institution.

This research is supported by the Australian Government Research Training Program.

Signature:

Production Note:
Signature removed prior to publication.

Date: 13/06/2019

ACKNOWLEDGEMENTS

I would like to express my sincere gratitude to a few special people in my life, without whose help, encouragement and guidance, the completion of this study would not have been possible.

I am grateful to my supervisors, Dr Najah Nassif, Dr Eileen McGowan and Dr Yiguang Lin, for their help, support and supervision during my postgraduate studies.

I would like to thank our collaborators from China, Dr Hongjie Chen, Dr Qiuxia Li, Dr Meijun Long and Prof Xiaofeng Zhu from the 3rd Affiliated Hospital of Sun Yat-sen University, who provided access to human clinical samples and helped in their processing in the second part of this thesis.

I owe my deepest gratitude to my father and mother, for their unconditional love, care and support. Although there are miles between us, we are never far apart. I can never thank you enough for what you have done for me. I would also like to thank my siblings Naghmeh and Navid, for their concern, kind words and support.

I would like to show my gratitude to my best friend and companion Oliver John Santos. Thanks for your constant support and encouragement. Thanks for always being there for me in hardship.

I am grateful to Maria Santos for her kind support and prayers.

I would like to thank my PhD colleagues Diana Hatoum and Chwee Fern Bok for their help in optimisation of PCR and initial work on SphK1, and I would like to thank Shohreh Razavy for her guidance in statistical analysis and Dr Sarah Bajan for her technical support.

I want to express my gratitude to the University of Technology Sydney for the award of an International Research Scholarship for the period of my PhD candidature.

LIST OF PUBLICATIONS AND PRESENTATIONS

JOURNAL ARTICLES

1. Haddadi N, Lin Y, Travis G, Simpson AM, Nassif NT, McGowen E: **PTEN/PTENP1: 'Regulating the regulator of RTK-dependent PI3K/Akt signalling', new targets for cancer therapy.** *Mol Cancer* 2018, **17:**37.

2. Haddadi N, Lin Y, Simpson AM, Nassif NT, McGowan EM: **"Dicing and Splicing" Sphingosine Kinase and Relevance to Cancer.** *Int J Mol Sci* 2017, **18**.

3. Hatoum D, Haddadi N, Lin Y, Nassif NT, McGowan EM: **Mammalian sphingosine kinase (SphK) isoenzymes and isoform expression: challenges for SphK as an oncotarget.** *Oncotarget* 2017, **8:**36898-36929.

4. **Haddadi N*,** Chen H*, Li Q*, Long M, Hatoum D, Bok CF, Zhu X, Nassif NT, Lin Y, McGowan EM: **Differential expression of sphingosine kinase 1 major Isoforms in human cancer patients and cancer cell lines: implications for cancer therapy.** (Submitted to Cancers).

5. Haddadi, N, Lin Y, McGowan, EM and Nassif, NT: **Cancer-associated mutations of PTEN alter PTEN function.** (Manuscript in preparation 2019).

PUBLISHED ABSTRACTS AND CONFERENCE PRESENTATIONS

1. Nahal Haddadi, Eileen McGowan, and Najah Nassif. Alteration Cellular Function by Cancer-associated Mutations of PTEN. **Frontiers in Cancer Science (FCS) 2017, Singapore.**

2. Nahal Haddadi, Eileen McGowan, and Najah Nassif. Cancer-Associated PTEN Mutations Alter PTEN Cellular Function. **Australasian Genomic Technologies Conference (AGTA) 2017, Hobart, TAS.**

3. Nahal Haddadi, Eileen McGowan, and Najah Nassif, Determining the Frequency and Involvement of PTEN Pseudogene (PTENP1) Expression in Cancer Cell Lines. **New Horizons Conference 2015, Sydney, NSW.**

AWARDS AND RECOGNITION

Recipient of UTS International Research Scholarship (UTS IRS), University of Technology Sydney (2015-2018).

LIST OF ABBREVIATIONS

Ab	Antibody
Amp	Ampicillin
AKT	AKT/protein kinase B
ATP	Adenosine triphosphate
BAD	Bcl-2 associated death promoter
Bp	Base pairs
BSA	Bovine serum albumin
Caspase	Cystein aspartate specific proteases
CBF1	Also known as recombination signal binding protein for immunoglobulin kappa J region (RBBJ)
cGMP	Cyclic guanosine monophosphate
CK	Creatine kinase
CK2	Casein kinase II
CMV	Cytomegalovirus
$C0_2$	Carbon dioxide
cDNA	Complementary DNA
CRC	Colorectal Cancer
CDK	Cyclin dependent kinase
DMEM	Dulbecco's Modified Eagle's Medium
DMSO	Dimethyl sulfoxide
dNTPs	deoxynucleotide triphosphates
DNA	Deoxyribonucleic acid
EDTA	Ethylenediamminetetraacetic acid
FCS	Foetal calf serum
Kb	Kilobase
MW	Molecular weight
PBS	Phosphate buffered saline
PCR	Polymerase chain reaction
PI	Propidium iodide

PIP2	Phosphoinositide 3,4,5-triphosphate
PIP3	Phosphoinositide 4,5-bisphosphate
PTEN	Phosphatase and tensin homologue deleted on chromosome 10
RNA	Ribonucleic acid
Tris	2-amino-2(hydroxymethyl-1,3-propaneldiol)

ABSTRACT

The *PTEN* tumour suppressor is the second most frequently mutated tumour suppressor gene in cancer. It is a lipid and protein phosphatase that negatively regulates the well-known pro-proliferative and anti-apoptotic phosphatidylinositol 3-kinase (PI3K)/AKT signalling pathway to modulate cell proliferation, cell cycle progression and cell survival. Sphingosine kinase 1 (SphK1), a known tumour promoter/oncogene, has been shown to activate the PI3K/Akt pathway to enhance resistance to apoptosis. The loss of function of PTEN and/or the overexpression of SphK1 contribute to tumorigenesis. This thesis describes the analysis of novel, cancer associated mutations of PTEN, to determine their effect(s) on wild type (WT) PTEN function, and also explores differential SphK1 isoform expression in cancers.

Previous work in our laboratory described 10 novel somatic mutations of PTEN in primary colorectal tumours. To determine the functional consequences of these novel cancer-associated PTEN mutations, the WT *PTEN* and the series of PTEN mutants (K62R, Y65C, K125E, K125X, E150Q, D153N, D153Y, N323K and the C124S and G129E controls) were transiently transfected into: (A) PTEN null U87MG glioblastoma cells, and WT PTEN expressing (A) HCT116 colon cancer and (C) MCF7 breast cancer cells. Transfected cells were then assayed for cell proliferation, cell cycle phase distribution and AKT phosphorylation. In U87MG cells, 50% of the PTEN mutants (Y65C, K125E, E150Q and D153Y) exhibited statistically significant reductions in cell proliferation, but not to the level of that of WT PTEN. In both the HCT116 and MCF7 cell lines, 80% of the PTEN mutants (K62R, Y65C, K125E, K125X, E150Q, D153Y and N323K) displayed reduced cell proliferation rates but none produced reductions comparable with WT PTEN. Further, relative to WT PTEN, 75% of PTEN mutants (K62R, K125X, E150Q, D153N and N323K) possessed functional deficiency in cell cycle inhibitory capacity in the G2 phase in U87MG cells. In contrast, 90% of PTEN mutants (K62R, K125E, K125X, E150Q, D153N, D153Y and N323K) possessed functional deficiency in the cell cycle inhibitory capacity in either the G1 or G2 phase in HCT116 cells. In MCF7 cells, 100% and 60% (K62R, Y65C, D153N, D153Y and N323K) of the PTEN mutants had functional deficiency in cell cycle inhibitory capacity in either the G1 or G2 phase, respectively. The analyses of endogenous suppression of phosphorylation of AKT revealed that 40% of PTEN mutants (K125E, K125X and D153N) show deficiency in pAKT suppression in the U87MG cell line while 60% of the mutants showed such deficiency in the HCT116 cell line (K125X, E150Q, D153N, D153Y and N323K). All but one (K62R) of the PTEN mutants showed a deficiency in the ability to suppress the level of endogenous phosphorylated AKT in the MCF7 cells. Overall, the results of the functional assays showed that the somatic mutations of the *PTEN* gene alter PTEN tumour suppressor function.

Expression of SphK1, a positive upstream regulator of the Akt pathway, is expressed as 2 major isoforms, SphK1-43kDa (SphK1a) and SphK1-51kDa (SphK1b), with similar SphK1 activity. However, to date, there is no literature on the expression of the two SphK1 isoforms in cell lines or human tissues. Profiling the expression of the two SphK isoforms in various cancer cell lines (n=24), primary cancer tissues (n=28) and paired adjacent tissues (n=28), demonstrated that the SphK1a isoform is expressed in all cell lines and tissues (both normal and cancer) studied, however, expression of SphK1b is cell and tissue specific, including breast, prostate and lung. Balancing signalling pathways and maintaining cellular homeostasis, as observed through the PTEN/SphK1 swinging pendulum is important and the study of these pathways is crucial in gaining further understanding the opposing regulatory mechanisms, which may be exploited for the future prevention and treatment of cancers.

TABLE OF CONTENTS

LIST OF FIGURES

LIST OF TABLES

General introduction

PTEN is a negative regulator of the PI3K/Akt pathway and mutations of PTEN were shown to alter its tumour suppressive function [1]. Work by various investigators has shown that PTEN plays a significant role not only in inducing cell cycle arrest and programming apoptosis, but also in other important aspects of cell physiology including the regulation of cell adhesion, migration and differentiation [2-8]. Work in our laboratory has shown the presence of PTEN gene mutations and/or deletions in 41% of primary colorectal tumours. Furthermore, evidence of the importance of these mutations was provided by the finding that all tumours harbouring alterations of the PTEN gene demonstrated either reduced or absent PTEN expression [9]. In the first chapter of this thesis a background to our current knowledge of PTEN; its involvement in cell function/ regulation as well as consequences of mutations/ loss of PTEN is provided. In the first part of this thesis we investigate the effect of 10 novel mutations of PTEN on its cellular function. On the other hand the subject of the second part of the thesis, SphK1, is a positive upstream regulator of the Akt pathway and, in contrast to the negative regulation of the pathway conferred by PTEN, SphK1 activates the PI3K/Akt pathway to promote cell proliferation [10-13]. The importance of the interplay between the two regulators converges on the Akt checkpoint (Figure 1.0) and it has been demonstrated that overexpression of SphK1 in some cell lines and xenograft models greatly enhances cell proliferation in the presence or absence of wild type PTEN and mutant PTEN. However, in some cases, PTEN inactivation, coupled with SphK1 activation has been linked to increased tumour aggressiveness and poor prognosis [10]. Although SphK1 is expressed as 2 major isoforms, SphK1-43kDa (SphK1a) and SphK1-51kDa (SphK1b), with similar SphK1 activity [14], most SphK1 experiments have focused

generically on the SphK1a isoform [15, 16]. To date there is no literature on the expression of the two SphK1 isoforms in cell lines or human tissues. The second part of the thesis addresses this important issue. During the course of this thesis I have published two reviews highlighting the importance of the SphK1 isoforms in cancer [15, 16]. This Chapter highlights the importance of SphK in general and defines the nomenclature of SphK, which forms part of the published review, "Dicing and splicing" sphingosine kinase and its relevance in cancer [15].

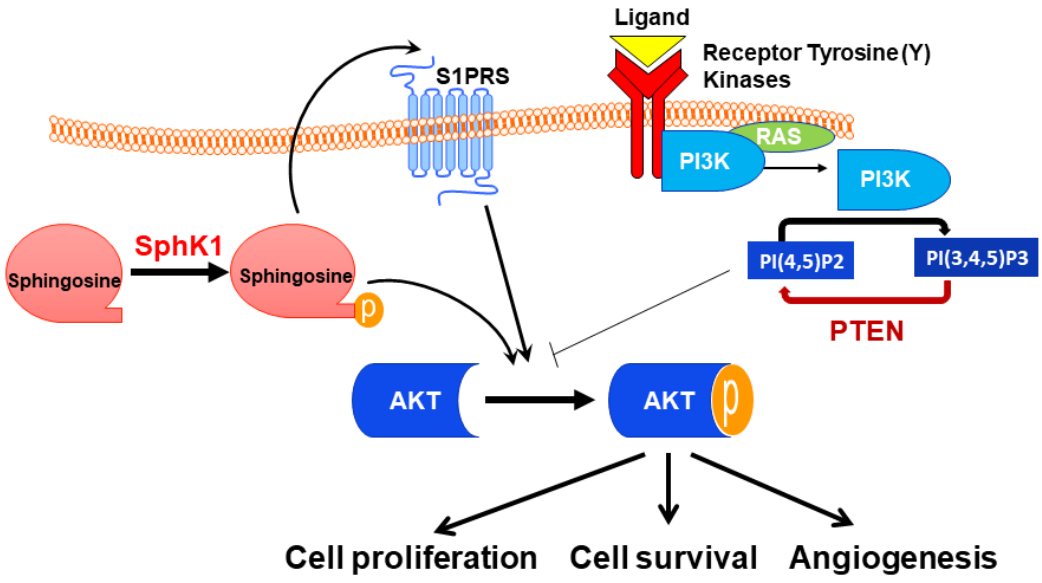

Figure 1.0 PTEN and SphK1 are opposing regulators of the PI3K/AKT Pathway. Binding a of ligand (e.g. growth factor, insulin, etc.) to a receptor tyrosine kinase activates PI3K, which, in turn, phosphorylates PIP2 to PIP3. Increases in PIP3 levels promote AKT activation and its downstream pathways to bring about enhanced cell proliferation and cell survival. PTEN is a direct antagonist of PI3K through the dephosphorylation of PIP3 to PIP and consequent inhibition of AKT activation. On the contrary, phosphorylation of sphingosine by SphK1 promotes the subsequent phosphorylation and activation of AKT, which leads to activation of downstream pathways, leading to a promotion of cell proliferation and survival.

PART 1

CHARACTERISATION OF PTEN TUMOUR SUPPRESSOR MUTATIONS IN CANCER

CHAPTER 1

INTRODUCTION TO TUMOUR SUPPRESSOR PTEN

Certificate of authorship and originality

Parts of this chapter have been published in Molecular Cancer Journal 2018. I certify that the work presented in this chapter has not previously been submitted as part of the requirements for a degree. I also certify that I carried out the majority of the work presented in this paper as the first author.

Principal supervisor

Dr Najah Nassif

Production Note:
Signature removed
prior to publication.

_____

Date: 25-09-2018

PhD candidate

Nahal Haddadi

Production Note:
Signature removed
prior to publication.

_____

Date: 25-09-2018

1.1 PTEN: an overview

The phosphatase and tensin homologue deleted on chromosome ten (*PTEN)* is a well-studied tumour suppressor located at chromosome 10q23.3 and known to be involved in the development and progression of multiple cancer types. PTEN is most commonly inactivated by mutation, deletion and/or epigenetic mechanisms in tumours of the brain, thyroid, breast, endometrium, ovarian tumours, prostate, melanoma and colon cancer [9, 12, 17-19], among others. Inactivation of *PTEN* is thought to be a primary contributor to tumorigenesis in the different tumour types described. *PTEN* was initially identified through deletion mapping studies in various human tumours and tumour cell lines [20]. The PTEN gene was also identified independently by two additional research groups who termed the gene *MMAC1* (mutated in multiple advanced cancers 1) [18] and *TEP1* (TGF β-regulated and epithelial cell enriched phosphatase 1) [17]. The name PTEN will be used from this point onwards, in this thesis.

Germline or inherited mutations of *PTEN* are the cause of the PTEN hamartoma tumour syndromes (PHTS) which are four rare autosomal-dominant syndromes, namely: (1) Cowden Syndrome (CS), (2) Bannayan-Riley-Ruvalcaba Syndrome (BRRS), (3) Proteus syndrome (PS) and (4) Lhermitte-Duclos syndrome. The four hamartoma syndromes show overlap in clinical features or manifestations and individuals with these

syndromes have an increased risk of developing thyroid, colon and endometrial cancers [21-24].

The PTEN protein is generally organised into two major domains, an N-terminal phosphatase domain, containing the phosphatase catalytic site, and a C-terminal domain. The phosphatase domain of PTEN possesses dual lipid and protein phosphatase activity [25, 26]. The protein phosphatase activity is regulatory and intermolecular, while the lipid phosphatase activity is linked more closely to the tumour suppressor function of PTEN [27]. The major substrate of PTEN is phosphatidylinositol-3,4,5-trisphosphate (PIP3), a lipid second messenger molecule [25, 28] formed by the phosphorylation of phosphatidylinositol-4,5-bisphosphate (PIP2) by the action of phosphoinositide-3-kinase (PI3K). The formation of PIP3 activates numerous downstream targets of the PI3K pathway, including the serine-threonine kinase protein kinase B (PKB)/Akt, which promotes cellular proliferation and inhibits apoptosis [29]. The major mechanism of PTEN-mediated tumour suppression is through negative regulation of the PI3K/Akt pathway, through dephosphorylation of PIP3, acting to inhibit both the pro-proliferative and anti-apoptotic cellular effects of this pathway (Figure 1.1) [6, 30-32]. PTEN also possesses protein phosphatase activity and its potential protein targets include focal adhesion kinase (FAK), Src homology collagen (Shc) and insulin receptor substrate 1 (IRS-1) [6, 25]. The protein phosphatase activity of PTEN is thought to be most important in the regulation of cell adhesion, migration, invasion, tumour metastasis and angiogenesis [33, 34].

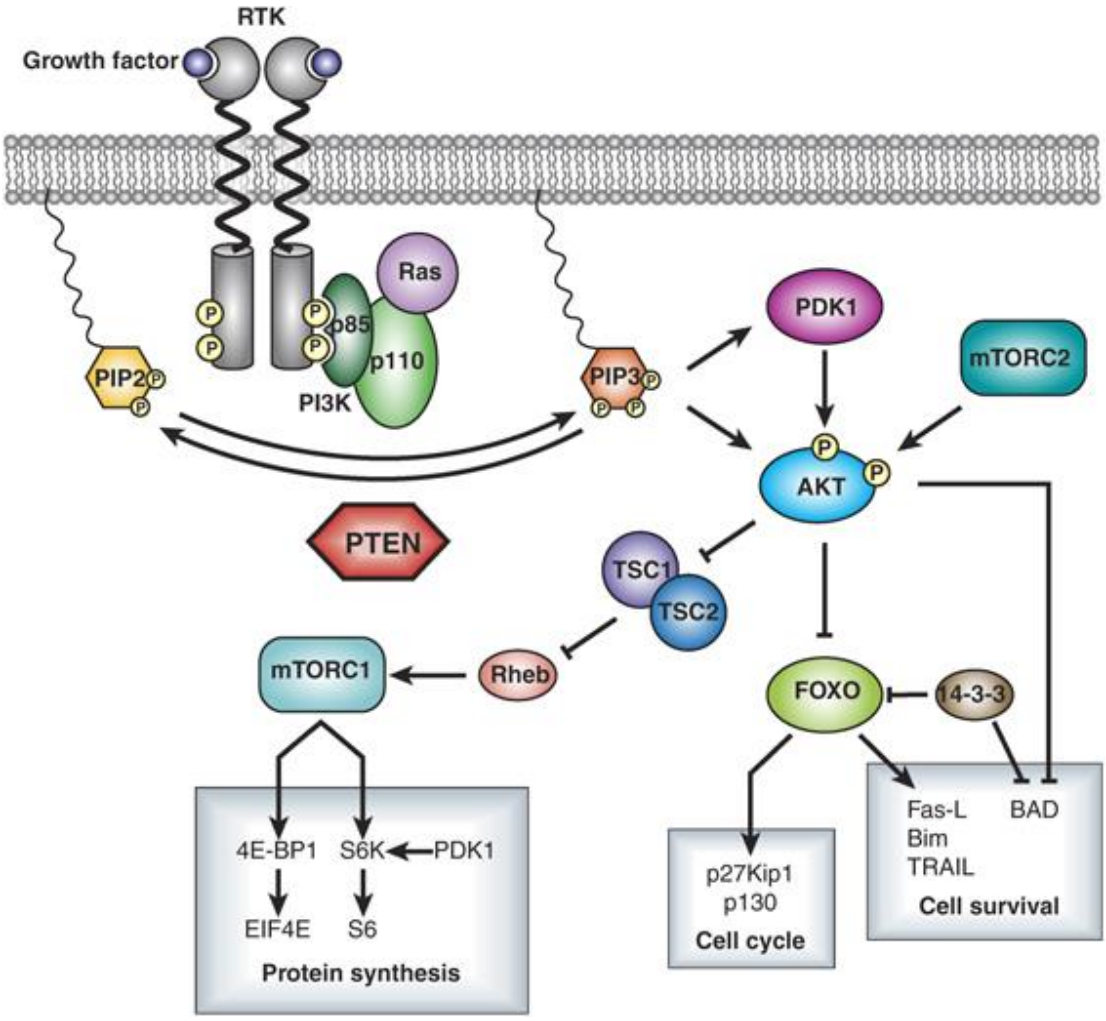

Figure 1.1 PTEN is a major negative regulator of the PI3K pathway. Binding of growth factors to receptor tyrosine kinases (RTK) leads to the activation of PI3K and phosphorylation of PIP2 to PIP3 and the recruitment of the serine/threonine kinases AKT and PDK1 to the cell membrane. After recruitment of AKT to the membrane, PDK1 and mTORC2 phosphorylate/activate AKT, which in turn activates a number of downstream targets to modulate cell growth, proliferation and survival. Taken from [35].

According to Knudson's hypothesis, both alleles of a tumour suppressor gene need to be inactivated for tumorigenesis to occur [36], however, inactivation of a single allele of *PTEN* has been shown to be sufficient for cancer development [37]. This is an example of haploinsufficiency, whereby expression from a single remaining allele is insufficient to maintain cellular integrity. PTEN cellular levels strongly influence cancer development, and subsequent cancer severity [38], thus the regulation and maintenance of cellular PTEN levels within a critical range is essential for preventing oncogenesis.

In addition to its role in the development and progression of various tumour types, *PTEN* has also been shown to play a key role in other diseases including diabetes [39], autism spectrum disorders [27] and neurological disorders such as Parkinson's disease and Alzheimer's disease [40-43]. The central involvement of PTEN in various cancers, and other disorders, confirms and strengthens the importance of this gene in the maintenance of normal cellular function and integrity, with alterations to its function or regulatory network being deleterious to cells.

1.2 PTEN Gene and Protein Structure

The *PTEN* gene is 160 kb in length and consists of 9 exons (Figure 1.2A). It is transcribed into a 5.572 kb mRNA transcript which encodes a 403 amino acid protein with an approximate molecular weight of 47.17 kDa [17, 18, 44-46]. The PTEN protein contains two major structural domains, the N-terminal phosphatase domain and the C-terminal domain, which encompass four functional domains [47]. Exons 1-6 of *PTEN* encode the N-terminal [$PI(4,5)P_2$]-binding (PBD)/phosphatase domain (residues 1-185), exons 7-9 encode the C-terminal domain (residues 186-403), which contains a C2 domain and the

carboxyl-terminal tail (C-tail) consisting of the C-terminal 50 amino acids. The last 3 amino acids make up the PDZ-binding domain (PDZ-BD). The structure of PTEN consists of five central β sheets with two α helices on one side and four on the other [2, 27, 48] (Figure 1.2B).

The N-terminal domain of PTEN (residues 1-185) contains a signature dual specificity protein tyrosine phosphatase (PTP) motif [$C(x)_5R$] at residues 123-130. This motif, located at the bottom of the active site pocket, is essential for enzymatic activity and tumour suppressor function of PTEN. Despite the similarity of this domain to other protein tyrosine phosphatases, its structure is mostly similar to dual specificity protein phosphatases (DUSP) [27, 49].

The C-terminal domain of *PTEN* (residues 186-403) is composed of two antiparallel β-sheets that are linked together by two short α-helices (Figure 1.2B) [48]. Within the C-terminal domain, the C2 domain (residues 186-351) is important for the correct positioning of PTEN at the site of its lipid substrate on the inner surface of the plasma membrane, where signalling takes place. Within the C-terminal tail of *PTEN* are two PEST (short intracellular half-life and protein degradation) homology regions, which are critical for PTEN stability, and a PDZ-binding site (Thr/Ser-x-Val-COOH) known to facilitate protein-protein interactions with other proteins containing PDZ domains [50]. The C-terminal tail region contains several phosphorylation sites (Ser362, Thr366, Ser370, Ser380, Thr382, Thr383 and Ser385) that are critical for PTEN activity and stability [22]. PTEN protein stability is dependent on the phosphorylation of Ser380, Thr382, and Thr383 by the protein kinase, casein kinase II (CK2) [26, 48]. Dephosphorylated PTEN is degraded by proteasome-mediated mechanisms [51, 52].

A

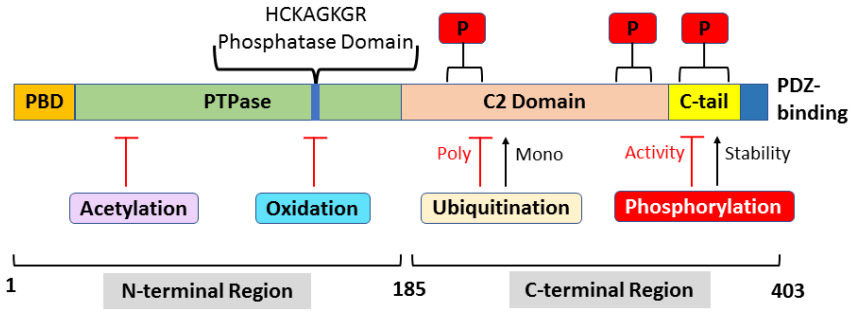

B

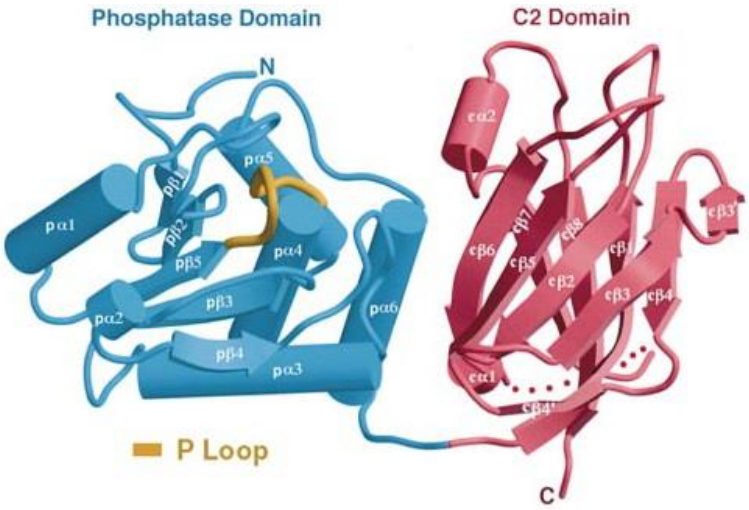

Figure 1.2 PTEN domain and 3D structure. A. PTEN is a 403 amino acid protein with five functional domains: a phosphatidylinositol-4,5-bisphosphate (PIP2)-binding domain (PBD), a phosphatase domain containing the catalytic core, a C2 domain with putative ubiquitination sites, two PEST (proline, glutamic acid, serine, threonine) domains for degradation, and a PDZ interaction motif for protein-protein interactions. Post-translational regulation of PTEN occurs by ubiquitination (Ub) of Lys residues within the PBD and C2 domain, by oxidation, SUMOylation of residues within the C2 domain, and acetylation on protein tyrosine phosphatase (PTPase) and PDZ-binding sites. Furthermore, PTEN is regulated by phosphorylation of specific serine and threonine residues within the C2 domain and C-terminal tail of PTEN (Modified from [2, 27]). **B.** The three-dimensional structure of PTEN. The N-terminal phosphatase domain is shown in blue and the HCxxGxxR phosphatase active site motif is shown in yellow. The C2 domain is shown in red. (Adapted from [53] and [48]).

1.3 Cellular functions of PTEN

PTEN has been shown to be able to translocate between the cytoplasm and nucleus of cells and is known to have specific functions in both cellular compartments. In the cytoplasm, PTEN plays a major role in the regulation of cell proliferation, cell cycle progression, apoptosis, cell adhesion, migration and cell invasion [6, 31]. Within the nucleus, PTEN plays a role in maintaining chromosomal stability and in DNA double strand break repair [28, 54], hence maintaining genome integrity. The mechanism by which PTEN is able to translocate between the nucleus and cytoplasm of cells is yet to be characterised but a number of mechanisms have been proposed and are discussed in section 1.3.3.

1.3.1 The cytoplasmic role(s) of PTEN

1.3.1.1 The PI3K pathway and regulation of cell proliferation and apoptosis

The attachment of an extracellular growth factor with a receptor tyrosine kinase (RTK) or G-protein coupled receptor (GPCR) leads to the recruitment of PI3K to the plasma membrane and phosphorylation of PIP2 to PIP3. The accumulation of PIP3 at the membrane allows recruitment of cellular proteins containing a pleckstrin homology (PH) domain (including serine-threonine kinase/protein kinase B (PKB/Akt)), which bind PIP3. Binding of Akt to PIP3 results in the translocation of Akt from the cytosol to the plasma membrane [55]. Upon membrane recruitment, Akt is activated by phosphorylation on Thr308 by pyruvate dehydrogenase kinase-1 (PDK1) and at Ser473 by mammalian target of rapamycin complex 2 (mTORC2). Activated Akt/PKB (phosphorylated form) is a well-established survival factor, exerting antiapoptotic effects by preventing the release of cytochrome C from mitochondria and inactivating

Forkhead transcription factors (FKHR), which are known to induce the expression of pro-apoptotic genes. Akt also phosphorylates, and inactivates, the proapoptotic factors BAD and caspase-9 in human cells [56]. These Akt targets or substrates play key roles in regulating critical cellular functions including proliferation, apoptosis, glucose homeostasis, nutrient response and DNA damage (Figure 1.3) [2, 28, 29, 37, 57]. PTEN acts as a direct antagonist of PI3K, dephosphorylating PIP3 to PIP2, and hence reduces the pro-proliferative effects of the PI3K pathway and restores the balance of cell growth, proliferation and death [27]. It is the loss of PTEN, or PTEN function, that promotes tumorigenesis in many cell types [58].

1.3.1.2 The role of PTEN in cell migration

Two cytoplasmic phosphoprotein substrates of PTEN are focal adhesion kinase (FAK) and the adaptor protein Shc [46, 59], which are central components of distinct signalling pathways. The FAK signalling pathway is activated by integrins and other growth factors and is linked to cell migration and other cellular activities. The Shc pathway is activated by receptors that include various tyrosine kinase receptors and integrins, and is part of a pathway that leads to activation of ERK MAP kinases, which is linked to cell motility (Figure 1.4) [60]. Overexpression of PTEN in mammalian cells decreases fibronectin-induced tyrosine phosphorylation of FAK [46, 59]. Dephosphorylation of FAK by PTEN inhibits cell spreading, suggesting that the protein-phosphatase activity of PTEN may be important in the regulation of cellular interactions [61].

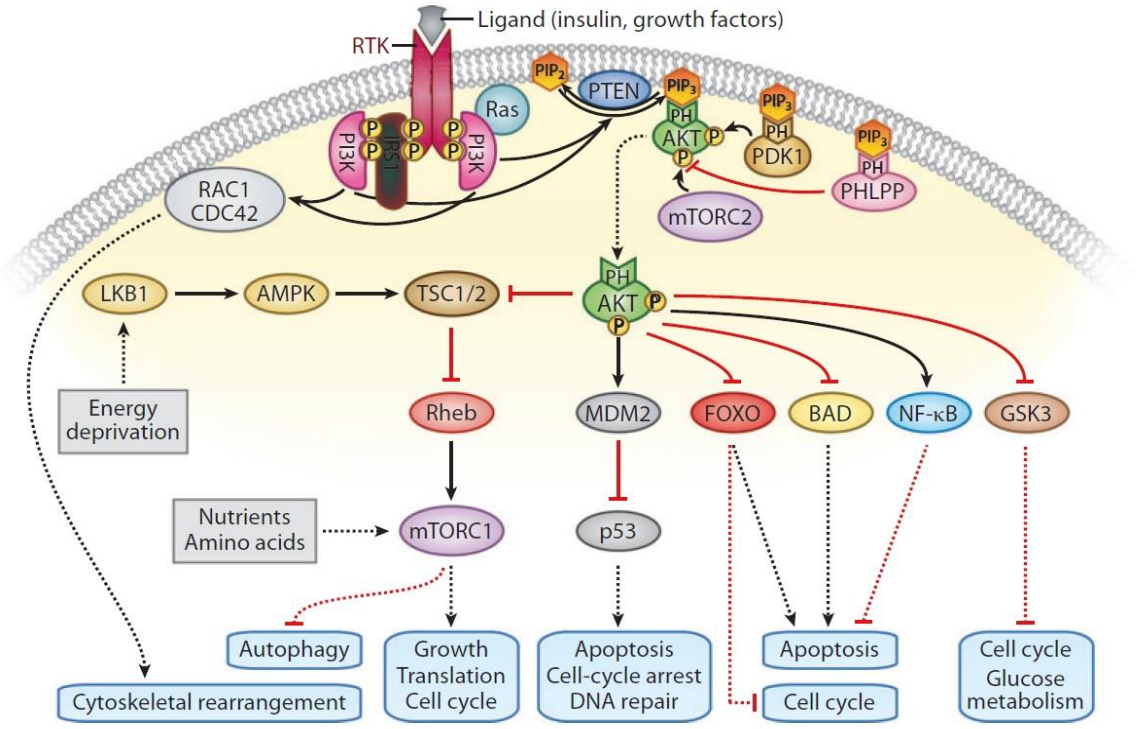

Figure 1.3 Role of PTEN in the PI3K/Akt signalling pathway. Growth factors bind G protein-coupled receptors or receptor tyrosine kinases on the outer side of the cell membrane, which leads to recruitment of PI3K (directly or through adaptor proteins) to the cell membrane through its regulatory subunit (P85) and phosphorylates PIP2 to PIP3 through its catalytic subunit (P110). The serine/threonine kinases AKT and PDK1 bind to the PH domain of PIP3 and recruit to the membrane. PDK1 and mTORC2 phosphorylate and activate AKT, which phosphorylates a number of downstream targets, resulting in the promotion of cell proliferation and survival. *PTEN* regulates the pathway at an early stage through the dephosphorylation of PIP3 to PIP2, directly antagonising the action of PI3 kinase (Modified from [2]).

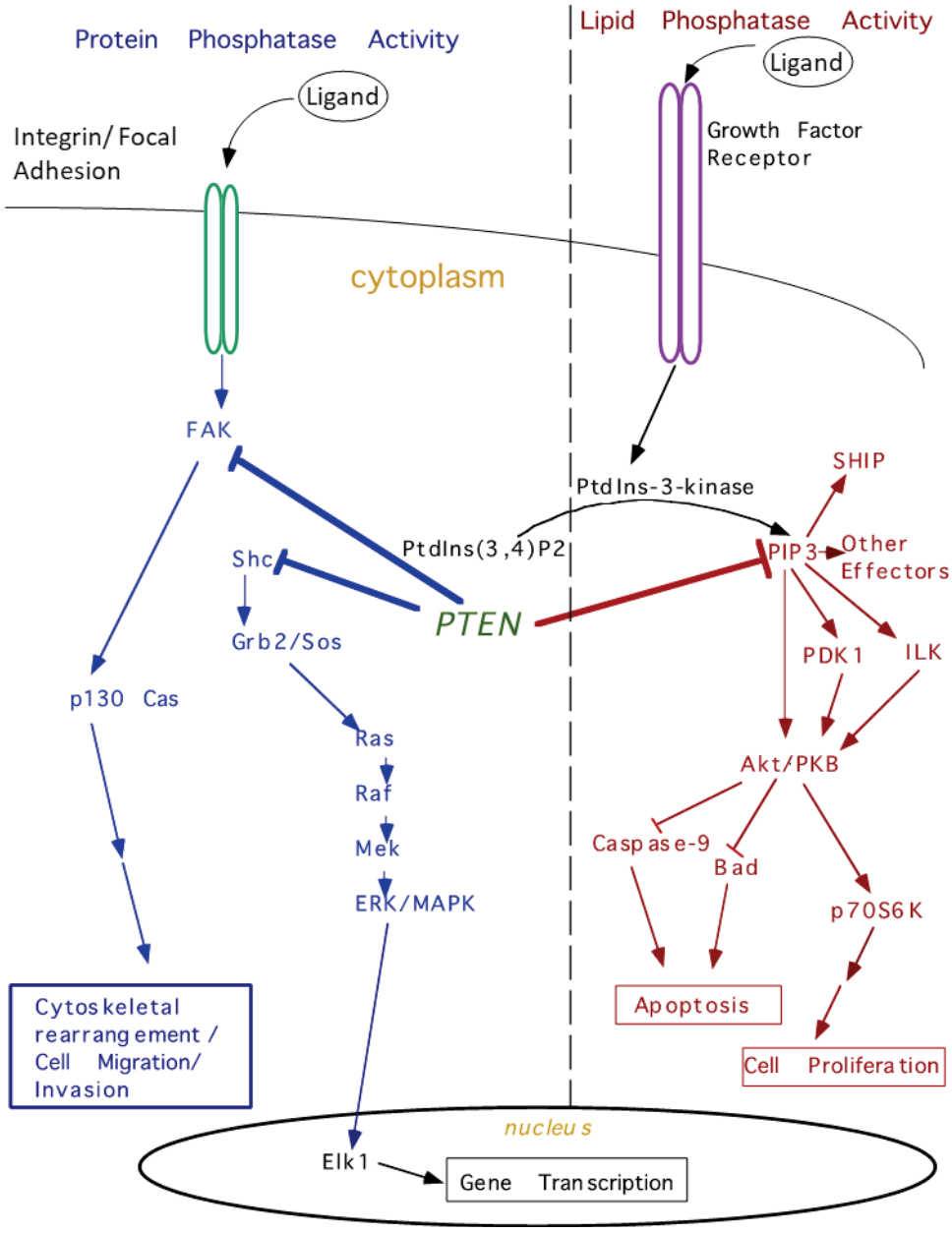

Figure 1.4 Cellular functions mediated by PTEN lipid and protein phosphatase activities. Schematic representation of the cellular pathways regulated by PTEN through its protein and lipid phosphatase activities. PTEN lipid phosphatase activity controls apoptosis and cell proliferation, while PTEN protein phosphatase activity controls cell migration and adhesion. Key: Shc, Src homology 2-containing protein; MAPK, mitogen-activated protein kinase; ERK, extracellular signal-regulated kinase; Akt/PKB, protein kinase B (Adapted from [6, 8, 62].

Dey et al (2008) suggest that both the protein and lipid phosphatase activities of PTEN are involved in the regulation of cell migration and identify a lipid phosphatase independent mechanism through regulation of vitronectin-directed migration [7]. Vitronectin is an abundant glycoprotein in blood plasma and various extracellular matrix sites, and cell interaction with vitronectin promotes cell adhesion, spreading and migration [63, 64]. Loss of PTEN expression has been shown to promote cell migration and increase tumour aggressiveness [27, 60, 65].

PTEN thus functions to **(a)** regulate apoptosis and growth through its lipid phosphatase activity, which regulates the level of PIP3, activation of Akt/PKB, and the process of apoptosis, as well as **(b)** play a role in regulating cell adhesion, migration, cell invasion, and mitogen activated protein (MAP) kinase activation, through its protein tyrosine phosphatase activity targeting focal adhesion kinase (FAK) and Shc [60].

1.3.1.3 Role of PTEN in tumour angiogenesis

The progression of tumours from a benign to a malignant state is associated with the initiation of angiogenesis, which is the production of new blood vessels from pre-existing vessels [66]. Angiogenesis, essential for tumour growth, is stimulated by a number of angiogenic factors, including vascular endothelial growth factor (VEGF) and hypoxia inducible factor 1 (HIF-1) [33]. HIF-1 is a transcription factor that activates the transcription of many genes, including VEGF. The loss of PTEN in tumours leads to a constitutive activation of the PI3K pathway leading to increased VEGF expression through HIF-1α stabilisation [67]. Reconstitution of PTEN expression in a $PTEN^{-/-}$ mouse brain tumour model led to decreased tumour growth *in vivo* and suppression of angiogenic activity [68]. AKT is the downstream target of PI3K in the regulation of

angiogenesis and tumour growth, and inhibition of angiogenesis by PTEN occurs through the inactivation of AKT and consequent decreases in HIF-1 and VEGF expression [33].

1.3.2 The roles of PTEN in the nucleus

PTEN has recently been shown to play important roles in maintaining chromosomal stability and in DNA double-strand break (DSB) repair and cells lacking nuclear PTEN are hypersensitive to DNA damage [69]. In the nucleus, PTEN interacts with centromere specific binding protein C (CENP-C) to modulate centrosome stability. Furthermore, PTEN is involved in DNA-damage responses, possibly through upregulation of Rad51, a member of the DNA repair family of proteins controlling homologous recombination-directed repair (HDR), a major mechanism of DSB repair [70]. Nuclear PTEN is also involved in regulating cell cycle progression through the reduction of cyclin D1 levels in the nucleus (Figure 1.5) [54, 60]. These functions of PTEN are independent of its phosphatase activity and, interestingly, provide a justification for tumour-suppressive activity of catalytically inactive PTEN [27].

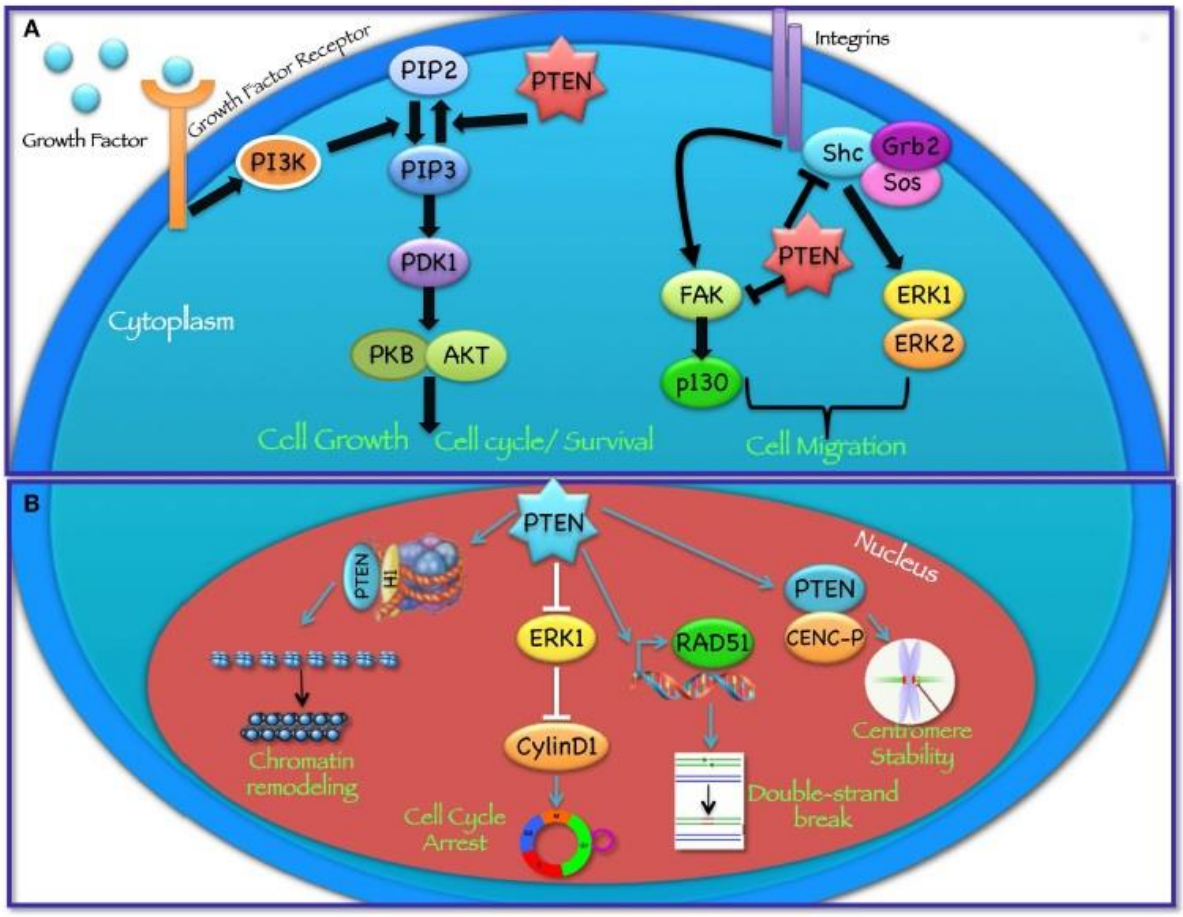

Figure 1.5 The cytoplasmic and nuclear functions of PTEN. (A) In the cytoplasm, PTEN acts as a direct antagonist of PI3K through the dephosphorylation of PIP3 to PIP2 leading to inhibition of cell growth, cell cycle progression and induction of apoptosis. Through its protein phosphatase activity, PTEN acts to regulate cell migration. (B) In the nucleus, PTEN plays roles in the repair of DNA double strand DNA breaks, the maintenance of genomic integrity, the regulation of cell cycle progression and chromatin remodelling. (Taken from [60]).

1.3.3 PTEN nucleocytoplasmic translocation

Despite the absence of a classic nuclear localisation signal (NLS), nuclear export sequence (NES) and indistinct mechanisms of PTEN nuclear translocation, PTEN has been clearly shown to localise to the nucleus where it is involved in a variety of biological functions as discussed in the previous section. Although the mechanism(s) of PTEN nuclear transport are not fully understood, several mechanisms have been proposed including: (a) active shuttling by the RAN GTPase or major vault protein (MVP), a nucleocytoplasmic transport protein [71], (b) simple diffusion, (c) cytoplasmic localisation signal-dependent export, (d) phosphorylation-dependent shuttling and (e) monoubiquitination-dependent nuclear import [72]. Interestingly, monoubiquitination of PTEN on Lys13 and Lys289 by NEDD4-1 promotes its nuclear import whereas PTEN polyubiquitination by NEDD4-1 leads to its cytoplasmic retention and degradation by proteasome mediated decay mechanisms [73, 74]. In fact, the compartmentalisation of PTEN to the cytoplasm and/or nucleus is currently considered to be another important mechanism of regulation of PTEN activity [75] and inappropriate compartmentalisation of PTEN has been linked with neoplastic transformation [9].

1.4 Involvement of *PTEN* in disease

1.4.1 Germline *PTEN* mutation and the PTEN hamartoma tumour syndromes

Germline mutations of PTEN have been linked to three inherited cancer syndromes with overlapping features: (1) Cowden Syndrome (CS), (2) Bannayan Riley Ruvalcaba syndrome (BRRS), and (3) Proteus syndrome (PS), all characterised by increased susceptibility to cancer [76]. These syndromes are notable for the presence of hamartomas, benign tumours in which differentiation is normal, but cells are highly

disorganised. In these seemingly unrelated syndromes, PTEN germline mutations account for 80% of CS, 60% of BRRS and 20% of PS patients. A detailed comparative list of PTEN mutations characterised in CS, BRRS and PS, including their gene position, any associated amino acid changes and disease associations is provided in Table 3 in reference [77].

Cowden syndrome (CS): The features of CS include hamartomatous overgrowth of tissues and a predisposition to developing tumours of the breast, thyroid, endometrium and, in some instances, colon cancer [78]. An additional feature of CS is an increase in insulin sensitivity, which has been linked with PTEN haploinsufficiency-associated enhancement of PI3K/Akt signalling [39]. The majority of CS patients have macrocephaly and some patients also have autism spectrum disorder related to germline mutations of PTEN [40, 41, 79-81]. Over 80 different germline PTEN mutations have been identified, with specific mutations, including the R130X and Y178X nonsense and H93R, D252G and F241S missense mutations shown to be associated with the autism and macrocephaly characteristics and leading to the proposal that PTEN sequencing may allow genetic phenotyping and subsequent diagnosis of a subset of autistic patients [33]. This disease is characterised by multiple hamartomas and an increased risk of breast, thyroid, endometrial and other cancers [23]. The most commonly reported phenotypes are thyroid abnormalities, mucocutaneous lesions, fibrocystic disease, macrocephaly, early-onset uterine leiomyoma and breast carcinoma [82]. Germline mutations in PTEN have been found in 80% of CS patients [83].

Bannayan-Riley-Ruvalcaba syndrome (BRRS): This disorder is characterised by macrocephaly, lipomatosis, hemangiomatosis and speckled penis. Germline mutations of *PTEN* have been identified in up to 60% of BRRS individuals [77, 84-86]. The *PTEN* mutational spectra for BBRS and CS show some overlap, lending formal proof that CS and BBRS are allelic [87]. There is some overlap in the germline mutations between CS and BRRS, however each syndrome has distinct PTEN germline mutations and, overall, distinct CS-associated mutations are located mainly in the 5' exon-encoded region whereas the BRRS specific mutations occur mainly in the 3'-encoded C2 domain region [77].

Proteus syndrome (PS): This is a rare disorder of mosaic growth dysregulation with the hallmark feature of overgrowth of multiple tissues including skin, bone, central nervous system and eye [88]. Patients with PS have an increased risk of developing tumours, mostly benign, generally developing by the age of 20 years and include meningioma, papillary adenocarcinoma of the testis, and cystadenoma of the ovaries [89]. At least three unique PS-associated PTEN mutations have been identified, W111R, C211X and M35T and PS-like syndrome has a common mutation linked with both CS and BRRS [77].

Lhermitte–Duclos disease (LDD): Also known as dysplastic gangliocytoma of the cerebellum, LDD is a hamartomatous overgrowth syndrome believed to be a component feature of Cowden syndrome together with megalocephaly [90]. Other neurological signs range from tremor and ataxia to epilepsy and mental retardation [91].

1.4.2 PTEN Somatic mutation and tumorigenesis

Mutations of PTEN have been identified in various sporadic cancers including glioblastoma, endometrial carcinoma, prostate carcinoma, melanoma, ovarian cancer, breast and lung cancers [17, 54, 92]. Point mutations and/or deletions and/or epigenetic silencing (through promoter hypermethylation) of one or both alleles can lead to PTEN inactivation [22, 93]. Interestingly, the loss of a single PTEN allele is often sufficient for the development of tumours (a property termed functional haploinsufficiency) [60]. The inactivation of both PTEN alleles occurs with low incidence but is observed more frequently in metastatic breast cancers, in glioblastoma, melanoma and prostate cancer [19, 54, 94, 95]. In tumours, PTEN is inactivated by various mechanisms, including not only mutations, but also deletions, transcriptional silencing through promoter hypermethylation, subcellular mislocalisation, and alterations of cellular stability and protein half-life as well as multiple mutations (reviewed in: [19, 54]).

Different tumour types appear to show certain PTEN inactivation mechanisms more frequently than others. For example, up to 70% of glioblastomas [17, 35, 60, 96] and 40% of breast cancers [19, 60] show inactivation of PTEN by deletion whereas in melanoma, about half of the tumours show PTEN inactivation by epigenetic silencing through promoter hypermethylation. PTEN loss or inactivation has been observed in up to 60% of sporadic colorectal cancers with the proportion of deletions and mutations resulting in PTEN inactivation or loss being almost the same [9, 19, 21, 60]. Table 1.1 shows the incidence, mode and significance of PTEN inactivation in various sporadic human cancers.

In addition, it is of note here that the presence of PTEN mutations and/or inactivation has been reported in a number disorders unrelated to cancer and include autism spectrum disorders, Alzheimer's disease (AD) and Parkinson's disease (PD) [40-43].

Glioblastoma Multiforme: Deletions of *PTEN* occur in approximately 70% of glioblastomas [17, 18] and gene deletion is the most common mechanism of PTEN inactivation in glioblastoma. Mutations of *PTEN* have been shown to occur in 20-44% of glioblastomas and glioblastoma cell lines and are often accompanied by loss of the remaining wild type allele [18, 20, 97-100].

Prostate cancer: The 10q23 region appears to be the most common region of loss in prostate cancer, with losses observed in up to 55 % of cases [101-105]. Furthermore, inactivation of *PTEN* by homozygous deletion has been shown to occur in 10-15 % of prostate carcinomas [103]. Interestingly, mutations of PTEN have been shown to occur more frequently in metastatic disease [103], while loss of PTEN expression has been correlated with pathological markers of poor prognosis [106].

Endometrial cancer: The frequency of *PTEN* mutations in endometrial carcinoma is approximately 35-55 % [107-110]. Loss of PTEN function by mutation or other mechanism (e.g. epigenetic events) is thought to be an early event in endometrial tumorigenesis [111].

Breast cancer: Mutations of *PTEN* have been shown to occur in approximately 5 % of breast cancers [105, 112, 113]. Subsequent studies have demonstrated a reduction or loss of PTEN expression in approximately 34 % of primary sporadic breast cancers [114].

PTEN is also implicated in many other cancer types (Table 1.1).

Table 1.1 Frequency of *PTEN* mutation, deletion and loss of PTEN expression in various sporadic tumour types. Approximate frequencies of mutation, loss of heterozygosity (LOH) and loss of expression of PTEN in different tumour types are shown. Data is derived from various studies as referenced.

Cancer Type	Frequency of PTEN Inactivation	Mechanism and Frequency of PTEN Inactivation				References
		LOH[1]	HD[2]	Mut[3]	Epigenetic	
Glioblastoma	17-70%	>70%	ND[4]	44%	ND	[17, 35, 60, 96]
Colorectal	60%	<19%	ND	<18%	ND	[9, 19, 21, 60]
Endometrial	34-83%	ND	ND	15–88%	38% (18% MET[5] & 20% LOE[6])	[19, 60, 115]
Breast	30-40%	<40%	ND	5%	90% (50% MET & 40% LOE)	[19, 60]
Thyroid	37%	ND	10%	ND	>50% MET	[19, 60]
Melanoma	32-33%	30-60%	ND	10-20%	>50% MET in patients with XP[7]	[19, 60, 115, 116]
Prostate	17-41%	ND	>20% HD and MUT		ND	[19, 60]
Leukaemia/ Lymphoma	75% of acute myeloid leukaemia	ND	10 % of T-ALL[8]	27% in T-ALL	ND	[19, 60]
Bladder	23%	23%	6%	23%	53% decreased or LOE	[19, 60, 117]
Pancreatic	50%	50%	15%	ND	70% loss of protein expression	[19, 60, 118]

[1]LOH, loss of heterozygosity; [2]HD, homozygous deletion; [3]MUT, mutation; [4]ND, not determined; [5]MET, promoter hypermethylation; [6]LOE, loss of expression; [7]XP, xeroderma pigmentosum; [8]T-ALL, T-cell acute lymphoblastic leukaemia.

1.5 Regulation of PTEN cellular abundance and activity

As small decreases in PTEN abundance or activity may lead to tumorigenesis, the maintenance of cellular levels of PTEN is tightly regulated by a variety of mechanisms acting at the transcriptional, post-transcriptional and post-translational levels [22, 37, 119]. These regulatory mechanisms maintain the activity and abundance of PTEN at the required level under different cellular circumstances and are discussed in the following sections.

1.5.1 Transcriptional regulation of *PTEN*

A number of transcription factors regulate *PTEN* transcription by directly binding to the PTEN promoter and either activating or repressing *PTEN* transcription. Known transcription factors characterised to date include the tumour suppressor p53 [120], early growth response 1 (EGR-1), activating transcription factor-2 (ATF2) [121], peroxisome proliferator-activated receptor γ (PPARγ) [122], Zinc finger protein encoded by the SNAIL gene (SNAIL), SLUG [123], cellular DNA-binding proteins encoded by the c-jun genes (c-Jun), polycomb complex protein encoded by the BMI-1 gene (BMI-1) and nuclear factor kappa-B (NFKB). Furthermore, the antisense transcript of the PTEN Pseudogene (PTENP1(AS)) is also known to regulate PTEN transcription (Figure1.6) [22, 124, 125].

Activators of PTEN transcription: The PTEN gene promoter contains a functional p53-binding site, which is required for p53-mediated transactivation [126]. p53 and PTEN share regulatory interactors and regulate each other in a feedback loop mechanism [127]. p53 upregulates PTEN transcription by binding to the functional p53 binding

element upstream of the PTEN promoter [128]. EGR binds to the PTEN promoter and upregulates PTEN expression in response to insulin-like growth factor 2 (IGF2) or

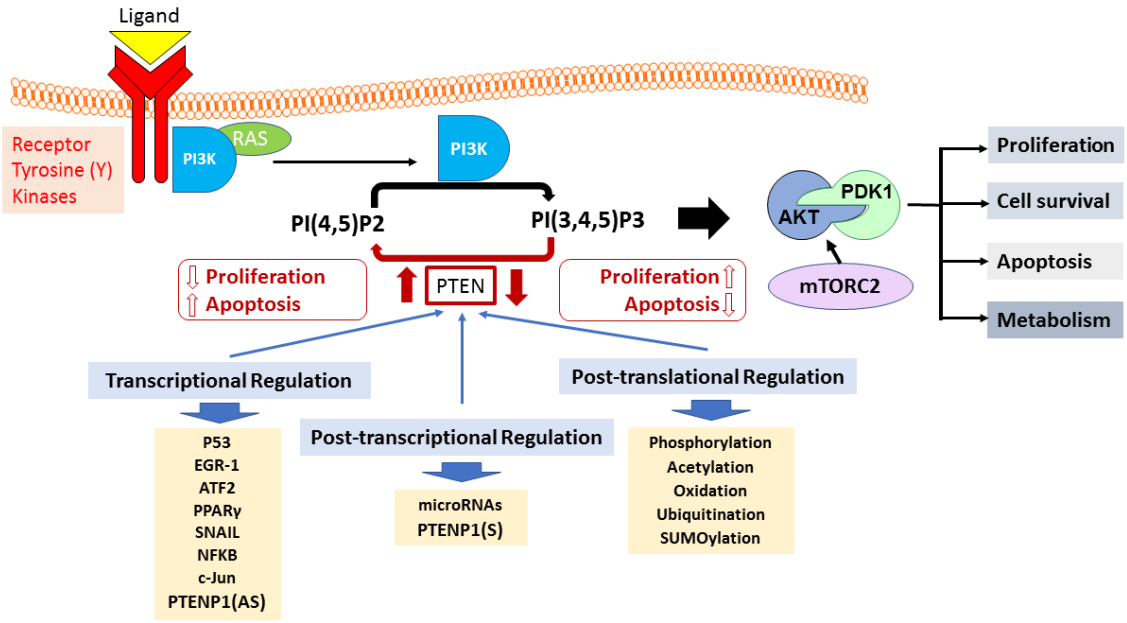

Figure 1.6 Regulation of PTEN, a major regulator of the PI3K/AKT signalling pathway. Growth factors bind receptor tyrosine kinases (RTKs) on the extracellular side of the cell membrane, which leads to the recruitment and binding of PI3K (directly or through adaptor proteins) to its cytoplasmic domain through its regulatory subunit (P85). Activated PI3K phosphorylates of PI(4,5)P2 to PI(3,4,5)P3, which occurs through its catalytic subunit (P110). The serine/threonine kinases Akt and PDK1 are recruited to the membrane after binding to the pleckstrin homology (PH) domain of PI(3,4,5)P3. PDK1 and mTORC2 phosphorylate and activate Akt, which phosphorylates a number of downstream protein targets with the overall effect of enhancing cell proliferation, metabolism and survival whilst inhibiting apoptosis. PTEN is a major negative regulator of PI3K/Akt signalling through its phosphoinositide phosphatase activity which acts to directly antagonise Pi3K activity by dephosphorylating PI(3,4,5)P3 to PI(4,5)P2. PTEN abundance and activity is highly regulated through various complementary mechanisms working at the transcriptional, post-transcriptional and post-translational levels (modified from [2]).

irradiation [129, 130]. Furthermore, PPARγ directly binds to two elements in the upstream region of the *PTEN* gene and increases *PTEN* expression [54, 131]. Another positive regulator of PTEN is ATF2, which, by binding to two sites in the *PTEN* promoter, also upregulates PTEN expression [121].

Repressors of PTEN transcription: On the contrary, Sal Like Protein 4 (SALL4), a zinc-finger transcription factor, represses *PTEN* transcription. Moreover, SNAIL homolog 1 (SNAL1) and DNA-binding 1 (ID1) can also inhibit PTEN transcription by competing with p53 for binding to the *PTEN* promoter [54]. BMI-1, a polycomb-group protein, and *c-Jun,* a proto-oncogene, also supress *PTEN* expression [132].

Of interest, C-repeat binding factor 1 (CBF-1), also known as RBP-JK is a transcription factor that has been shown to be able to either activate or suppress *PTEN* transcription under different cellular conditions [133].

1.5.2 Post transcriptional regulation of PTEN by microRNAs and PTENP1

PTEN is now known to be regulated at the post-transcriptional level through the binding of specific microRNAs (miRNAs), which act to inactivate or repress PTEN translation [134]. Furthermore, the transcription of a processed pseudogene of PTEN (*PTENP1*), has been shown to produce a transcript that is able to regulate PTEN cellular levels by binding to PTEN-targeting miRNAs and freeing PTEN from miRNA-mediated repression [95]. The transcript of PTENP1 is not translated and acts, within the cell, as a regulatory long non-coding RNA.

1.5.2.1 Post-transcriptional regulation of PTEN by microRNAs

PTEN is regulated at the post-transcriptional level by a number of different miRNAs. These small noncoding RNAs (ncRNAs), approximately 14-24 nt in length [134], bind to their target messenger RNA (mRNA) at seed regions, known as miRNA recognition elements [135, 136], which are located within the 3'untranslated region (UTR) of the specific target mRNAs (Figure 1.7) [137, 138].

Interestingly, recent studies have revealed miRNA binding sites are also present in the coding regions, the 5'UTR region and even the promoter region of target mRNAs [138-140]. miRNA function is dependent upon the binding affinity of the specific miRNA with the target mRNA, such that binding of miRNAs can either lead to degradation of the target through perfect complementary binding or inhibition of translation through imperfect binding [141, 142]. PTEN is known to be post-transcriptionally regulated by miRNAs binding within its 3'UTR, which results in blockage of translation, and a consequent decrease in PTEN abundance [143].

miRNAs commonly known to bind to, and repress PTEN include miR-17, miR-19, miR-21, miR-26, and miR-214 [95, 144, 145]. MicroRNAs have been shown to possess functional roles in cancer development and progression [146], and a variety of oncogenic miRNAs (oncomirs) have recently been shown to bind specifically to PTEN transcripts, blocking PTEN translation in a cancer-type dependent manner. Overexpression of PTEN-specific miRNAs has the potential to enhance cancer progression, and specific PTEN-targeting oncomirs have been linked to the development and progression of hepatocellular carcinomas, prostate cancer, clear-cell renal carcinoma, breast cancer and endometrial cancer (Table 1.2).

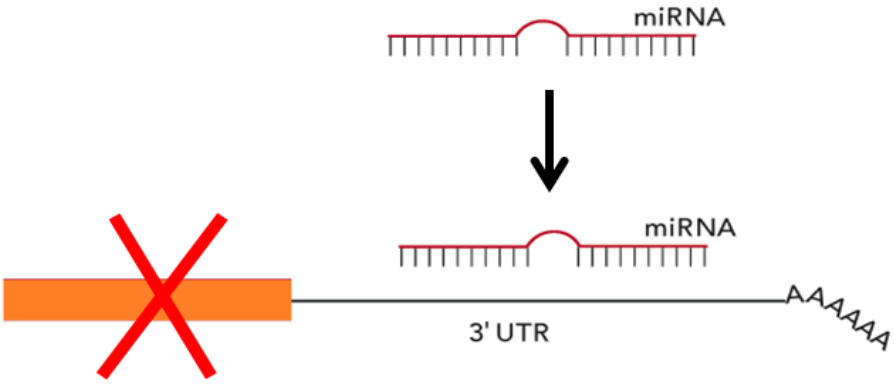

Figure 1.7 Regulation of protein coding mRNAs by miRNAs. Attachment of the short miRNAs to the 3′ UTR of target coding mRNAs inhibits translation and protein production. (Adapted from [147]).

Table 1.2 PTEN-targeting miRNAs identified in various cancer types.

Cancer	microRNAs (miRNA, mIR)	References
Prostate	miR-17, miR-19, miR-21, miR-26 and miR-214	[95]
Hepatocellular	miR-17, miR-19b and miR-20a	[148]
Clear-cell renal	miR-21	[149]
Glioma	miR152	[150]
Breast	miR-106b and miR-93	[151]
Endometrial	miR-200a, miR-200b and miR-200C	[3, 152]

In 2010, a processed pseudogene of PTEN (PTENP1) was found to be transcribed to produce a transcript with high sequence similarity with the PTEN transcript. Further, this pseudogene transcript was ascribed a novel function of acting as a 'decoy' for miRNA binding of PTEN-targeting miRNAs, as discussed in more detail below [95].

1.5.2.2 Regulation of PTEN abundance by PTENP1

1.5.2.2.1 PTENP1 pseudogene and its regulation of PTEN

The *PTEN* pseudogene, *PTENP1*, is a processed pseudogene located on chromosome 9p13.3, with extensive nucleotide sequence identity to the PTEN transcript sequence with only 18 nucleotide mismatches within the coding region [153, 154]. The nucleotide sequence identity between the two transcripts extends into parts of the 5' UTR and 3' UTR [95].

Poliseno et al [155] have shown that the PTENP1 transcript acts as a miRNA decoy, binding to a number of PTEN-targeting miRNAs and reducing the cellular concentration of these miRNAs. This therefore provides an opportunity for PTEN to escape its miRNA-mediated repression, hence restoring PTEN function. Thus, PTENP1 can regulate the cellular level of PTEN and PTENP1 knockdown results in decreased PTEN mRNA and protein (Figure 1.8) [155]. The levels of PTEN and PTENP1 appear to be inversely correlated in prostate cancer samples and deletion of PTENP1 has been shown to be a frequent event in some sporadic cancers including colon and prostate cancers, attributing a tumour suppressor function to PTENP1 that is independent of its effect on PTEN abundance [3, 155, 156].

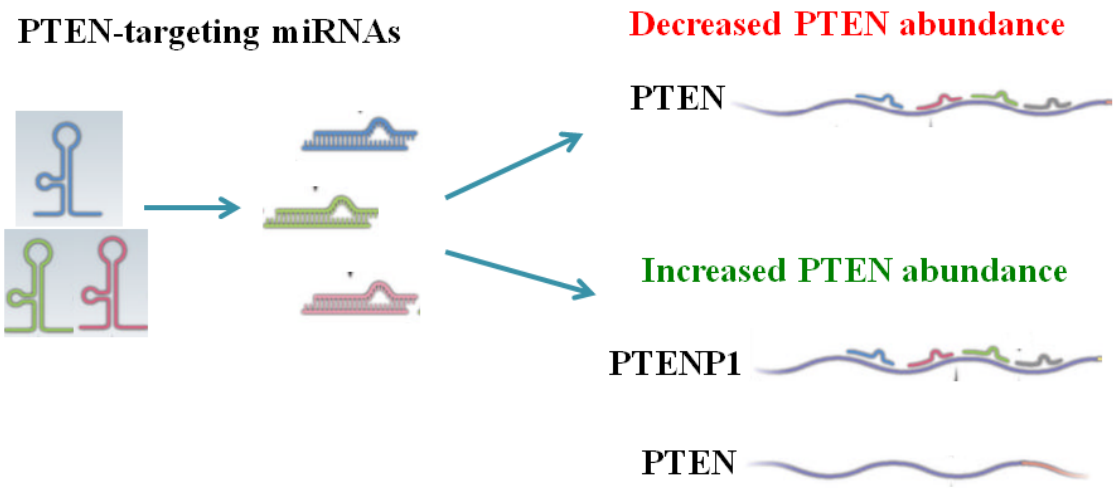

Figure 1.8 Post-transcriptional regulation of PTEN by miRNAs and PTENP1. In the absence of PTENP1, PTEN-targeting miRNAs bind to PTEN and repress PTEN translation, decreasing its cellular abundance. In the presence of the PTENP1 transcript, both PTEN and PTENP1 transcripts compete for the binding of PTEN-targeting miRNAs. Binding of these miRNAs to PTENP1 means less miRNA binding to PTEN and a lifting of the miRNA-mediated repression of PTEN translation and increased PTEN abundance.

1.5.3 Regulation of PTEN by post-translational mechanisms

1.5.3.1 ***Regulation of PTEN by phosphorylation:*** Phosphorylation of serine and threonine residues in the C2 and C-terminal tail of PTEN by specific protein kinases can alter PTEN activity and stability. Phosphorylation of T366, S370, S380, T382, T383 and S385 by casein kinase 2α (CK2α) stabilises PTEN by creating a closed conformation with increased cellular half-life but with reduced phosphatase activity, reduced interactions with other binding partners and decreased plasma membrane localisation [157]. Liver kinase B1 (LKB1) can inactivate PTEN by phosphorylation on S385 [158] while glycogen synthase kinase 3β (GSK3b) decreases PTEN activity through phosphorylation of S362 and T366 [159]. Phosphorylated PTEN adopts a closed conformation with decreased activity but increased stability but can be re-activated by dephosphorylation of the specific Ser and Thr residues in the C-terminal tail by the action of PTEN itself through auto-dephosphorylation. Dephosphorylated PTEN adopts an open-conformation with increased phosphatase activity but decreased cellular half-life (Figure 1.9) [22, 54, 160].

1.5.3.2 ***Regulation of PTEN by acetylation***: In response to growth factor stimulation, the P300/CBP-associated factor (PCAF), also known as KAT2B, acetylates residues K125 and K128, located in the catalytic pocket of PTEN, resulting in negative regulation of PTEN enzymatic activity [161]. PTEN is also acetylated by CREB-binding protein (CBP) on K402 in the PDZ domain-binding motif of PTEN, which affects PTEN interaction with other PDZ domain-containing partners [162]. The acetylation may be reversed by the action of Sirtuin 1 (SIRT1), which reconstitutes the phosphatase activity of PTEN [162].

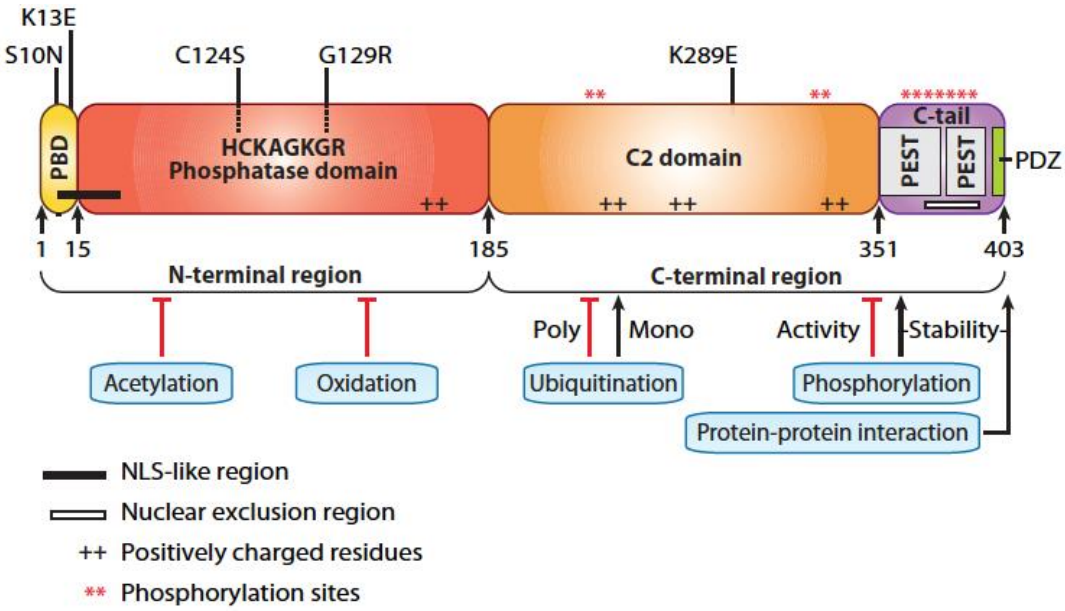

Figure 1.9 PTEN protein domain structure and sites of post-translational modification. PTEN is composed of 403 amino acids and is characterised by five functional domains: a phosphatidylinositol-4,5-bisphosphate (PIP2)-binding domain (PBD), a phosphatase domain containing the catalytic core, a C2 domain with putative ubiquitination sites, two PEST (proline, glutamic acid, serine, threonine enriched) domains for degradation, and a PDZ interaction motif for protein-protein interactions. Also depicted are an N-terminal nuclear localisation signal-like region, a C-terminal nuclear exclusion signal, and several charged residues and phosphorylation sites important for subcellular localisation and stability (Taken from [2]).

1.5.3.3 Regulation of PTEN by oxidation: The oxidation of PTEN by H_2O_2 leads to the formation of a disulphide bond between the residues C124 and C71, leading to inactivation of PTEN catalytic activity. The reverse reaction is possible with thiol compounds such as thioredoxin [163, 164].

1.5.3.4 ***Regulation of PTEN by ubiquitination***: The conserved C-terminal tail of PTEN (residues 352-403) interacts with the C2 domain, creating a loop (residues 283-309) containing a major ubiquitination site (K289). Neural precursor cell expressed developmentally downregulated-4-1 (NEDD4-1) can ubiquitinate PTEN when this loop is released. Mono-ubiquitination of PTEN, at K13 or K289, leads to the translocation of PTEN to the nucleus while polyubiquitination targets PTEN for degradation by cytoplasmic proteasomes [119].

1.6 Background to the project and aims

The significance of the role of PTEN in normal cellular function and the involvement of PTEN alterations (mutations and deletions) in tumorigenesis has been highlighted by the frequency of its deregulation in cancer. The importance of this gene in cellular function is further highlighted by the strict regulation of its activity and abundance by a number of regulatory mechanisms acting at the various levels of gene expression. An understanding of the mechanism(s) by which *PTEN* mutations and other alterations contribute to the development and progression of cancer is imperative for the development of future therapies.

Previous work in our laboratory described a high frequency (41%) of *PTEN* gene alterations (mutation and/or deletion) in primary sporadic colorectal cancer, with the

occurrence of PTEN gene mutations in 25% of tumours [9] . This data redefined the role of this important tumour suppressor gene in colon cancer as previous reports had showed *PTEN* mutations to be infrequent and to occur almost exclusively in tumours with microsatellite instability. Overall, 10 novel cancer-associated somatic mutations of PTEN were described (Figure 1.10 and Table 1.3). Based on their position, and work in other tumours, most of the mutations were predicted to alter the lipid phosphatase activity essential for PTEN tumour suppressor function. All tumours harbouring alterations of the *PTEN* gene demonstrated either reduced or absent PTEN expression and there was a strong correlation between reduced or absent PTEN staining and later clinical stage of tumour at presentation. This suggested the involvement of *PTEN* in a distinct pathway of colorectal tumorigenesis that is distinct from the pathway of mismatch repair deficiency.

The overall aim of this part of the research is to study the effect of these novel, cancer-associated *PTEN* mutations on PTEN function, specifically its regulation of cell growth and proliferation, cell cycle regulation and PI3K pathway activation *in vivo*.

It is vital to examine the functional significance of these tumour-associated *PTEN* mutations, as PTEN plays a major role in regulating cell survival by inhibiting cell cycle progression and cellular proliferation. Improving our understanding of this gene and its role in colorectal, and other, tumours may lead to better prognostic indicators as well as molecular targets for therapy for colorectal and other cancer patients.

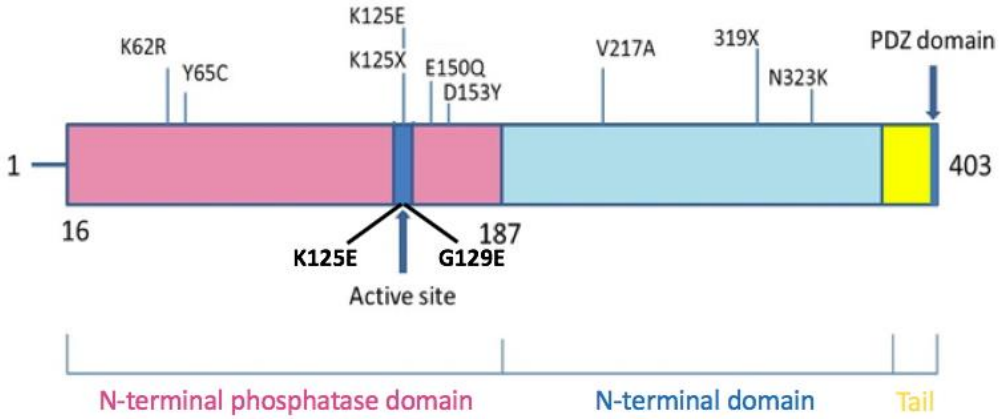

Figure 1.10 Somatic mutations of PTEN detected in primary sporadic colorectal tumours. The type and location of each of the detected mutations are shown above the PTEN protein sequence. Mutations are distributed throughout the length of the protein with the majority being missense mutations. Mutations shown below the protein sequence (C124S and G129E) are the known PTEN phosphatase deficient mutants [83, 165] produced for use as controls for comparison with WT PTEN and the detected mutants.

Table 1.3 Summary of the properties of each of the 10 novel cancer-associated PTEN mutations to be studied in this project.

Mutant sequence	Mutation type	Location	Protein Location
K62R	missense	exon 3	N –terminal phosphatase domain
Y65C	missense	exon 3	N –terminal phosphatase domain
K125E	missense	exon 5	N –terminal phosphatase domain | Active site
K125X	nonsense	exon 5	N –terminal phosphatase domain | Active site
E150Q	missense	exon 5	N –terminal phosphatase domain
D153N	missense	exon 5	N –terminal phosphatase domain
D153Y	missense	exon 5	N –terminal phosphatase domain
N323K	missense	exon 8	C- terminal, C2 domain
[#]C124S	missense	exon 5	N –terminal phosphatase domain | Active site
[#]G129E	missense	exon 5	N –terminal phosphatase domain | Active site

[#]Previously characterised and known PTEN phosphatase deficient mutants [83, 165].

1.6.1 Project objectives

It was hypothesised that inactivating mutations of the *PTEN* gene will alter its tumour suppressive function with consequent effects on cell proliferation, cell cycle regulation and PI3K pathway activation.

The overall aim of this project is to determine the effects of the unique cancer-associated *PTEN* gene mutations on the tumour suppressive function of the mutant PTEN protein. This project will generate data to complete and strengthen preliminary data.

The overall aim of this work will be achieved through fulfilment of the following specific experimental aims:

1. To prepare, and verify by sequencing, the set of PTEN expression constructs (consisting of the wild type (WT) PTEN, each of the mutant PTEN sequences and appropriate controls) required for PTEN functional analysis *in vitro*.

2. To determine the effect of WT PTEN, and each of the PTEN mutants on the rate of cell proliferation in different cancer cell lines (U87MG, HCT116 and MCF7).

3. To determine the effect of WT PTEN, and each of the PTEN mutants on the cell cycle phase distribution of different cancer cell lines (U87MG, HCT116 and MCF7).

4. To determine the ability of WT PTEN and each of the PTEN mutants to suppress the phosphorylation and activation of AKT (a key indicator of PI3K pathway activation).

An understanding of the biological effect of the detected *PTEN* mutations will help elucidate the role of *PTEN* in sporadic colorectal tumorigenesis, as well as other cancers and further enhance our understanding of the function of this important gene.

CHAPTER 2

GENERAL MATERIALS AND METHODS

This section includes the general materials and methodologies used in both parts of the research work described in this thesis (part 1 and part 2). Specific materials and methodologies unique to either part 1 or part 2 only, are described in the relevant sections of the thesis where they are used.

2.1 General Materials and Reagents

All reagents used were either of molecular biological or analytical grade. Agarose (molecular biology grade), ampicillin sodium salt, yeast extract, tryptone, phosphate buffered saline (PBS) tablets, sodium chloride (NaCl), dimethyl sulphoxide (DMSO) and Tris-EDTA (TE) buffer (100X concentrate) were obtained from Sigma Aldrich. Fetal Bovine Serum (FBS), TRIZOL Reagent and HANKS buffered salt solution were purchased from Life Technologies. Tris-Acetate electrophoresis buffer (TAE, 10X concentrate) was purchased from Astral Scientific. Gel Red nucleic acid stain was obtained from Biotium. Bromophenol blue was provided by Biolabs.

2.1.1 Cell lines

The U87MG (ATCC® HTB-14™) human glioblastoma cell line was kindly donated by Dr Kerry McDonald (Kolling Institute of Medical Research, Sydney, Australia). The MCF7 (ATCC® HTB-22™) breast cancer cell line was available at the University of Technology Sydney. The HCT116 colon cancer cell line was kindly provided by Professor Robert Sutherland and Gillian Lehrbach (Garvan Institute of Medical Research, Sydney, Australia). All the cell lines were maintained as adherent cell lines and were certified mycoplasma free. All cell lines were regularly tested for mycoplasma using the Lonza MycoAlertTM Plus mycoplasma detection kit.

2.1.2 Antibodies and stains

The PTEN poly-clonal antibody (ab44712) was obtained from Abcam and Hoechst 33342 from Thermo Fisher Scientific. Alexa Fluor 568 goat anti mouse IgG was purchased from Invitrogen. Anti-flag m2 mouse F1804-1MG from Sigma Aldrich was kindly donated by Dr Sarah Bajan (UTS). Wheat Germ Agglutinin (WGA) Alexa Fluor 488 conjugate (Invitrogen), was generously provided by Dr Michael Johnson (UTS).

2.1.3 Molecular weight markers for electrophoresis

DNA molecular weight standards were used to estimate the sizes of PCR products. The DNA size standards used were the PCR marker, Hyperladder I (Bioline), Hyperladder IV (Bioline), Hyperladder V (Bioline) and 100bp PCR ladder (Sigma). The sizes of the specific markers in each standard are listed below (in bp units):

PCR marker: [50, 150, 300, 500, 766]

Hyperladder I: [200, 400, 600, 800, 1000, 1500, 2000, 2500, 3000, 4000, 5000, 6000, 8000, 10,000]

Hyperladder IV: [100, 200, 300, 400, 500, 600, 700, 800, 900, 1000]

Hyperladder V: [25, 50, 75, 100, 125, 150, 175, 200, 250, 300, 400, 500]

100bp PCR ladder: [100, 200, 300, 400, 500, 600, 700, 800, 900, 1000]

2.1.4 Protein molecular weight standards

The protein size standards used were the See Blue Plus 2 prestained standards from Life Technologies. These were used to determine protein sizes in the 4-250 kDa molecular weight range and consisted of bands of the following molecular weights (in kDa): 188, 98, 62, 49, 38, 28, 17, 14, 6 and 3 kDa.

2.2 General methods

2.2.1 Sterility and containment of biological materials

All heat stable solutions and plasticware items, such as disposable pipette tips and microcentrifuge tubes, were sterilised by autoclaving (121°C, 20 min) prior to use. Glassware was sterilised by autoclaving or by heating at 180°C (2 h to overnight) in a hot air oven.

2.2.2 Measurement of nucleic acid concentration

RNA and DNA concentration were determined by measuring the absorbance of appropriately diluted samples at 260 nm and 280 nm using the Nanodrop spectrophotometer (Nanodrop ND-1000 V3.8.1, Biolab) and One Viewer (version 1.2.0.367) software according to the manufacturer's instructions. An A260/A280 ratio above 1.8 was indicative of high purity nucleic acid preparations.

2.2.3 Agarose gel electrophoresis

Agarose gels of 1-2% (w/v) were used to visualise and analyse the quality of extracted RNA samples and amplified PCR products respectively. Agarose gels were prepared in 1X TAE buffer and contained 0.01% (v/v) GelRed. Gels were electrophoresed submerged in 1X TAE buffer. Prior to loading, 0.2-0.3 vol of loading buffer (60% sucrose, 100 mM Tris-HCl, pH 8.0, 10 mM EDTA, 0.02% bromophenol blue and 0.02% xylene cyanol) was added to all samples to be electrophoresed. All gels were electrophoresed at 80-100V for 45-60 min and electrophoresed products were visualised on a UV

transilluminator using the Syngene Ingenius 3 gel documentation system (Syngene International) and Genesys version 1.5.0.0 software.

2.2.4 Preparation and growth of plasmid clones

2.2.4.1 Bacterial growth and maintenance

LB medium contained 5 g/L yeast extract, 10 g/L tryptone and 10 g/L NaCl. 2X YT medium contained 10 g/L yeast extract, 20 g/L tryptone and 5 g/L NaCl. Media for plates contained 20-30 g/L agar-agar or 20 g/L agarose and 100 µg/mL ampicillin accordingly. Similarly, for liquid culture, media (either LB or 2X YT) contained 100 µg/mL ampicillin.

LB medium or 2X YT medium containing 100µg/mL ampicillin was inoculated with a single plasmid containing colony and incubated at 37°C with shaking (200 rpm) overnight. The cells were harvested by centrifugation (4,500 xg, 10 mins at RT) for subsequent plasmid preparation.

2.2.5 Preparation of plasmid DNA

2.2.5.1 Small scale preparation (mini-prep) of plasmid DNA

Plasmid DNA was isolated from 1.5 mL of bacterial culture using the PureLink Quick Plasmid Miniprep system (Invitrogen) according to the manufacturer's instructions. The isolated plasmid DNA was eluted in TE buffer and the concentration and quality of the plasmid DNA was determined using the nanodrop spectrophotometer and agarose gel electrophoresis.

2.2.5.2 Large scale preparation (midi-prep and maxi-prep) of plasmid DNA

Plasmid DNA was prepared for transient transfection using a scaled-up version of the mini-prep system. Plasmid DNA was isolated from either 100 mL (for midi-prep) or 200 mL (for maxi-prep) 2X YT medium, which had been inoculated with a single colony and grown overnight at 37^{o}C, using the PureLink midi-prep or maxi-prep (Invitrogen) system according to the manufacturer's instructions. The isolated plasmid DNA was eluted in either 100 µL or 200 µL of TE buffer for midi-prep or maxi prep, respectively.

2.2.6 Tissue culture methods

2.2.6.1 Tissue culture materials

Vented cap tissue culture flasks (T25, T75 and T175) and sterile serological pipettes were obtained from BD Bioscience. TrypLE Express trypsin substitute, Dulbecco's Modified Eagle Medium (DMEM) and Fetal Bovine Serum (FBS) were obtained from Life Technologies.

2.2.6.2 Maintenance of human cancer cell lines

Frozen cells (stored in liquid nitrogen) were thawed quickly at 37°C and, once thawed, were placed into pre-warmed fresh medium in T75 flasks. After overnight growth (37^{o}C and 5% CO_2), the culture medium was replaced. All cell lines used (HCT116 human colon carcinoma cell line, U87MG glioblastoma cell line and MCF7 breast cancer cell line) were adherent cell lines and were maintained in DMEM supplemented with 10% FCS in a humidified system containing 5% (v/v) CO_2 at 37°C. To passage cells, the monolayer of cells was washed with 1.5 mL of 1X Dulbecco's phosphate-buffered saline (DPBS) (Thermo Fisher Scientific). Cells were detached from the surface using 1-2 mL

TrypLE Express and incubation for 4-8 min at 37°C). Cells were harvested by centrifugation (1000 rpm for 5 mins) and resuspended in culture medium. Cells were counted using a haemocytometer and reseeded into new flasks. Cells were passaged once they reached 80% confluence and harvested for subsequent cellular assays.

2.2.6.3. Determining cell growth characteristics and growth curve preparation

To determine cell growth characteristics of all cell lines used, growth curves were generated. To achieve this, cells were seeded at a density of 1.5 x 10^5 cells in T25 flasks and incubated at 37°C and 5% CO_2, with cells being harvested and counted at 24 hr intervals over 5-7 days. At the conclusion of the time period, the numbers of cells counted at each time point was plotted against time to obtain doubling times for each cell line. Six replicates were analysed in each experiment (i.e. for each cell line) and each experiment was performed three times.

2.2.6.4 Determination of cancer cell doubling time

The doubling time of each cell line used was calculated using the formula:

$$(t2 - t1)/ (\log n2 - \log n1)$$

[where t2 = doubling time (hr); Ln = natural log of the number; n2 = final cell number; n1 = initial cell number; t = time interval between n1 and n2 (hr)] (Butler, 1999).

2.2.6.5 Preparation of frozen cell stocks

Cells were harvested by trypsinisation and collected by centrifugation (1000 rpm, 5 min). The cell pellet was resuspended in freezing medium (90% FBS and 10% DMSO) to achieve a density of 1-2 x 10^6 cells/mL. Cells were placed in sterile labelled cryovials (in

1 mL aliquots) on ice and stored at -80°C overnight before being transferred and stored in liquid nitrogen.

2.2.7 Methods for the preparation and analysis of RNA

2.2.7.1 Isolation of total RNA from cell lines

Total RNA was isolated from cultured cells using either (A) a method combining TRIzol (Life Technologies) extraction and the RNeasy Plus Mini system (Qiagen), or (B) the Maxwell ESC simply RNA cells system (Promega) and the Maxwell RSC Instrument (Promega), using the relevant manufacturers' protocols.

(A) In the case of the combined TRIzol (Life Technologies) and RNeasy Plus Mini system, cultured cells were harvested by the addition of TRIzol to the cells (1 mL per 10 cm^2 of culture dish surface area) and scraping of the surface of the culture dish to collect the cells in a microcentrifuge tube. Tubes containing the cells were stored at -80°C until required for RNA extraction. To process the RNA, each tube was thawed at room temperature, then 0.2 mL of chloroform was added per 1 mL TRIzol. The mixture was vortexed and centrifuged for 15 min at 12000 rpm and 4°C. The collected aqueous layer containing the RNA was passed through a gDNA eliminator column of the RNeasy system to remove any potential contaminating genomic DNA, and RNA was purified using the RNeasy Plus Mini system following the manufacturer's protocol.

(B) When the Maxwell system was used, RNA was extracted from $1x10^6$-$5x10^6$ cells using the automated Maxwell RSC Instrument from Promega, according to the manufacturer's instructions.

In all cases, RNA quality was determined by agarose gel electrophoresis and Nanodrop absorbance measurements. Unless otherwise stated, extracted RNA was either used immediately for cDNA synthesis or stored at -80°C until required.

2.2.8 Reverse transcription and synthesis of cDNA

Reverse transcription was performed using the SuperScript III First Strand Synthesis SuperMix (Life Technologies) with oligo (dT) priming, according to the manufacturer's protocol. In all cases, 1 ug of total RNA was used for cDNA synthesis. The synthesised cDNA was either used immediately for PCR or stored at -20°C until required.

2.2.9 Polymerase chain reaction (PCR)

PCRs were typically carried out in a 50 uL reaction volume, which contained PCR master mix (1X), 0.5 U Taq DNA Polymerase, and 20 pmol each primer. PCR reactions typically contained 40 ng cDNA template. PCR was usually started with a denaturation step (95°C, 3 min), followed by 35 cycles of denaturation (95°C, 30 s), annealing (55-65°C, 30 s) and extension (72°C, 30 s). PCR was ended with a final extension step (72°C, 10 min).

All RT-PCR reactions were initially optimised for annealing temperature, and, once optimised, the PCR protocols were used for amplification reactions. A negative control, containing H_2O in place of the template, was included in all PCR reactions. A no reverse transcriptase control was also included to test for any genomic DNA contamination. All PCR reactions were conducted using the Eppendorf master cycler gradient instrument (Eppendorf). After PCR, amplification products (0.2 vol) were typically analysed by agarose gel electrophoresis.

2.2.10 Protein analysis methods

2.2.10.1 Materials for protein analysis

Pre-cast 4-12 % bis-tris polyacrylamide (NuPage Novex Bis-Tris Gels) gels, 2-(N-morpholino ethane sulfonic acid) (MES) running buffer, NuPage LDS sample buffer, NuPage transfer buffer and antioxidant were purchased from Thermo Fisher Scientific. PBS was also obtained from Thermo Fisher Scientific and PBST consisted of 1X PBS with 0.05 % Tween-20.

2.2.10.2 Protein extraction for western blotting

Transfected cells (40 hours after transfection) were harvested, washed with PBS and resuspended in 2X SDS lysing buffer containing loading dye [125 mM Tris-HCl (pH 6.8), 20% (v/v) glycerol, 4% (w/v) sodium dodecyl sulfate (SDS), 0.04% (w/v) Bromophenol blue and 200 mM 1,4-dithiothreitol (DTT)]. Prior to loading on to polyacrylamide gels, samples were heated at 95°C for 5 minutes, placed on ice for at least 1 minute and then centrifuged to gather all the contents at the bottom of the tube.

2.2.10.3 Polyacrylamide gel electrophoresis of proteins

Protein concentration was estimated using the BioRad BCA assay (Biorad Lab Inc. CA) and equal amounts of protein were loaded into each well of a 4-12% Bis-Tris polyacrylamide (NuPage Novex Bis-Tris Gel) gel and separated by SDS-PAGE. Gel electrophoresis was then carried out for 60 minutes at 150 V, in MES running buffer containing antioxidant.

After electrophoresis, separated proteins were transferred to PVDF membranes using the XCell II blot system (Thermo Fisher Scientific), based on the manufacturer's

instructions (30 V for 60 min). Thereafter, to verify the efficacy of the transfer, the membrane was stained with Ponceau S stain (Ponceau S 0.1 g, trichloroacetic acid 1.0 g/mL), with shaking, for 1 minute. The membrane was then washed with de-ionised water to visualise the pink coloured protein bands. After verification of protein transfer, the membrane was washed 3 times with water, once in PBS and once in PBST (5 min each wash).

2.2.10.4 Western blot analysis

The membrane was then incubated in blocking buffer (PBST containing 4-5% skim milk powder) overnight at 4°C, with gentle agitation. The membrane was quickly washed 3 times with PBST, then washed for a further 20 minutes (with gentle agitation) in PBST. Membranes were incubated with the optimal primary antibody dilution for a minimum of 2 hours and up to overnight, with gentle agitation. Thereafter the membrane was washed 2 times with PBST (20 min each wash), followed by a third wash in PBST (overnight at 4°C). The secondary antibody, Alexa Fluor 568 goat anti mouse IgG (Invitrogen) was then incubated with the membrane, with gentle agitation, for 60 minutes. The membrane was then washed twice with PBST (20 min each at room temperature) and once with PBS for 10 min. Detection of hybridised bands on the membrane membrane was carried out using the enhanced chemiluminescence (ECL) substrate (Amersham ECL prime western blotting detection reagent from GE Healthcare) according to the manufacturer's instructions. ECL reagent A was mixed with reagent B in a 1:1 ratio and the liquid used to cover the membrane (0.125 mL/cm^2). After 3-5 min incubation the membrane was visualised and images captured using an Amersham Imager 600 (GE Healthcare). The exposure time was optimised

prior to final image capture. The molecular weight of the hybridised proteins (PTEN, AKT, p-AKT, β-actin and SphK1) was determined by reference to the protein molecular weight marker (SeeBlue Plus2 Pre-stained Protein Standard - Thermo Fisher Scientific).

Images of the blots were taken at identical exposure times and were used for densitometry analysis using the Amersham Imager 600 software. After subtraction of background, the band density was calculated by the software. The protein band density was normalised individually against β-actin bands for gel loading differences.

2.2.11 Software and bioinformatics

The analysis and alignment of all sequence data was carried out using the Blast functionality on NCBI (National Centre for Biotechnology Information) and Clustal Omega from EMBL-EBI (The European Bioinformatics Institute).

2.2.12 Statistics

Statistical analyses were carried out using Microsoft Excel and IBM SPSS (version 25) statistical software. Paired-sample t-tests were used in chapters 3 and 4 to determine whether the mean difference between paired observations were statistically significant (further details are presented within the respective chapters). Independent t-tests were used to analyse the difference between the means of two independent groups (e.g. WT PTEN vs mutant PTEN) to determine whether the differences observed were statistically significant between the sets of groups analysed (further details are presented within the relevant chapter sections). A p-value of less than 0.05 was considered statistically significant.

CHAPTER 3

RESULTS

OPTIMISATION OF EXPERIMENTAL PARAMETERS FOR PTEN CELLULAR AND FUNCTIONAL ANALYSES

3.1 Introduction

The aims of part 1 of the research were to analyse the effect of wild type and mutant PTEN function on cell proliferation, cell cycle phase distribution and Akt activation in order to determine if any of the cancer-associated PTEN mutations altered the wild function of PTEN. To this end, a panel of cancer cell lines was to be used to determine the presence of any cell-type specific effects. The panel of cell lines to be used were (1) U87MG glioblastoma cells, (2) HCT116 colon cancer cells and (3) MCF7 breast cancer cells. Cellular and functional analyses were to be carried after transfection of each of the cell lines with the wild type, and each of the mutant, PTEN constructs.

Prior to carrying out any experiments to determine and compare wild type and mutant PTEN function, all the PTEN expression construct sequences were to be verified and a series of optimisation experiments were undertaken. This results chapter outlines the sequence verification and optimisation steps and validation of the parameters to be used for the analysis of wild type and mutant PTEN functional and cellular analyses. Optimisation was initially carried out to ensure that the parameters used in the cellular assays were optimal to allow accurate determination of functional changes in PTEN action brought about by mutation. Optimisation included determining optimal transfection parameters, optimal cell densities for analysis and other analysis parameters described in the subsequent sections. Once optimised, the conditions and parameters determined were used for subsequent assays of wild type and mutant PTEN function.

3.2 Materials and methods

3.2.1 Cloning vectors and bacterial Host Strains

The wild type PTEN, and each of the PTEN mutants were constructed in the pFLAG-CMV-5b expression vector (Sigma) and stored as glycerol stocks in the laboratory. Each of the PTEN point mutations had been produced by site-directed mutagenesis of the WT PTEN sequence. The truncating PTEN mutant was produced by cloning the region of PTEN encompassing codons 1-124 to produce a truncated PTEN protein. All PTEN constructs were expressed as FLAG-tagged proteins within the cell. The glycerol stocks were used to reconstitute the WT and each of the mutant PTEN sequences. After growth and maxi-prep of all clones, the PTEN constructs were all re-sequenced to ensure that sequences were correct and that no additional mutations had been introduced in the preparation process. Preparation of clones from DNA stocks was completed after transformation of the relevant clones into competent *E. coli* DH5α cells (Invitrogen, now ThermoFisher Scientific). Upon subsequent transfection of cells, the WT and mutant PTEN constructs are expressed as C-terminal FLAG tagged PTEN proteins.

The Spectrin B-GFP marker plasmid was also available in the laboratory and provided for this project. This construct was produced by the cloning of the Spectrin B sequence with a 3' GFP fusion in the pcDNA 3.1 vector (Invitrogen, now ThermoFisher Scientific). Upon transfection, spectrin B is expressed, within cells, as a fusion protein with a GFP tag, allowing transfected cells to be detected by their green fluorescence.

3.2.1.1 Verification of PTEN expression construct sequences

Sequencing of the wild type and mutant PTEN expression constructs was carried out by Macrogen Inc. (South Korea) using primers specific to the vector sequence and present on either side of the inserted sequence. The primer sequences were: CMV 30 sequencing primer (forward), 5'-AAT-GTC-GTA-ATA-ACC-CCG-CCC-CGT-TGA-CGC-3' and CMV 24 sequencing primer (reverse) 5'-TAT-TAG-GAC-AAG-GCT-GGT-GGG-CAC-3'). The sequences of the constructs were determined with significant sequence overlaps.

3.2.2 Transfection protocols and cellular analysis: optimisation and pilot analysis

3.2.2.1 Optimisation of transfection efficiency by flow cytometry

Before carrying out any transfection experiments, the transfection protocol was optimised to determine the optimal conditions for high efficiency transfection. For optimising transfection efficiency, the appropriate cells were seeded at a density of $2x10^5$ cells/well in 6 well plates and, after overnight growth, transfection was carried out. Transfection optimisation experiments were carried out using the spectrin-GFP plasmid. The amount of plasmid DNA used for transfection was varied to determine the optimal DNA amount for the highest transfection efficiency. Once determined, this optimal DNA amount was used in subsequent experiments to determine the optimal lipofectamine 2000 concentration by testing varying concentrations of this reagent and measuring transfection efficiency at the differing concentrations (see section 3.2.2.2 below). After determination of optimal amount of DNA and transfection reagent for this assay based on the literature co-transfection of GFP plasmid with wild type or mutant PTEN constructs was used [166, 167]. In all cases, transfection was carried out, and the

culture medium was changed 5 hours after transfection. After 40 hours post transfection, the medium was removed, and the cells washed twice with 5 mL PBS per well. Cells were then harvested by trypsinisation, collected by centrifugation and resuspended in 1 mL PBS. Cells were then passed through the cell strainer cap of falcon tubes (BD) and analysed by flow cytometry using the LSRII flow cytometer (Beckman Coulter). A total of 30,000 events were acquired and analysed using BD FACSDiva 8.0.1 software. The use of the Spectrin B-GFP plasmid for these experiments allowed live cell analysis of protein expression by flow cytometry.

3.2.2.2 Optimising transfection parameters for transient transfection in 6 well plates

In the case of transfection optimisation for 6-well plates, cells were seeded at a density of $3x10^5$ cells per well and grown overnight prior to transfection the following day. For transfection, solution A, containing plasmid DNA (1-10 µg) and Opti-MEM (serum free medium), at a total volume of 100 µL and solution B, containing lipofectamine 2000 (2-10 uL) and Opti-MEM, to a final volume of 100 uL, were made. Solution A was then combined with solution B and the mixture incubated at room temperature for 20 minutes. The DNA-Lipofectamine 2000 lipid complex (200 uL total) was added drop wise to each well. After 4-6 hours, the culture medium was changed and all subsequent cellular analyses were carried out after 40 hours incubation at 37°C and 5% (v/v) CO_2.

3.2.2.3 Optimising transfection parameters for transient transfection in 96-well plates

When using 96 well plates, the relevant cells were seeded at the optimal density of $2.5x10^3$ cells per well in the appropriate culture medium (see section 3.2.3 below). The cells were transfected as described in section 3.2.2.2 with the difference that for

transfection of the cells in each well, solution A contained 0.066 µg plasmid DNA and Opti-MEM in final volume of 5 µl and solution B consisted of 0.3 µL lipofectamine 2000 and 4.7 µL Opti-MEM. After incubation of DNA-Lipofectamine solution at RT for 20 min, a total volume of 10 µL was added in each well. Again, the culture medium was changed after 4-6 hours.

3.2.3 Determining the seeding density of individual cancer cell lines for the SYBR green-based cell proliferation assay

To determine the seeding density of individual cancer cell lines, to ensure cells are in the exponential phase of growth during the cell proliferation analysis (3-4 days), cells were seeded in 96-well plates at 4 concentrations (500, 1000, 1500, 2000) with 6 replicates for each cell seeding density. Cells were grown at 37^{o}C and 5% CO_2 and a replicate plate was removed from the incubator at 24 hour intervals. Upon removal of the plate, the growth medium was removed and the plates stored at -80˚C for at least 24 hours to facilitate the breakdown of the cell membrane. Cells were then stained with 200 uL/well of SYBR Green I (Invitrogen) diluted 1:4000 in a hypotonic lysis buffer (10 mM Tris HCl pH 8, 2.5 mM EDTA, 0.1% Triton X-100) for 72 hours in the dark at 4°C and the fluorescence quantified by fluorimetry at 535 nm emission with 485 nm excitation, using a Tecan Infinite 200 pro reader. The fluorescence reading is proportional to number of nuclei and provides an indication of the number of cells in each well at each time point (0, 24, 48, 72, 96 and 120 hours).

3.3 Results

3.3.1 Verification of wild type (WT) and mutant PTEN sequences

Prior to carrying out any of the PTEN functional and cellular analysis experiments, all the available expression clones were sequenced completely to verify that all clones contained the PTEN sequence and that the only change the PTEN mutant clones carried was that of the mutation of interest. Sequencing was conducted using primers within the vector sequence that bordered both ends of the PTEN insert sequence. Upon checking of the sequences obtained against the GenBank entry for PTEN, the wild type and each of the mutant PTEN construct sequences were verified as such (Figure 3.1) and it was confirmed that no additional sequence changes were apparent.

3.3.2 Optimal cell seeding density for cell proliferation analysis differs for the different cell lines

To determine the optimal cell seeding density for the analysis of cell proliferation, the cell proliferation rates of the U87MG, HCT116 and MCF7 cell lines were determined using varying seeding densities with cell proliferation measured at 24-hour intervals using the SYBR Green-based assay (section 3.2.3). Such an analysis generated series of growth curves for each cell line at the different cell seeding density used. As 6 replicates were analysed for each density for every time point, an accurate picture of the growth characteristics of each cell line was observed (Figure 3.2). It was evident from the generated growth curves that the optimal seeding density was slightly different for each of the cell lines due to their differing growth rates, shapes and cell volumes.

At low cell densities, all three cell types show a proportionate increase in fluorescence intensity with increasing cell number, however, at high cell densities the increase in

fluorescence intensity is no longer proportional to cell density and therefore becomes unreliable for further analyses. Considering the growth curves generated, the optimal seeding density for cell proliferation experiments is 1500 cells/well for U87MG cells and 2000 cells/well for both MCF7 and HTC116 cells in 96 well plates.

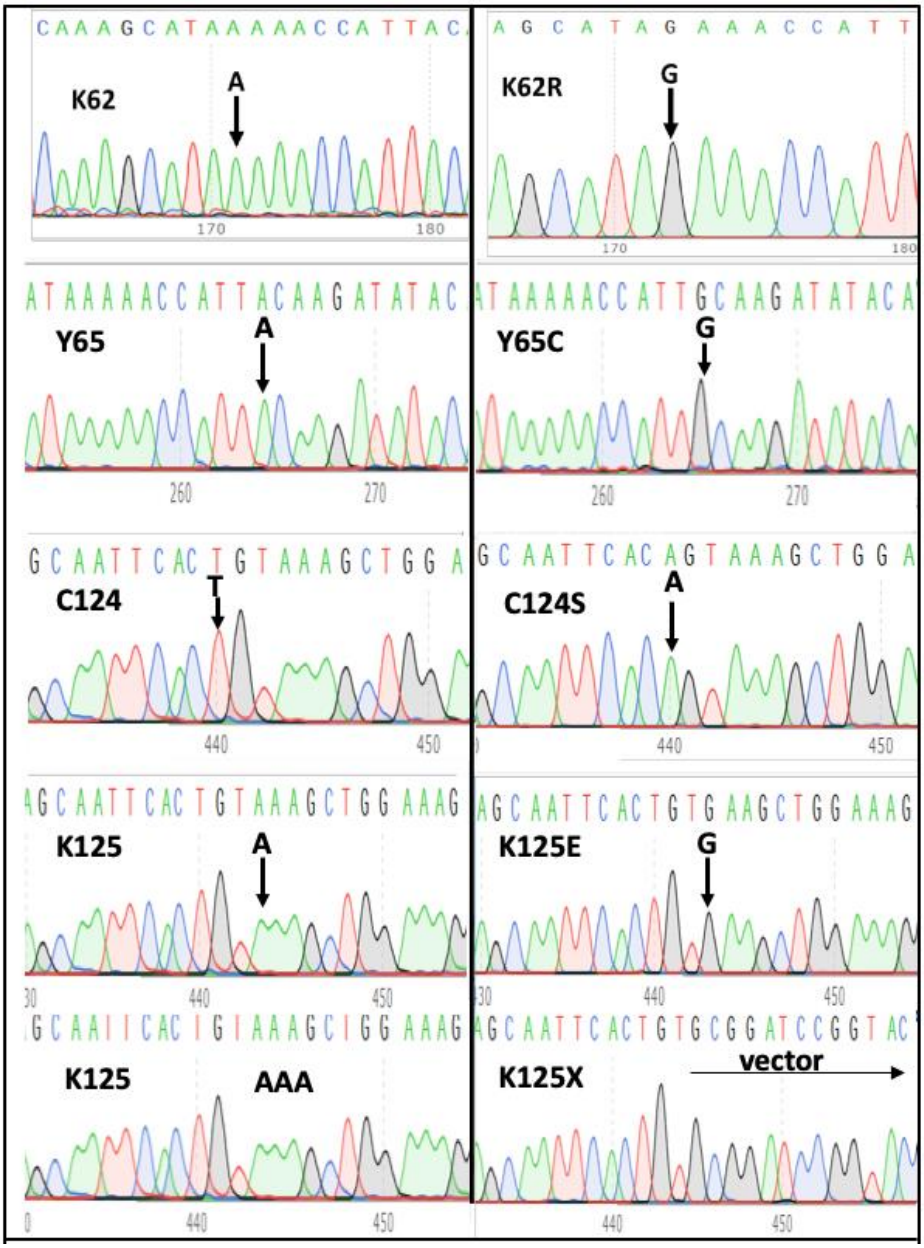

Figure 3.1 WT and mutant PTEN expression construct sequence verification. All PTEN expression clones were sequenced completely to ensure each construct carried the relevant cloned PTEN sequence (wild type and/or mutant). Sequences in the left side of each panel represent the wild type sequence and those on the right show the

corresponding mutant sequence present in the relevant PTEN expression construct. The K125X truncating mutant contains a shortened PTEN sequence ending at codon C124 and lacking the stop codon. Sequences after codon 124 correspond to the FLAG fusion epitope and vector sequences. These are indicated by the arrow with the vector notation above.

(Figure 3.1 continued on the following page)

(Figure 3.1 continued from previous page)

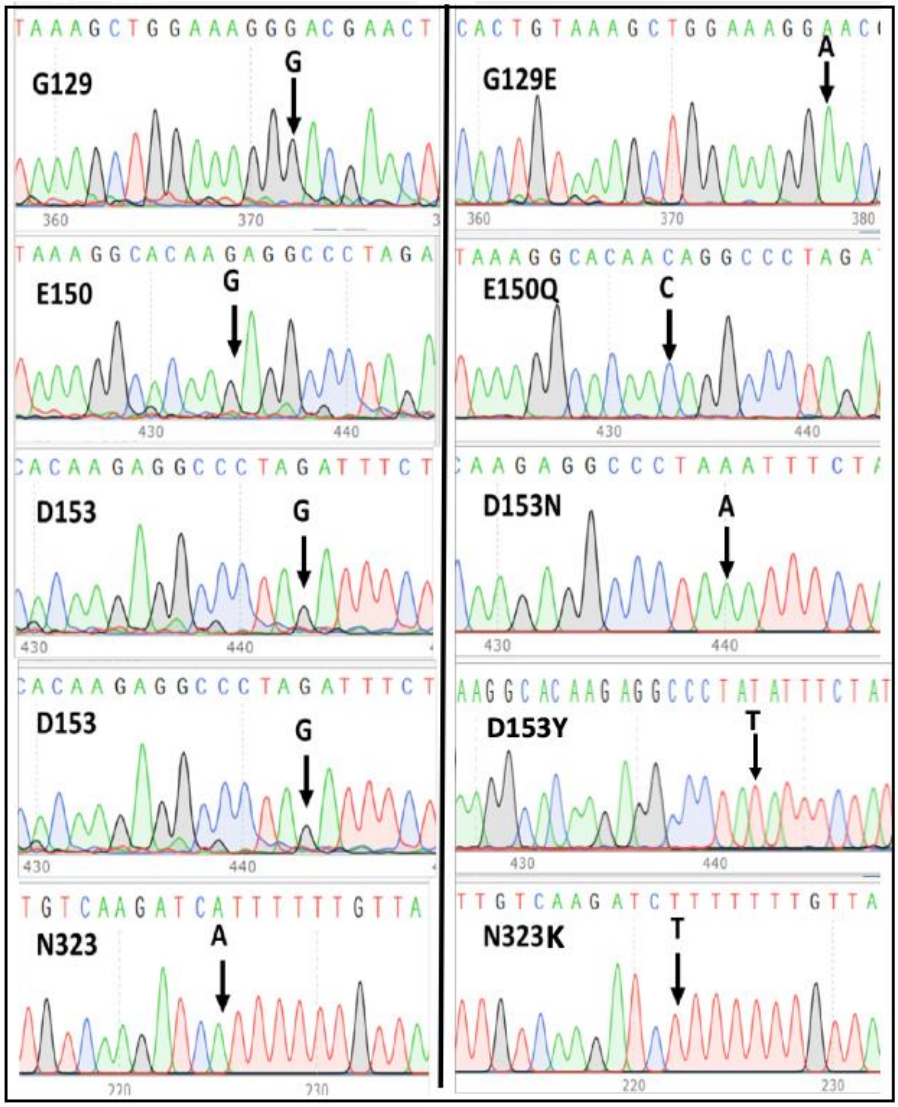

3.3.3 Optimal cell seeding density for cell proliferation analysis differs for the different cell lines

To determine the optimal cell seeding density for the analysis of cell proliferation, the cell proliferation rates of the U87MG, HCT116 and MCF7 cell lines were determined using varying seeding densities with cell proliferation measured at 24-hour intervals using the SYBR Green-based assay (section 3.2.3). Such an analysis generated series of growth curves for each cell line at the different cell seeding density used. As 6 replicates were analysed for each density for every time point, an accurate picture of the growth characteristics of each cell line was observed (Figure 3.2). It was evident from the generated growth curves that the optimal seeding density was slightly different for each of the cell lines due to their differing growth rates, shapes and cell volumes.

At low cell densities, all three cell types show a proportionate increase in fluorescence intensity with increasing cell number, however, at high cell densities the increase in fluorescence intensity is no longer proportional to cell density and therefore becomes unreliable for further analyses. Considering the growth curves generated, the optimal seeding density for cell proliferation experiments is 1500 cells/well for U87MG cells and 2000 cells/well for both MCF7 and HTC116 cells in 96 well plates.

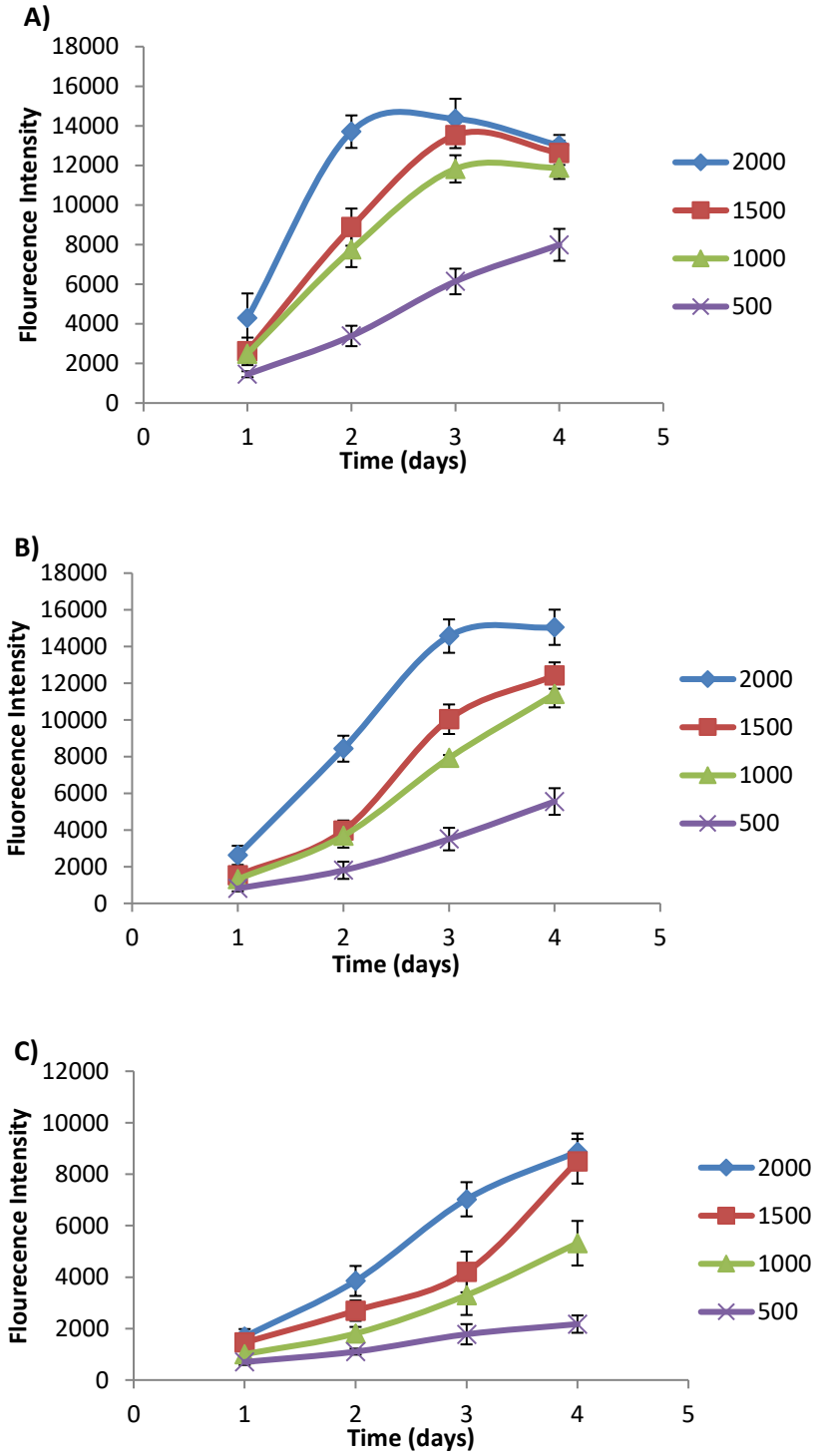

Figure 3.2 Determining optimal cell seeding densities for U87MG, HCT116 and MCF7 cells. Cells were seeded at varying densities (500, 1000, 1500 and 2000 cells per well) (6 replicates) in 96 well plates. Cells were grown at 37°C and 5% CO_2 and a replicate plate removed at 24-hour intervals for SYBR green treatment and fluorescence reading at 535 nm emission with 485 nm excitation. **(A)** U87MG growth curves, **(B)** HCT116 growth curves and **(C)** MCF7 growth curves. The error bars represent the standard deviation.

3.4 DNA and Lipofectamine concentrations were determined for optimal transfection efficiency

Transfection efficiency was optimised by varying, individually, (a) the amount of DNA and (b) Lipofectamine 2000 used for transfection. In this case, U87MG cells were seeded in 6 well plates at the optimal density of $2.5x10^5$ cells/well. The plasmid expression construct used for transfection was the Spectrin B-GFP plasmid in which spectrin is expressed with a C-terminal GFP tag. The GFP tag would allow the detection of transfected cells as GFP expression could be detected by the presence of green fluorescence. U87MG cells were initially transfected with varying amounts of plasmid DNA (1µg, 2 µg, 3 µg, 4 µg, 5 µg, 6 µg, 7 µg and 8 µg) and a fixed volume of lipofectamine (2 µL) per well. At 40 hours after transfection, the cells were analysed by flow cytometry, with gating on the green fluorescence. Cells were also visualised by fluorescence microscopy to view the green fluorescing transfected cells expressing spectrin-GFP (Figure 3.3A). The results of these transfection experiments showed that the highest transfection efficiency of 32% was obtained when cells were transfected with 2 µg plasmid DNA/well.

Once the optimal amount of DNA was determined, it was used to optimise the volume of Lipofectamine 2000 to be used. In these experiments, 2 µg plasmid DNA was combined with varying lipofectamine volumes (2-10 µL) for transfection in 6 well plates. Analysis of the cells by flow cytometry (40 hours after transfection) indicated that a lipofectamine volume of 8 µL/well provided the highest transfection efficiency of 33.8% successfully transfected cells in total of 30,000 events (Figure 3.3B). The optimal transfection parameters were now determined for subsequent transfection

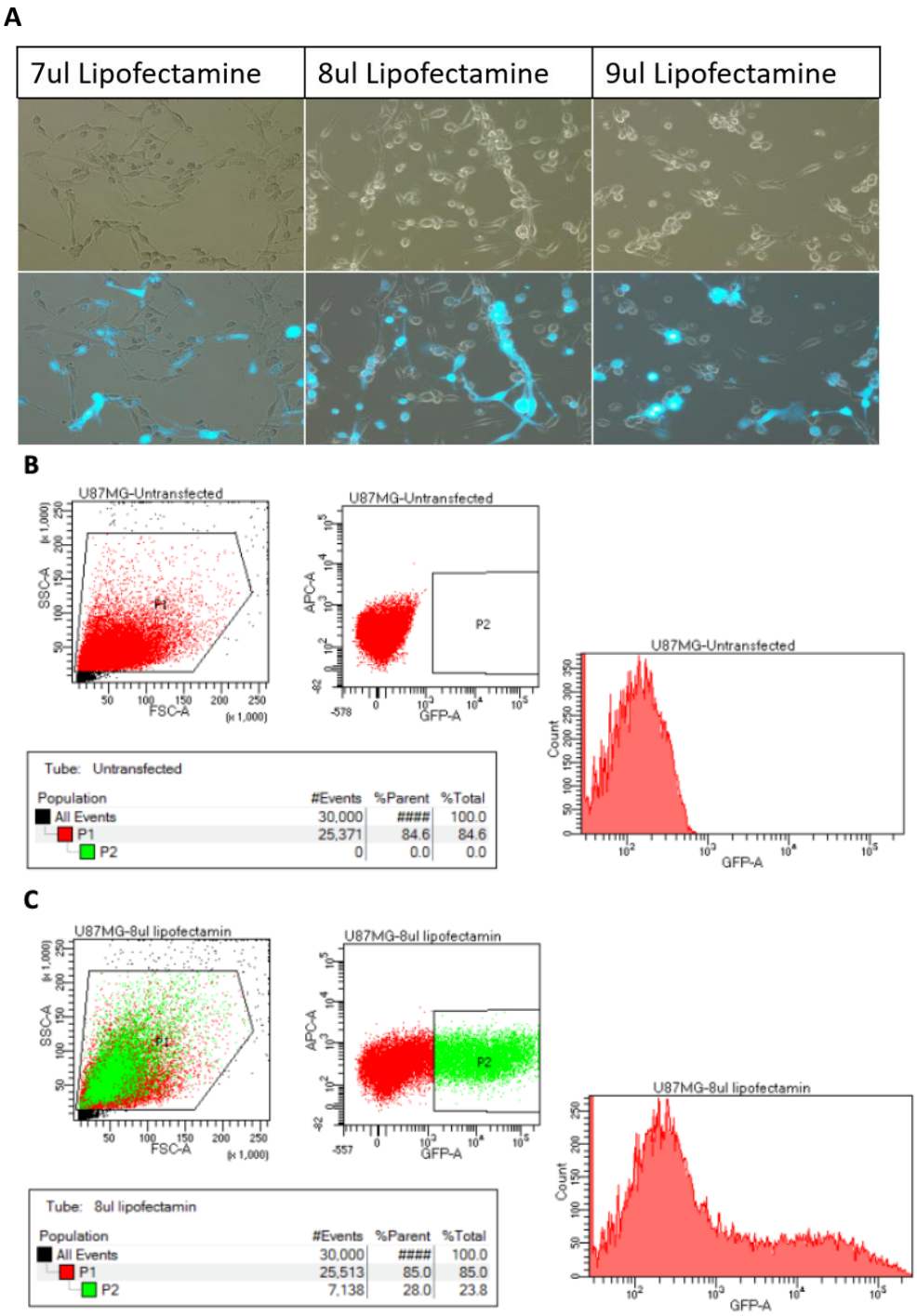

Figure 3.3 Determining parameters for optimal transfection efficiency. U87MG cells were transfected with 2 ug of spectrin-GFP plasmid DNA and varying lipofectamine volumes (2-10 uL) per 6 well plate. Cells were analysed 48 hours after transfection by **(A)** fluorescence microscopy and **(B and C)** flow cytometry. **(B)** Untransfected cells showing viable cells (dot-blot and histogram) with no green fluorescence in the control cells. **(C)** Transfected cells showing green fluorescence. The histogram shows the green fluorescence on the x-axis and the cell count on the Y axis (in total of 30,000 events).

While analysis of the effect of PTEN on cell cycle phase distribution would be carried out in 6-well plates, the cell proliferation assays were to be conducted in 96 well plates, to allow multiple replicates at each time point. Additionally, as the PTEN constructs did not possess a fluorescent tag for subsequent detection by flow cytometry, each PTEN construct would be co-transfected with the GFP-spectrin plasmid. To this end, the optimal transfection parameters determined for 6-well plates were scaled down accordingly for 96 well plates. U87MG cells were seeded at the optimal density of 1500 cells/well and transfection carried out accordingly with the wild type PTEN construct and the spectrin-GFP plasmid. Five replicates were included and the transfection experiments were repeated 3 times. After transfection (40 hours) cells were analysed by flow cytometry to determine transfection efficiency based on the numbers of green fluorescent cells. The flow cytometry data indicated a transfection efficiency of 75% of cells successfully transfected in 10,000 events (Figure 3.4). Thus, using the scaled down parameters of 0.066 µg plasmid DNA (PTEN and Spectrin GFP combined) with 0.3 uL lipofectamine, a transfection efficiency of 75% could be expected. These were the conditions that would be used for the transfections of the wild type and mutant PTEN constructs for subsequent functional analyses (described in chapter 4).

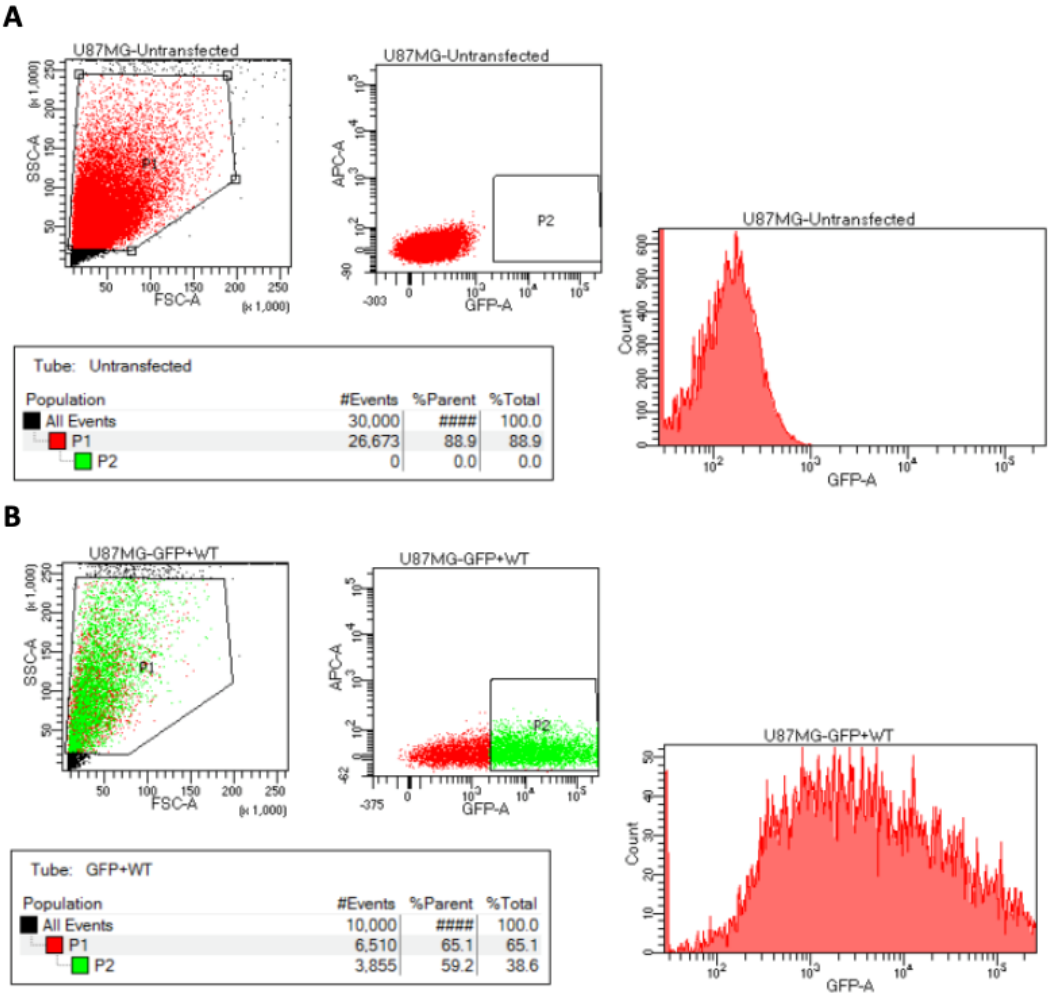

Figure 3.4 Optimising transfection efficiency for PTEN functional and cellular analysis. U87MG cells were seeded at 1500 cells/well in 96 well plates and immediately transiently co-transfected with the wild type PTEN and spectrin-GFP expression constructs. After transfection, (40 hours), cells were analysed by flow cytometry, gating on the viable population of cells (SSC vs FSC) and cells expressing the green fluorescence (APC vs GFP). In the above histograms, the X axis represents the green fluorescence and the Y axis represents the cell count. **(A)** Illustration of untransfected cells. **(B)** Wild type and GFP transfected cells.

3.4.1 Verification PTEN expression status of cancer cell lines

In order to determine and verify the PTEN expression status of each of the cancer cell lines to be used in this study (U87MG, HCT116 and MCF7), western blot was used using a PTEN antibody. The results of the western analysis showed the presence of PTEN protein, at varying levels in each of the three cell lines (Figure 3.5 B). Overall, the intensity of the PTEN bands were much lower than those of the β-actin bands, used as the loading control.

3.4.2 Verification of PTEN expression post transfection

In order to confirm exogenous overexpression of PTEN in each of the cancer cell lines after transfection, the wild type PTEN construct was transfected into each of the cancer cell lines. After transfection (40 hours), western analysis was carried out on extracted protein using a FLAG primary antibody to selectively detect exogenous PTEN expression (Figure 3.5 A). As can be seen from the results of the western analysis, all three cell lines expressed high levels of exogenous wild type PTEN. In this case, the intensity of the PTEN protein expression bands is approximately equivalent in intensity to the β-actin loading control.

To further verify that all PTEN expression constructs (wild type and mutant PTEN) were expressed equally well for the purpose of the functional analysis, the wild type, and each mutant PTEN construct were transfected into the PTEN null U87MG cell line. After transfection (40 hours), cells were harvested and protein extracted for western analysis using the FLAG antibody (Figure 3.6). The results showed that high level exogenous expression of wild and mutant PTEN was achieved in the U87MG cells.

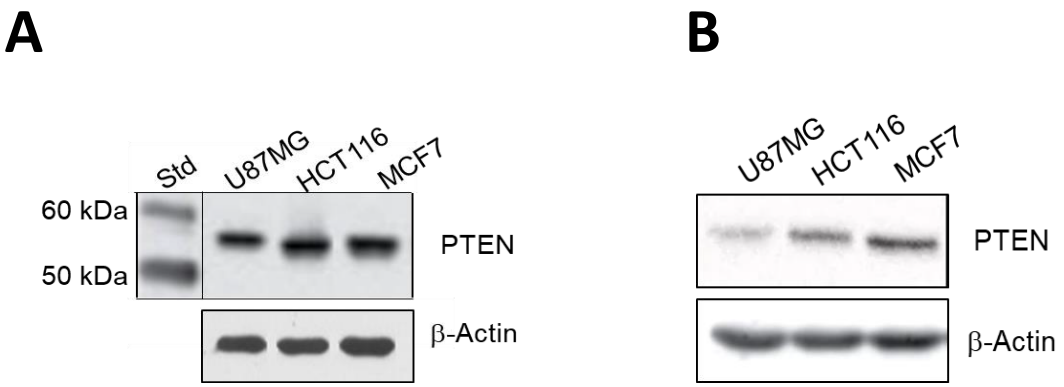

Figure 3.5 Detection of both endogenously, and exogenously, expressed PTEN by western analysis. **A.** Detection of exogenously-expressed wild type PTEN (40 hours post-transfection) in cancer cells using the FLAG Antibody. **B.** Detection of endogenously-expressed PTEN in cancer cells using a specific PTEN antibody. β-actin is included as a loading control on each gel. Key: Std, molecular weight marker.

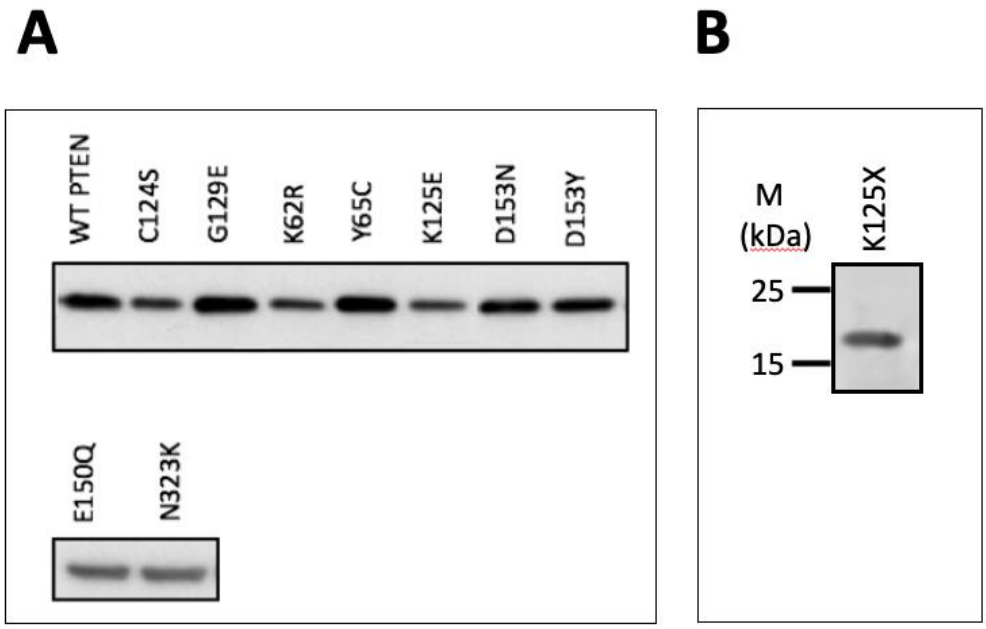

Figure 3.6 Detection of exogenously expressed wild type and mutant PTEN in U87MG cells by western analysis. Exogenously-expressed wild type and mutant PTEN was detected in U87MG cells, after transfection (40 hours), by western analysis using a primary FLAG antibody. **A.** WT PTEN and full length PTEN mutants harbouring point mutations and single amino acid changes. **B.** Truncating PTEN mutant K125X expresses a FLAG-tagged truncated form of PTEN containing amino acids 1-124, with a lower molecular weight. Key: M, molecular weight marker.

3.4.3 Summary

With optimised transfection protocols confirmed and clone sequence verification completed, along with confirmation of the expression of wild type PTEN in each cancer cell line after transfection, functional and cellular analysis to determine the effect of PTEN mutation on PTEN function cold be commenced.

To confirm that all PTEN expression constructs (wild type and mutant PTEN) were expressed equally well for the purpose of the functional analysis, the wild type, and each mutant PTEN construct were transfected into the PTEN null U87MG cell line. After transfection (40 hours), cells were harvested and protein extracted for western analysis using the FLAG antibody (Figure 3.6). The results showed that high level exogenous expression of wild and mutant PTEN in the U87MG cells.

CHAPTER 4

RESULTS

DETERMINING THE EFFECT OF *PTEN* MUTATIONS ON PTEN CELLULAR FUNCTION

4.1 Introduction

This chapter is divided into 3 sections, in which will be presented the results of the cellular analysis to determine the effect of the different cancer-associated mutations on PTEN function. The first section of this chapter (section 4.2) will present the results, and discussion of the experiments testing the effect of wild type and mutant PTEN on the cell proliferation of cancer cells. The second section of the chapter (section 4.3) will present the results and some discussion of the work assessing the effect of wild type and mutant PTEN on the cell cycle phase distribution of cancer cells. The final section of this chapter (section 4.4) will present the results and some discussion of the work investigating the effect of wild type and mutant PTEN on Akt phosphorylation (and activation) in cancer cells. In all cases, each of the functional assays were carried out in the three cancer cell lines, U87MG glioblastoma cells, HCT116 colon cancer cells and MCF7 breast cancer cells. Wild type PTEN and each of the cancer-associated mutations of PTEN (K62R, Y65C, K125E, K125X, E150Q, D153N, D153Y and N323K) were tested in each of the functional assays in all three cell lines. All experiments utilised a set of controls which included: (a) Untransfected cells, (b) vector transfected cells, (c) mock transfected cells (i.e. H_2O replaced DNA in the transfection), (d) known PTEN phosphatase deficient mutants C124S and (e) G129E.

Cellular and functional analyses were all conducted after transfection of each of the wild type and mutant PTEN constructs in each of the cell lines to be studied, using the pre-optimised transfection parameters (see chapter 3).

4.2 Specific materials and methods

4.2.1 Analysis of cancer cell proliferation using a SYBR Green based assay

The analysis of cell proliferation was carried out using a SYBR green-based assay, which relies on the labelling of DNA with SYBR® green I and subsequent measurement of cellular DNA content by fluorimetry. Cells (either U87MG, HCT116 or MCF7) were seeded in 96-well plates in sets of 5 replicates at the optimal seeding density of $2.5x10^3$ cells/well for each cell line. Cells were grown overnight to establish adherence and transfection of cells was completed on the following day. Transient transfection of cells with wild type (WT) and mutant PTEN expression constructs (K62R, Y65C, K125E, K125X, E150Q, D153N, D153Y, N323K, C124S control and G129E control) was carried out (section 3.2.2.2). After transfection, a replicate 96-well plate was removed from the incubator at 24-hour intervals for subsequent analysis by fluorimetry to determine cell proliferation level. Upon removal of the samples at each time point, the culture medium was aspirated and the sample plate placed at -80°C for at least 24 hours. After 24 hours, 200 uL of SYBR green staining solution (SYBR green 1 diluted 1:4000 in a hypotonic lysis buffer containing 10 mM Tris HCl pH 8, 2.5 mM EDTA and 0.1% Triton X-100) was placed in each well and plates placed at 4°C for 72 hours, in the dark. Quantification of cell florescence of samples was carried out by fluorimetry at 535 nm emission with 485 nm excitation, on a Tecan plate reader. Readings were taken from all samples at every time point of analysis. Each experiment was repeated on three separate occasions and five replicates for each sample were included in each experiment. All experiments contained the same set of controls (un-transfected cells, mock transfected cells and vector transfected cells) to ensure consistency of analysis across all cell lines studied.

4.2.2 Data analysis for cell proliferation experiments

The means ± standard deviations for all samples (wild type and mutant PTEN), in each experimental set (U87MG, HCT116 and MCF7), were calculated and graphed using Microsoft Excel. The rates of cell proliferation of each cell line, transfected with mutant PTEN, was compared with the proliferation data of the same cells transfected with the wild type PTEN and p-values were determined. Statistical analyses were carried out using Microsoft Excel and IBM SPSS (version 25) statistical software. Paired-sample t-tests were used to determine whether the mean difference between paired observations were statistically significant. Independent t-tests were used to analyse the difference between the means of two independent groups (e.g. WT PTEN vs mutant PTEN) to determine whether the differences observed were statistically significant between the sets of groups analysed. A p-value of less than 0.05 was considered statistically significant.

4.2.3 Analysis of cell cycle phase distribution of cancer cells

Cell cycle phase distribution of the transfected cancer cells was determined by flow cytometry 40 hours after transfection. All three cell lines (U87MG, HCT116 and MCF7) were transfected with wild type or mutant PTEN constructs (K62R, Y65C, K125E, K125X, E150Q, D153N, D153Y, N323K, C124S control and G129E control). Cells were seeded at a density of $2.5x10^3$ cells/well in 6-well plates and grown overnight (37^oC and 5% CO_2) to establish adherence and transfection of cells was carried out on the following day. Cells were co-transfected with a PTEN expression construct (wild type, mutant or control) and the spectrin B-GFP plasmid using a total DNA amount of 4 ug/transfection (2 ug PTEN construct and 2 ug spectrin B-GFP construct) with 8 uL Lipofectamine

2000/transfection (section 3.2.2.2). After transfection (40 hours), the culture medium was aspirated and cells were harvested by trypsinisation (100 uL TrypLE Express per well) and collected by centrifugation (600 g for 6 min at room temperature). After removal of the medium, cells were washed twice with warm PBS and re-centrifuged with the same centrifugation settings. The cell pellet was then resuspended in PBS and the cells fixed by the addition of 0.5 mL cold 95% (v/v) ethanol. Fixed cells were then washed twice in cold PBS with centrifugation (700 g for 3 min at room temperature) between washes. Cells were then resuspended in 0.5 mL PBS and incubated with RNase A (10 ug/mL) for 5 min at room temperature. Propidium iodide (PI) was added to the cells (20 ug/mL), which were then analysed by flow cytometry on a FACS Calibur flow cytometer (Becton Dickinson). Linear emission of PI was collected in the FL-3 channel (for 25,000 GFP positive cells) gated in the FL-1 (green) channel. The FL-2 channel was used for doublet discrimination. A total of 25,000 events were typically analysed using the Cell-Quest software (Becton Dickinson). The percentage of cells in the different cell cycle phases were determined using ModFit-LT software. All samples were analysed in duplicates in each experiment, and all experiments were repeated three times, on separate occasions, for verification of results. The number of cells in each cell cycle phase (as a percentage) was determined using the following formula:

$$\textit{Cell cycle phase distribution(\%)} = \frac{No.\ of\ cells\ in\ either\ G1,G2\ or\ S\ phase}{Total\ number\ of\ cells\ counted} \times 100$$

4.2.4 Detection of total AKT and phosphorylated AKT

Detection of total Akt and phosphorylated Akt (pAkt) in cancer cells by western analysis

All three cancer cells transiently transfected with either wild type or mutant PTEN constructs in 6-well plates (section 3.2.2.2) and, 40 hours after transfection, cells were harvested, washed and protein extracted for western analysis (2.2.10.2). After protein extraction from lysed cells, equal amounts of protein were loaded onto SDS-PAGE gels and transferred to PVDF membranes. Western analysis was carried out essentially as described in section 2.2.10. Hybridising bands were detected on the membranes using chemiluminescence (ECL) (Amersham ECL prime western blotting detection reagent from GE Healthcare), according to the manufacturer's instruction. ECL reagent (A) was mixed with reagent (B) in a 1:1 ratio with sufficient volume to cover the membrane (0.125 mL/cm^2). After 3-5 min incubation, the membrane was visualised and images captured using the Amersham Imager 600 from GE Healthcare. The exposure time was optimised for image capture. The molecular weight of the hybridised proteins (PTEN, AKT, p-AKT, and β-actin) was determined by the use of a protein molecular marker (SeeBlue Plus2 Pre-stained Protein Standard from ThermoFisher Scientific). For determining AKT phosphorylation status, membranes were initially incubated with the p-AKT (phospho-specific akt Ser473 antibody, Cell Signalling Technologies), followed by membrane stripping and re-hybridisation with the AKT (total AKT protein, Cell Signalling Technologies) antibody. Membranes were stripped by washing in stripping buffer (62.5 mM Tris HCL, 14.3 M β-mercaptoethanol, 20% SDS, pH 6.8) at 50˚C for 30 minutes, with agitation. The membranes were then washed in PBST buffer three times (10 min each at room temperature) following by overnight incubation in blocking

buffer, according to section 2.2.10. The membrane was then used for detection of total AKT. Images were then taken with identical exposure times (as described above).

4.2.5 Determining p-AKT level using densitometry

Images of the western blots, taken at the optimal, and identical exposure settings, were used for densitometry on the Amersham Imager 600 software. After subtraction of background, the band density was determined by the software. The protein density was normalised individually against β-actin bands to account for any gel loading differences. The p-AKT level changes were calculated using the normalised densities of the bands and the p-AKT/AKT ratio.

4.3 RESULTS 1: DETERMINING THE EFFECT OF WILD TYPE AND MUTANT PTEN ON THE PROLIFERATION OF CANCER CELLS

4.3.1 Background

PTEN is an evolutionarily conserved phosphatase, with the ability to influence multiple essential cellular processes. One of the key roles of PTEN in cells is the regulation of cell proliferation, thought to be modulated through its lipid phosphatase activity [6, 8]. The role of wild type PTEN in the regulation of cell proliferation, through its negative regulation of the PI3K/Akt pathway is well documented [2, 28, 29, 37, 57]. Through negative regulation of the PI3K pathway, PTEN reduces the pro-proliferative effects of this pathway to restore the balance of cell growth, proliferation and death (Figure 4.1) [27]. It is the loss of PTEN that promotes tumorigenesis in many cell types [58].

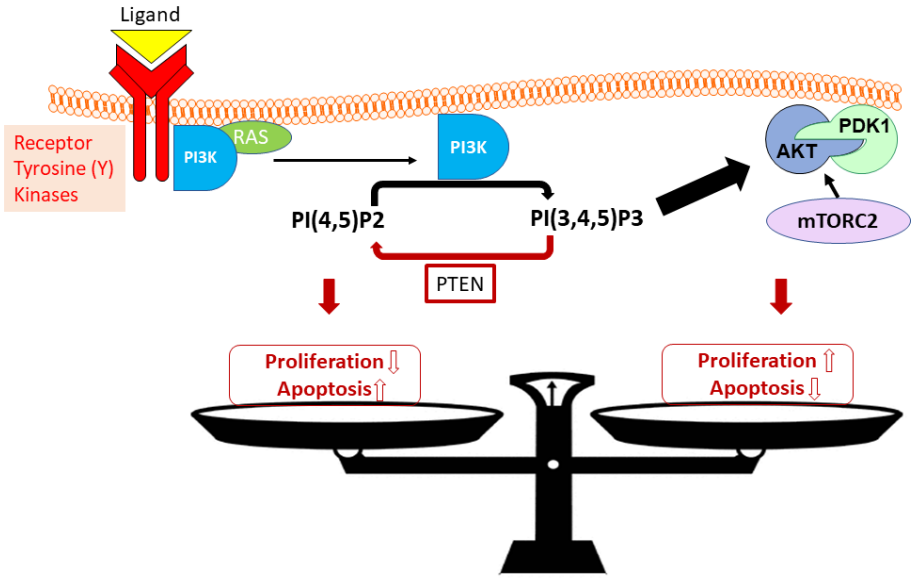

Figure 4.1 PTEN is a negative regulator of cell proliferation. Binding of a ligand/growth factor, to its receptor on the cell membrane leads to activation of PI3K, which phosphorylates PIP2 to PIP3, resulting in recruitment of PDK1 to the plasma membrane and phosphorylation of AKT and activation of downstream pathways resulting in overall increased cell proliferation and decreased apoptosis. On the contrary, the presence of functional PTEN antagonises PI3K, by dephosphorylation of PIP3 to PIP2, and hence maintains the balance between cell proliferation and cell death.

4.3.2 Mutant PTEN decreases U87MG glioblastoma cell proliferation with reduced efficacy compared to wild type PTEN

U87MG cells were transiently transfected with the wild type, and each of the mutant PTEN constructs, followed by measurements of cell proliferation, before and after transfection, using the SYBR green based assay. Initial experiments utilising the control plasmids, showed that the cell proliferation rate of the untransfected U87MG cells, mock transfected and vector only transfected cells were almost identical with no significant difference in growth rates (P-value>0.05). As all three control cell transfections gave similar results, the mock transfected cells were selected as the untransfected cell reference point, to which the results of the WT PTEN were compared. The cell proliferation rates of each of the PTEN mutants were subsequently compared to that of both the mock-transfected and the wild type transfected cells. Comparison with the mock-transfected cells provided an indicator to determine whether a particular mutant PTEN altered cell proliferation, and comparison with the wild type PTEN allowed a determination of how well each PTEN mutant performed its function. All data presented are derived from three independent experiments in which 5 replicates were included within each experiment. Overall, transient transfection of WT or mutant PTEN led to a 60%-85% reduction in the cell proliferation rate of U87MG cells in comparison to mock transfected cells. The level of reduction in cell proliferation varied and was dependent upon the particular PTEN mutant being studied (Figure 4.2).

The WT-PTEN transfected cells showed a decreased cell proliferation rate that was only approximately 15% of the rate of the mock transfected, or untransfected, cells. Thus, WT PTEN decreased the cell proliferation rate of U87MG cells by up to 85% (Figure

4.2C). U87MG cells expressing the control, phosphatase deficient mutants, C124S and G129E, showed higher proliferation rates, decreasing cell proliferation by approximately 65% and 60%, respectively. Thus, the control phosphatase deficient mutants reduced the cell proliferation rate of U87MG cells to 35% and 40%, respectively, of the mock-transfected cell rate. In comparison to wild type PTEN, these phosphatase deficient mutants do not slow cell proliferation as well as wild type PTEN with only half the rate of cell proliferation of wild type ($p<0.05$).

Expression of the E150Q and D153Y mutants of PTEN showed U87MG proliferation rates (37% and 30% the rate of the mock-transfected cells) that were comparable to that observed with the control phosphatase deficient mutants, indicating that these mutations altered the ability of PTEN to slow cell proliferation to wild type levels (37% for E150Q and 30% for D153Y vs 15% for WT PTEN, $p<0.05$) in U87MG. This corresponds to an 85% slowing of cell proliferation by WT PTEN compared to 63% and 65% slowing by the E150Q and D153Y mutants of PTEN, respectively.

Interestingly, the K62R (20% cell proliferation rate of mock-transfected cells), Y65C (23%), K125E (25%), K125X (22%) and D153N (22%) mutants of PTEN produced decreased U87MG cell proliferation that was not as low as that of the WT PTEN level of 15%. When compared to the WT PTEN the cell proliferation reductions produced by Y65C and K125E were significantly different to that produced by WT PTEN (23% for Y65C and 25% for K125E vs 15% for WT PTEN, $p<0.05$), indicating that these mutations potentially altered PTEN function in U87MG cells. When compared to WT PTEN, the levels of reduction in cell proliferation produced by the K125X and D153N mutants did not reach statistical significance.

Finally, the N323K mutant of PTEN appears to produce reduced U87MG cell proliferation comparable to WT PTEN indicating little alteration in PTEN function produced by the mutation in this cell line.

A

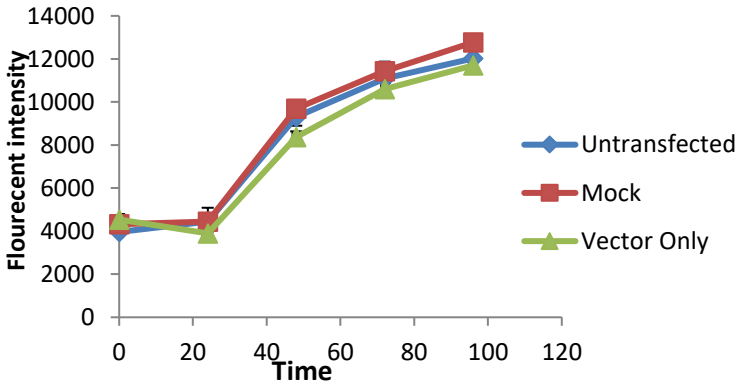

B

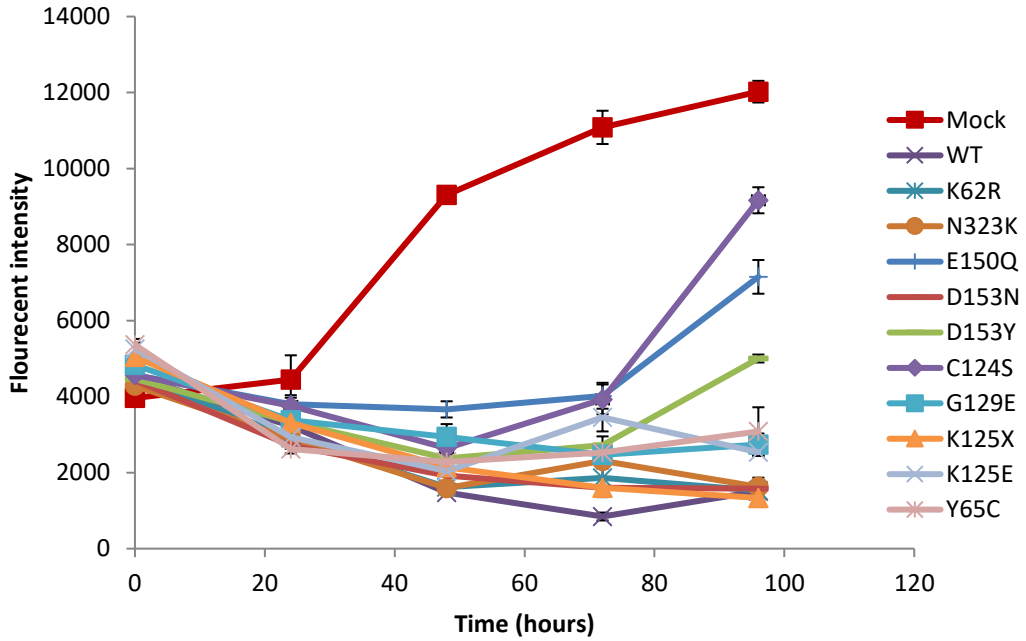

Figure 4.2 is continued on the following page.

C

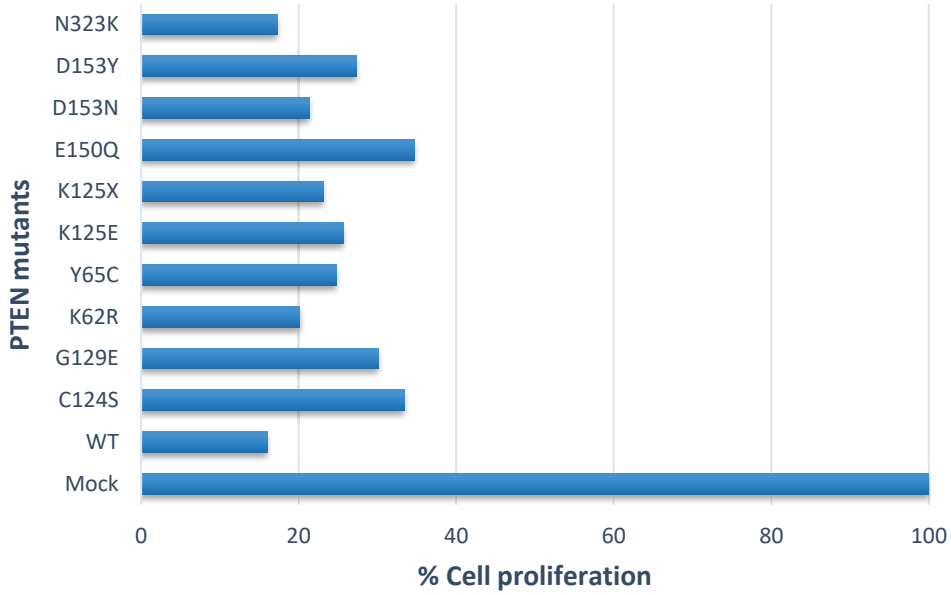

Figure 4.2 Analysis of cell proliferation rate of U87MG glioblastoma cells transfected with wild type and mutant PTEN. **A.** Growth curves of untransfected, mock transfected and vector-transfected U87MG cells. **B.** Growth curves of U87MG cells transfected with wild type and mutant PTEN. Three independent experiments were conducted with 5 replicates within each experiment. Each time point on the growth curves is an average of five replicates (at 0, 24, 48, 72 and 96 hours after transfection). The error bars represent the standard deviations. **C.** Relative cell proliferation rates of WT and mutant PTEN transfected U87MG cells, expressed as a percentage of the proliferation rate of the mock transfected cells which were assigned a proliferation of 100% (at the 72-hour time point).

4.3.3 The effect of wild type and mutant PTEN on the proliferation of HCT116 colon cancer cells

HCT116 colon cancer cells were transiently transfected with the wild type, and each of the mutant PTEN constructs, followed by measurements of cell proliferation using the SYBR green based assay. As previously indicated, all data presented are derived from three independent experiments in which 5 replicates were included within each experiment. As observed with the U87MG experiments, transfection of HCT116 cells with the control plasmids, showed that the cell proliferation rates of the untransfected, mock transfected and vector only transfected cells were almost identical with no significant difference in cell proliferation rates ($p>0.05$). Again, the mock transfected cells were selected as the untransfected cell reference point, to which the cell proliferation rates of the wild type, and each of the PTEN mutant-transfected cells were subsequently compared.

Overall, transient transfection of WT or mutant PTEN led to an approximate 20%-60% reduction range in the cell proliferation rate of U87MG cells in comparison to the mock transfected cells. The level of reduction of cell proliferation was variable and dependent upon the particular PTEN mutant being studied (Figure 4.3).

The WT-PTEN transfected cells showed a decreased cell proliferation rate that was approximately 45% of the rate of the mock transfected, or untransfected, cells. Thus, WT PTEN decreased the cell proliferation rate of HCT116 cells by approximately 53% (Figure 4.3C). HCT116 cells expressing the control, phosphatase deficient mutants, C124S and G129E, showed slightly higher proliferation rates, decreasing cell proliferation by approximately 50% and 45% of mock transfected cells, respectively.

Thus, the control phosphatase deficient mutants reduced the cell proliferation rate of HCT116 cells to 50% and 55%, respectively, of the mock-transfected cell rate. In comparison to wild type PTEN, these phosphatase deficient mutants do not slow cell proliferation as well as wild type PTEN, but the effect is small with differences of 5-10% greater than the mock transfected cells (50% for C124S and 55% for G129E vs 45% for WT, $P<0.05$).

Expression of the K62R, Y65C, K125E, K125X, E150Q and N323K mutants of PTEN produced cell proliferation rates that were significantly higher than the wild type proliferation rate ($p<0.05$) and ranged between 60-80% of the rate of the mock-transfected cells. Interestingly, this set of PTEN mutants produced cell proliferation rates that were higher than those of the control phosphatase deficient mutants of PTEN ($p<0.05$). The higher cell proliferation rates observed are indicating of altered PTEN function with decreased ability to slow cell proliferation to wild type levels in HCT116 cells.

Finally, the D153N and D153Y PTEN mutants appear to produce a reduction in HCT116 cell proliferation comparable to that of WT PTEN indicating little alteration in PTEN function produced by these mutations in this cell line (48% for D153N and 43% for D153Y vs 45% for WT, $p>0.05$).

A

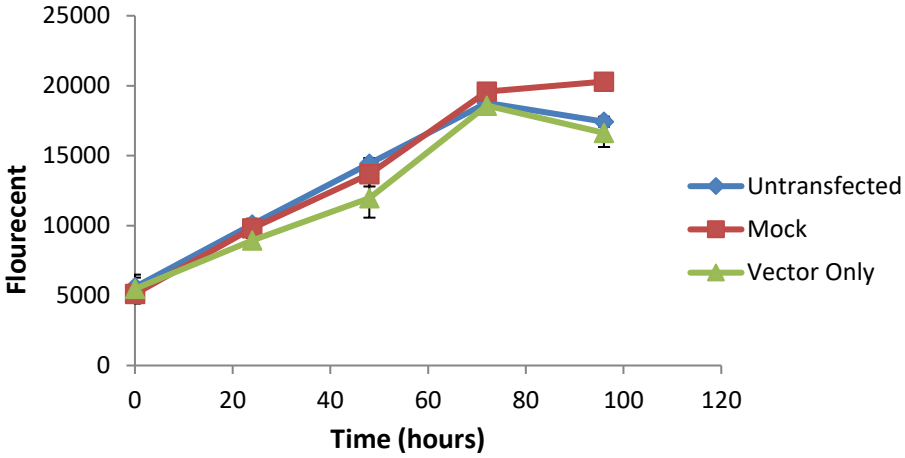

B

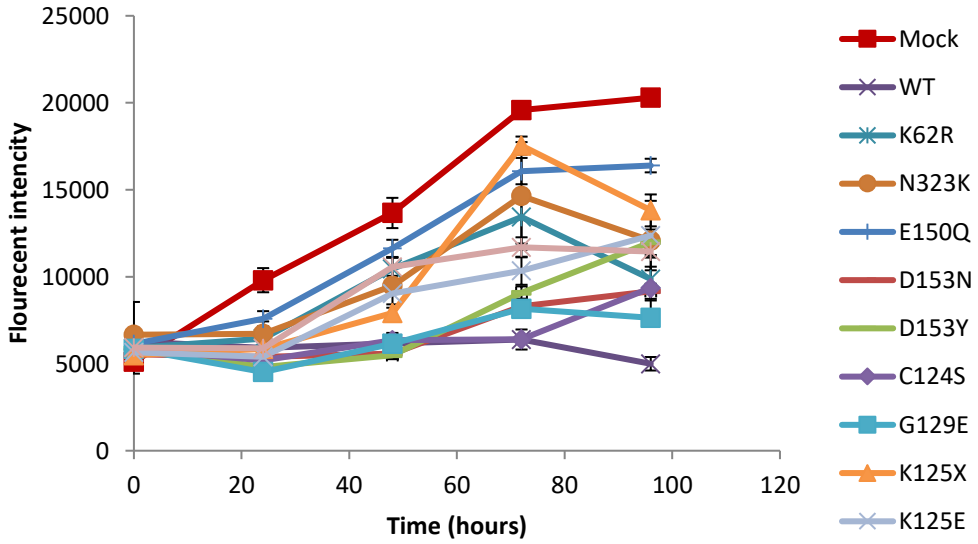

Figure 4.3 is continued on the following page

C

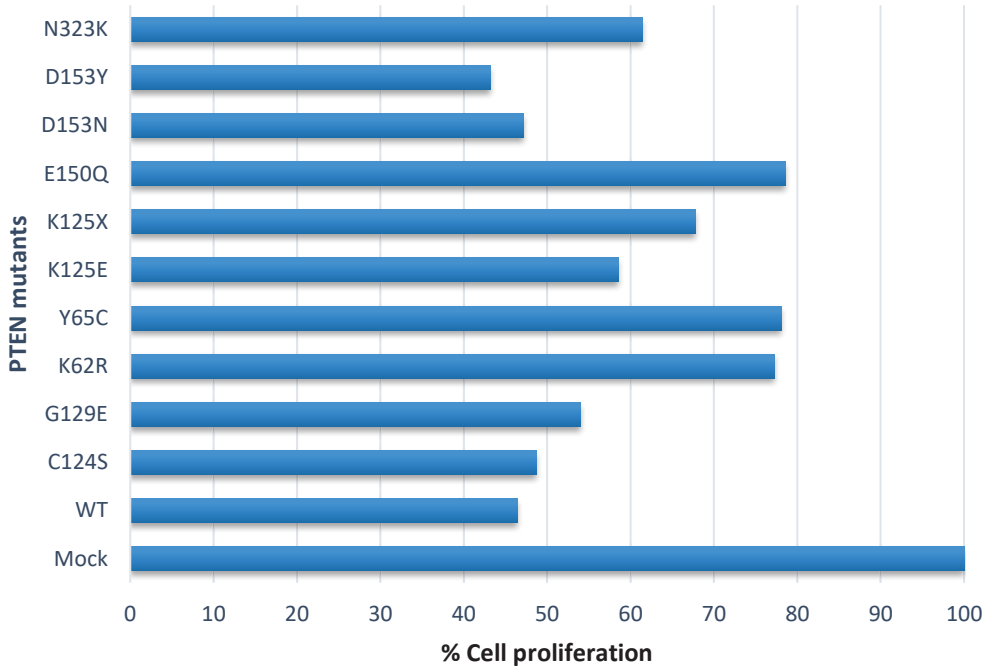

Figure 4.3 Analysis of cell proliferation rate of HCT116 colon cancer cells transfected with wild type and mutant PTEN. **A.** Growth curves of untransfected, mock transfected and vector-transfected HCT116 cells. **B.** Growth curves of HCT116 cells transfected with wild type and mutant PTEN. Three independent experiments were conducted with 5 replicates within each experiment. Each time point on the growth curves is an average of five replicates (at 0, 24, 48, 72 and 96 hours after transfection). The error bars represent the standard deviations. **C.** Relative cell proliferation rates of WT and mutant PTEN transfected HCT116 cells, expressed as a percentage of the proliferation rate of the mock transfected cells which were assigned a proliferation of 100% (at the 72-hour time point).

4.3.4 The effect of wild type and mutant PTEN on the proliferation of MCF7 breast cancer cells

MCF7 breast cancer cells were transiently transfected with the wild type, and each of the mutant PTEN constructs, followed by measurements of cell proliferation using the SYBR green based assay. As with the other 2 cell lines, all data presented are derived from three independent experiments in which 5 replicates were included within each experiment. As observed with both the U87MG and HCT116 cells, transfection of MCF7 cells with the control plasmids, showed that the cell proliferation rates of the untransfected, mock transfected and vector only transfected cells were almost identical with no significant difference in cell proliferation rates (Figure 4.4A) ($p>0.05$). Again, the mock transfected cells were selected as the untransfected cell reference point, to which the cell proliferation rates of the wild type, and each of the PTEN mutant-transfected cells were compared.

Overall, transient transfection of WT or mutant PTEN led to a reduction in the cell proliferation rate of MCF7 cells in the range of 45-80% of the rate of the mock transfected, or untransfected, cells. The level of reduction of cell proliferation was again variable and dependent upon the particular PTEN mutation (Figure 4.4).

The WT-PTEN transfected cells showed a decreased cell proliferation rate that was approximately 45% of the rate of the mock transfected, or untransfected, cells. Thus WT PTEN decreased the cell proliferation rate of MCF7 cells by approximately 55% (Figure 4.4C). MCF7 cells expressing the control, phosphatase deficient mutants, C124S and G129E, showed higher cell proliferation rates, decreasing cell proliferation by approximately 25% and 50% of mock transfected cells, respectively. Thus the control

phosphatase deficient mutants reduced cell the proliferation rate of MCF7 cells to 75% and 50%, respectively, of the mock-transfected cell proliferation rate. In comparison to wild type PTEN, these phosphatase deficient mutants do not slow cell proliferation as well as wild type PTEN, with the effect being greater with the C24S mutant (75% for C124S and 50% for G129E vs 45% for WT, $p<0.05$ in both cases).

Expression of the K62R, Y65C, K125E, K125X, D153Y and N323K mutants of PTEN produced cell proliferation rates that were significantly higher than the wild type cell proliferation rate and ranged between 60-80% of the rate of the mock-transfected cells ($p<0.05$ for all vs 45% for WT PTEN). Interestingly, this set of PTEN mutants produced cell proliferation rates that were higher than those of the G129E control phosphatase deficient mutant of PTEN ($p<0.05$ for all vs 50% for G129E). The higher cell proliferation rates observed are indicative of altered PTEN function with decreased ability to slow cell proliferation to wild type levels in MCF7 cells.

Finally, the E150Q and D153N PTEN mutants appear to produce a reduction in MCF7 cell proliferation that is close to that of WT PTEN indicating only minor alteration in PTEN function produced by these mutations in this cell line (50% for E150Q and 50% for D153N vs 45% for WT, $p<0.05$) (Table 4.1).

A

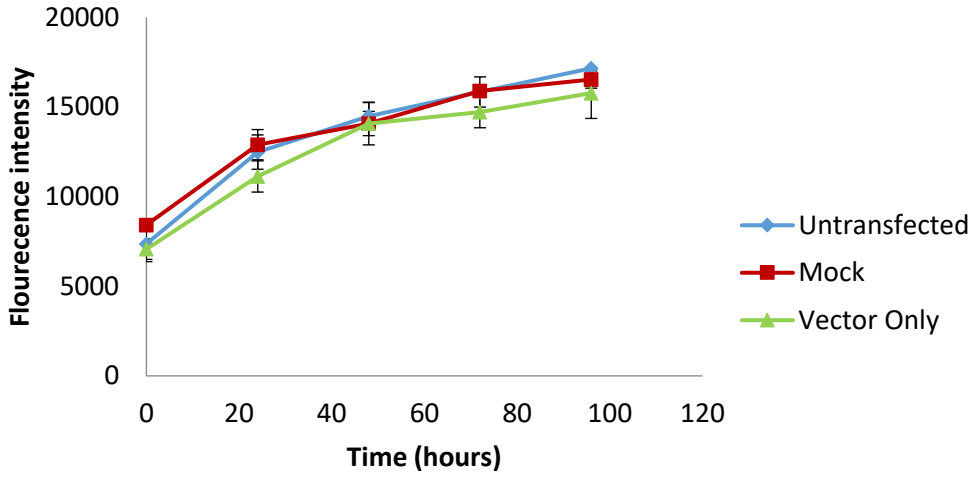

B

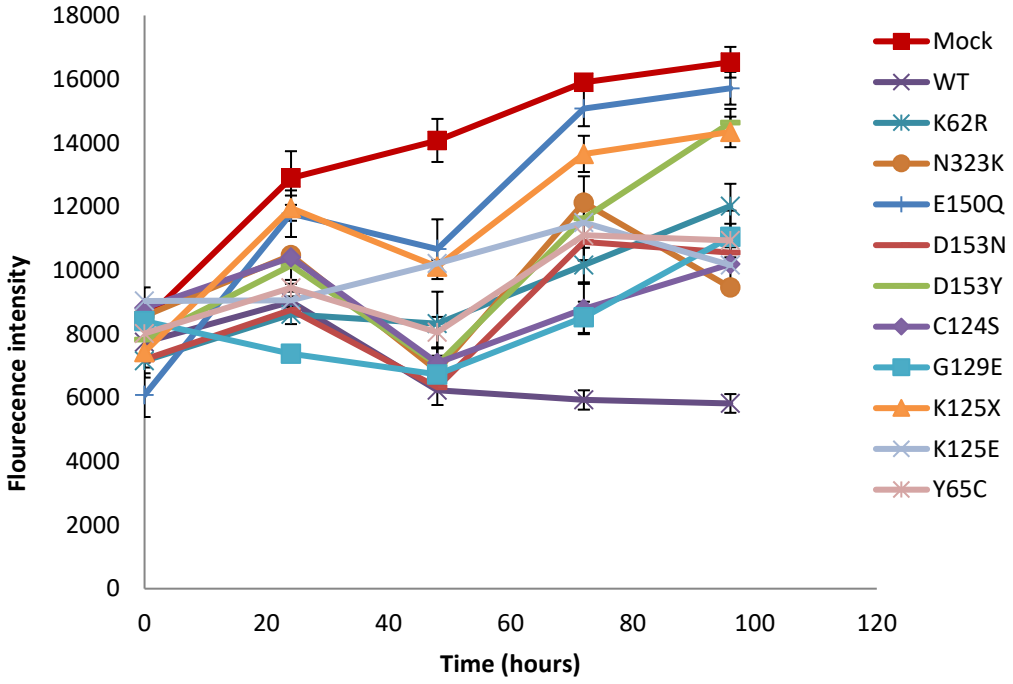

Figure 4.4 is continued on the following page.

C

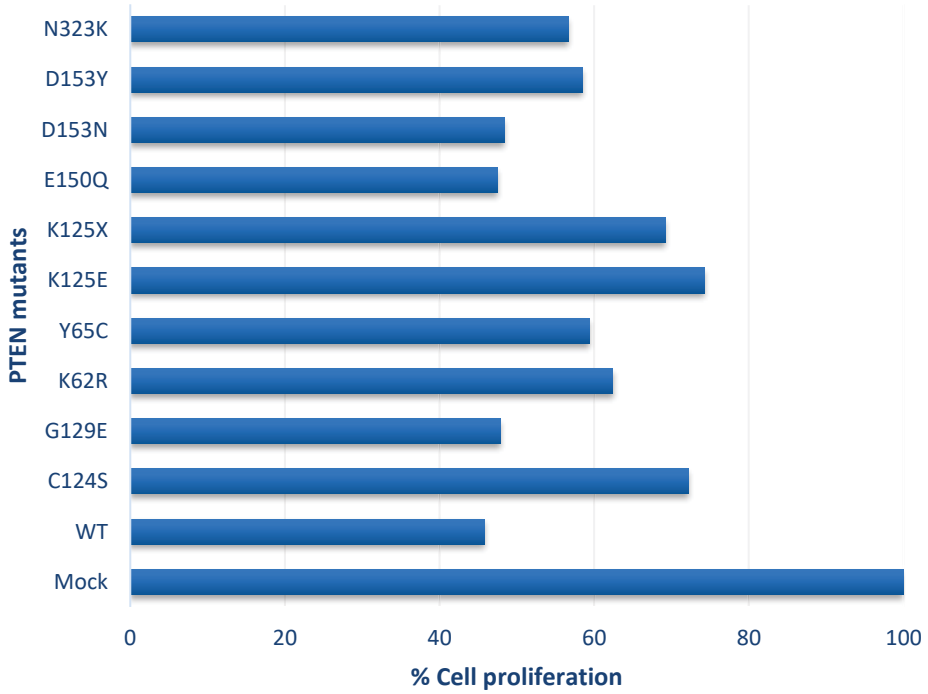

Figure 4.4 Analysis of cell proliferation rate of MCF7 breast cancer cells transfected with wild type and mutant PTEN. **A.** Growth curves of untransfected, mock transfected and vector-transfected MCF7 cells. **B.** Growth curves of U87MG cells transfected with wild type and mutant PTEN. Three independent experiments were conducted with 5 replicates within each experiment. Each time point on the growth curves is an average of five replicates (at 0, 24, 48, 72 and 96 hours after transfection). The error bars represent the standard deviations. **C.** Relative cell proliferation rates of WT and mutant PTEN transfected MCF7 cells, expressed as a percentage of the proliferation rate of the mock transfected cells which were assigned a proliferation of 100% (at the 72-hour time point).

Table 4.1 Comparison of the effect of wild type or mutant PTEN on the cell proliferation of U87MG, HCT116 and MCF7 cells. The results of the cell proliferation experiments are summarised, showing the effect of each PTEN mutant on cell proliferation in comparison to the effect of wild type PTEN. Results shown in the bold red text indicate those PTEN mutants showing greatest changes from the wild type PTEN.

Mutant	U87MG	HCT116	MCF7
WT vs **K62R**	No ↑	**Yes ↑**	**Yes ↑**
WT vs **Y65C**	Yes ↑	**Yes ↑**	**Yes ↑**
WT vs **C124S**	Yes ↑	No ↑	Yes ↑
WT vs **K125E**	Yes ↑	**Yes ↑**	**Yes ↑**
WT vs **K125X**	Yes ↑	**Yes ↑**	**Yes ↑**
WT vs **G129E**	Yes ↑	No ↑	No ↑
WT vs **E150Q**	**Yes ↑**	**Yes ↑**	No ↑
WT vs **D153N**	**Yes ↑**	No ↑	No ↑
WT vs **D153Y**	Yes ↑	No ↑	**Yes ↑**
WT vs **N323K**	No ↑	**Yes ↑**	**Yes ↑**

Legend
Yes – indicates a change in cell proliferation that was statistically significant
No – indicates difference is not statistically significant
↑ - Indicates cell proliferation was increased compared to the WT PTEN rate

4.4 RESULTS 2: DETERMINING THE EFFECT OF WILD TYPE AND MUTANT PTEN ON THE CELL CYCLE PHASE DISTRIBUTION OF CANCER CELLS

4.4.1 Introduction and background

The cell cycle is a series of strictly regulated stages of cell growth, division, proliferation and apoptosis. The cycle of cell division is made of four phases: (i and ii) two gap phases (G1 and G2) during which cells are occupied with protein synthesis and growth, (iii) S phase, in which DNA replication occurs and (iv) M phase, in which mitosis or cell division occurs [168]. Progress through the cell cycle is tightly regulated by various regulatory proteins including the cyclins, cyclin-dependent kinases (CDKs) and CDK inhibitors, to ensure that cells grow and replicate with intact, mutation-free DNA [168].

PTEN is known to modulate cell cycle progression in the cytoplasm through antagonism of the PI3K pathway and subsequent downregulation of downstream events within this signalling pathway. Additionally, regulation of ERK phosphorylation by PTEN, and reduction of cyclin D1 in the nucleus through increased phosphorylation of beta-catenin, enhances the rate of beta-catenin degradation and modulates cell cycle progression [54, 60, 169]. It is noteworthy to mention that PTEN nuclear function is independent of its phosphatase activity and, interestingly, provides a justification for the tumour-suppressive activity of catalytically inactive PTEN [27].

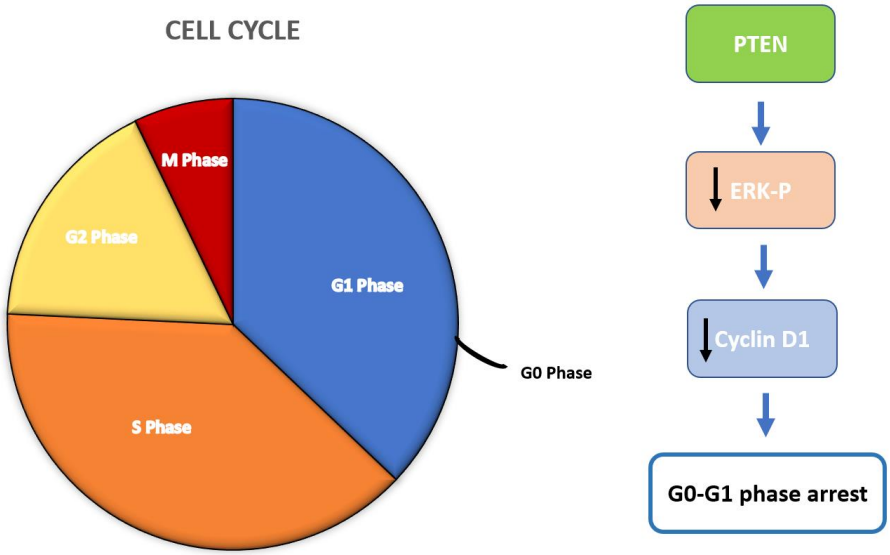

Figure 4.5 The cell cycle and the role of PTEN in cell cycle regulation. The four phases of the mammalian cell cycle (G1, G2, S and M phases) are shown. Active PTEN downregulates the MAPK (ERK) pathway, the dephosphorylation of ERK, leading to reduced cyclin D1 levels and consequent cell cycle arrest in the G0-G1 phase.

Exogenous transient expression of PTEN is known to cause cell cycle arrest in various cell lines including U87MG [4, 5, 170] and MCF7 cancer cell lines [5, 44, 45, 171, 172], but stable transfection of PTEN in breast cancer cells (MCF7) resulted in both cell cycle arrest in the G1 phase and apoptosis [32]. This indicated the possibility of activity of PTEN through cell type specific pathways to produce the observed varying effects in different cell types. It is possible, however, that the resulting apoptosis observed in some studies, may be attributed to the high level of overexpression of PTEN achieved in the cell lines (MCF7 breast cancer) [32, 173], prostate cancer (LNCaP) [174] and glioma (U251) [175] used.

In light of these studies, the effect of the wild type and mutant PTEN on the cell cycle phase distribution of U87MG, HCT116 and MCF7 cells was undertaken. The WT PTEN and each mutant PTEN were examined for their functional ability to induce cell cycle arrest, and/or alter the cell cycle phase distribution of these cell lines. Pilot experiments conducted prior to the experimental work indicated that analysis of the cell cycle phases by flow cytometry was optimal at the 40 hours post transfection time point for all cell lines (data not shown).

4.4.2 Effect of expression of wild type and mutant PTEN on the cell cycle phase distribution of U87MG glioblastoma cells

The wild type, and each of the PTEN mutants were transiently co-transfected with spectrin B-GFP into the PTEN null U87MG cells and, 40 hours after transfection, the cell cycle phase distribution was determined by flow cytometry. Gating was initially on the viable cell population (FCS vs SSC) followed by gating on the green fluorescence, for positively-transfected cells, then red fluorescence (DNA content) through the FL3-H channel. After flow cytometry analysis, all flow histograms were analysed using the ModFIT software (Figure 4.6). The data shown represent the average of 4 separate experiments, in which samples were analysed in duplicate within each experiment.

Relative to the vector-transfected cells, the wild type PTEN transfected cells showed a higher proportion of cells in the G1 phase (50% of cells in G1 for vector transfected vs 65% for WT PTEN transfected, $p<0.05$), almost identical proportions in the G2 phase proportions and a lower proportions in the S-phase, indicating a marked G1 arrest brought about by WT PTEN (Figure 4.7). Transfection with the C124S phosphatase deficient mutant led to a lower number of cells in the G1 phase compared to WT PTEN,

indicating a reduced ability of this mutant to bring about G1 arrest (40% in G1 for C124S and 65% for WT PTEN, $p<0.05$) (Table 4.2).

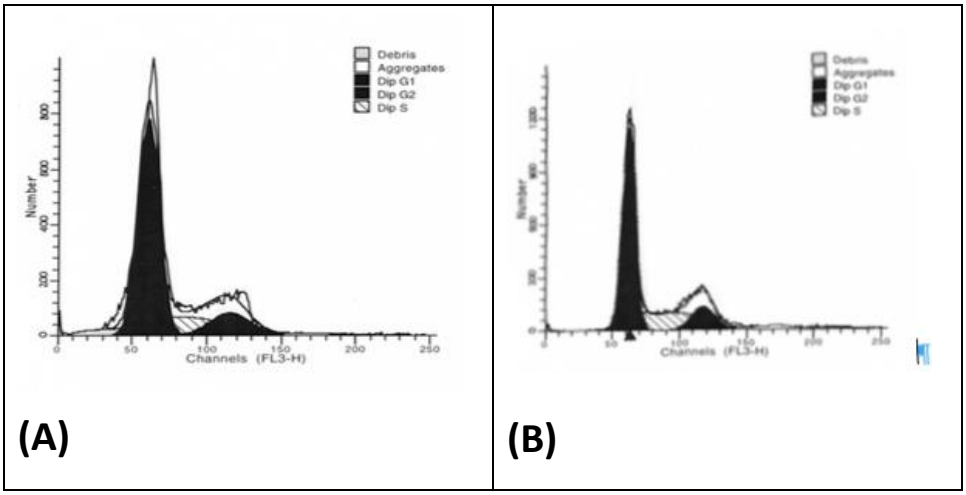

Figure 4.6 Cell cycle analysis of transfected U87MG cells using ModFIT software. Representative cell cycle phase peak profiles of U87MG cells transfected with **(A)** spectrin B-GFP alone and **(B)** co-transfected with spectrin B-GFP and wild type PTEN. The flow cytometry histograms were converted to cell cycle phase distribution plots by the ModFIT software.

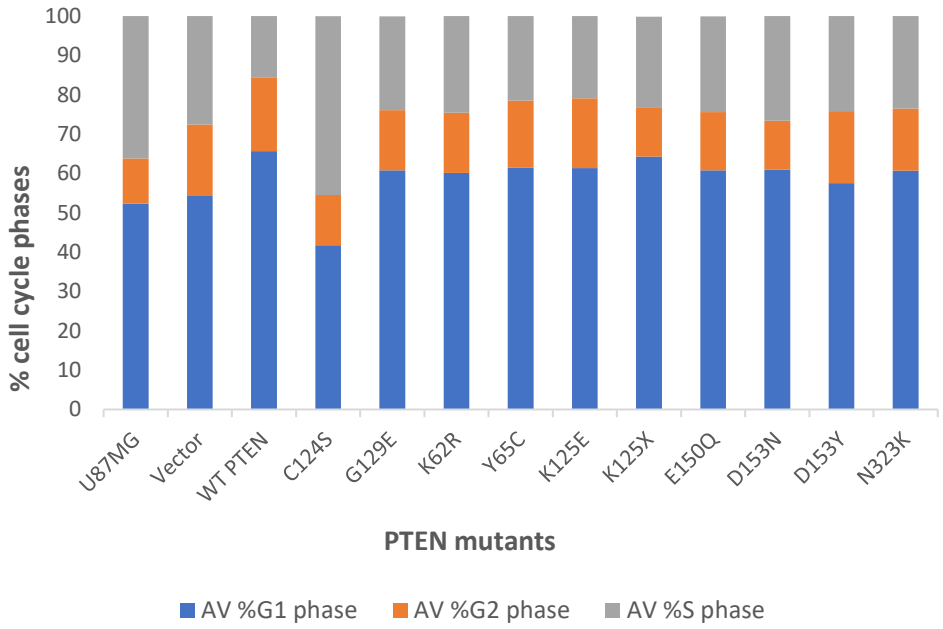

Figure 4.7 Cell cycle phase distribution of wild type and mutant PTEN expressing U87MG glioblastoma cells. Cell cycle phase distribution (by percentage of total cells) was determined from flow cytometry histograms using the ModFit software. The data shown represent the average of 4 experiments, in which samples were analysed in duplicate within each experiment.

The remainder of the PTEN mutants (K62R, Y65C, G129E, K125E, K125X, E150Q, D153N, D153Y and N323K) showed very modest G1 arrest, the magnitude of which was only marginally smaller than the WT PTEN level, indicating variable levels of functional deficiency of the PTEN mutants (Figure 4.7 and Table 4.2). Additionally, some PTEN mutants produced a marginal, but significant ($P<0.05$) decrease in the proportion of cells the G2 phase in comparison to WT PTEN transfected cells (C124S, K125X and D153N vs WT PTEN) (Table 4.2).

Table 4.2 Comparison of the G1 and G2 cell cycle phase distribution of WT and mutant PTEN transfected U87MG cells. Mutation shown in the red font signify those PTEN mutants that significantly alter either the G1 or G2 cell cycle phase distribution compared to WT PTEN.

Independent comparison T-test	G1		G2	
	P-value	*Significant?	P-value	*Significant?
WT vs. C124S	.000	Yes	.000	Yes
WT vs. G129E	.053	No	.009	Yes
WT vs. K62R	.090	No	.001	Yes
WT vs. Y65C	.099	No	.013	Yes
WT vs. K125E	.208	No	.105	No
WT vs. K125X	.620	No	.000	Yes
WT vs. E150Q	.127	No	.000	Yes
WT vs. D153N	.150	No	.000	Yes
WT vs. D153Y	.016	Yes	.449	No
WT vs. N323K	.150	No	.015	Yes

* Assumption of homogeneity of variances were met (p>.05).

4.4.3 Effect of expression of wild type and mutant PTEN on the on the cell cycle phase distribution of HCT116 colon cancer cells

In this series of experiments, the wild type, and each of the PTEN mutants were transiently co-transfected with spectrin B-GFP into the HCT116 colon cancer cell line and, 40 hours after transfection, the cell cycle phase distributions were determined by flow cytometry (gating on the red and green fluorescence) followed by analysis of the flow histograms using the ModFIT software (Figure 4.8). As the mutations being studied were initially detected in primary colon cancers, the results for this cell line would be of great interest. The data shown represent the average of 4 separate experiments, in which samples were analysed in duplicate within each experiment.

Relative to the vector-transfected, or untransfected cells, wild type PTEN transfection of HCT116 cells led to a higher population of cells in the G1 phase (60% of cells in G1 for vector transfected vs 80% for WT PTEN transfected, $p<0.05$), and a lower number of cells in the G2 (20% of cells in G2 for vector transfected vs 10% for WT PTEN transfected, $p<0.05$) and S phases (20% of cells in S phase for vector transfected vs 10% for WT PTEN transfected, $p<0.05$) (Figure 4.8). The C124S and G129E phosphatase deficient mutants produced similar effects on cell cycle phase distribution with a decreased number of cells in the G1 phase and an increased number of cells in the G2 and S phases compared to WT PTEN, indicating a reduced ability of these PTEN mutants to bring about G1 arrest (45% in G1 for C124S and G129E vs 80% for WT PTEN, $p<0.05$) (Figure 4.8 and Table 4.3).

Most notably, in comparison to the WT PTEN expressing cells, a large number of the PTEN mutants produce a marked induction of the G2 phase, longer than that observed

with the phosphatase control mutants C124S and G129E, indicating a G2 phase arrest. This was observed upon transient expression of the K62R, K125E, K125X, E150Q, D153N and D153Y mutants of PTEN in HCT116. Such an effect was not observed in the U87MG cells ($P<0.05$ for all compared to WT PTEN) (Table 4.3).

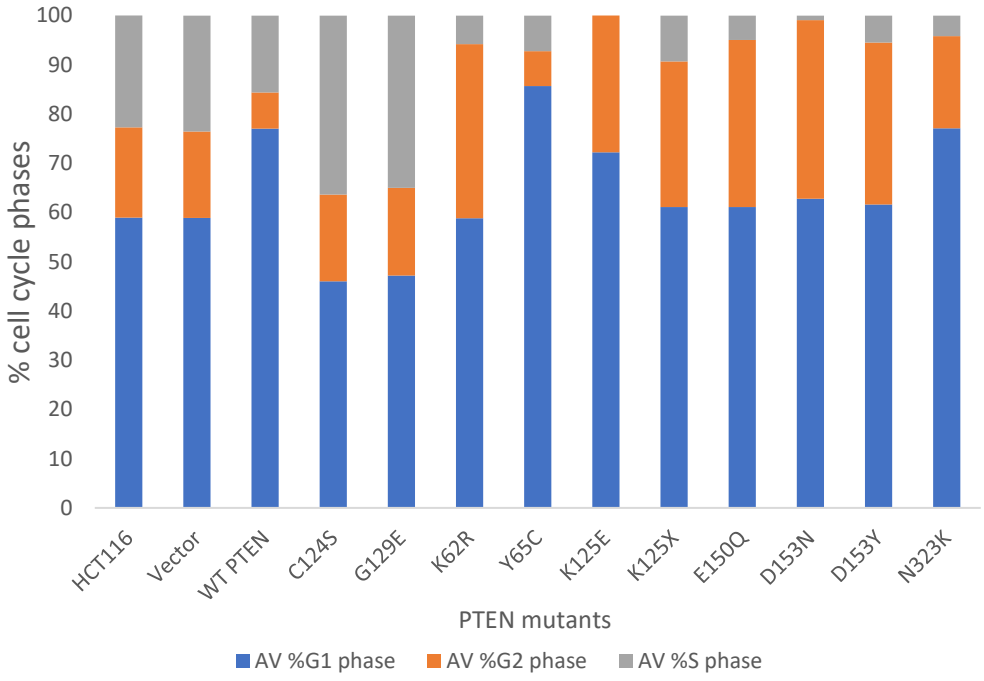

Figure 4.8 Cell cycle phase distribution of wild type and mutant PTEN expressing HCT116 colon cancer cells. Cell cycle phase distribution (by percentage of total cells) was determined from flow cytometry histograms using the ModFit software. The data shown represent the average of 4 experiments, in which samples were analysed in duplicate within each experiment.

Table 4.3 Comparison of the G1 and G2 cell cycle phase distribution of WT and mutant PTEN transfected HCT116 cells. Mutation shown in the red font signify those PTEN mutants that significantly alter either the G1 or G2 (or both) cell cycle phase distribution compared to WT PTEN.

Independent comparison T-test	G1		G2	
	P-value	*Significant?	P-value	*Significant?
WT vs. C124S	.000	Yes	.000	Yes
WT vs. G129E	.044	Yes	.000	Yes
WT vs. K62R	.000	Yes	.000	Yes
WT vs. Y65C	.101	No	.999	No
WT vs. K125E	.001	Yes	.000	Yes
WT vs. K125X	.000	Yes	.000	Yes
WT vs. E150Q	.005	Yes	.000	Yes
WT vs. D153N	.002	Yes	.000	Yes
WT vs. D153Y	.001	Yes	.000	Yes
WT vs. N323K	.475	No	.000	Yes

* Assumption of homogeneity of variances were met (p>.05).

4.4.4 Effect of expression of wild type and mutant PTEN on the on the cell cycle phase distribution of MCF7 breast cancer cells

In this series of experiments, the wild type, and each of the PTEN mutants were transiently co-transfected with spectrin B-GFP into the MCF7 breast cancer cell line and, 40 hours after transfection, the cell cycle phase distributions were determined by flow cytometry followed by analysis of the flow histograms using the ModFIT software (Figure 4.9). The data shown represent the average of 4 separate experiments, in which samples were analysed in duplicate within each experiment.

Relative to the vector-transfected, or untransfected, cells, wild type PTEN transfection of MCF7 cells led to an increase in the number of cells in the G1 phase (50% of cells in G1 for vector transfected vs 75% for WT PTEN transfected, $p<0.05$), and a decrease in the number of the cells in the G2 (20% of cells in G2 for vector transfected vs 10% for WT PTEN transfected, $p<0.05$) and S phases (30% of cells in S phase for vector transfected vs 15% for WT PTEN transfected, $p<0.05$) (Figure 4.9). The C124S and G129E phosphatase deficient mutants produced similar effects on cell cycle phase distribution as the vector-transfected cells indicating functional deficiency of the two mutants. Both mutants show a lower proportion of cells in the G1 phase and a larger proportion of cells in the G2 and S phases compared to WT PTEN, indicating a reduced ability of these PTEN mutants to bring about G1 arrest (45% in G1 for C124S and G129E vs 75% for WT PTEN, $p<0.05$) (Figure 4.9 and Table 4.4).

Most notably, in comparison to the WT PTEN expressing cells, the K125E and K125X mutants produce an increase in the number of cells in the S-phase with a reduction in the number of cells in the G1 phase, indicating reduced ability to produce G1 arrest but

bring about S phase inhibition. The K62R, E150Q and D153N appear to produce a G1 arrest, but the effect is below that of WT PTEN indicating a reduced ability of these mutants of PTEN to bring about cell cycle arrest in G1 (Figure4.9 and Table 4.4).

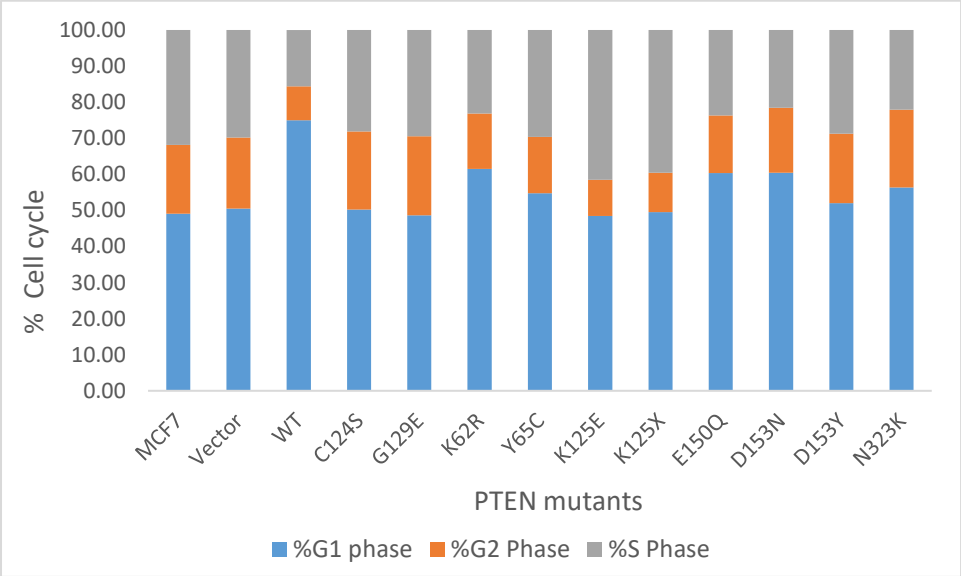

Figure 4.9 Cell cycle phase distribution of wild type and mutant PTEN expressing MCF7 breast cancer cells. Cell cycle phase distribution (by percentage of total cells) was determined from flow cytometry histograms using the ModFit software. The data shown represent the average of 4 experiments, in which samples were analysed in duplicate within each experiment.

Table 4.4 Comparison of the G1 and G2 cell cycle phase distribution of WT and mutant PTEN transfected MCF7 cells. Mutation shown in the red font signify those PTEN mutants that significantly alter either the G1 or G2 cell cycle phase distribution compared to WT PTEN.

Independent comparison T-test	G1		G2	
	P-value	*Significant?	P-value	*Significant?
WT vs. C124S	.006	Yes	.002	Yes
WT vs. G129E	.003	Yes	.002	Yes
WT vs. K62R	.008	Yes	.008	Yes
WT vs. Y65C	.003	Yes	.040	Yes
WT vs. K125E	.002	Yes	.332	No
WT vs. K125X	.002	Yes	.304	No
WT vs. E150Q	.004	Yes	.069	No
WT vs. D153N	.018	Yes	.004	Yes
WT vs. D153Y	.007	Yes	.031	Yes
WT vs. N323K	.004	Yes	.006	Yes

* Assumption of homogeneity of variances were met (p>.05).

The effect of mutants on cell cycle distribution in comparison with wild type PTEN in all three cell lines are summarised in the Table 4.5. Although the trend caused by each mutant in various cell lines is similar in most cases, but it is speculated that variation of their effect on G2 phase distribution in a few of the mutants are cell type dependent as well including K62R, Y65C, K125X, E150Q, D153N, N323K.

Table 4.5 Summary of the effect of wild type and mutant PTEN on the cell cycle distribution in cancer cells. The results of the cell cycle experiments are summarised, showing the effect of each PTEN mutant on cell cycle distribution in comparison to the effect of wild type PTEN. Results shown in the bold red text indicate those PTEN mutants showing greatest changes from the wild type PTEN.

PTEN sequence	Cell line	Detectable Change in Cell Cycle Phase Distribution			
		G1 Phase	Direction of Change	G2 Phase	Direction of Change
K62R	U87MG	No	↓	**Yes**	**↓**
	HCT116	No	↓	**Yes**	**↑**
	MCF7	**Yes**	**↓**	**Yes**	**↑**
Y65C	U87MG	No	↓	Yes	↓
	HCT116	Yes	↓	Yes	↓
	MCF7	No	↓	**Yes**	**↑**
K125E	U87MG	No	↓	No	↑
	HCT116	Yes	↓	**Yes**	**↑**
	MCF7	**Yes**	**↓**	No	↑
K125X	U87MG	No	↓	**Yes**	**↓**
	HCT116	**Yes**	**↓**	**Yes**	**↑**
	MCF7	**Yes**	**↓**	No	↑
E150Q	U87MG	No	↓	**Yes**	**↓**
	HCT116	**Yes**	**↓**	**Yes**	**↑**
	MCF7	**Yes**	**↓**	**Yes**	**↑**
D153N	U87MG	No	↓	**Yes**	**↓**
	HCT116	**Yes**	**↓**	**Yes**	**↑**
	MCF7	**Yes**	**↓**	**Yes**	**↑**
D153Y	U87MG	Yes	↓	No	↑
	HCT116	**Yes**	**↓**	**Yes**	**↑**
	MCF7	**Yes**	**↓**	**Yes**	**↑**
N323K	U87MG	No	↓	Yes	↓
	HCT116	No	↓	**Yes**	**↑**
	MCF7	**Yes**	**↓**	**Yes**	**↑**

Legend

No - indicates no significant change in the distribution of cells in the relevant cell cycle phase in comparison to WT PTEN.

Yes indicates a significant change in the distribution of cells in the relevant cell cycle phase in comparison to WT PTEN.

The direction of the arrows indicate either an increase (↑) or decrease (↓) in the distribution of cells in the relevant cell cycle phase in comparison to WT PTEN.

4.5 RESULT 3: DETERMINING THE EFFECT OF WILD TYPE AND MUTANT PTEN ON AKT PHOSPHORYLATION IN CANCER CELLS

4.5.1 Background

The PI3K/AKT pathway is major signalling pathway regulating cell survival, growth and apoptosis. As a member of this signalling pathway, AKT is activated in response to the binding of a number of growth factors to their extracellular receptors. Phosphorylated AKT (pAKT) is the active form of this protein, that, once activated, is able to regulate downstream targets within the PI3K lipid signalling pathway [170, 176]. Activation of AKT occurs through phosphorylation of Thr-308 and Ser-473 [177, 178]. PTEN modulates the activation of AKT by reducing levels of PtdIns(3,4,5)P3 through direct antagonism of PI3K [179, 180] (Figure 4.10). Thus loss of PTEN (by deletion or mutation) occurs in many cancers and leads to constitutive activation of the PI3K pathway with high levels of active, phosphorylated AKT, and re-expression of PTEN has been shown to reduce the PtdIns(3,4,5)P3 levels and decrease the level of AKT phosphorylation, and activation, in various cell lines [45, 175, 181, 182].

This section examines the ability of wild type and mutant PTEN to suppress the phosphorylation of AKT (at Ser473) as measure of PTEN lipid phosphatase functionality.

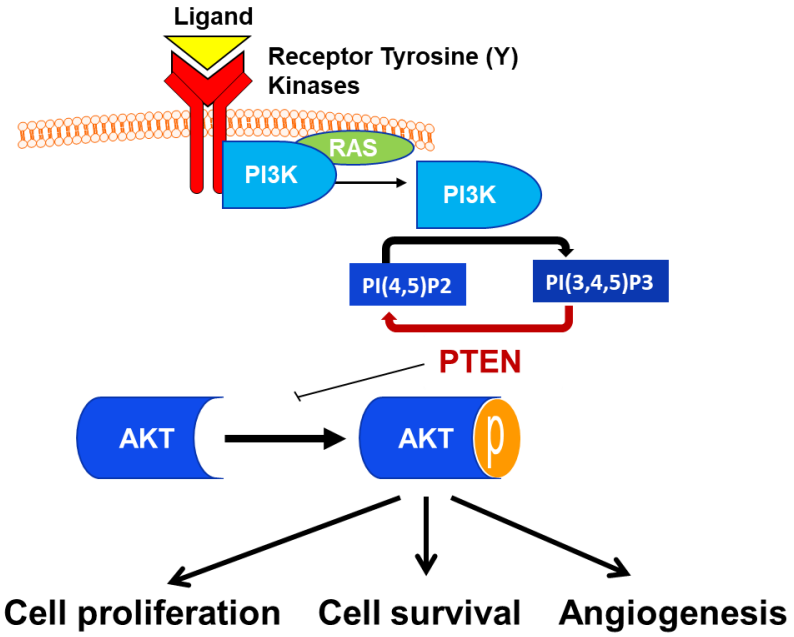

Figure 4.10 PTEN is a negative regulator of the PI3K/AKT pathway through dephosphorylation of PIP3. The PI3K/AKT pathway is activated by the binding of a ligand (such as insulin or growth factor) to its receptor tyrosine kinases on the membrane. This in turn leads to phosphorylation of PtdIns(4,5)P2 (PIP2) to PtdIns(3,4,5)P3 (PIP3) by PI3 kinase and consequent activation of the downstream members of the pathway, leading to enhanced cell proliferation, cell growth and survival and decreased apoptosis. PTEN inhibits AKT activation through the dephosphorylation of PIP3 back to PIP2 with consequent decreased AKT phosphorylation and activation.

4.5.2 Expression of mutant PTEN suppresses AKT phosphorylation with reduced efficacy compared to wild type PTEN in U87MG glioblastoma cells

To determine the ability of wild type, and each PTEN mutant to suppress the phosphorylation and activation of AKT, the wild type and mutant PTEN expression constructs (K62R, Y65C, K125X, K125E, D153N, D153Y, E150Q and N323K) were transiently expressed in U87MG cells and, 40 hours post transfection, total protein was isolated from cell lysates and western analysis was carried out using antibodies specific for phosphorylated AKT (pAKT) at Ser473, and total AKT. Subsequent densitometric analysis allowed the proportion pAKT to total AKT to be determined and to follow the variation in the level of pAKT produced by expression of the different mutants of PTEN.

The expression of exogenous WT-PTEN suppressed the level of pAKT in U87MG cells, when compared to the untransfected, or vector-transfected cells (Figure 4.11). In contrast, the C124S and G129E phosphatase deficient control mutants produced little to no suppression of the level of pAKT. The K62R, Y65C, E150Q, D153Y and N323K mutants of PTEN all produced similar levels of pAKT suppression as the wild type PTEN in the U87MG cells (Figure 4.11). Additionally, the expression of the K125X, K125E and D153N PTEN mutants also showed little suppression of AKT phosphorylation in U87MG cells.

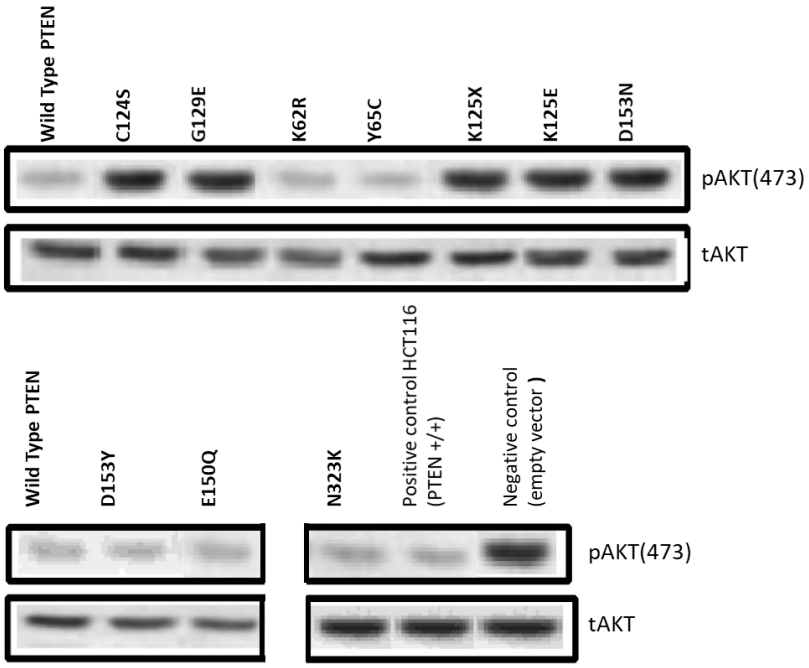

Figure 4.11 The effect of wild type and mutant PTEN expression on the phosphorylation of AKT in U87MG glioblastoma cells. Wild type and mutant PTEN was transiently expressed U87MG cells. After transfection (40 hours), protein was extracted and western analysis was conducted using antibodies specific for AKT and the phosphorylated AKT. β-Actin was included as a loading control.

4.5.3 Expression of mutant PTEN suppresses AKT phosphorylation with reduced efficacy compared to wild type PTEN in HCT116 cells

The wild type and mutant PTEN expression constructs (K62R, Y65C, K125X, K125E, D153N, D153Y, E150Q and N323K) were transiently expressed in HCT116 colon cancer cells and, 40 hours post transfection, total protein was isolated from cell lysates and western analysis was carried out using antibodies specific for phosphorylated AKT (pAKT) at Ser473, and total AKT. Subsequent densitometric analysis allowed the

proportion pAKT to total AKT to be determined and to follow the variation in the level of pAKT produced by expression of the different mutants of PTEN. As HCT116 cells express endogenous wild type PTEN, the level of phosphorylated AKT (pAKT) is lower than that of U87MG cells.

The expression of exogenous WT-PTEN produced a very low degree of suppression of the level of pAKT in HCT116 cells, when compared to the untransfected, or vector-transfected cells (Figure 4.12). The C124S and G129E phosphatase deficient control mutants produced a lower level of pAKT suppression compared to the wild type level. The K62R, Y65C and K125E mutants of PTEN produced similar levels of pAKT suppression as the wild type PTEN in the HCT116 cells (Figure 4.12). Expression of the K125X, E150Q, D153N, D153Y and N323K PTEN mutants showed little to no suppression of AKT phosphorylation compared to cells expressing wild type PTEN.

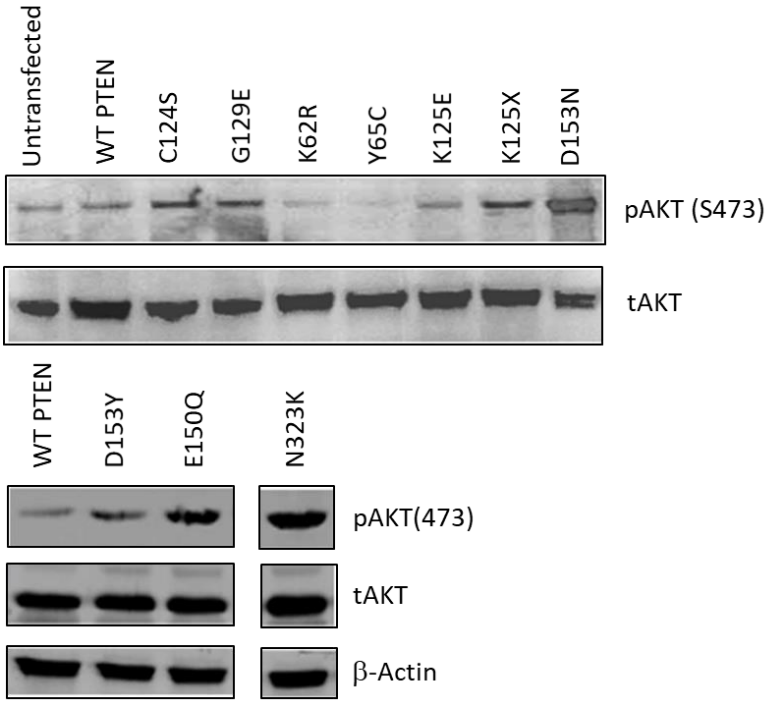

Figure 4.12 The effect of wild type and mutant PTEN expression on the phosphorylation of AKT in HCT116 colon cancer cells. Wild type and mutant PTEN was transiently expressed in HCT116 colon cancer cells. After transfection (40 hours), protein was extracted and western analysis was conducted using antibodies specific for AKT and the phosphorylated AKT. β-Actin was included as a loading control.

4.5.4 Expression of mutant PTEN suppresses AKT phosphorylation with reduced efficacy compared to wild type PTEN in MCF7 breast cancer cells

The wild type and mutant PTEN expression constructs (K62R, Y65C, K125X, K125E, D153N, D153Y, E150Q and N323K) were also transiently expressed in MCF7 breast cancer cells and, 40 hours post transfection, total protein was isolated from cell lysates and western analysis was carried out using antibodies specific for phosphorylated AKT (pAKT) at Ser473, and total AKT. Subsequent densitometric analysis allowed the proportion pAKT to total AKT to be determined and to follow the variation in the level

of pAKT produced by expression of the different mutants of PTEN. Similar to the HCT116 cells, MCF7 cells also express endogenous wild type PTEN, and hence the level of phosphorylated AKT (pAKT) is again lower than that of U87MG cells.

The expression of exogenous WT-PTEN produced a low degree of suppression of the level of pAKT in MCF7 cells, when compared to the untransfected, or vector-transfected cells (Figure 4.13). Expression of the C124S and G129E phosphatase deficient control mutants produced a lower level of pAKT suppression compared to the wild type level with marginally darker pAKT bands in the mutant lane compared to the wild type sample (Figure 4.13). The K62R mutant produced similar levels of pAKT suppression as the wild type PTEN expressing MCF7 cells (Figure 4.13), indicating little deficit in PTEN function with the presence of this mutation. Expression of the Y65C, K125E, K125X, E150Q, D153N, D153Y and N323K PTEN mutants showed little to no suppression of AKT phosphorylation compared to cells expressing wild type PTEN, indicating a level of functional deficit of these PTEN mutants (Figure 4.13 and Table 4.6).

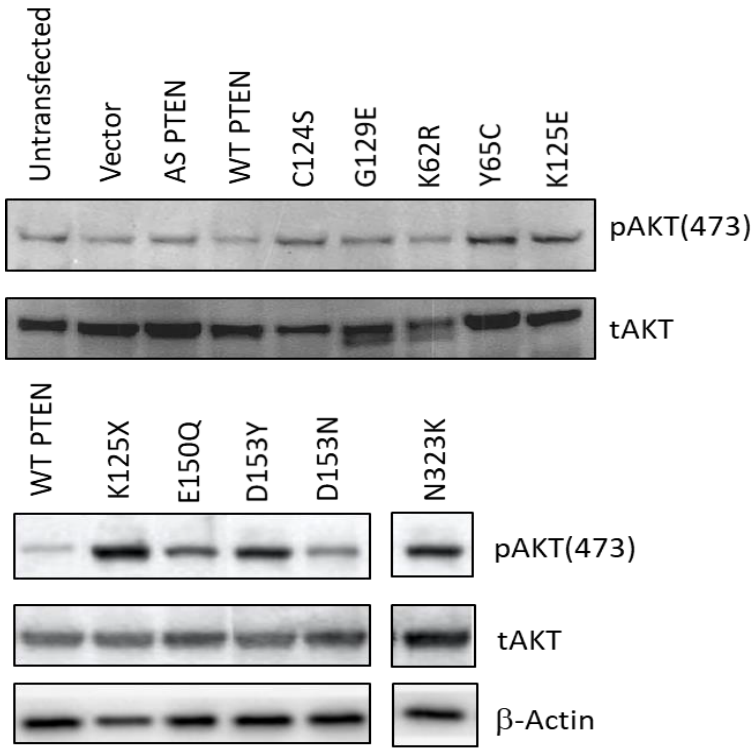

Figure 4.13 The effect of wild type and mutant PTEN expression on the phosphorylation of AKT in MCF7 breast cancer cells. Wild type and mutant PTEN was transiently expressed in MCF7 cells. After transfection (40 hours), protein was extracted and western analysis was conducted using antibodies specific for AKT and the phosphorylated AKT. β-actin was included as a loading control.

Table 4.6 Summary of the effect of wild type and mutant PTEN on the level of pAKT in cancer cells. The pAKT/total AKT ratio, determined from densitometric analysis, has been used to compare the pAKT status for each of the PTEN sequences in each of the 3 cell lines. The pAKT/total AKT ratio for the each of the untransfected cells was assigned a value of 1 (equivalent to 5 stars) and each of the ratios for the mutant PTEN were adjusted accordingly to represent a proportion of the corresponding untransfected cell ratio (range from 1-5 stars). Mutations shown in the red font signify those PTEN mutants that, in comparison to WT PTEN, led to high levels of pAKT as a result of altered tumour suppressor function.

	U87MG	HCT116	MCF7
UNTRANSFECTED	*****	*****	*****
WILD TYPE	*	**	**
C124S	*****	*****	****
G129E	*****	****	****
K62R	*	**	***
Y65C	*	**	*****
K125E	*****	***	****
K125X	*****	****	*****
E150Q	**	*****	*****
D153N	*****	*****	*****
D153Y	**	****	*****
N323K	**	*****	*****

4.6 DISCUSSION

The functional and cellular analyses described for the wild type and mutant PTEN showed some overall interesting and though provoking results. In each of the functional assays, expression of wild type PTEN showed an overall suppressive function within the cancer cell lines studied with observed reductions in cell proliferation, induction of G1 (and/or G2) cell cycle arrest and reduction in the levels of phosphorylated AKT in all three cell lines studied. Interestingly, expression of the known phosphatase deficient mutants of PTEN, namely C124S and G129E, showed marked reductions in the suppressive effects observed for wild type PTEN, indicating, as expected, functional deficit of PTEN carrying these mutations. Interestingly, the C124S mutant appeared to be the least suppressive of the two phosphatase deficient mutants in the reduction of cell proliferation in MCF7 cells.

The cancer associated mutations tested showed suppressive capabilities that ranged from being comparable to wild type PTEN for some of the mutants, to being comparable to the control phosphatase deficient mutants of PTEN for others. Overall, the effect of each of the mutants on PTEN function was both mutation, and cell type, dependent, with some PTEN mutations showing changes in suppressive function in one cell type, that were not observed one, or both, of the other cell lines. The fact these cancer associated PTEN mutations showed a decrease in the suppressive effects of PTEN indicate a potential role for these PTEN mutants in the development, or progression, of the cancers (colorectal cancer) in which they were detected, as well as other cancers. The results of these analyses highlight specific mutants of PTEN for further study of the specific mechanism(s) of their involvement in cancer development and for cancer

therapeutic strategies. The results for the specific mutations and their effects on PTEN function are summarised in Table 4.6 and discussed in detail below.

4.6.1 Effect of wild type and mutant PTEN on cancer cell proliferation

Previous studies have shown that the expression of wild type PTEN in U87MG (functionally PTEN null) cells antagonises the PI3K/AKT signalling pathway through replacement of functional PTEN expression in these cells [5, 172]. Studies in glioma, prostate cancer, thyroid cancer, breast cancer and lung cancer have further shown that the expression of exogenous wild type PTEN significantly inhibits cell proliferation, brings about cell cycle arrest in the G1 phase and promotes apoptosis [25, 44, 174, 183, 184]. Even though some of these cell types expressed PTEN at varying levels, transfection of exogenous wild type PTEN led to suppression of cell proliferation independent of the presence of endogenously expressed PTEN [184, 185]. Exogenous expression of wild type and mutant PTEN had differing effects on cell proliferation in the cell lines used. Expression of exogenous WT-PTEN reduced cell proliferation in cells expressing endogenous PTEN, but the repressive effect was of greater magnitude in cells with an absence of endogenous PTEN expression [185]. Based on the cell type and endogenous PTEN expression status of the cell lines used, the PTEN null U87MG glioblastoma cells showed the greatest level of reduction of cell proliferation by WT PTEN compared to that observed with the HCT116 and MCF7 cells, which express endogenous functional PTEN. This observation was consistent with the literature [5, 32, 186, 187].

Table 4.7 Summary of results of the functional effects of the different PTEN mutations on the functions of PTEN in the regulation of cell proliferation, the cell cycle and AKT phosphorylation status in cancer cells (U87MG, HCT116 and MCF7). Values and trends indicated in the red font signify results that were significantly different to the effect produced by WT PTEN.

PTEN sequence	Cell line	Cell proliferation	Cell cycle		pAKT Status
			G1	G2	
K62R	U87MG	No ↑	No↓	**Yes ↓**	-
	HCT116	Yes ↑	No↓	**Yes ↑**	-
	MCF7	Yes ↑	**Yes ↓**	**Yes ↑**	↑
Y65C	U87MG	Yes ↑	No↓	Yes ↓	-
	HCT116	Yes ↑	Yes ↓	Yes ↓	-
	MCF7	Yes ↑	No↓	**Yes ↑**	↑
K125E	U87MG	Yes ↑	No↓	No↑	↑
	HCT116	Yes ↑	Yes ↓	**Yes ↑**	↑
	MCF7	Yes ↑	**Yes ↓**	No↑	↑
K125X	U87MG	Yes ↑	No↓	**Yes ↓**	↑
	HCT116	Yes ↑	**Yes ↓**	**Yes ↑**	↑
	MCF7	Yes ↑	**Yes ↓**	No↑	↑
E150Q	U87MG	Yes ↑	No↓	**Yes ↓**	↑
	HCT116	Yes ↑	**Yes ↓**	**Yes ↑**	↑
	MCF7	No ↑	**Yes ↓**	**Yes ↑**	↑
D153N	U87MG	Yes ↑	No↓	**Yes ↓**	↑
	HCT116	No ↑	**Yes ↓**	**Yes ↑**	↑
	MCF7	No ↑	**Yes ↓**	**Yes ↑**	↑
D153Y	U87MG	Yes ↑	Yes ↓	No↑	↑
	HCT116	No ↑	**Yes ↓**	**Yes ↑**	↑
	MCF7	Yes ↑	**Yes ↓**	**Yes ↑**	↑
N323K	U87MG	No ↑	No↓	Yes ↓	↑
	HCT116	Yes ↑	No↓	**Yes ↑**	↑
	MCF7	Yes ↑	**Yes ↓**	**Yes ↑**	↑

The C124S PTEN mutant is associated with endometrial cancer and is known to be catalytically inactive due to loss of both lipid and protein phosphatase activity [45, 165]. Transient transfection and exogenous expression of the C124S phosphatase deficient mutant of PTEN resulted in very little reduction of cell proliferation for all three cancer cell lines, with no evidence of any increase in the presence of apoptotic cells across the time of the experiment (data not shown), highlighting the importance of the lipid phosphatase function of PTEN in the regulation of cell proliferation, and consistent with other reports showing loss of function of PTEN carrying this mutation [5, 8, 44, 188].

The G129E mutation of PTEN was initially described in Cowden syndrome and is known to cause a loss the phosphoinositide phosphatase activity of PTEN, while retaining the protein phosphatase activity [45, 77]. Previous reports have shown increased cell proliferation of U87MG and MCF7 cells, compared to wild type PTEN [173, 189], and hence these mutations were included as a reference in the work presented in this thesis. Expression of the G129E mutation brought about modest, but statistically significant, increases (5-15%) in cell proliferation in all three cell lines studied, with the largest effect observed in the U87MG cell line (15% increase from the WT PTEN proliferation rate, $p<0.05$). Increased cell proliferation has been observed for this mutation in other studies, and, while these results are consistent with the literature, the magnitude of the effect of this mutant on cell proliferation is somewhat smaller in comparison. The sequences of the expression constructs had been verified, ensuring the correct mutant sequences were present, and hence the smaller effect cannot be attributed to any sequence alteration of PTEN within the expression construct.

However, PTEN phosphatase activity is crucial in modulating cell growth and apoptosis, and there are some indications that the amounts of enzyme needed for its phoshotyrosine phosphatase activity in cells are more stoichiometric rather than catalytic [190] and, if this consideration is extended to its lipid phosphatase activity, might have had an impact in these results.

Moreover, some new studies report PTEN-mediated reductions in cell proliferation that independent of its effect on AKT activation/inactivation [191] and this may be of interest to follow up further as it may partially explain this observation. The reported AKT-independent mechanisms of PTEN tumour suppression include activation of the JNK signalling pathway [192], cell size checkpoint control [193], activation of the SRC signalling pathway [194], inactivation of the PKR-eIF2α phosphorylation pathway through PTEN protein-protein interaction [195] and oncogenic transformation of cells by 58-kDa microspherule protein (MSP58) [196]. Furthermore, previous reports of the effect of these two phosphatase mutants of PTEN were predominantly carried out using the MTT, MTS or viability cell count assays [44, 174, 184]. The basis of the MTT and MTS assays is the measurement of mitochondrial metabolic activity, which may prove misleading as increased mitochondrial activity detected by these assays may be due to an increase in mitochondrial biomass or metabolic activity, and not necessarily due to increased cell proliferation. On the other hand, reductions in cell proliferation rate may be due to cell cycle arrest, with cells remaining viable [197]. In a previous study on the accuracy and reliability of various cell proliferation assays, it was demonstrated that the SYBR-green assay (measurement of DNA content through

intercalation of SYBR green dye into DNA) was a more reproducible and reliable method of measuring cell proliferation changes compared to MTS assays [197].

The PTEN mutants K62R and Y65C decreased cell proliferation to similar levels in both HCT116 and MCF7 cells, with a greater reduction in U87MG cells. In all cases, the levels of reduction in cell proliferation produced by these mutants were not as high as that of wild type PTEN (5-8% greater proliferation than WT PTEN in U87MG, 31-32% greater proliferation in HCT116 cells and 15-17% greater proliferation than WT PTEN in MCF7 cells), indicating a level of functional PTEN deficit brought about by these mutations. This is interesting as both of these mutations were originally detected in a single tumour from a colorectal cancer patient. Both mutation occur on the same allele and the tumour showed decreased PTEN expression [9]. Although HCT116 cells contain endogenous, WT-PTEN, loss of a single PTEN allele is sufficient for tumorigenesis [37]. Hemizygous PTEN knockout mice show that monoallelic loss of PTEN is sufficient for tumour initiation and growth [181, 183, 198].

The lysine residue on codon 125, located in the phosphatase active site of PTEN, was found to be the target of two mutations, mutants K125E and K125X. The level of reduction of cell proliferation produced by these mutants was very similar in the HCT116 and MCF7 cells, and of lower magnitude in the U87MG cells. In all cases, the level of reduction in cell proliferation achieved was not as great as that produced by WT PTEN (7-10% greater proliferation than WT PTEN in U87MG, 12-21% greater proliferation in HCT116 cells and 27-32% greater proliferation than WT PTEN in MCF7 cells). Based on a structural analysis of PTEN, the K125 residue interacts with phosphate groups at the D1 and D5 positions of the inositol ring [48]. Cancer-

associated mutants K62R, Y65C, K25E and K125X are located within the N-terminal phosphatase domain of PTEN (residues 1-185), with the K125E and K125X mutants specifically located within the ATP-binding motif of the active site within this protein domain. Mutations in this region of PTEN may result in nuclear mislocalisation [199], may alter anchorage-dependent growth [200], cellular proliferation [200], and dysregulated PTEN expression and activity [201]. In particular, the K125E/X mutations lie in the catalytic core motif (HCXXGXXR) of PTEN (residues123-130) [48], and only a single amino acid away from the catalytic C124 residue important for both PTEN lipid and protein phosphatase activity. It was hypothesised that mutations in this region would interfere the tumour suppressor function of PTEN through diminishing the phosphatase activity of PTEN phosphatase activity, and the results presented as part support this hypothesis. Subsequent to this work, Costa and colleagues have reported that the PTEN mutation A126G produces a gain-of-function effect, shifting the function of PTEN from a phosphoinositide (PI) 3-phosphatase to a phosphoinositide (PI) 5-phosphatase [202].

PTEN interacts with P53 through its C2 domain, forming a stable complex of PTEN/P53, and upregulates P53 protein level and activity [120]. In a study of exogenous expression of mutants of PTEN with loss of ATP-binding capacity, downregulation of P53 was found to be phosphatase-independent and MDM2-independent in MCF7 cells [201]. The authors reported that the K125E mutant of PTEN produced a higher cellular proliferation rate, faster clonogenicity and lowest P53 transcriptional activity, behaving as a phosphatase deficient mutant with observed nuclear mis-localisation [200, 201].

They believe that the balance between dosage, mis-localisation and phosphatase activity of ATP motif mutants is important in their effect on cells [201].

The missense mutations E150Q, D153Y and D153N fall within the N-terminal phosphatase domain of PTEN (residues 7-185). Around 30% of all PTEN mutations occur in this region and have been shown to cause loss of lipid phosphatase activity [23]. E150Q was found as a homozygous somatic mutation, however it was not present in the matched polyp sample of the same patient suggesting that this mutation may be involved in colorectal cancer progression [9]. Our data indicates reduced function of PTEN carrying these three mutations in all three cell lines. In all cases, mutants reduced cell proliferation, with the level of reduction being variable in each of the cell lines, and not as great as that produced by WT PTEN (7-17% greater proliferation than WT PTEN in U87MG, 2-32% greater proliferation in HCT116 cells and 5-17% greater proliferation than WT PTEN in MCF7 cells). The E150Q mutation produced the greatest effect in HCT116 cells, reducing the WT PTEN proliferation rate by 32% ($p<0.05$).

The N323K missense mutation is located in the C-terminal domain of PTEN (residues 186-351). This region is also important for the tumour suppressor function of PTEN as loss of phosphatase activity has been reported as a result of mutations in this domain of the PTEN protein [203, 204]. Interestingly, cells expressing this PTEN mutant showed increased cell proliferation compared to WT PTEN expressing cell, with the effect more significant in the HCT116 and MCF7 cells than U87MG cells (3% greater proliferation than WT PTEN in U87MG, $p>0.05$; 15% greater proliferation in HCT116 and MCF7 cells, $P<0.05$ for both). Specifically, while only in HCT116 this mutation was unable to reduce

the cell proliferation rate compared to transiently transfected WT-PTEN in the same cell line.

In summary, the cell proliferation analysis highlighted all the cancer-associated mutations of PTEN to have reduced capacity to suppress cell proliferation but with variable effects in the different cell lines. The K62R, Y65C, K125E, K125X and N323K mutants are least effective, compared to wild type PTEN, in the HCT116 and MCF7 cells, whereas the D153N mutant is least effective in U87MG cells. The E150Q mutant is highlighted as having lowered suppressive effect in the U87MG and HCT116 cells, indicating the cell type specificity of the effect on cell proliferation.

4.6.2 Effect of wild type and mutant PTEN expression on the cell cycle phase distribution of cancer cells (U87MG, HCT116 and MCF7)

Analysis of cell cycle phase distribution after exogenous expression of wild type, and each of the cancer-associated mutations of PTEN, showed differences in the lengths of the G1 and/or G2 phases, depending on the mutation studied and the cell type being used. Previous studies have reported the induction of G1 phase block upon expression of wild type PTEN in PTEN-null cells [5, 32, 172, 205] and this was also observed in this study. Exogenous expression of wild type PTEN was shown to bring about G1 cell cycle arrest in the U87MG glioblastoma, HCT116 colon cancer and MCF7 breast cancer cells. Thus wild type PTEN caused G1 arrest in both PTEN null (U87MG) and wild type PTEN expressing cells (HCT116 and MCF7) alike.

The C124S control phosphatase deficient mutant of PTEN, lacking both the lipid and protein phosphatase activity, did not produce any G1 arrest, while the G129E lipid phosphatase deficient mutant produced a marginal G1 arrest in U87MG cells, which

was not apparent in either HCT116 or MCF7 cells. Interestingly, the G129E mutant was found not to be able to bring about a G1 phase arrest in PTEN-null 786-O renal carcinoma cells [172]. This provided further evidence of the cell-type specificity of PTEN function and dysfunction.

The cancer associated mutants K62R, K125E, K125X, E150Q, D153N and D153Y, all produced varying levels of G1 arrest that were below the level produced by wild type PTEN in the U87MG, HCT116 and MCF7 cells, indicative of functional alteration of PTEN carrying these mutations. The K62R, Y65C and K125E mutations of PTEN are located in the ATP binding motif of PTEN, and it has been shown that these mutants cause nuclear mis-localisation of PTEN and alter anchorage-dependent growth, cell proliferation and apoptosis in MCF7 cells [200]. It was further reported that these mutants deregulate PTEN expression and abrogate the phosphatase activity, which is important for cell cycle regulation, however no changes in cyclin D1 level was reported [201]. As the ATP binding motif is within the phosphatase domain (residues 1-185) of PTEN, impaired phosphatase activity for mutants occurring within this region is reasonable, especially if they occur within the core catalytic motif of PTEN (residues 123-130) [48], namely K125E and K125X. The K62R and Y65C are located in the ATP-binding motif A (residues 60-73) (Figure 4.14) [201].

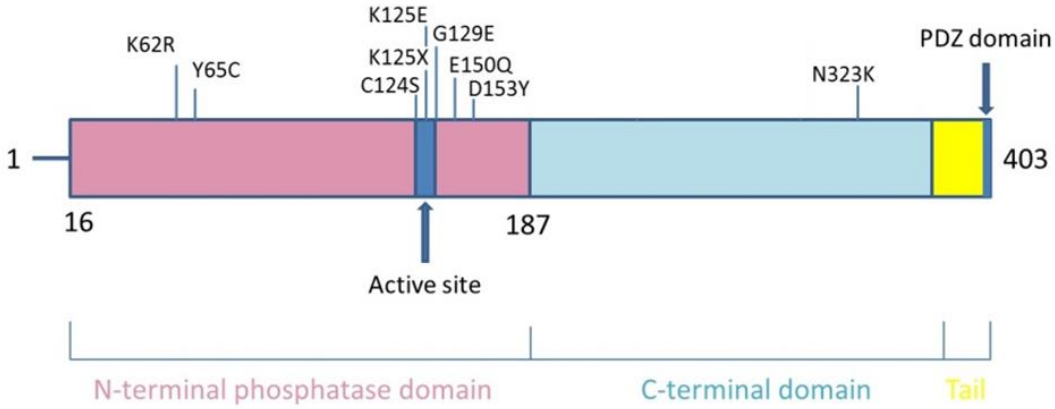

Figure 4.14 Location of the cancer-associated mutations of PTEN within the PTEN protein sequence and domain structure.

Interaction between PTEN and P53 is reported to upregulate the P53 level and activity in cells [206]. PTEN contains an ATP-binding site within its N-terminal domain, involved in modulation of PTEN subcellular localisation [199, 200]. Ectopic expression of ATP-binding mutants of PTEN in MCF7 cells led to downregulation of P53 levels, thought to be mediated through a phosphatase independent and MDM2-independent manner [201]. The results presented in this thesis demonstrate that, in U87MG cells, in addition to a marginal decrease in the length of the G1 phase, compared to wild type PTEN, the effect of these mutants (K62R, Y65C, K125E and K125X) caused a statistically significant increase in the G2 phase length. In HCT116 cells, PTEN mutants K62R, K125E and K125X decreased the level of G1 arrest, compared to WT PTEN, but brought about a G2 arrest in HCT116 cells.

Based on the structural analysis of PTEN, the K125 residue is located in the tyrosine phosphatase motif (residues 122-132) HCxxGRxxR in the P loop of the phosphatase active site [48]. Mutations of K125 have been shown to have up to a 75% decrease in

lipid phosphatase activity. This residue interacts with the D1 position of the inositol ring through charge-charge interaction [26, 48, 204], hence when mutated, a reduced affinity for phosphoinositides containing the D1 position is expected [28].

The N323K mutant, located within the C-terminal C2 domain of PTEN [48], brought about arrest in both the G1 and G2 phases. Compared to the wild type PTEN, this mutation was not as effective at bringing about a G1 arrest in U87MG and MCF7 cells, however it also brought about a G2 arrest, not observed with wild type PTEN expression, in HCT116 and MCF7 cells. It has been suggested that mutations within the C2 domain have little effect on PTEN activity, however the results shown in this thesis would suggest otherwise [207].

Thus, it is suggested that PTEN modulates the cell cycle progression by targeting further downstream targets in the pathway like AKT, as in a study the introduction of active AKT overruled the cell cycle arrest of G1 in cells with exogenous WT-PTEN [185].

4.6.3 Effect of wild type and mutant PTEN expression on AKT phosphorylation of cancer cells (U87MG, HCT116 and MCF7)

The proto-oncogene Akt, a target of PI3 kinase activation, has a central role in a signalling pathway of which many components have been linked to metabolism, protein synthesis, cell proliferation, survival, and transcriptional regulation. It is overexpressed as well as activated in numerous human cancers. Conversely, cell lines that lack PTEN expression show increased levels of PIP3 levels and Akt activity. Aberrant activation of the PI3K pathway is oncogenic and plays critical roles in a variety of cancer types. In contrast, PTEN dephosphorylates and inactivates the lipid second messenger phosphorylated by PI3K, thereby acting as a tumour suppressor [208]. Disruption of

PTEN activity results in increased growth signals and promotion of tumour formation [198, 209]. Numerous *in vitro* studies demonstrate the important role of PI3K in colorectal neoplasia [210].

Although PTEN is capable of dephosphorylating both phosphotyrosine and phosphothreonine [211], its primary substrates are the 3-phosphoinositides, PIP2 and PIP3 [45, 212]. Akt is activated by a dual regulatory mechanism that requires both translocation to the plasma membrane and phosphorylation at Thr308 in the activation loop of the kinase and Ser 473 at the C-terminus [213, 214]. Binding of the pleckstrin homology domain (PH) of Akt to phosphatidylinositol 3,4,5, triphosphate (PIP_3) on the inner leaflet of the plasma membrane releases the autoinhibitory function of this domain allowing phosphoinositide-dependent kinase 1(PDK1) to phosphorylate Akt on Ser 473 [178, 215]. Phosphorylation of Akt is required for its function. Thus, Akt activity is positively regulated by PI3K, which phosphorylates phosphatidylinositol-4, 5-bisphosphate (PIP_2) to produce PIP_3 [216].

The tumour cell lines with mutant PTEN retained elevated levels of PtdIns(3,4,5)P3 and Akt activity, and the introduction of wild-type PTEN reduced the levels of both [181, 182]. Furthermore, analysis of the PTEN crystal structure indicates that the phosphatase active site of PTEN is larger than that of the PTPs and that the COOH-terminal portion has a structure similar to the C2 domain and actually binds to phospholipid membranes *in vitro* [48]. To elucidate the most important tumour suppressor function of PTEN, the analysis of the effect of the missense mutations on currently known functional properties of PTEN will be beneficial until all of the functions of PTEN are clarified.

Overall, the analysis of the results of the assays of PTEN function, indicate that the mutations detected in sporadic colorectal cancer show decreased ability to suppress the level of endogenous phosphorylated AKT in all three cancer cell lines: U87MG, HCT116 and MCF7 cells. In all cases, expression of the wild PTEN produced the highest level of pAKT suppression. Expression of the control phosphatase deficient mutants of PTEN, C124S and G129E, produced the least amount of pAKT suppression across all three cells lines, indicating functional deficit induced by these mutations of PTEN.

The PTEN N-terminal domain mutants, K62R and Y65C produced little suppression of pAKT levels in the MCF7 cells but the level of suppression was higher in the U87MG and HCT116 cells, again highlighting the cell-type dependency of the effect of PTEN. The remaining N-terminal domain mutants, K125E, K125X, E150Q, D153N and D153Y, produced very little pAKT suppression, indicating some loss of this PTEN functionality, in all three cells lines studied. The greatest loss of this function was observed in the MCF7 cells (Table 4.5). Interestingly, biochemical analyses from previous studies have shown that most missense mutations found in the phosphatase domain dramatically decrease or inactivate the phosphatase activity of PTEN [211, 217].

The mutation N323K is a missense mutation found on the C terminal domain of PTEN. In comparison to wild type PTEN, expression of this mutant abolished the ability of PTEN to suppress pAKT levels in the HCT116 and MCF7 cells. It has been shown that missense mutations in the C-terminal region inactivate the tumour-suppressor function of PTEN by affecting its intrinsic phosphatase activity, most likely as a result of conformational changes. This effect is reflected also by the persistence of PKB/Akt activation in cells expressing these mutants [203]. This region is also essential for tumour suppressor

function, and partial or total absence of phosphatase activity has been demonstrated to result from amino-acid changes outside the phosphatase domain [203, 204]. This could explain the behaviour of this mutant PTEN as a partial loss of function mutant, as observed in this study. Additionally, mutations within the C2 domain can also decrease the protein stability.

The K125E and K125X mutations are located in the N-terminal phosphatase domain of PTEN and were predicted to alter at least the lipid phosphatase activity essential for the PTEN tumour suppressor function [48, 204]. Interestingly, codon 125, an invariant lysine residue, appears to be a target with two distinct mutations occurring at this site. Molecular modelling of the PTEN structure with the PIP3 soluble head group analog inositol 1,3,4,5-tetrakisphosphate indicates that Lys 125 and Lys128/His93 are positioned to coordinate the D1 and D5 phosphate groups of the inositol ring, respectively, by charge–charge interactions [48]. PTEN mutants in which Lys125 and Lys128 have been substituted with Met display a substantial decrease in lipid phosphatase activity, which further supports the concept that charge interactions are critical determinants for PTEN specificity toward PIP3 [48]. The possible mechanism reported for this is that modification of lysine residues within the catalytic pocket may interfere with substrate binding [161].

However, the K125 site is located in the flexible catalytic domain P-loop structure of PTEN [48], which suggests that the addition of small acetyl groups would not physically impede interaction with substrate. Alternatively, acetylation of these lysine residues might cause the loss of a positive charge in the catalytic cleft known to be required for selectivity of the negatively charged PI(3,4,5)P3 substrate, as well as its orientation

within the cleft [48]. This could be the reason why both K125E and K125X behave like lipid phosphatase inactive mutants.

Because loss of PTEN function is a common molecular abnormality in human cancer, defining its mechanism of growth suppression is of critical importance. The preliminary functional evidence presented here from expression studies and from analysis of these ten novel mutations indicates that PTEN functions to inhibit the PI3-kinase AKT pathway, presumably through dephosphorylation of the PI3-kinase substrate PIP3. With this knowledge, therapeutic strategies that target the PI3K-Akt pathway may be particularly effective in cancers lacking PTEN function because some of these mutant tumours show higher levels of pathway activation.

CHAPTER 5

INTRODUCTION TO SPHINGOSINE KINASE 1 (SPHK1) ISOFORMS

Certificate of authorship and originality

Parts of this chapter have been published in two review papers in *Oncotarget* and *International Journal of Molecular Sciences* in 2017. I certify that the work presented in this chapter has not previously been submitted as part of the requirements for a degree. I also certify that I carried out the majority of the work presented in these papers as the first author.

Principal supervisor

Dr Najah Nassif

Production Note:
Signature removed
prior to publication.

_____

Date: 25-09-2018

PhD candidate

Nahal Haddadi

Production Note:
Signature removed
prior to publication.

_____

Date: 25-09-2018

Prelude: SphK1 and PTEN are related through their common, but opposing, regulation of the PI3K/Akt pathway

As observed in the preceding section of this thesis, PTEN is a negative regulator of the PI3K/Akt pathway and mutations of PTEN were shown to alter its tumour suppressive function. On the other hand, SphK1, the subject of this second part of the thesis, is a positive upstream regulator of the Akt pathway and, in contrast to the negative regulation of the pathway conferred by PTEN, SphK1 activates the PI3K/Akt pathway to promote cell proliferation [10-13]. The importance of the interplay between the two regulators converges on the Akt checkpoint (Figure 5.1) and it has been demonstrated that overexpression of SphK1 in some cell lines and xenograft models greatly enhances cell proliferation in the presence or absence of wild type PTEN and mutant PTEN. However, in some cases, PTEN inactivation, coupled with SphK1 activation has been linked to increased tumour aggressiveness and poor prognosis [10]. Although SphK1 is expressed as 2 major isoforms, SphK1-43kDa (SphK1a) and SphK1-51kDa (SphK1b), with similar SphK1 activity [14], most SphK1 experiments have focused generically on the SphK1a isoform [15, 16]. To date there is no literature on the expression of the two SphK1 isoforms in cell lines or human tissues. This part of the thesis addresses this important issue. During the course of this thesis I have published two reviews highlighting the importance of the SphK1 isoforms in cancer [15, 16]. This Chapter highlights the importance of SphK in general and defines the nomenclature of SphK, which forms part of the published review, “Dicing and splicing” sphingosine kinase and its relevance in cancer [15].

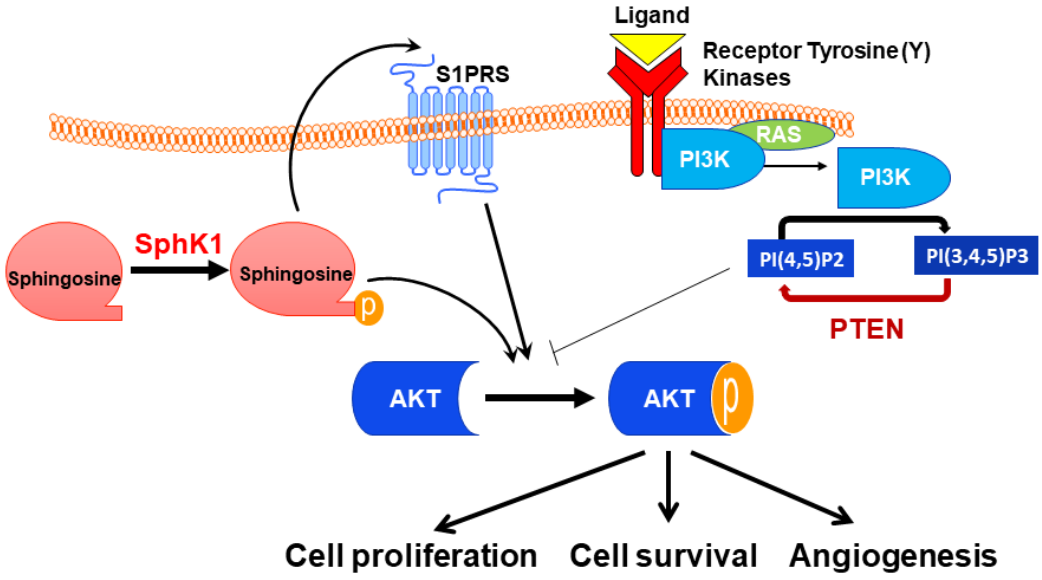

Figure 5.1 PTEN and SphK1 are opposing regulators of the PI3K/AKT Pathway. Binding a of ligand (e.g. growth factor, insulin, etc.) to a receptor tyrosine kinase activates PI3K, which, in turn, phosphorylates PIP2 to PIP3. Increases in PIP3 levels promote AKT activation and its downstream pathways to bring about enhanced cell proliferation and cell survival. PTEN is a direct antagonist of PI3K through the dephosphorylation of PIP3 to PIP and consequent inhibition of AKT activation. On the contrary, phosphorylation of sphingosine by SphK1 promotes the subsequent phosphorylation and activation of AKT, which leads to activation of downstream pathways, leading to a promotion of cell proliferation and survival.

5.1 SphK1: an overview

Sphingosine kinase (SphK), categorised as a bioactive lipid enzyme, is a central player in the sphingolipid rheostat [218-222]. The sphingolipid rheostat was first coined in the mid-nineties to describe the repression of ceramide-mediated programmed cell death through the conversion of sphingosine, a metabolite of ceramide, to sphingosine-1-phosphate (S1P) [222-224]. In this role, SphK modulates the balance between S1P, sphingosine and ceramides to maintain physiological levels of sphingosine and ceramide [225-227]. Activity of SphK/S1P is enhanced through cytokines, hormones, and growth

factor stimulation [227-231]. Thus, SphK is the rate-limiting enzyme that maintains the level of S1P for cell survival and normal cell proliferation and function. Conversely, S1P is enzymatically degraded by S1P lyase to maintain the level of S1P at normal physiological levels (Figure 5.1) [225, 232]. As will be described in this chapter, SphK has two major isoenzymes (isozymes), SphK1 and SphK2, and each isozyme is expressed as a number of isoforms [233-235]. Differences in conformation and dimerisation properties, in addition to the varying subcellular localisations of SphK isozymes and isoforms, contribute to the diversity in SphK functions. SphK isozymes have some redundancy and compensatory functions in "normal" physiology, as described in mouse models. SphK knockout mice with deletion of either isozyme show no obvious phenotypic abnormalities [236-238]. Deletion of both isozymes results in embryonic fatality [236]. Recently our attention has been drawn to the diversity in biological functions of the SphK1 and SphK2 isoforms whereby each isozyme has multiple isoforms differing only at the N-termini [219, 233, 239, 240]. There is a strong suggestion that imbalances of SphK1 isoform abundance may play a crucial role in the pathophysiology of diverse diseases, may contribute to resistance to current anti-cancer drug therapies [241-243], and may have consequences for therapies targeting SphK1 and S1P in the presence of comorbid conditions [14, 232]. Importantly, emerging evidence suggests that although high expression of both SphK-1a and -1b isoforms are associated with oncogenicity, the aberrant expression of the isoforms may be important to the efficacy of anti-SphK1 drug therapies [14, 241, 242]. Thus, SphK isoform function and role in normal physiology and disease initiation and progression certainly merit further examination.

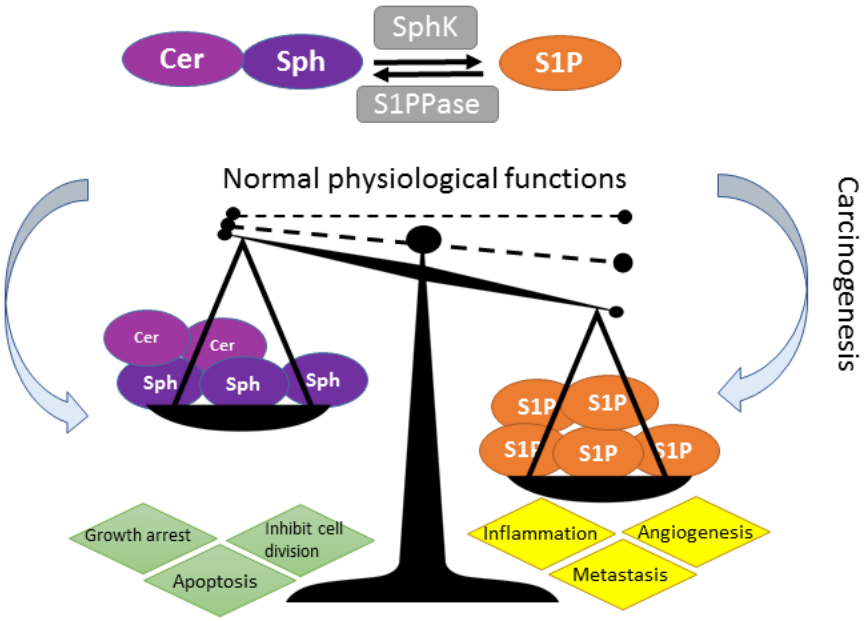

Figure 5.2 The SphK rheostat: tipping the sphingosine-sphingosine kinase (SphK) sphingosine-1-phosphate (S1P) rheostat in favour of cancer. Ceramide (Cer) and sphingosine (Sph), upstream in the SphK rheostat, are pro-apoptotic while SphK conversion of sphingosine to S1P tips the balance in favour of cell survival and cell maintenance (as shown by the arrows and dashed lines). Imbalance (increase) in S1P expression, through overexpression of SphK activity, illustrated by dashed lines to solid line, is causally associated with cancer development, inflammation, angiogenesis and metastasis [244].

5.2 Importance of isoenzymes (isozymes) and variant isoforms in the future of Cancer treatment

Multiple isozymes occur mainly through gene duplication throughout evolution and each isozyme can produce many alternatively spliced transcripts and variant protein isoforms. Alternative splicing of a single gene allows for selective inclusion and exclusion of specific exons within a gene and provides for greater proteomic multiplicity and physiological functionality [245]. Dicing and splicing of introns and exons to produce variant isoforms is a common process occurring in 95% of all multi-exon genes [245].

Advantages of alternative exon splicing in different tissues allows for variations in protein-protein interactions with consequent modulation of specific interacting networks in the cell to allow variations in function [246]. On the other hand, a switch in splicing preference, aberrant splicing of isoforms, or loss of isoforms, have been shown to correlate with the development and/or progression of malignancy [247-249]. Therefore, targeting alternative splicing pathways may be a potential avenue for therapeutic intervention and identification of aberrantly spliced variants, and/or novel protein isoforms, which may be useful as a diagnostic biomarker in cancer. The SphK family of proteins, which is part of a much larger superfamily of structurally related lipid signalling kinases [250], is derived from alternate splicing of two different isozymes which lead to the expression of many variant isoforms that act to direct many physiological functions in the cell. There is strong evidence associating SphK overexpression and the development and progression of many different cancer types (Table 5.1).

Table 5.1 Overexpression of SphK is causally linked to cancer.

Cancer Sub-Type	Reference(s)
Breast	[228, 231, 251-265]
Leukaemia	[276-280]
Lung	[11, 281-284]
Pancreas	[285-288]
Renal	[289]
Colon	[290-292]
Ovarian	[293-298]*
Brain	[299-302]
Uterine Cervical	[303]*
Liver	[304-308]*

*SphK has been identified as potential diagnostic markers in human cancer patients. (Table updated from [16]).

In the absence of any known cancer-associated mutations in the SphK isozymes or isoforms, the term ‘oncogenic addiction’, where the cancer cell becomes reliant on SphK-S1P signalling for survival, has been proposed [309]. The relevance of aberrant dicing and splicing of SphK1 and SphK2 isozymes and the production of variant SphK isoforms in the development and progression of malignancy is very much underexplored. This review highlights and discusses our current knowledge of the SphK aberrant signalling that may contribute or drive SphK-coupled oncogenicity with particular interest directed towards the current understanding of SphK isozymes, alternatively spliced isoforms ‘dicing and splicing’ and the potential contribution of these isoforms to cancer cell biology and their influence on SphK/S1P based cancer therapeutics.

5.3 SphK isozymes and isoforms

5.3.1 Clarification of sphk nomenclature

Due to the disparity in SphK nomenclature in the literature, in this review SphK1 and SphK2 are referred to as isozymes (isoenzymes) and the variant SphK1 and SphK2 isoform identities are derived from GenBank and the literature and are summarised in Table 5.2.

Table 5.2 Nomenclature of SphK1 and SphK2 isozymes and protein isoforms.

Isozymes	Isoform Name	Isoform No.	Variant No.	GenBank Accession	Uniprot ID
Sphingosine kinase 1 (SphK1; SK1)	SphK1a	Isoform 3	Variant 3	NM_001142601	Q9NYA1-1
			Variant 4	NM_001142602	
			Variant X1*	XM-005257766	
	SphK1b	Isoform 2	Variant 2	NM_182965	Q9NYA1-2
	SphK1c SphK1a+14	Isoform 1	Variant 1	NM_021972	Q9NYA1-3
Sphingosine kinase 2 (SphK2; SK2)	SphK2a SphK2-L	Isoform 1 and 3	Variant 1	NM_020126	Q9NRA0-1
			Variant 3**	NM_001204159	Q9NRA0-3
	SphK2b SphK-S	Isoform 2	Variant 2	NM_001204158	Q9NRA0-2
	SphK2c	Isoform 4	Variant 4	NM_001204160	Q9NRA0-4
	SphK2d	Isoform 5	Variant 5	NM_001243876	Q9NRA0-5
			Variant X1	XM_017027008	Q9NRA0-5
			Variant X2	XM_011527133	Q9NRA0-1
			Variant X3	XM_006723292	Q9NRA0-2
			Variant X4	XM_011527134	Q9NRA0-2
			Variant X5	XM_017027009	
			Variant X6	XM_017027010	

*Variant X1 has been annotated using gene prediction methods supported by mRNA and expressed sequence tag (EST) evidence. ** Variant 3 also has the Uniprot ID Q9NRA0-1. Note: The nomenclature in this Table is derived from the GenBank and Uniprot entries. In some studies, SphK1b is referred to as SphK1c [310], however for direct comparison between studies, the Genbank accession numbers are consistent between studies.

5.3.2 SphK1 and SphK2 isozymes are transcribed from different genes and evolutionary conserved

It is less than 20 years since the human SphK isozymes were sequenced [311-313], substantiating evolutionary conservation across a wide range of organisms from mammalian species and plants, to yeast [240]. The first two human SphK isozymes described were SphK1a (isoform 3) [311] and SphK2a (isoform 2) [312]. Each isozyme is located on a different chromosome, SphK1 is located on chromosome 17 (17q25.2) and SphK2 is located on chromosome 19 (19q13.2) [312]. There is high sequence homology between the two SphK isozymes, believed to have evolved from a much larger superfamily of sphingosine and diacylglycerol (DAG) lipid signalling kinases, and not just a product of a simple gene duplication event [240, 250, 312]. The 3D structure of SphK, as illustrated by the SphK1a structure determined by Wang and colleagues, is very distinct from other protein kinase and lipid kinase families [314].

There is 47% identity in the N-termini and 43% identity in the C-termini of the SphK isozymes, with 80% similarity in their enzymatic activity [315]. The N-termini of both SphK isozymes contain five conserved domains (C1-C3) and the C-termini contain the C4 and C5 domain [218, 312]. Within the C1-C3 of both SphK isozymes resides a DAG kinase catalytic domain, conserved across the DAG and ceramide kinases [316]. Although the binding site for ATP has been found to be present within the conserved C2 domain, structural studies of SphK1 have shown that all the C1-C5 motifs contribute to ADP binding [218]. The C4 domain appears to be unique to the SphK family, setting SphKs apart from other lipids and enabling their unique ability to catalyse the conversion of sphingosine to S1P, thus making SphKs the sole source of S1P [218, 317]. Albeit this C4

sequence has the greatest diversity between the SphK1 and SphK2 isozymes, the domain responsible for sphingosine binding, suggesting this domain is responsible for preferred sphingosine substrate specificity [218, 317].

The major differences in the alignment of the two-original human SphK sequences are that SphK2 possesses an additional 236 amino acids at the N-terminal, a proline-rich insertion in the middle of the SphK2 C-terminal sequence [240, 312, 318] and a pro-apoptotic BH3 binding domain [319]. Although the crystal structure of SphK2 has yet to be solved, the unique upstream N-terminal region and the proline–rich insert of the SphK2 allow for major differences in conformational motility and protein-protein interactions between the two isozymes.

The extra sequence at the N-terminal of SphK2 provides for binding of a greater number of substrates such as the immunomodulatory SphK2 drug FTY720, which is now used in the clinic as a therapy for multiple sclerosis, and has already provided a prime example [258, 320].

Given both isozymes catalyse the conversion of sphingosine to its S1P active form, it is intriguing to note that different and opposing functions have been assigned to the two SphK isozymes, SphK1 is pro-survival whereas SphK2 is pro-apoptotic [321]. Explanations for this dichotomy is partly found in the subcellular localisation of these isozymes. SphK1 is predominantly cytoplasmic and upon agonist activation, such as growth factors [231], TNFα [322], and hormones [323], mainly mediated through ERK1/2 phosphorylation, which increases its activity and translocation to the plasma membrane [324]. Therefore, S1P can act as a dual 'inside-outside' messenger. Intracellular S1P catalysed by SphK can function as a second messenger inside the cell or S1P is exported outside the cell [258,

325]. Secreted extracellular S1P binds directly to S1P receptors (S1PRs) on the cell surface and signals in an autocrine and/or paracrine manner, termed as an 'inside-outside' mechanism of S1P action (Figure 5.2) [325]. Directed localisation of SphK1 post stimulation by agonists has also been found to increase its catalytic activity [234], for example agonist-induced translocation to the nuclear/perinuclear space, potentially the endosomal compartments showed a major increase in SphK1 enzymatic activity [326].

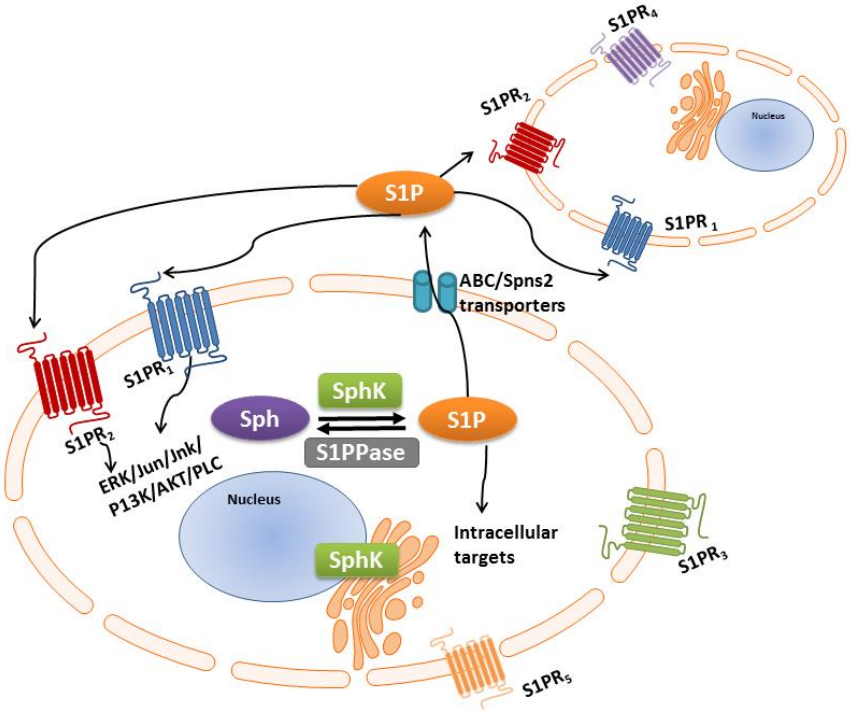

Figure 5.3 Complexity of SphK-S1P 'inside-outside' signalling. SphK is a lipid enzyme catalysing the phosphorylation sphingosine to its active form S1P. S1P can act in an autocrine or paracrine manner. S1P is exported extracellularly through the ABC [327] and Spns2 (Sphingolipid Transporter) 2 [328, 329] transmembrane proteins or can act intracellularly on yet unknown targets. S1P extracellularly activity occurs through the binding of one or more S1P receptors (S1P1-5) located on the plasma membrane, which are coupled to different internal G proteins which in turn activate or inhibit downstream signalling pathways. This complex S1P signalling paradigm extends the repertoire of diverse cellular and biological processes of the SphK family of lipid isozymes and isoforms.

On the other hand, SphK2 contains a nuclear localisation sequence (NLS) in its unique 236 N-terminal allowing both nuclear and cytoplasmic sub-cellular localisation depending on the cell milieu [318, 330].

Inside the nucleus, S1P produced by SphK2 activation can bind and inhibit histone deacetylases (HDAC)1/2 [318, 330, 331] and human telomerase reverse transcriptase (tHERT) [332], directly modulating cell cycle signalling cascades. In the cytosol, SphK2-endoplasmic reticulum generated S1P appears to be directed into biosynthesis of pro-apoptotic ceramide [321]. Additional studies have also shown the extra SphK2 BH3-binding domain inhibits the anti-apoptotic protein BCL-xL [318, 319], thereby conferring pro-apoptotic or anti-tumourigenic functions to SphK2. It is noted that there is emerging evidence that a small proportion of SphK isozymes are released into the extracellular milieu and produce S1P directly in the extracellular environment [310]. The exact function of SphKs in the extra-cellular environment is still unclear.

Further insights into the structure-function of SphKs, mainly focusing on the SphK1 structure, can be found in the recent article by Adams et al. [333].

5.4 Lessons from the SphK 'Isozyme' knockout mouse models from mouse to human

Most of the groundbreaking work in understanding the roles of mammalian SphK isozymes is from the SphKs knockout mouse models. Most importantly, although the two SphK isozymes have seemingly opposing functions, each have complementary and compensatory mechanisms. SphK1 and SphK2 knockout mice have provided exemplary models to study the effect on one or both isozymes in vivo [312]. During embryonic mouse development SphKs are temporally differentially expressed. SphK1 peaks at day

7 and decreases thereafter, whereas SphK2 gradually increases in expression up to day 17 [312]. Although SphK activity is present in all adult mouse tissues [334], a predominance of SphK1 is found in blood, lung, kidney, colon, spleen and lungs [334], whereas SphK2 predominance occurs in liver, kidney, brain, and heart [312]. In addition to differences in tissue distribution and sub-cellular localisation, differences are observed in isozyme kinetic properties in response to alteration in ionic strength and detergents, and differences in their preferred sphingosine substrates, whereby SphK1 has a preference for D-erythro-sphingosine and D-erythro-dihydrosphingosine over other substrates, where SphK2 also phosphorylates phytosphingosine [234]. Albeit major differences are observed in SphK isozyme expression in both embryological and adult tissues, ablation of one of the isozymes is not embryonically lethal, mice are viable and fertile with no obvious pathophysiology [237, 238, 335, 336]. These findings in SphK1$^{-/-}$ and SphK2$^{-/-}$ mouse models clearly demonstrate that the two isozymes have overlapping functions in development. In reality, both SphKs have been found in the extra-cellular environment, therefore able to generate S1P both intra- and extra-cellular thus expanding their repertoires and rapidity of signalling events [310]. In contrast, when both SphK isozymes are ablated mouse embryos do not survive, presenting with neurological and vascular developmental defects, thereby determining an undisputable role for SphKs/S1P signalling in mammalian development [236].

On further scrutiny, pathological differences in the SphK1$^{-/-}$ and SphK2$^{-/-}$ mice have started to emerge. A few examples include, mice deficient in SphK1 were rendered lymphopenic by FTY720 [238], endogenous SphK1 demonstrated a protective role in renal ischemia whereas SphK2 had a detrimental role [337], and in separate studies SphK1$^{-/-}$mice demonstrated a very poor survival following cardiac arrest [338]. Recently,

mice lacking SphK2 were found to have 85-90% reduction of brain S1P and impairment of contextual fear memory [339]. In addition, in a breakthrough finding, presented SphK2/S1PR2 signalling, not SphK1, as an important enzymatic pathway involved in regulating hepatic lipid metabolism [340-344]. Dysregulation of the SphK2/S1P2 signalling pathway in mice fed on a high-fat diet were more susceptible to the development of fatty liver and related diseases through regulation of conjugated bile acids, important hormones produced during the feed/fast cycle [344]. Impaired bile formation and flow (cholestasis) has been associated with increased SphK2/S1P/S1PR2 activation and blocking this pathway with the specific S1PR2 inhibitor (JTE-013) reduced cholestatic liver injury through reduction of total bile acid levels in serum [345].

In the context of cancer development, there is some suggestion that SphK1 depletion may have some protective effect against the development of some cancers, for example $SphK1^{-/-}$ mice were less inclined to develop colon cancer [292, 346]. Treatment of tumour-bearing mice with SK1-I (SphK1 inhibitor), decreased S1P levels in both circulation and the tumour that significantly decreased the tumour see, angiogenesis and lymphangiogenesis [260]. In $SphK2^{-/-}$ mice, SphK1 was upregulated to compensate for the loss of SphK2 associated with increased circulating S1P [346]. The increased S1P levels were associated with inflammation and risk of colitis-associated cancer [346].

The lessons we may take from these mouse studies are that although there are no overt physiological differences observed when one SphK isozyme is depleted, there are downstream consequences for how the body compensates for this loss and potentially increased vulnerability to cancer and other diseases.

5.5 SphK1 and SphK2 isozymes transcribe multiple variant isoforms

Sphingosine kinase isozymes have multiple alternatively spliced isoforms, which are listed in Table 5.2. The variant isoforms of both SphK1 and SphK2 identified provide greater functional diversity to this lipid kinase family. Whilst many alternative human SphK variant isoforms have been identified and characterised, determining the function of each isoform is yet to be completed. Our knowledge of SphK isoform specificity and function in humans is severely limited, mainly due to the strong overlapping and compensatory roles of the isozymes and isoforms in normal physiology. All the SphK isozymes and isoforms catalyse the same reaction (sphingosine-S1P) making it extremely difficult to extrapolate individual and compensatory functions for each of the isozymes and more so for the isoforms. Most of the early studies on human SphK1 and SphK2 did not specify the isoform examined, and as the S1P activity has been shown to be similar between the different isoforms it has not been a high priority research area. Only a few studies have focused on the differences between the SphK isoforms and these have focused on the major SphK1a and SphK1b and the SphK2-S and SphK2-L. In addition, although the SphK2a gene was cloned in both human and murine cells in 2000 [312], the SphK2 larger isoform SphK2-L (SphK2b) was not found in mice [345]. Since SphK2 isoform 2 (b) appears to be specific to humans, studies on this isoform 2b have been performed in cell lines only [318]. Currently only the overexpression of each human SphK 'isoform' in cell culture has shed some light into how they control different signalling pathways within the cell, and the functional consequences of overexpressing SphK individual isoforms against a background of endogenous SphK expression.

5.6 SphK1 variant isoforms—differences in dicing, splicing and localisation

Three unique SphK1 isoforms have been characterised in humans which differ only in their N-terminal region (Table 5.2; Figure 5.3). Isoform 2 is the longest isoform with a molecular weight of 51KDa, whereas the shortest isoform is isoform 3, 42.5kDa, and isoform 1 has an extra 14 amino acids, 43.9kDa. In addition, NCBI reports a predicted variant known as variant X1 which is not identified as protein and has been annotated using a gene prediction method and supported by mRNA and EST evidence. These isoforms are the result of alternative splicing variants, variant 1 and variant 2 encode isoforms 1 and 2 respectively, while variant 3 and variant 4 both encode isoform 3 (Figure 5.3). Distinguishing isoforms 1 and 3 on SDS PAGE is not plausible as they have a very similar molecular weight, while isoform 2 with an extra 86 amino acids is easy to be separated [347, 348]. Comparison of the mammalian SphK1 and Sphk2 indicated that they all contain five highly conserved regions involved in the ATP binding and catalytic conversion of sphingosine to S1P.

Only a few studies have shown the localisation of different isoforms in various tissue types. Most of the studies used the overexpression of the isoform 1 or 2 in human cells for characterisation and determination of their biological significance [347-350]. Moreover, most of these *in vitro* studies used the SphK1 isoform 1 to study the function and structure of the SphK1 [333]. Both isoforms 1 and 2 translocate to the cell membrane, interestingly, the SphK1a (isoform 3) has been shown to be secreted from cells with more involvement in S1P/S1PR1 extracellular activity compared to SphK1b (isoform 2) and SphK1c (isoform 1) which appeared to remain mainly in the plasma membrane [350].

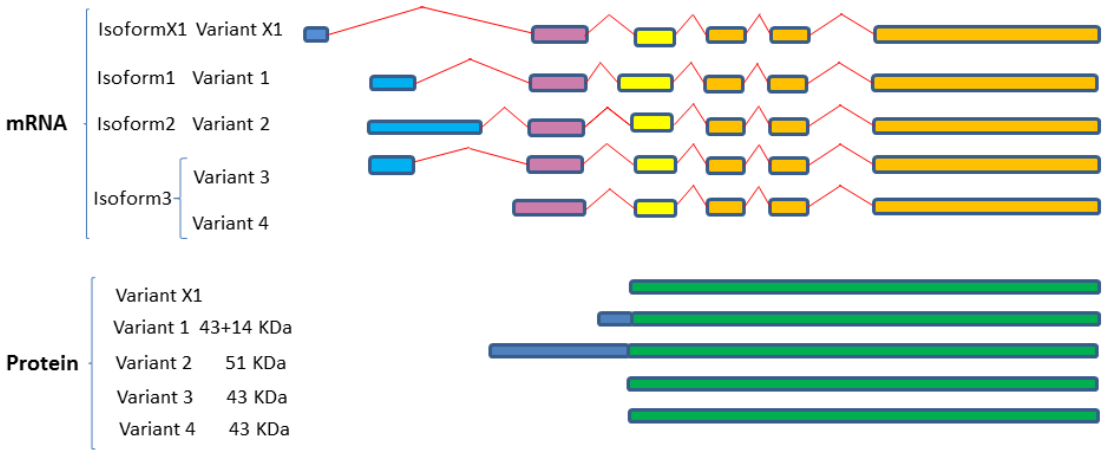

Figure 5.4 Variant splicing and dicing of human SphK1 isoforms. Schematic diagram of SphK1 splice variants and protein isoforms based on mRNA and protein sequences acquired from GenBank. Colored boxes are representative of different RNA fragments and protein fragments, same color boxes are originated from the same origin of DNA sequences and are identical/similar sequences. Expression from four variant mRNA transcripts (variants 1–4) results in three SphK1 isoforms (isoforms 1–3). A predicted fifth human SphK1 splice variant (variant X1), based on sequence prediction methods, results in a predicted fourth isoform (isoform X1) (annotated using gene prediction software and further evidenced by mRNA and EST). SphK1 sequences were aligned using Clustal Omega (V1.2.4) multiple sequence alignment (Available online: http://www.ebi.ac.uk/Tools/msa/clustalo/).

5.7 Over-active sphk-s1p signalling and relevance to cancer

Although there is a strong, indisputable, causal association between adverse SphK/S1P signalling and cancer, to date there have been no reports of SphK/S1PR mutations linked to cancer development and it has been suggested that cancer cells develop a dependence on SphK cellular signalling, referred to as 'non-oncogene addiction' [309]. In addition, overactive SphK signalling is causally associated with treatment resistance, in particular endocrine resistant tumours [351]. In a recent review S1P levels were a

good indicator of clinical outcome in breast cancer patients, increased S1P was associated with drug resistance to common drug therapies (hormone, herceptin (HER2) and chemotherapies) [262]. To this end, novel inhibitors of SphK activity have been designed and successfully tested and characterised in human cancer cells and primary cancer cells from patient samples as listed in Table 5.3.

Table 5.3 SphK inhibitors tested in human cancer cells and primary human cancer cells.

SPHK Inhibitor	Cancer Cell Type	SphK Selectivity	References
B5354-c	Prostate (LNCaP, Du145 and PC-3) Breast (MDA-MB-231)	SphK1	[268, 352]
F-12509a	Leukaemia (HL-60, LAMA-84 and HL-60 MDR) Chronic Myeloid Leukaemia blasts	SphK1	[353]
SK1-I	Glioma (U87MG, LN229 and U373) and Primary Glioma Cells (GBM6) Leukaemia (U937, HL-60 and Jurkat) and Acute Myeloid Leukaemia blasts Breast cancer (MDA-MB-231, MCF-7 and MCF-7 HER2) Prostate [LNCaP]	SphK1	[10, 260, 347, 354-356]
SKI-II	Prostate (LNCaP, C4-2B and PC-3) Pancreas (Panc-1 and BXPC-3) Bladder (T24) Breast (MCF7)	SphK1 and SphK2	[267, 274, 357-360]
ABC294640	Pancreatic (clinical trial) and (Panc-1) Colorectal (HT-29 and Caco-2) Breast (MCF-7, MDA-MB-231) Ovarian (SK-OV-3) Prostate (DU145) Kidney (A-498) Melanoma (1025LU) Bladder (T24) Liver (Hep-G2)	SphK2	[360-362]

Safingol	Solid tumours (clinical trial)	SphK1 and SphK2	[361, 363, 364]
	Glioblastomas		
	Colorectal tumour		
	Colorectal (HCT116)		
	Adrenal cortical carcinoma		
	Sarcoma		
N,*N*-dimethyl-D-*erythro*-sphingosine (DMS)	Acute myeloid leukemia (HL-60, U937, CMK7)	SphK1 and SphK2	[365-371]
	Chronic myeloid leukemia (JFP1, K562)		[372]
	Gastric (MKN45, MKN74, Kato III)		[373, 374]
	Acute lymphoid leukemia (Jurkat)		[375, 376]
	Lung (LU65, NCI-1169, A549)		[373]
	Cervix carcinoma (KB-3-1)		[377]
	Colon (Colo205, SW48, SW403, SW1116, SW1417, HT29, LS174T, LS180, HRT18)		[367, 373]
	Pheochromocytoma (PC-12)		[378, 379]
	Prostate adenocarcinoma (LNCaP)		[380]
	Melanoma (M1733, F10, F1, BL6)		[373]
	Hepatoma (Hep3B)		[381]
	Epidermoid carcinoma (A431)		[367, 373]
	Breast adenocarcinoma (MCF7)		[255]
	Acute myeloid leukemia (HL-60, P388, U937, NB4)		[369, 370, 382, 383]
	Lymphoma (WEHI-231)		
L-*threo*-dihydrosphingosine (DHS)	Breast adenocarcinoma (MCF7)	SphK1 and SphK2	[384, 385]
	Hepatoma (Hep3B)		[184]
	Neuroblastoma (SH-SY5Y)		
	Melanoma (A2058, 939, C8161)		[386]
	Prostate (PC-3, LNCaP-C4-2B, and DU145)		[387-391]
FTY720 (fingolimod)	Ovarian cancer (OV2008, IGROV-1, A2780, SKOV-3, R182)	SphK1	[191]
	Bladder (T24, UMUC3 and HT1197)		[192]
	Glioblastoma (U251MG and U87MG)		[193]
	Hepatoma (HepG2, Huh-7 and Hep3B)		[194]
K145	Leukemia (U937)	SphK2	[392]

5.8 SphK1 isozyme is overexpressed in multiple cancer types

Functionally SphK1 is the major isoform linked with many of the hallmarks of cancer and it has historically been identified as a major driver of cancer with a shorter overall survival in many human cancer patients [393], contributing to chemoresistance and poor survival. Overexpression of SphK1 is linked to oncogenicity through various mechanisms such as imbalance of SphK1/S1P, enhancing oncogene Ras, promoting cancer stem cell proliferation to increase tumorigenesis, and imbalance between intracellular and extracellular S1P [394]. Aberrant SphK1 is also involved in the neovascularisation of tumours involving paracrine angiogenesis and lymphangiogenesis [356, 395, 396]. Knockdown of SphK1 in breast and glioma cancer cells have been found to reduce migration and tube formation [356]. There have been numerous compounds designed to target SphK, albeit with limited efficacy in clinical trials [397]. However, given the importance of SphK1 in malignancy, it is anticipated that new SphK1 targets will be discovered, especially for hard to treat cancers that overexpress SphK1. For example, recently, Zhu et al [298] found that a calcium and integrin binding protein CIB2 proved to be a novel and valuable target, which downregulated SphK1 signalling in ovarian cancer, suggesting CIB2 as a new therapeutic SphK1-targeted candidate for ovarian cancer.

5.9 'Dicing and splicing' sphingosine kinase variant isoforms and relevance to cancer

Due to the heterogeneity of cancers, the major problem with cancer treatments and the major cause of cancer-related deaths is resistance and recurrence to current therapies resulting in metastasis. Coming into the limelight as switches in cancer progression are

the ‘dicers and splicers’ of introns and exons, whereby aberrant splicing and the loss of expression of particular isoforms of importance are associated with malignancy [247-249]. SphK is no exception in this case.

5.10 Homing into SphK1 isoform expression in anti-cancer targets

Although little is known about alternative splicing of SphK in cancer, we know that alterations in SphK isoform expression lead to changes in the direction of SphK signalling pathways [35]. The additional N-terminal 86 amino acids of SphK1b allows for specific partner binding to this unique region. As described by Yagoub and colleagues [35], in general, isoform-specific interactions were more frequently observed with the SphK1b (51 kDa) isoform. This N-terminal amino acid extension of SphK1b also allows for conformational differences between the two major isoforms, thus also facilitating SphK1a, as well as SphK1b, isoform-specific partner interaction [35]. These results present a case for alterations in isoform abundance ratios conveying differences and similarities in SphK downstream signalling events. That said, we and others have shown that both isoforms have the same S1P activity and do not exhibit any overt phenotypic changes in cell morphology or function [35,132,133]. On further scrutiny, what we are finding is that changes in SphK1a and SphK1b expression levels can make cancer cells more vulnerable to treatment resistance. For example, in the immunoprecipitation study of Yagoub and colleagues, SphK1b interacted preferentially with dipeptidyl peptidase 2 (DPP2), a protein targeted in diabetic therapy and involved in the regulation of glucose metabolism [35]. Treatment with a DDP2/4 inhibitor in hormone-dependent breast cancer cells enhanced SphK1b expression with no change in SphK1a. Similarly, Pyne and colleagues demonstrated differences in the treatment response in prostate

cancer depending on enhancement of specific SphK1 isoform expression [132,133]. Enhancement of SphK1b in androgen-independent prostate cancer cells altered anti-SphK drug efficacy [47,132,133]. Although there are no current studies exploring the expression of SphK specific isoforms in cancer patients, these initial in vitro studies in cancer cell lines, suggest that differences in SphK1 isoform expression may be relevant in anti-SphK/S1P/S1PR cancer-based therapies.

5.11 Aims of the study

As the importance of the functional differences between the two SphK1 isoforms becomes apparent, the question of whether both SphK1 isoforms are expressed in the same cell, or whether all cells express one or both SphK1 isoforms becomes a critical one to answer. To answer these basic questions, the aims of this part of the thesis are:

1) To design PCR primers and optimise PCR amplification parameters for SphK1 isoform specific amplification and detection of SphK1 isoform expression.
2) To investigate and determine the frequency of expression of the two SphK1 isoforms, SphK1a and SphK1b, in a series of cancer cell lines.
3) To investigate and determine the frequency of expression of the two SphK1 isoforms, SphK1a and SphK1b, in different primary cancer and adjacent patient tissue samples.

CHAPTER 6

OPTIMISATION OF METHODOLOGY FOR DETECTION OF SPHK1 ISOFORM EXPRESSION

6.1 Introduction

This Chapter addresses the first aim of Part 2 of this thesis: *to design and optimise SphK1 specific isoform PCR primers for the identification of SphK1 isoform expression.*

The SphK1a and SphK1b differ only at the N-terminal, whereby SphK1b has a unique additional region of 86 amino acids (Figure 5.3). Two SphK1 constructs, SphK1-43kDa (SphK1a) and SphK1-51kDa (SphK1b) have been previously constructed and stably transfected into MCF-7 cells as described in methods and results below. These cell lines were used as controls in all experiments to verify the SphK1-PCR conditions in cell lines (*in vitro*) and human tissues (*in vivo*). Specific primers were designed to overlap the unique SphK1b region to determine the presence of the SphK1b isoform, and primers designed within the common SphK1a and SphK1b region. From the designed primers two primer sets, one overlapping the upstream SphK1b-SphK1a region and one within the SphK1a region, that were proved to be the most efficient, were used for all further experiments to investigate and determine the expression of SphK1 isoforms in all cell lines and tissue samples tested.

6.2 Methods and Results

6.2.1 SphK1 isoform expression in MCF7 stable cell lines

SphK1a and SphK1b were isolated from human placenta, umbilical vein endothelial cells (HUVEC), then inserted into cDNA3.1 vectors (containing Flag-TAG) and sequenced [14, 398]. SphK1a and SphK1b sequences were verified in our laboratory and neither SphK1 sequence contained the extra 14 amino acids described for the SphK1c variant (Figure 5.3). Overexpression of the isoforms in MCF-7SphK1a and MCF-

7SphK1b was verified by western blot analysis using Anti-flag m2 mouse F1804-1MG from Sigma Aldrich (Figure 6.1).

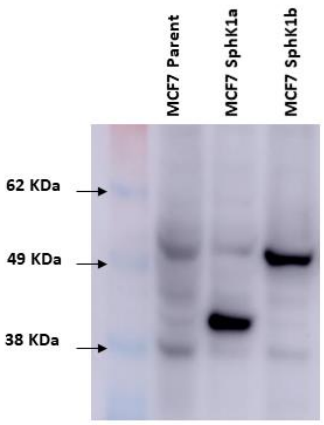

Figure 6.1. Verification of expression of exogenous SphK1a and SphK1b in stably MCF7 transfected cells by western blot. MCF-7SphK1a an MCF-7SphK1b cells were lysed and equal amounts of protein were loaded onto SDS-PAGE gels and transferred to PVDF membranes. Membranes were probed with anti-FLAG antibody. MCF-7 parent cells were used as a control.

6.2.2 Optimisation of PCR parameters

6.2.2.1 Optimisation of the SphK1-PCR primers

To investigate the expression of SphK1-51kDa (SphK1b) and SphK1-43kDa (SphK1a), 12 SphK1-specific PCR primers were designed (Figure 6.2). Two forward primers were located in the unique SphK1b-51kDa upstream region of the gene (Figure 6.2A) and 10 primers (forward and reverse) were located within the SphK1a-43kDa region (Figure

6.2A). The locations of the PCR primers are shown on the SphK1 sequences downloaded from the ncbi website (accession number NM_182965.2) (Figure 2B). The projected size of the SphK1-PCR amplified products, alongside the SphK1 sequence locations are listed in Figure 6.2C. Each of the 6 primer sets (Figure 6.2C) were tested to determine the optimal PCR conditions for each primer set using the MCF-7-SphK1b stably transfected cells.

All cell lines were cultured until 70% confluency and RT-PCRs were performed as described in Chapter 2, sections 2.2.6 to 2.2.8. Figure 6.3 shows a representative agarose gel with the test results for the optimal annealing temperatures for SphK1 primers F3-R4. A direct comparison of each of the 6 sets of SphK1-primers was performed using the MCF-7 parent cells (P) and MCF-7-SphK1a (43) and MCF-7SphK1b (51). The results are shown in Figure 6.3C. Primer sets F1-R2, and F5-R6 were specific for the SphK1b isoform as the primers crossed the SphK1-51-43 boundary (Figure 6.3A). Primers F1-R2 picked up the endogenous SphK1b in the MCF-7 parent (P), and MCF-7SphK1a (43) and a very clear band was observed in the MCF-7SphK1b cells, which overexpressed the SphK1b isoform (Figure 6.3C). Primers F5-R6 were not as effective at amplifying the SphK1 product compared to primers F1-R2 (Figure 6.3C). Primer sets F3-R4, F7-R8, F9-R10 and F11-R12 were all located in the SphK1a domain, common to both isoforms. Efficiency of PCR amplification was, F3-R4 > F7-R8 > F9-R10 > F11-R12, with primer set F3-R4 being the most efficient and F11-R12 performing poorly, as depicted by the PCR band intensity.

A.

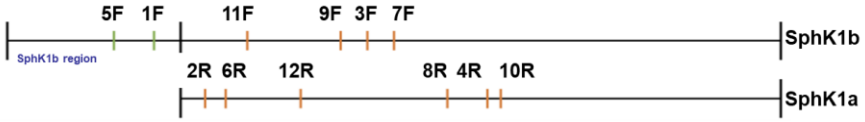

B.

```
   1 agtgccctcc ccgctccgcg gcgccggctg cgaagttgag cgaaaagttt gaggccggag
  61 ggagcgaggc cggggagtcc gctccagcgg ggcgctccag tccctcagac gtgggctgag
 121 cttgggacga gctgcgttcc gccccaggcc actgtaggga acggcggtgg cgcctcccca
 181 gcaaaccgga ccgactgggt agggccgccc accctgcctt cgcgccgctc gtggctcctg
 241 tgcggcccgc cctcgcgggg ccccgggaac tgggccactt gtcgcttggg cgagagcagg
 301 cggcagctgg tggcccggtt cgggcttggc tttggcgcga cccgggagcg gctcccacga
 361 gcgccgcgcg cgtcgcaacg gagcggggcc ctgagaagcg cgcgccgcgg ctcccaccgc
 421 tctggagctc cgggcagggg acacggcaac ctggatggct ggggcaggga tcctctccca
 481 gaacttcgtg cccagcaatg tccgctcaag ttctgggatt tttacgcagc tggactcccc
 541 tccccctggc agccccgagg ggtccagccg ccgcagggaa tgacgccggt gctcctgcag
 601 ccacggctcc gggcggggaa ggcgagcccc acagccggcc ctgcgacgcc cgcctgggca
 661 gcacctataa ggagctgaag gcacgagccg ccgccacggg cagcgccccc acagcgccag
 721 ggacccctg gcagcgggag ccgcggggtcg aggttatgga tccagcgggc ggcccccggg
 781 gcgtgctccc gcggccctgc cgcgtgctgg tgctgctgaa cccgcgcggc ggcaagggca
 841 aggccttgca gctcttccgg agtcacgtgc agccccttt ggctgaggct gaaatctcct
 901 tcacgctgat gctcactgag cggcggaacc acgcgcggga gctggtgcgg tcggaggagc
 961 tgggccgctg ggacggtctg gtggtcatgt ctggagacgg gctgatgcac gaggtggtga
1021 acgggctcat ggagcggcct gactgggaga ccgccatcca gaagcccctg tgtagcctcc
1081 cagcaggctc tggcaacgcg ctggcagctt ccttgaacca ttatgctggc tatgagcagg
1141 tcaccaatga agacctcctg accaactgca cgctattgct gtgccgccgg ctgctgtcac
1201 ccatgaacct gctgtctctg cacacggctt cggggctgcg cctcttctct gtgctcagcc
```

C.

Primer No.	Primer Sequence		Mapping position	Length of PCR Products (bp)
F1 -R2	SK1-F1	5' TTTACGCAGCTGGACTCCCCT	521 – 541	164 bp
	SK1-R2	5' CTGCCTTCAGCTCCTTATCGG	664 – 684	
F3 -R4	SK1-F3	5' GGCTGAGGCTGAAATCTCCTT	881 – 902	289 bp
	SK1-R4	5' GCAGTTGGTCAGGAGGTCTTC	1149 – 1169	
F5 -R6	SK1-F5	5' CGCTCAAGTTCTGGGATTTTT	503 – 523	185 bp
	SK1-R6	5' CTCCTGCCTTCAGCTCCTTAT	667 – 687	
F7 -R8	SK1-F7	5' ATCTCCTTCACGCTGATGCT	894 – 913	103 bp
	SK1-R8	5' CTCCAGACATGACCACCAGA	977 – 996	
F9 -R10	SK1-F9	5' TTTGGCTGAGGCTGAAATCT	878 – 897	306 bp
	SK1-R10	5' CACAGCAATAGCGTGCAGTT	1164 – 1183	
F11 -R12	SK1-F11	5' ATAAGGAGCTGAAGGCAGGAG	667 – 687	100 bp
	SK1-R12	5' GCTGGATCCATAACCTCGAC	747 – 766	

Note: F = Forward primer, R = Reverse primer

Figure 6.2 SphK1 forward and reverse PCR primer sequences and locations. SphK1 (SK1) accession number NM_182965.2 was accessed using the Blast search engine from the NCBI website (http://blast.ncbi.nlm.nih.gov/Blast.cgi). **A.** Schematic showing the approximate position of the SphK1 primers. **B.** SphK1 PCR specific primers (Forward and reverse) positions are mapped and highlighted. **C.** Tabulation of each PCR primer (forward and reverse) show the exact mapped position and the size of the expected amplified SphK1-PCR product. Note: the colours of the mapping positions are colour coded in B and C.

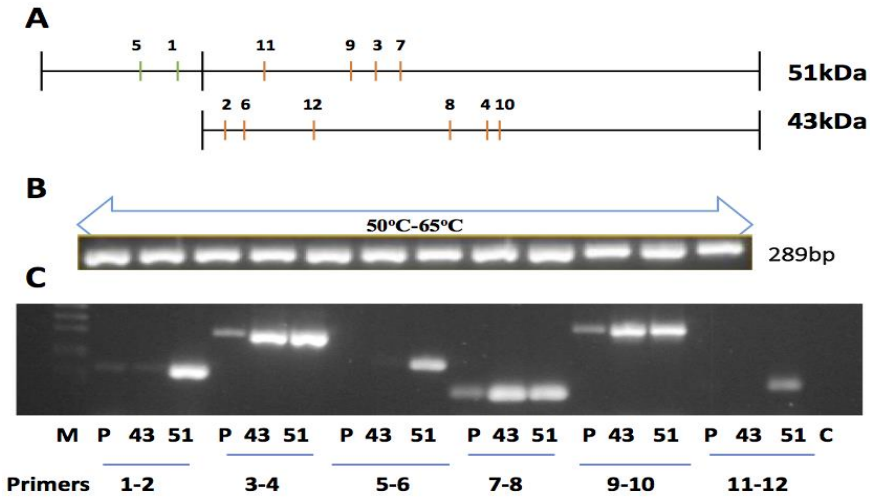

Figure 6.3. Optimisation and selection of SphK1 isoform PCR primers. Each of the primer sets shown in Fig. 6.2C were optimised to determine the most efficient amplification procedures. (A) The schematic showing the SphK1-specific forward and reverse PCR primers is reiterated to show relative positions for the forward and reverse primers. All SphK1 primer sets were optimised at a gradient annealing temperature of 50°C-65°C, tested using MCF-7 stably transfected SphK1-51kDa cells. (B) Representative electrophoresis gel using SphK1 primers F3-R4. (C) SphK1 primer sets (F1-R2, F3-R4, F5-R6, F7-R8, F9-R10, F11-R12) were tested in parent MCF-7 (P), MCF-7-SphK1a (43), and MCF-7-SphK1b (51) cell lines. C = control, no primers. M = bioRad 100bp marker.

Different combinations of SphK1 primers were explored, however any attempt to amplify across the region located between nucleotides 766-878 on SphK1a, proved unsuccessful. Thus, this region was subsequently referred to as the "SphK1 Bermuda Triangle" (Figure 6.4). SphK1 primer sets that crossed this region, including primer sets, F11-R8, F11-R4, and F9-R8, did not produce a PCR product. However, SphK1 primers used outside this domain (and did not overlap the region 766-878), including primer sets F1-R2, F3-R4, F3-R8, F9-R8, produced a SphK1 product. This 766-878 region was GC rich and upon further investigation contained hairpin-loops, which accounted for the difficulty in using this region for SPhK1-PCR amplification.

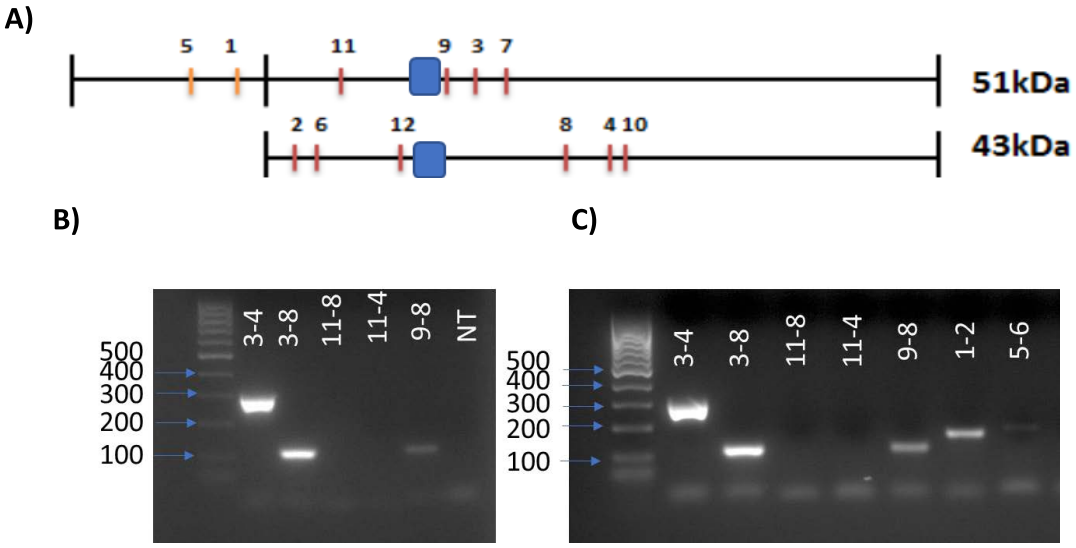

Figure 6.4 SphK1 'Bermuda triangle'. A) Schematic of the SphK1 primer locations showing the "SphK1 Bermuda Triangle' domain" (shown in blue). No combination of SphK1 primers crossing this section, between nucleotides 766-878 on SphK1a, produced a clear PCR amplification product. B) PCR with SphK1 primer combinations, F3-R4, F3-R8, F11-R8, F11-R4, F9-R8, amplified from MCF7 SphK1a cells. C) PCR with SphK1 primer combinations, F3-R4, F3-R8, F11-R8, F11-R4, F9-R8, F1-R2, F5-R6, F1-R4 amplified from MCF7 SphK1b cells.

6.3 Summary and conclusion

In this section, 6-sets of SphK1-specific primers, to identify if SphK1a and 1b were expressed in the same cell or same human tissue, were designed, optimised and compared. Further, different combinations of individual SphK1 primers were trialled to determine the most efficient and simple PCR amplification for SphK1 isoform identification. The most effective and efficient SphK1-primers proved to be primer set F1-R2, which was specific for Sphk1b (crossing the SphK1a-SphK1b boundary), and primer set F3-R4, which was used to detect SphK1a, although common to both isoforms (summarised in Figure 6.5). These SphK1 primers were used in all further experiments, both *in vitro,* in cell lines, and in *vivo,* in human tissue samples, to determine if one or

both isoforms were expressed in different cell lines and human cancers. An interesting observation was that, even though the RT-PCR results were qualitative, not quantitative, both isoforms were amplified in the parent MCF-7 breast cancer cells using both primer sets, suggesting, from this optimisation step that both isoforms are expressed in MCF7 breast cancer cells.

While similarities between the isoform sequences presented a limitation, this was overcome by using a variety of specific primer pairs and repetition of all the PCR assays to ensure reproducibility.

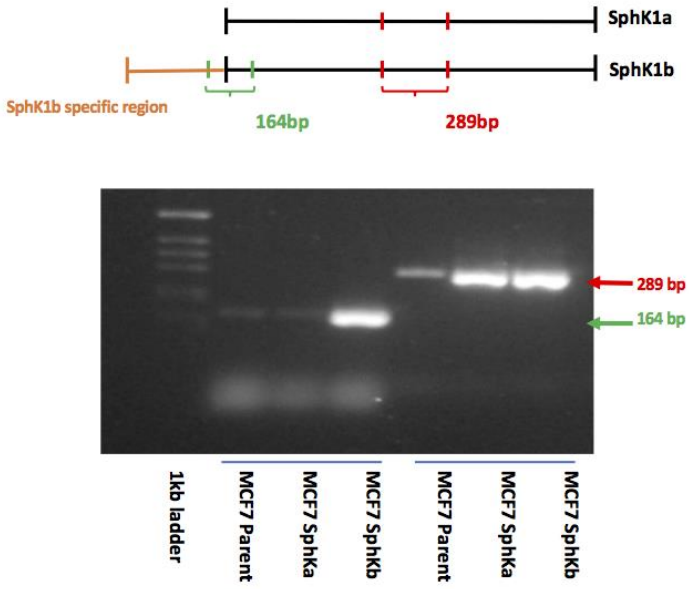

Figure 6.5 MCF-7 cells express both SphK1b and SPhK1 isoforms. The top schematic shows the positions of Primers F1-R2, and F3-R4. Primers F1-R2 amplify a 164bp SphK1b specific product which lies across the SphK1b and SphK1a border. Primers F3-R4, are located within the SphK1a region and amplify a product of 289bp. Agarose gel: results from the PCR amplification in MCF-7 parent, MCF-7SphK1a and MCF-7SphK1b using primers F1-R2 and F3-R4. Primers F1-R2 amplified a strong band in the SphK1b cells and a faint (endogenous) band in the parent and SphK1a expressing cells. Primers F3-R4 amplified a strong band in both SphK1a and 1b expressing cells, and a faint endogenous SphK1 band in the parent cell line.

CHAPTER 7

SPHK1 ISOFORM ANALYSIS

7.1 Introduction

High expression of SphK1 is causally associated with cancer and reduced overall 5-year survival rates [271, 393]. However, as SphK1 positivity differs in different cancer types and in different patients, it is difficult to predict whether SphK1 is a good predictor of patient outcome in all cancers. This is exemplified when we used the Kaplan Meier Plotter (KMplot.com), an online survival analysis tool, to determine SphK1 as a predictor of specific cancer outcome.

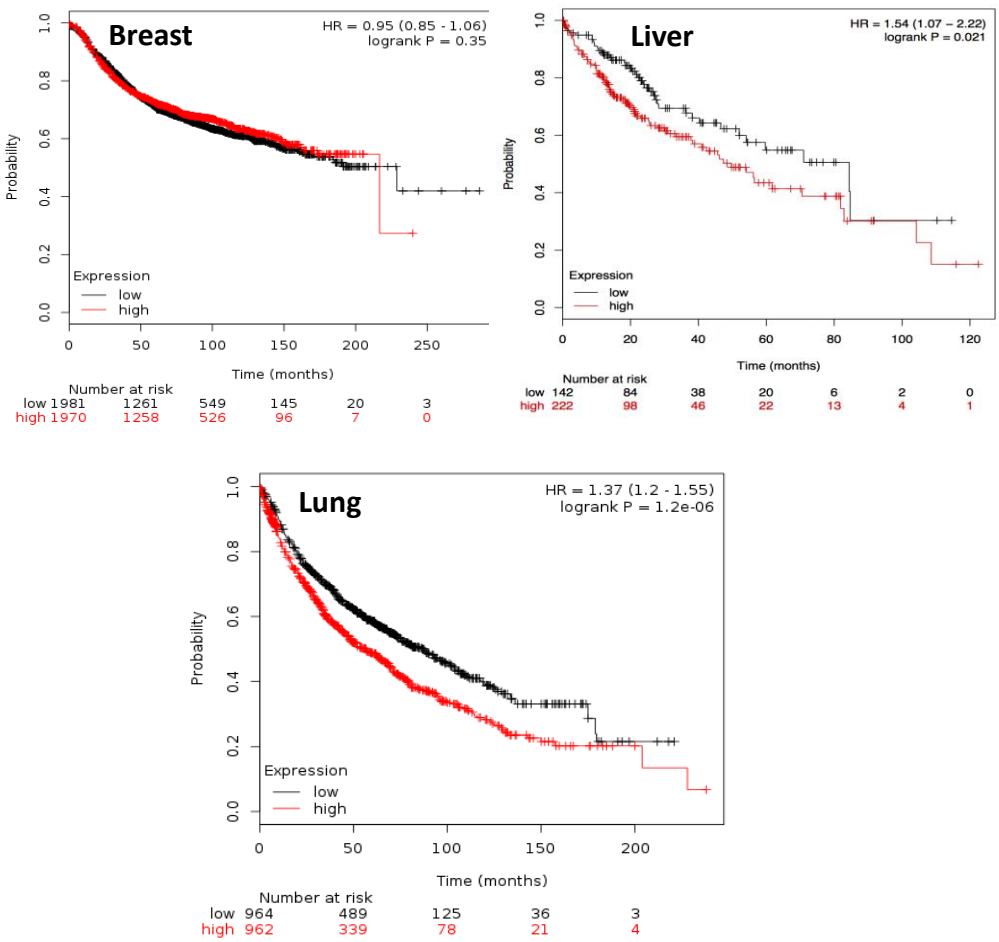

Figure 7.1 SphK1 is not a predictor of RFS in all cancers. The KMPlot (kmplot.com) was used to determine SphK1 as a predictor of RFS in breast [399], liver [400] and lung [401] cancers. As denoted on the graphs, the black lines refer to low SphK1 expression and the red line refers to high SphK1 expression.

As shown in Figure 7.1, overall relapse free survival (RFS) in nearly 3000 breast cancer patients without treatment showed no significant difference in patients with low or high expression of SphK1. Conversely, in liver (364 patients) and lung cancers (1926 patients) SphK1 expression was a significant predictor of poor RFS ($P<0.05$). There was a significant correlation of SphK1. Despite these generalised predictions, in some cases different cancers may respond differently to treatment if SphK1 is overexpressed. An example being breast cancer where *in vitro* studies causally associate endocrine resistance with SphK1 overexpression [351].

From our limited knowledge differences in the expression of individual SphK1 isoforms in human cancers may have consequences leading to either increased or decreased vulnerability to resistance to cancer treatments [259, 347, 348]. To date, we have no information on the expression of the various SphK1 isoforms in normal and malignant human tissues, however what is emerging is that different tissues express different SphK isozymes and S1P receptors, and it is, therefore, not unreasonable to expect differential SphK1 isoform expression through alternative splicing events that is dictated by the cellular and metabolic milieu. The possibility and consequences of SphK1 isoform instability in human cancers is yet unexplored, even though aberrant SphK isozymes and altered expression and sub-cellular location of isoforms has been observed and, together, may contribute to cellular transformation and cancer. With current knowledge exposing the increasing complexity of SphK/S1P/S1PR signalling and the dependency on this signalling pathway in different cancer cell types, it is apparent that further study is of importance to characterise the specificity of SphK1 isoforms in cancer tissues when seeking new diagnostic targets and therapeutic interventions.

This Chapter addresses Part 2: Aims 2 and 3 as outlined below:

2) To investigate and determine the frequency of the expression of the two SphK1 isoforms SphK1a and SphK1b in cancer cell lines.
3) To investigate and determine the frequency of the expression of the two SphK1 isoforms SphK1a and SphK1b in cancer and adjacent patient tissue samples.

Note: The experiments conducted in this Chapter are qualitative, not quantitative data. The aims were, as a first step, to determine if both SphK1 isoforms were expressed in all cancer and normal tissues tested. This question has not been previously addressed.

7.2 Methods

7.2.1 Cell culture.

Cells lines tested for expression of SphK1 isoforms are listed in Table 1. Cancer cells were cultured in DMEM with 10% FBS or RPMI1640 with 10% FCS depending on the cell type. Primary cell lines were cultured in alpha-Minimum Essential medium (α-MEM) supplemented with 2 mM L-glutamine, 100 U/ml penicillin/streptomycin, 20% FCS, 10ng/mL recombinant basic-fibroblastic growth factor. All cell lines were regularly tested for mycoplasma using the Lonza MycoAlert^{TM} Plus mycoplasma detection kit and were mycoplasma free.

7.2.2 Cell lines:

Cell lines used for the identification of SphK1 isoforms are listed in Table 7.1. Mesothelioma cell lines were kindly donated by Dr Glen Reid Asbestos Disease Research Institute (ADRI). The prostate cancer cell lines were kindly donated by the late Robert Sutherland, Garvan Institute, Sydney.

Table 7.1 Cell lines used for the identification of SphK1 isoforms

Cancer type	Reference/source
Breast Cancer (epithelial)	
MCF-7 luminal A (ER+/PR+/HER2-)	ATCC® HTB-22™
T-47D luminal A (ER+/PR+/HER2-)	ATCC® HTB-133™
Cervical cancer	
HeLa	ATCC® CCL-2™
Bone cancer (Epithelial)	
U-2OS	ATCC® HTB-96™
Prostate cancer (Epithelial)	
DU 145 (androgen independent)	ATCC® HTB-81™
LNCaP (androgen dependent)	ATCC® CRL-1740™
PC-3 (androgen independent)	ATCC® CRL-1435™
VCaP (androgen independent)	ATCC® CRL-2876™
Colon cancer (Epithelial)	
HCT 116	ATCC® CCL-247™
HT29	ATCC® HTB-38™
Brain cancer (Epithelial)	
U-87MG	ATCC® HTB-14™
Mesothelioma (Epithelioid)	ATCC® CRL-5820™
NCL-H28	ATCC® CRL-5820™
NCL-H226	ATCC® CRL-5826™
NCL-H2052	ATCC® CRL-5915™
NCL-H2452	ATCC® CRL-5946™
MM05	[402]*
VAMC23	[403]**
Mesothelioma (Biphasic)	
MSTO-211h	ATCC® CRL-2081™
SPC111	[404]**
M38K P5	[405]
Mesothelioma (Benign)	
REN -both	[406]
MeT-5A	ATCC® CRL-9444™
LP9	[407]
Non-tumourigenic	
HEK293	ATCC® CRL-1573™

*A/Prof Rayleen Bowman (UQ Thoracic Research Centre, Prince Charles Hospital, Brisbane, Australia)

**Prof Walter Berger (Institute of Cancer Research) & Prof Walter Klepetko (Division of Thoracic Surgery, Medical University of Vienna, Austria)

Note: RNA from the mesothelioma cell lines were kindly provided by Dr Glen Reid and Patrick Winata (ADRI)

7.2.3 Clinical tissue samples:

Tissue samples where obtained from the following sources: (a) human liver cancer tissue samples were kindly provided by Prof Xiaofeng Zhu, The First Affiliated Hospital of Sun Yat-sen University, Guangzhou; (b) human breast and prostate cancer and adjacent tissue samples were kindly provided by Dr Meijun Long, Dr Hongjie Chen and Dr Qiuxia Li, The 3rd Affiliated Hospital of Sun Yat-sen University, Guangzhou. The use of human tissues for this project was approved by the relevant institutional human ethics committee for both sites with overall human ethics approval number GZSCHE 2016-00122. Resections from patients with liver (hepatocellular) carcinoma, prostate and breast cancer were conducted and tumour tissue, as well as tissue adjacent to the tumour site, were collected for diagnostic purposes and for research (with informed consent as per the ethics protocols). Once collected, tissue segments were harvested and submerged in RNA*later* Stabilisation Solution (Thermo Fisher) to stabilise and protect the RNA until the RNA was extracted. RNA was subsequently extracted using TRIzol™ according to the manufacturer's instructions.

7.2.4 RT-PCR amplification

RT-PCR sample preparation is described in Chapter 2, sections 2.2.6 to 2.2.8. RNA extracts from the mesothelioma cell lines was kindly provided by Patrick Winata, ADRI. RNA extraction and RT-PCR for clinical samples were prepared by Dr Long.

7.3 Results

Differential SphK1 isoform expression in different cell types *in vitro* demonstrated by RT-PCR. RNA was extracted from 6 different cell types, breast, prostate, colon, brain, ovarian, and mesothelioma, as well as benign mesothelioma and human embryonic kidney as listed in Table 7.1. Quantity and quality of all RNA samples were verified using the nanodrop as described in Chapter 2, as sections 2.2.6 to 2.2.8. Visual representation of SphK1a and SphK1b primer products for each cell line alongside MCF-7 parent, MCF-7SphK1a, and MCF-7SphK1b as controls for PCR primer specificity (Figure 7.2). All cell lines, irrespective of cell type, amplified the 289bp PCR product located in the SphK1a domain, albeit expression varied dependent on the cell type (Figure 7.2). In contrast the PCR-164bp, which is specific for the SphK1b isoform was only expressed in breast and mesothelioma cells in relatively low amounts. All the prostate cancers, independent of characteristics such as androgen dependent or independent, colon cancers, ovarian, brain and bone did not express the SphK1b isoform in cell culture. Out of the 2 breast cancer cell lines tested only one cell line (MCF-7 cells) showed the expression of SphK1b. In contrast, in T-47D breast cancer cells no SphK1b product was observed and very low amounts of the SphK1a product was amplified (Fig. 7.2). The majority of the mesothelioma cell lines expressed SphK1b (7/9 and 2/3 benign). In addition, the expression of the SphK1b specific product appeared to be relatively unstable as expression of the SphK1b PCR product was not consistent and varied with passage number in the mesothelioma cells (Table 7.2).

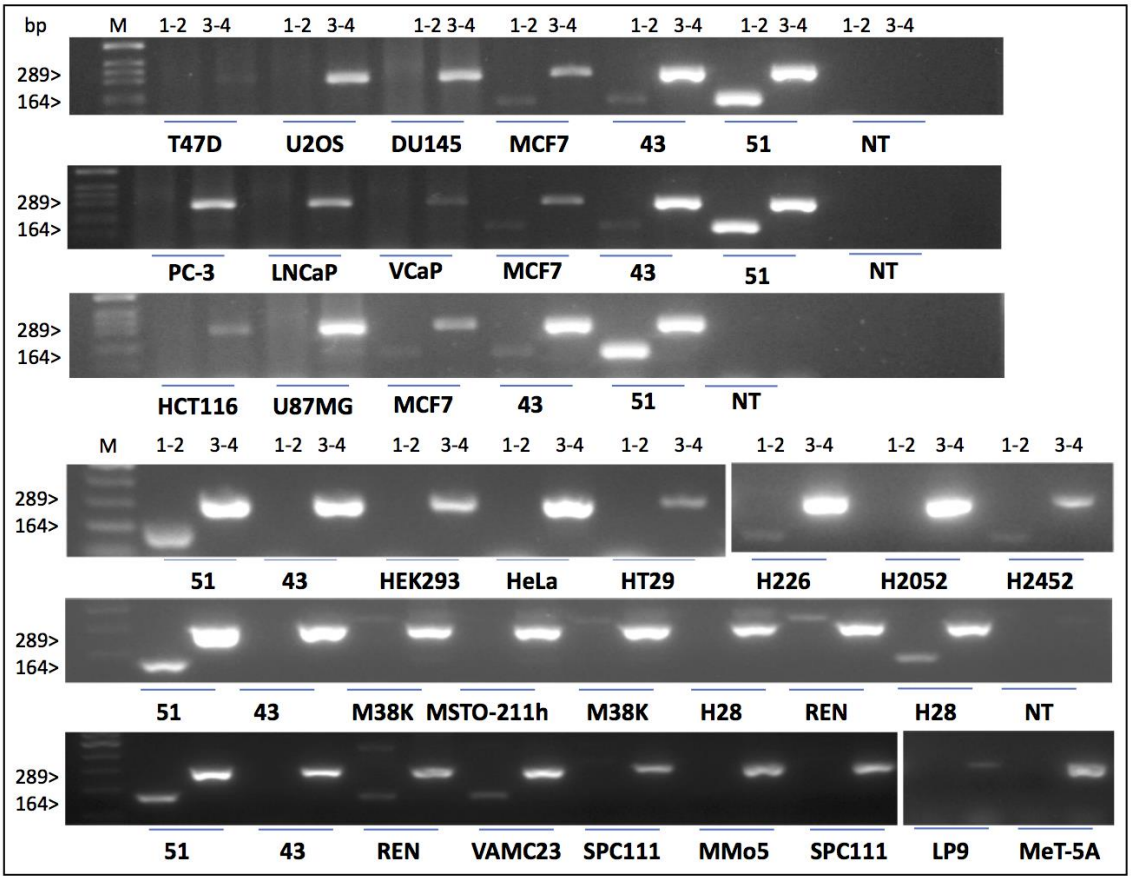

Figure 7.2 Differential expression of SphK1 isoform in cancer cells *in vitro*. Representative gel electrophoreses of SphK1 isoform RT-PCR amplification products from cancer and benign cell lines (described in Tables 7.1 and 7.2). Cells were harvested at 70% confluency. RNA was extracted using TRIzol™ and quality and quantify verified using the Nanodrop spectrophotometer. RT-PCR was performed using SphK1 primers 1-2 and 3-4 (as described in Chapter 6). Primers 1-2 amplified a product of 164 nucleotide base pairs (bp) and primers 3-4 amplified a product of 289 bp. MCF-7SphK1b (51) and MCF-7SphK1a (43) and no DNA template (NT) were used as controls for every RT-PCR. These panels are representative of repeat experiments.

Table 7.2 Comparison of SphK1a- and SphK1b -PCR products in cancer cell lines.

Cancer type	(SphK1a: primers 3-4)	SphK1b: primers 1-2)
Breast Cancer (epithelial)		
MCF-7	++	+
MCF-7 -SphK1a	++++++	+
MCF-7 -SphK1b	++++++	+++++++
T-47D luminal A (ER+/PR+/HER2-)	+	-
Cervical cancer		
HeLa	++++++	-
Bone cancer (Epithelial)		
U-2OS	+++	-
Prostate cancer (Epithelial)		
DU 145 (androgen independent)	+++	-
LNCaP (androgen dependent)	++	-
PC-3 (androgen independent)	+++	-
VCaP (androgen independent)	+	-
Colon cancer (Epithelial)		
HCT 116	+	-
HT29	+	-
Brain cancer (Epithelial)		
U-87MG	+++++	-
Mesothelioma (Epithelioid)		
NCL-H28 (*p113)	+++	-
NCL-H28 (*p114)	+++	+
NCL-H226 (*p74)	+++	++
NCL-H226 (*p75)	++	+
NCL-H2052 (*p51)	+++	+
NCL-H2052 (*p89)	++	-
NCL-H2452 (*p=36)	++	+
NCL-H2452 (*p=37)	+	-
MM05 (*p=25)	++	-
MM05 (*p=32)	++	-
VAMC23 (*p57)	+++	++
Mesothelioma (Biphasic)		
MSTO-211h (*p=45)	+++	++
MSTO-211h (*p=56)	+++	-
SPC111 (*p=14)	++	-
SPC111 (*p=16)	++	-
M38K P5 (*p=5)	+++	-
M38K P5 (*p=6)	+++	-
Mesothelioma (Benign)		
REN (*p=14)	+++	+
REN (*p=15)	+++	+
MeT-5A (1A)	+++	-
MeT-5A (1B)	+++	-
LP9 (*p=3)	++	+
LP9 (*p=14)	+	-
Non-tumourigenic		
HEK293	++	-

Note *p = passage number

7.3.1 Only SphK1a isoform is expressed in hepatocellular carcinoma patient tissue in vivo

Resections from 6 patients diagnosed with liver (hepatocellular carcinoma) were processed as described in section 7.2.2 and RNA extracted and RT-PCR performed as described in Chapter 2, sections 2.2.6 to 2.2.8. Samples were collected from the liver cancer tissue and the adjacent tissue. The patients' details, age of diagnosis and gender are listed in Table 7.3. No other background patient details were made available.

Table 7.3 Characteristics and expression of SphK1 isoform expression in liver cancer patients.

Sample ID	Nature	Age/Sex	Diagnosis	Sub type
A1T	Cancer	62/Male	Liver cancer	HCC
A1P	Adjacent			
A2T	Cancer	63/M	Liver cancer	HCC
A2P	Adjacent			
A3T	Cancer	62/F	Liver cancer	HCC
A3P	Adjacent			
A4T	Cancer	66/M	Liver cancer	HCC
A4P	Adjacent			
A5T	Cancer	36/M	Liver cancer	HCC
A5P	Adjacent			
A6T	Cancer	66/M	Liver cancer	HCC
A6P	Adjacent			

HCC – hepatocellular carcinoma

Visual representation of SphK1a and SphK1b PCR amplified products alongside MCF-7 parent, MCF-7SphK1a, and MCF-7SphK1b as controls for PCR primer specificity are shown in Figure 7.3 (amplification is shown for the 289bp PCR product located in the SphK1a domain and the 164bp specific for the SphK1b isoform). Without exception, SphK1a was expressed in all the liver cancer tissue and the corresponding adjacent tissue, albeit in varying expression levels (Table 7.4). Within the limitation that the RT-PCR experiment was not quantitative, the trend suggested there was no consistent variation between the expression of SphK1a in the cancer and corresponding adjacent tissue, although the expression of SphK1a did vary between patients. Interestingly, SphK1b was not detected in any of the liver patients' cancer tissue or corresponding adjacent tissue (Figure 7.3, Table 7.4).

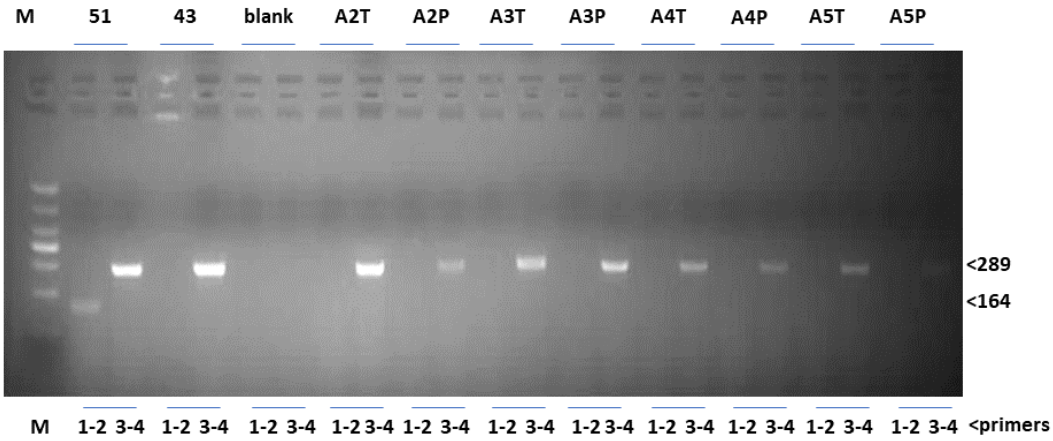

Figure 7.3 Comparative analysis of SphK1a and SphK1b isoform expression in liver cancer and adjacent samples. Representative gel electrophoreses of SphK1 isoform RT-PCR amplification products from liver cancer and adjacent tissue samples (described in Table 7.4). RNA was extracted from tissue using TRIzol™ and quality and quantify verified using the Nanodrop spectrophotometer. RT-PCR was performed using SphK1 primers 1-2 and 3-4 (as described in Chapter 6). Primers 1-2 amplified a product of 164 nucleotide bp and primers 3-4 amplified a product of 289 bp. MCF-7SphK1b (51) and MCF-7SphK1a (43) and no DNA template (NT) were used as controls for the RT-PCR specificity. T = tumour, P= adjacent tissue. Each sample was amplified 2x with similar results.

Table 7.4 SphK1 isoform expression in liver cancer patients.

Sample ID	Nature	Sphk1a	Sphk1b
A1T	Cancer	+++	-
A1P	Adjacent	+++	-
A2T	Cancer	+++	-
A2P	Adjacent	++	-
A3T	Cancer	+++	-
A3P	Adjacent	+++	-
A4T	Cancer	++	-
A4P	Adjacent	++	
A5T	Cancer	+	-
A5P	Adjacent		
A6T	Cancer	++	-
A6P	Adjacent	+	-

HCC – hepatocellular carcinoma

7.3.2 Differential expression of SphK1a and SphK1b isoforms in prostate cancer patient tissue in vivo

Resections from 7 patients diagnosed with prostate cancer were processed as described above for the human liver cancer tissue samples. The patients' details, age of diagnosis and prostate cancer sub-type are listed in Table 7.5. No other background patient details were available.

Table 7.5 Characteristics of Prostate Cancer Samples

Sample ID	Nature	Age/Sex	Diagnosis	Subclass/staging*
9	Cancer	57/M	Prostate cancer	pT3a stage
10	Adjacent	57/M		
14,15	Cancer	75/M	Prostate cancer	pT2c stage
16	Adjacent	75/M		
17,18	Cancer	72/M	Prostate cancer	pT2c stage
19	Adjacent	72/M		
21,22	Cancer	70/M	Prostate cancer	pT3b stage
23,24	Adjacent	70/M		
25	Cancer	75/M	Prostate cancer	pT2a stage
26	Adjacent	75/M		
27	Cancer	69/M	Prostate cancer	pT3b stage
28	Adjacent	69/M		
29	Cancer	64/M	Prostate cancer	pT3b stage
30	Adjacent	64/M		

*Clinical stage of prostate cancer

Visual representation of SphK1a and SphK1b PCR amplified products for prostate cancer and adjacent tissue are shown in Figure 7.4. MCF-7 parent, MCF-7SphK1a, and MCF-7SphK1b as controls for PCR primer specificity. All prostate patient samples, both cancer and adjacent tissue, expressed the SphK1a isoform. With the exception of a few obvious samples (9T and 10P) there was no overt difference in the expression of SphK1a in the cancer and adjacent samples (Figure 7.4). SphK1b was detected in both prostate cancer patients' tissue and corresponding adjacent tissue, albeit the SphK1b expression was very low and in some cases undetectable (Figure 7.4 and Table 7.6).

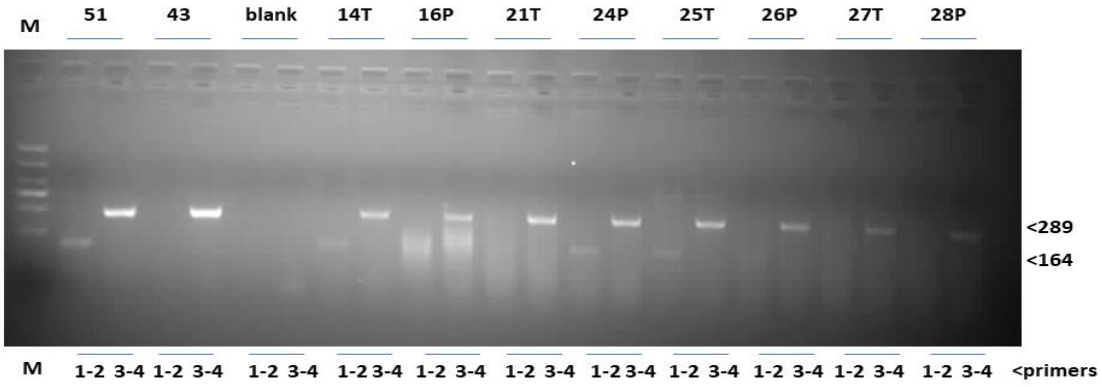

Figure 7.4 Comparative analysis of SphK1a and SphK1b isoform expression in prostate cancer and adjacent samples. Representative gel electrophoreses of SphK1 isoform RT-PCR amplification products from prostate cancer and adjacent tissue samples (described in Table 7.3.4). SphK1a and SphK1b RT-PCR was amplified as described in Figure 7.3.2. Primers 1-2 amplified a product of 164 nucleotide bp and primers 3-4 amplified a product of 289 bp. MCF-7SphK1b (51) and MCF-7SphK1a (43) and no DNA template (NT) were used as controls for the RT-PCR specificity. T = tumour, P= adjacent tissue. Each sample was amplified 2x with similar results.

Table 7.6 SphK1 isoform expression in prostate cancer clinical samples

Sample ID	Nature	SphK1a	SphK1b
9T	Cancer	+	+?
10P	Adjacent	+++	+
14T	Cancer	++	+
16P	Adjacent	++	++
17T	Cancer	+	+?
19P	Adjacent		
21T	Cancer	++	-
24P	Adjacent	++	+
25T	Cancer	++	+
26P	Adjacent	++	+
27T	Cancer	+	-
28P	Adjacent	+	-
29T	Cancer	+	+
30P	Adjacent	+	-

+? = very low expression

7.3.3 Differential SphK1 isoform expression by RT-PCR in breast cancer patients.

Fresh breast tissue from the breast cancer and adjacent tissue was processed as described for liver and prostate cancer clinical samples. The characteristics of the breast samples, including Grade, sex and hormonal status are listed in Table 7.7.

Table 7.7 Characteristics of Breast Cancer Samples

Sample ID	Nature	Age/Sex	Diagnosis	Subclass
1T	Tumour	34/F	Breast Cancer	30% IDC(Grade:3); 70% DCIS (High Grade)/(ER+、PR-、HER2-)
1P	Adjacent	34/F		
2T	Tumour	42/F	Breast Cancer	IDC(Grade:3)/(ER-, PR-, HER2+)
2P	Adjacent	42/F		
3T	Tumour	47/F	Breast Cancer	IDC(Grade:3)/(ER+、PR+、HER2+)
3P	Adjacent	47/F		
4T	Tumour	66/F	Breast Cancer	8% IDC(Grade2); 92% DCIS (Medium Grade)/(ER-、PR-、HER2+)
4P	Adjacent	66/F		
5T	Tumour	32/F	Breast Cancer	IDC (Grade 2)/(ER-、PR+、HER2+)
5P	Adjacent	32/F		
6T	Tumour	60/F	Breast Cancer	IDC (Grade 2)
6P	Adjacent	60/F		
7T	Tumour	61/F	Breast Cancer	IDC (Grade 2)/(ER-、PR+、HER2+)
7P	Adjacent	61/F		
8T	Tumour	62/F	Breast Cancer	10% IDC (Grade 1); 90% DCIS (Low Grade)/(ER+、PR+、HER2+)
8P	Adjacent	62/F		
9T	Tumour	47/F	Breast Cancer	ILC
9P	Adjacent	47/F		
10T	Tumour	60/F	Breast Cancer	IDC (Grade 2)/(ER+, PR+, HER2+)
10P	Adjacent	60/F		
11T	Tumour	76/F	Breast Cancer	IDC (Grade 2)/(ER+, PR+, HER2+)
11P	Adjacent	76/F		
12T	Tumour	53/F	Breast Cancer	90% IDC (Grade 2); 10% DCIS/(ER+, PR+, HER2+)
12P	Adjacent	53/F		
13T	Tumour	54/F	Breast Cancer	IDC (Grade 3)/ER-、PR-、HER2-)

13P	Adjacent	54/F		
14T	Tumour	43/F	Breast Cancer	IDC (Grade 3)/ER+、PR+、HER2+)
14P	Adjacent	43/F		
15T	Tumour	50/F	Breast Cancer	IDC (Grade 3)/ER+、PR+、HER2+)
15P	Adjacent	50/F		

Note: Tumour: breast cancer tissue, Adjacent: non-tumour tissue adjacent to breast cancer, IDC: invasive ductal carcinoma, ILC: invasive lobular carcinoma, ILC: invasive lobular carcinoma。

A visual representation of SphK1a and SphK1b PCR products amplified in breast cancer tissue and adjacent tissue is shown in Figure 7.5. MCF-7 parent, MCF-7SphK1a, and MCF-7SphK1b are loaded as controls for PCR primer specificity.

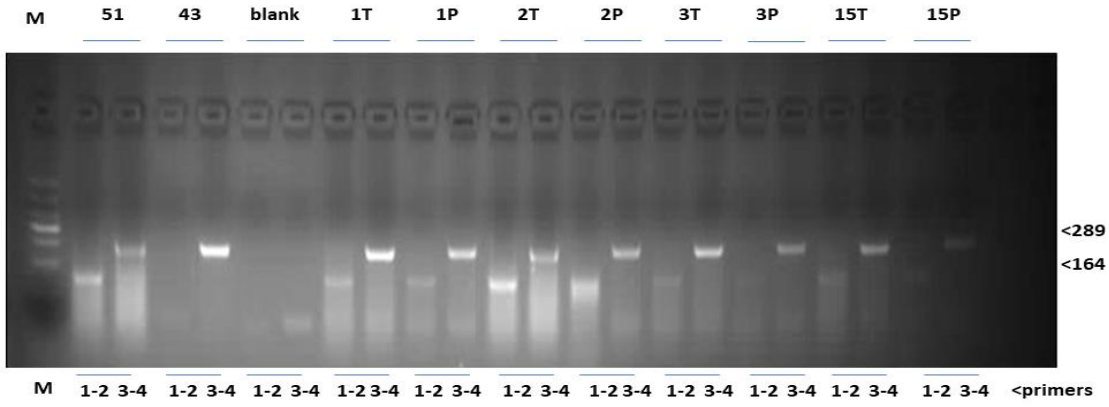

Figure 7.5 Comparative analysis of SphK1a and SphK1b isoform expression in breast cancer and adjacent samples. Representative gel electrophoreses of SphK1 isoform RT-PCR amplification products from breast cancer and adjacent tissue samples (described in Table 7.8). SphK1a and SphK1b RT-PCR was amplified as described in Figure 7.3.2. Primers 1-2 amplified a product of 164 nucleotide base pairs (bp) and primers 3-4 amplified a product of 289 bp. MCF-7SphK1b (51) and MCF-7SphK1a (43) and no DNA template (NT) were used as controls for the RT-PCR specificity. T = tumour, P= adjacent tissue. Each sample was amplified 2x with similar results.

Relative comparative expression of SphK1a and SphK1b is presented in Table 7.8. Most breast patient samples, both cancer and adjacent tissue, expressed the SphK1a isoform. Similar to liver and prostate cancers the levels of Sphk1a expression varied between breast cancer patient samples. However, there was some discrepancy between breast cancer and corresponding adjacent tissue in the majority of breast cancer patients: whereby an SphK1 PCR product was detected more often in the cancer tissue (with greater band intensity) compared to the adjacent tissue (Table 7.8). The most interesting finding was that SphK1b was expressed in over 50% of breast cancer patient samples and adjacent tissues (Table 7.8). The SphK1b isoform was lowly expressed, or not expressed, in the majority of breast tissue, with the exception of the breast cancer tissue sample 2T and the corresponding adjacent tissue 2P (Table 7.8). In these 2 samples, the two SphK1a (3-4) and SphK1b PCR (1-2) primers amplified similar product amounts, thus making it difficult to determine if this was the product of SphK1b isoform, in preference to the SphK1a isoform.

Expression of SphK1 isoforms was assessed by breast cancer Grade, Grades 1-3 and Invasive lobular carcinoma (Table 7.9) and by hormonal status (Table 7.10). An interesting observation was that most of the Grade 2 tumours had undetectable levels of SphK1b, whereas all the Grade 3 breast tissues proved positive for SphK1b expression, albeit to varying levels (Table 7.9). SphK1b expression was not confined to the cancer tissue, but was equally observed in the resected adjacent breast tissues.

Table 7.8 SphK1 isoform expression in breast cancer clinical samples

Sample ID	Nature	SphK1a	SphK1b
1T	Tumour	+++	+
1P	Adjacent	+++	+
2T	Tumour	++	+++
2P	Adjacent	++	++
3T	Tumour	+++	+
3P	Adjacent	++	+
4T	Tumour	+++	-
4P	Adjacent	-	-
5T	Tumour	+++	+
5P	Adjacent	-	-
6T	Tumour	+	-
6P	Adjacent	?	?
7T	Tumour	-	-
7P	Adjacent	+	+
8T	Tumour	++	+
8P	Adjacent	+	?
9T	Tumour	+	-
9P	Adjacent	-	-
10T	Tumour	+	-
10P	Adjacent	+	+
11T	Tumour	+	-
11P	Adjacent	-	-
12T	Tumour	+	+
12P	Adjacent	+	-
13T	Tumour	+	+
13P	Adjacent	+	+
14T	Tumour	+	+
14P	Adjacent	+	+
15T	Tumour	++	+
15P	Adjacent	+	+

Table 7.9 Analysis of SphK1 isoform expression in breast cancer patients by Grade

Grade	Total no.	Cancer		Adjacent	
		SphK1a	SphK1b	SphK1a	SphK1b
Grade 1	1/15	1/1	1/1	1/1	0/1
Grade 2	7/15	6/7	1/7	3/7	2/7
Grade 3	6/15	6/6	6/6	6/6	6/6
ILC	1/15	1/1	0/1	0/1	0/1

ILC = Invasive lobular carcinoma.

Table 7.10 Analysis of SphK1 isoform expression in breast cancer patients by hormonal status.

Type	Total no.	Cancer		Adjacent	
		SphK1a	SphK1b	SphK1a	SphK1b
Breast overall	15	14/15	9/15	10/15	8/15
ER+ (8/15)	8	8/8	6/8	8/8	5/8
ER- (5/15)	5	4/5	2/5	3/5	3/5
UN (2/15)	2	2/2	0/2	0/2	0/2
HER2+ (11/15)	11	9/11	7/11	8/11	6/11
HER2- (2/15)	2	2/2	2/2	2/2	2/2

ER = estrogen receptor positive; UN=unknown; HER2 = Herceptin 2.

ILC = Invasive lobular carcinoma.

Given the few samples in each category, there was obvious correlation between hormone status and difference in SphK1 isoform expression.

7.4.1 SphK1 isoform mRNA stability

At the protein level, the unique 86 amino acids at the SphK1b N-terminal allows for conformational changes to facilitated isoform preferential interaction with proteasomal proteins, and ubiquitin-protein ligase, thereby making SphK1b more susceptible to protein degradation [14]. However, we know little about the structure and stability of the SphK1 isoforms at the mRNA level. In our cell lines and patient tissue samples, SphK1b mRNA was detected at low levels compared to SphK1a (i.e. the PCR product for SphK1b was fainter than that for SphK1a). It is possible that the SphK1b mRNA may be more unstable than SphK1a transcript, as demonstrated by the inconsistency of detection of a SphK1b PCR product between increasing passage numbers of the same mesothelioma cells. However, to test for this, specific experiments will need to be carried out to measure mRNA half-life. As an initial test, we explored the predicted SphK1b and SphK1a mRNA structure and inferred information about stability based on computer structural predictions.

Determination of mRNA secondary structure, three-dimensional (3D) structure and their dynamics through experimental methods is expensive and limited to X-Ray crystallography, cryo-electron and NMR spectroscopy [408, 409]. However, many computational models have been developed that predict the folded secondary and 3D structures of mRNA and their stability [410]. Here, mRNA secondary structure fold predictions were performed based on highly probable base pairs and the lowest free energy structure for each sequence as determined by Mathews lab Computational Biology of RNA online website (https://rna.urmc.rochester.edu). Presented here are the structure predictions that may have higher fidelity of the predicted structures for each

SphK1a and SphK1b isoform (Figure 7.6 A and B). Based on these data, it may be of importance to consider RNA stability testing, which involves standardised conditions and inhibition of *de novo* RNA synthesis to determine the SphK1b mRNA stability.

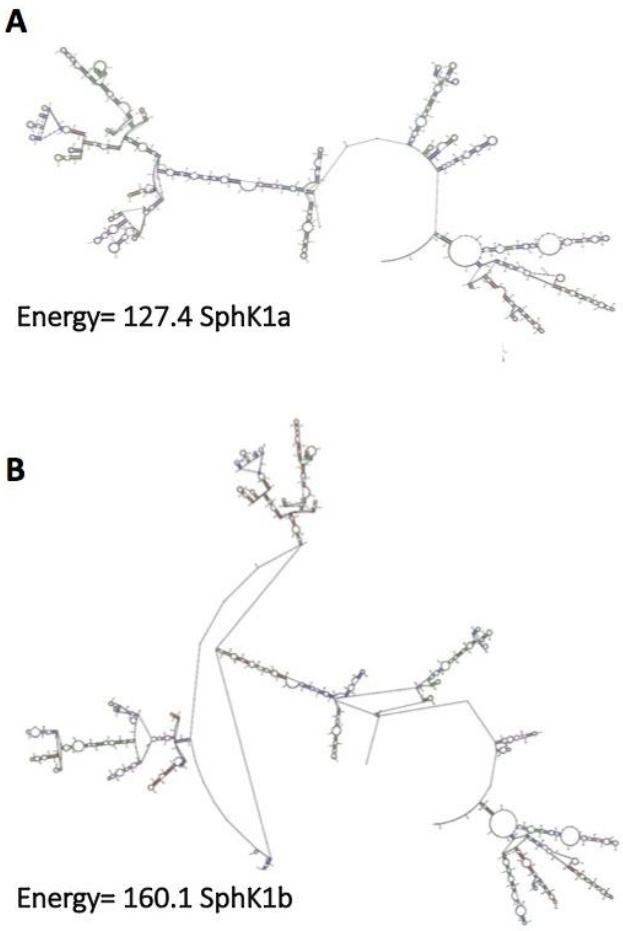

Figure 7.6 Predicted secondary structure of SphK1a and SphK1b based on the lowest free energy structure. Structural predictions for SphK1a and SphK1b isoforms suggest that SphK1a (A) is more stable than the SphK1b isoform (B) (https://rna.urmc.rochester.edu). More detailed description is provided in section 7.3.5.

mRNAs associated with stress have higher free energy, longer loop length and more single strands that enable them to have conformational changes in response to their environment [411]. Also, some mRNA isoforms transcribed from a single gene can have different half-lives depending on their environmental conditions [412, 413]. Investigations by Geisberg and his group, examining stabilising and destabilising elements on mRNAs and isoform half-lives, suggested that the double-stranded structures at the 3' region are crucial in mRNA stability [414]. Taking all these predictions into account, SphK1b with the higher free energy and the longer loop length is predicted to be less stable than the SphK1a isoform. These predictions may provide a reason why SphK1b is seemingly lowly expressed compared to its shorter 1a isoform, *in vitro* (cell lines) and *in vivo* (patient tissue samples). In addition, it may explain why SphK1b is not consistently expressed over different passage numbers as it may be more susceptible to degradation within the cell milieu or, alternatively may be more susceptible to degradation in mRNA preparation.

7.5 Discussion

This study, is the first report to explicatively examine the differential expression of SphK1a and SphK1b in a wide range of cancer cell lines and cancer patients. Expression of SphK1a and SphK1b isoforms were compared to cells engineered to overexpress either the SphK1a or SphK1b isoform, to determine correct size and specificity. The most widespread finding was that the SphK1a (43kDa) isoform was expressed in all cancer types, albeit SphK1a expression was not uniform and expression levels were dependent on the nature of the cancer. In contrast, the longer SphK1b isoform was not detected in

most cell types tested, *in vitro* (Table 7.2), and not detectable in all patient cancer and adjacent tissues (Table 7.4, 7.6 and 7.8). The longer SphK1b isoform was detected in one breast cancer cell line and most of the mesothelioma cell lines tested in cell culture conditions, SphK1b was not detected in colon, cervical, brain and bone cancer cells (Table 7.2). The SphK1b isoform, when expressed, was either generically more lowly expressed than its 1a-counterpart in all cell types, alternatively the SphK1b mRNA was more unstable and more susceptible to degradation. The endogenous 1b-isoform expression was also dependent on the cell culture passage and/or conditions, again questioning the stability of the 1b- isoform. Comparing the mRNA structure of the 2 isoforms, the b-isoform was predicted to be more unstable.

In patient samples, SphK1a was detected in all cancer types and adjacent tissue. This implies that generic expression of SphK1a, both *in vitro* and *in vivo,* in tumour and non-tumourigenic tissue, is important for basic cell function. SphK1b was not detected in liver cancer patients but was expressed in prostate and breast cancer patient tissues. The unpredictable and notable absent of the SphK1b isoform in most cells, independent of cell type, culture conditions, and independent of patient cancer type, suggests that SphK1b has specific cellular functions. Speculatively, a possible function in reproductive tissues (prostate and breast) may be hormone related. The little published information available suggests that expression of SphK1b may alter treatment outcome in breast cancer. Previous study demonstrated the important differences of SphK1a and SphK1b as drivers of distinct as well as 'in-common' signalling pathways of the two major SphK1 isoforms in a hormone responsive breast cancer cell model [14], providing some insight into the importance of the two isoforms in directing cell function. The findings that both

isoforms are expressed in hormone responsive patient breast cancer samples and adjacent tissue support the diverse signalling pathways of both isoforms are important in the cell's normal as well as abnormal function.

At this stage we have no direct evidence to suggest SphK1 isoform association with chemoresistance or hormone resistance. Nonetheless, aberrant SphK1 isoform expression has been causally associated with prostate cancer therapy resistance in pre-clinical laboratory experiments. Although SphK1 inhibitors have been successful in increasing chemosensitivity [387, 415, 416], there are examples demonstrating discriminatory chemosensitivity depending on the expression of the two major SphK1 isoforms in prostate hormone dependent and independent cell lines [241, 242]. Therefore, from a cancer prognostic viewpoint, understanding SphK1 isoform expression may have relevance for treatment outcome in patients with hormone responsive cancers.

SphK1 expression is portrayed as a major contributor underpinning cancer progression, with high expression significantly associated with many cancer types with poorer overall clinical outcomes and survival [393]. In the absence of mutations in SphK1, it has been suggested that cancer cells become reliant on SphK1 function for survival, termed "non-oncogenic addition" [309] - how and why is unknown. As overexpression of SphK1 has been widely reported as important in cancer development and progression as shown in Table 5.1 chapter 5. This study was focused on determining if one or both isoforms are expressed in normal and cancer cells. The greater the Grade of breast cancer the higher level of SphK1 was detected and in Grade 3 both isoforms were detected. The abnormal expression of the two isoforms may be important in hormonal signalling, however, it is

important to note, we found that in many cancer cell types and adjacent tissue, the SphK1b isoform is not present at detectable levels. This strongly signifies overexpression of SphK1-S1P signalling and activity causally associated with cancer and other disease states [16, 219, 232] is dependent on the SphK1a isoform in most cell types. As more light is shed on the 'in common' and discrete functions of SphK1 isoforms and the subtle but importance in changing cell function response will aid in designing more efficient therapies.

CHAPTER 8

OVERALL DISCUSSION AND CONCLUSION

8.1 The effect of PTEN mutations on the suppressive functions of PTEN

The work described in the first part of this thesis has shown, for the first time, that the novel cancer-associated mutations of PTEN, detected in colon cancer (K62R, Y65C, K125E, K125E, E150Q, D153N, D153Y and N323K) alter, to varying degrees, the suppressive function of PTEN to enhance cell proliferation, decrease the cell cycle inhibitory effect and reduce the ability to suppress the phosphorylation of AKT (Figure 8.1). The results described are reproducible and confirmed in replicate experiments. The deficits in PTEN function conferred by these mutations, combined with their overall propensity to promote cell growth and activate the PI3K/AKT pathway in HCT116 colon cancer cells, could conceivably have contributed to the development and progression of the primary colorectal tumours in which they were detected. The fact that these PTEN mutants conferred similar growth enhancing effects in the U87MG glioblastoma and MCF7 breast cancer cells indicated that these mutations could potentially contribute to the development of other cancer types.

The studied mutations are novel mutations and their functional effects were unknown prior to this study. This work has shown that the effect of each of the mutations on PTEN function is mutation dependent, and cell specific. Particular mutations did not bring about the same effect in all three cell lines. Interestingly, mutations occurring outside the catalytically important N-terminal phosphatase domain of PTEN were able to reduce the suppressive function of PTEN with equal efficacy to those occurring within the phosphatase domain.

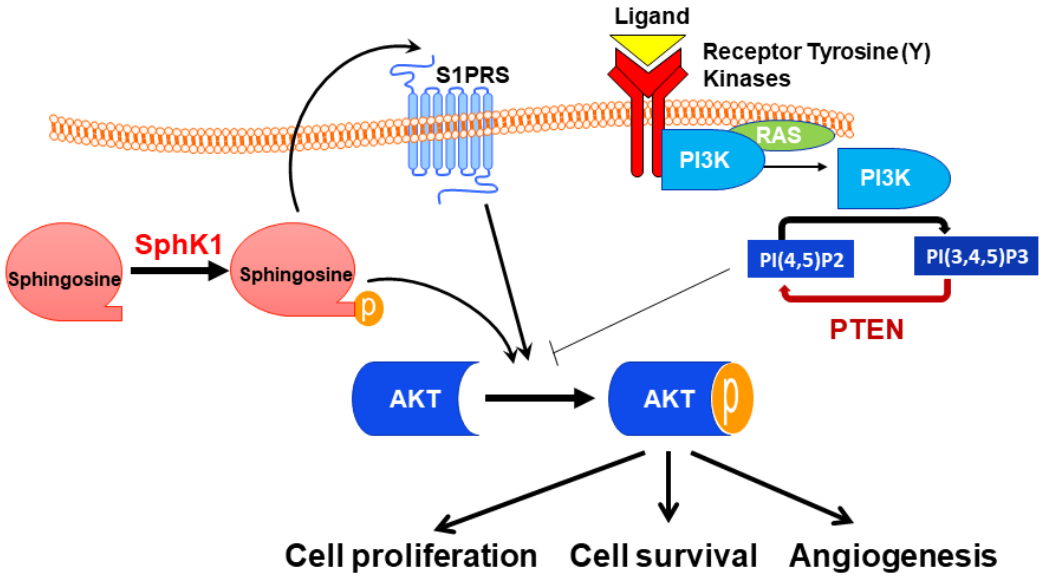

Figure 8.1 PTEN Suppresses and SphK1 Activates the PI3K/AKT Pathway. Binding of ligand (growth factor, insulin etc) to receptor tyrosine kinases activated PI3K, that in turn phosphorylates PIP2 to PIP3. PIP3 promotes the AKT activation and its downstream pathways causing increase in the cell proliferation, cell survival and angiogenesis. PTEN is a direct antagonist of PI3/AKT pathways by dephosphorylating PIP3 and inhibiting AKT activation. On the contrary, SphK1 by phosphorylating sphingosine promotes the phosphorylation and activation of AKT, which leads to activation of downstream pathways.

In future studies arising from this work, it would be of interest to produce cell lines stably expressing some of the PTEN mutants in an inducible manner to allow the study of the effects before and after the induction of expression of the mutants. Additionally, the use of a stable expression system would allow the effects of the expression of PTEN mutants to be monitored over a longer time period than can be studied after transient transfection. The use of an expression vector with a fluorescent tag would allow the expressed PTEN to be tracked within cells to determine if any of the PTEN mutations altered the subcellular localisation of PTEN in comparison to the wild type PTEN. Further studies of the effect of the described mutations of PTEN in additional functional that are known to be regulated by the protein phosphatase activity of PTEN, including cell migration and cell invasion assays, could provide further information on the effects of these mutations on PTEN function. Also, study of the effect of Rapamycin/mTOR inhibitors and anti-proliferative drugs on stable mutant PTEN expressing cells could be beneficial in treating colorectal patients with PTEN mutation.

8.2 Profiling SphK1 isoform expression in cancer cells and primary human cancer tissues

The second part of thesis explored SphK1 isoform expression in different cancer cell lines and primary cancer tissues. SphK1 is associated with many disease types including cancer (Table 5.1). Unlike PTEN, where mutations are associated with cancer phenotype, mutations have not been reported in SphK1 in association with any cancer phenotype [307]. Instead, SphK1 acts as oncogene through overexpression, or non-oncogenic addiction [307].

The multiplicity of SphK1 isoform expression is emerging as an important feature of the cancer phenotype and a number of reports indicate that an alteration/ imbalance in SphK and SphKb isoform expression is linked to resistance to conventional cancer treatments [239, 346]. The work presented in this part of the thesis represents the first investigation of the frequency of SphK isoform expression in various cell lines and cancers. The results of this work have shown that SphK1a is the generic isoform of SphK1 in cells as the SphK1a isoform was present in the majority of all cancer cell lines and human sample tissues tested in this study. The absence of the SphK1b isoform in most cells indicated that this isoform has cell specific functions. The 1b-isoform was poorly detected in most cancer cells and tissues. This may be due to low RNA expression, or, alternatively, to decreased stability or reduced half life of this longer mRNA.

We do not know if aberrant SphK1 isoform expression is associated with cancer, however, interestingly, the two hormone-related tissues, the prostate and the breast, expressed both isoforms, albeit not in all the tissue samples tested. There are reports that changes in SphK1a and SphK1b expression levels lead to cancer cell resistance to treatment in both the prostate and the breast. Treatment of hormone-dependent breast cancer cells with a dipeptidyl peptidase 2 (DPP2) inhibitor (a regulator of glucose metabolism interacting with SphK1b) increased the SphK1b expression with no change in SphK1a [241, 348]. Also, the presence or increase of the SphK1b isoform in androgen-independent prostate cancer cells is important to understand as the presence of the 1b-isoform may affect the efficacy of anti-SphK drugs [271, 348]. However, these experiments were conducted *in vitro* (cell culture) and may not necessarily reflect the patient outcome. Despite our limited knowledge of the involvement and mode of

actions of the SphK1 isoforms, this initial study, exploring the expression of SphK1 isoforms, merits further investigation as isoform expression may be of value in anti-SphK/S1P cancer-based therapies.

8.3 Conclusions and future directions

From the present study, we now have a basic understanding of SphK1 isoform expression in different cancers, additional studies are needed to further clarify the roles of the two isoforms. This is especially important in the reproductive tissues, the prostate and breast where both isoforms are expressed and have been identified in altering the cancer phenotype. In line with the understanding that PTEN and SphK1 converge on the PI3K/AKT signalling, producing opposing outcomes, it would be interesting to further investigate the expression of WT and mutant PTEN in cell lines overexpressing the SphK1a and SphK1b isoforms. As PTEN mutants also have the ability to alter the cancer phenotype, reduction of the tumour suppressor function of mutant PTEN, alongside SphK1 activation, would lead to the convergence of the effects of these two players to induce the development of more aggressive, treatment resistant cancer types (Figure 8.1).

APPENDIX-I

Table A.1.1. Statistical analysis of cell proliferation data in U87MG cells. Paired T-tests for cell proliferation data comparing each the results of each PTEN construct against the mock-transfected U87MG cells

		Mean	Std. Deviation	Std. Error Mean	Sig.(2-tailed)	Significant?
Pair 1	U87MG	9391.0000	615.36128	275.19793	.576	No
	Mock	9581.20	298.966	133.702		
Pair 2	U87MG	9391.0000	615.36128	275.19793	.593	No
	Vector	9248.2000	526.07290	235.26695		
Pair 3	U87MG	9391.0000	615.36128	275.19793	.000	Yes
	WT	3204.0000	830.78968	371.54044		
Pair 4	U87MG	9391.0000	615.36128	275.19793	.000	Yes
	K62R	1931.4000	444.92617	198.97703		
Pair 5	U87MG	9391.0000	615.36128	275.19793	.000	Yes
	Y65C	2370.4000	284.07534	127.04236		
Pair 6	U87MG	9391.0000	615.36128	275.19793	.000	Yes
	C124S	2042.2000	340.68343	152.35826		
Pair 7	U87MG	9391.0000	615.36128	275.19793	.000	Yes
	K125E	2458.0000	633.51283	283.31555		
Pair 8	U87MG	9391.0000	615.36128	275.19793	.000	Yes
	K125X	2220.6000	360.35857	161.15725		
Pair 9	U87MG	9391.0000	615.36128	275.19793	.000	Yes
	G129E	2889.8000	600.62026	268.60555		
Pair 10	U87MG	9391.0000	615.36128	275.19793	.000	Yes
	E150Q	3330.2000	481.19196	215.19559		
Pair 11	U87MG	9391.0000	615.36128	275.19793	.000	Yes
	D153N	1539.4000	218.95502	97.91966		
Pair 12	U87MG	9391.0000	615.36128	275.19793	.000	Yes
	D153Y	2615.6000	341.83081	152.87138		
Pair 13	U87MG	9391.0000	615.36128	275.19793	.000	Yes
	N323K	1659.8000	208.19510	93.10768		

Table A.1.2. Independent T-Test of U87MG results, cell proliferation data acquired for each mutant against WT at 48 hours post transfection in U87MG cells.

Manipulated	Mean	Std. Deviation	Std. Error Mean	Sig. (2-tailed)	Significant?
WT	3204.0000	830.78968	371.54044	.017	Yes
K62R	1931.4000	444.92617	198.97703		
WT	3204.0000	830.78968	371.54044	.067	No
Y65C	2370.4000	284.07534	127.04236		
WT	3204.0000	830.78968	371.54044	.020	Yes
C124S	2042.2000	340.68343	152.35826		
WT	3204.0000	830.78968	371.54044	.149	No
K125E	2458.0000	633.51283	283.31555		
WT	3204.0000	830.78968	371.54044	.041	Yes
K125X	2220.6000	360.35857	161.15725		
WT	3204.0000	830.78968	371.54044	.513	No
G129E	2889.8000	600.62026	268.60555		
WT	3204.0000	830.78968	371.54044	.776	No
E150Q	3330.2000	481.19196	215.19559		
WT	3204.0000	830.78968	371.54044	.003	Yes
D153N	1539.4000	218.95502	97.91966		
WT	3204.0000	830.78968	371.54044	.181	No
D153Y	2615.6000	341.83081	152.87138		
WT	3204.0000	830.78968	371.54044	.012	Yes
N323K	1659.8000	208.19510	93.10768		

Table A.1.3. Statistical analysis of cell proliferation data in HCT116 cells. Paired T-tests for cell proliferation data comparing each the results of each PTEN construct against the mock-transfected HCT116 cells.

		Mean	Std. Deviation	Std. Error Mean	Sig. (2-tailed)	Significant?
Pair 1	HCT116	14693.8000	483.32463	216.14935	.189	No
	Mock	13711.80	1395.866	624.250		
Pair 2	HCT116	14693.8000	483.32463	216.14935	.076	No
	Vector	12919.4000	1669.30803	746.53725		
Pair 3	HCT116	14693.8000	483.32463	216.14935	.002	Yes
	WT	9295.6000	1925.49456	861.10735		
Pair 4	HCT116	14693.8000	483.32463	216.14935	.002	Yes
	K62R	10594.2000	1536.68481	687.22634		
Pair 5	HCT116	14693.8000	483.32463	216.14935	.010	Yes
	Y65C	10710.2000	2201.36996	984.48257		
Pair 6	HCT116	14693.8000	483.32463	216.14935	.000	Yes
	C124S	6675.8000	503.13388	225.00831		
Pair 7	HCT116	14693.8000	483.32463	216.14935	.000	Yes
	K125E	8033.6000	1490.70681	666.66435		
Pair 8	HCT116	14693.8000	483.32463	216.14935	.000	Yes
	K125X	6360.6000	979.85448	438.20424		
Pair 9	HCT116	14693.8000	483.32463	216.14935	.001	Yes
	G129E	7409.2000	1934.68892	865.21919		
Pair 10	HCT116	14693.8000	483.32463	216.14935	.005	Yes
	E150Q	10768.4000	1483.52664	663.45328		
Pair 11	HCT116	14693.8000	483.32463	216.14935	.000	Yes
	D153N	6467.4000	1279.27765	572.11036		
Pair 12	HCT116	14693.8000	483.32463	216.14935	.000	Yes
	D153Y	5929.2000	1453.08042	649.83732		
Pair 13	HCT116	14693.8000	483.32463	216.14935	.001	Yes
	N323K	8422.2000	1572.08737	703.05885		

Table A.1.4. Independent T-Test of HCT116 results, cell proliferation data acquired for each mutant against WT at 48 hours post transfection in HCT116 cells.

Manipulated	Mean	Std. Deviation	Std. Error Mean	Sig. (2-tailed)	Significant?
WT	9295.6000	1925.49456	861.10735	.272	No
K62R	10594.2000	1536.68481	687.22634		
WT	9295.6000	1925.49456	861.10735	.311	No
Y65C	10710.2000	2201.36996	984.48257		
WT	9295.6000	1925.49456	861.10735	.019	Yes
C124S	6675.8000	503.13388	225.00831		
WT	9295.6000	1925.49456	861.10735	.280	No
K125E	8033.6000	1490.70681	666.66435		
WT	9295.6000	1925.49456	861.10735	.016	Yes
K125X	6360.6000	979.85448	438.20424		
WT	9295.6000	1925.49456	861.10735	.161	No
G129E	7409.2000	1934.68892	865.21919		
WT	9295.6000	1925.49456	861.10735	.212	No
E150Q	10768.4000	1483.52664	663.45328		
WT	9295.6000	1925.49456	861.10735	.026	Yes
D153N	6467.4000	1279.27765	572.11036		
WT	9295.6000	1925.49456	861.10735	.014	Yes
D153Y	5929.2000	1453.08042	649.83732		
WT	9295.6000	1925.49456	861.10735	.455	No
N323K	8422.2000	1572.08737	703.05885		

Table A.1.5. Statistical analysis of cell proliferation data in MCF7 cells. Paired T-tests for cell proliferation data comparing each the results of each PTEN construct against the mock-transfected MCF cells

		Mean	Std. Deviation	Std. Error Mean	Sig. (2-tailed)	Significant?
Pair 1	MCF7	13185.8000	1232.85895	551.35129	.789	No
	Mock	13455.00	1248.595	558.388		
Pair 2	MCF7	13185.8000	1232.85895	551.35129	.743	No
	Vector	13030.8000	997.24506	445.98155		
Pair 3	MCF7	13185.8000	1232.85895	551.35129	.009	Yes
	WT	9319.8000	1298.51923	580.71546		
Pair 4	MCF7	13185.8000	1232.85895	551.35129	.012	Yes
	K62R	8398.6000	1832.54408	819.53863		
Pair 5	MCF7	13185.8000	1232.85895	551.35129	.002	Yes
	Y65C	7993.2000	940.70250	420.69495		
Pair 6	MCF7	13185.8000	1232.85895	551.35129	.000	Yes
	C124S	6397.6000	1062.51226	475.16993		
Pair 7	MCF7	13185.8000	1232.85895	551.35129	.001	Yes
	K125E	9994.6000	614.91528	274.99847		
Pair 8	MCF7	13185.8000	1232.85895	551.35129	.000	Yes
	K125X	6158.0000	507.29134	226.86758		
Pair 9	MCF7	13185.8000	1232.85895	551.35129	.000	Yes
	G129E	6447.6000	887.83123	397.05020		
Pair 10	MCF7	13185.8000	1232.85895	551.35129	.040	Yes
	E150Q	9717.2000	1459.44363	652.68303		
Pair 11	MCF7	13185.8000	1232.85895	551.35129	.002	Yes
	D153N	6507.0000	1532.44788	685.33153		
Pair 12	MCF7	13185.8000	1232.85895	551.35129	.005	Yes
	D153Y	7868.4000	1197.39501	535.49133		
Pair 13	MCF7	13185.8000	1232.85895	551.35129	.002	Yes
	N323K	7627.4000	1177.63292	526.65345		

Table A.1.6. Independent T-test analysis of cell proliferation data comparing cell proliferation of each PTEN mutation against that of WT PTEN in MCF7 cells.

Manipulated	Mean	Std. Deviation	Std. Error Mean	Sig. (2-tailed)	Significant?
WT	9319.8000	1298.51923	580.71546	.386	No
K62R	8398.6000	1832.54408	819.53863		
WT	9319.8000	1298.51923	580.71546	.101	No
Y65C	7993.2000	940.70250	420.69495		
WT	9319.8000	1298.51923	580.71546	.005	Yes
C124S	6397.6000	1062.51226	475.16993		
WT	9319.8000	1298.51923	580.71546	.324	No
K125E	9994.6000	614.91528	274.99847		
WT	9319.8000	1298.51923	580.71546	.001	Yes
K125X	6158.0000	507.29134	226.86758		
WT	9319.8000	1298.51923	580.71546	.004	Yes
G129E	6447.6000	887.83123	397.05020		
WT	9319.8000	1298.51923	580.71546	.661	No
E150Q	9717.2000	1459.44363	652.68303		
WT	9319.8000	1298.51923	580.71546	.014	Yes
D153N	6507.0000	1532.44788	685.33153		
WT	9319.8000	1298.51923	580.71546	.103	No
D153Y	7868.4000	1197.39501	535.49133		
WT	9319.8000	1298.51923	580.71546	.063	No
N323K	7627.4000	1177.63292	526.65345		

APPENDIX II

Table A.2.1. Statistical analysis of cell cycle phase distribution data in U87MG cells. Paired T-tests for G1 cell cycle data comparing the G1 phase distribution results of each PTEN construct against that of the vector transfected U87MG cells.

		Mean	Std. Deviation	Std. Error Mean	Sig. (2-tailed)	Significant?
Pair 1	U87MG	10480.5000	189.01411	94.50705	.466	No
	Vector	10625.0000	216.32383	108.16192		
Pair 2	U87MG	10480.5000	189.01411	94.50705	.004	Yes
	WT	12878.5000	665.02205	332.51103		
Pair 3	U87MG	10480.5000	189.01411	94.50705	.000	Yes
	C124S	8261.5000	302.52879	151.26439		
Pair 4	U87MG	10480.5000	189.01411	94.50705	.006	Yes
	G129E	11966.5000	367.52279	183.76139		
Pair 5	U87MG	10480.5000	189.01411	94.50705	.024	Yes
	K62R	12005.0000	552.88215	276.44107		
Pair 6	U87MG	10480.5000	189.01411	94.50705	.005	Yes
	Y65C	12045.5000	536.42117	268.21058		
Pair 7	U87MG	10480.5000	189.01411	94.50705	.001	Yes
	K125E	12382.5000	227.37561	113.68780		
Pair 8	U87MG	10480.5000	189.01411	94.50705	.000	Yes
	K125X	12690.0000	277.43107	138.71554		
Pair 9	U87MG	10480.5000	189.01411	94.50705	.000	Yes
	E150Q	12182.0000	42.61455	21.30728		
Pair 10	U87MG	10480.5000	189.01411	94.50705	.002	Yes
	D153N	12296.0000	238.18760	119.09380		
Pair 11	U87MG	10480.5000	189.01411	94.50705	.038	Yes
	D153Y	11479.5000	515.31835	257.65917		
Pair 12	U87MG	10480.5000	189.01411	94.50705	.001	Yes
	N323K	12286.0000	269.48346	134.74173		

Table A.2.2. Independent T-test analysis of G1 cell cycle phase distribution data comparing the G1 phase distribution of each PTEN mutation against that of WT PTEN in U87MG cells.

Manipulated	Mean	Std. Deviation	Std. Error Mean	Sig. (2-tailed)	Significant?
WT	12878.5000	665.02205	332.51103	.000	Yes
C124S	8261.5000	302.52879	151.26439		
WT	12878.5000	665.02205	332.51103	.053	No
G129E	11966.5000	367.52279	183.76139		
WT	12878.5000	665.02205	332.51103	.090	No
K62R	12005.0000	552.88215	276.44107		
WT	12878.5000	665.02205	332.51103	.099	No
Y65C	12045.5000	536.42117	268.21058		
WT	12878.5000	665.02205	332.51103	.208	No
K125E	12382.5000	227.37561	113.68780		
WT	12878.5000	665.02205	332.51103	.620	No
K125X	12690.0000	277.43107	138.71554		
WT	12878.5000	665.02205	332.51103	.127	No
E150Q	12182.0000	42.61455	21.30728		
WT	12878.5000	665.02205	332.51103	.150	No
D153N	12296.0000	238.18760	119.09380		
WT	12878.5000	665.02205	332.51103	.016	Yes
D153Y	11479.5000	515.31835	257.65917		
WT	12878.5000	665.02205	332.51103	.150	No
N323K	12286.0000	269.48346	134.74173		

Table A.2.3. Statistical analysis of cell cycle phase distribution data in U87MG cells. Paired T-tests for G2 cell cycle data comparing the G2 phase distribution results of each PTEN construct against that of the vector transfected U87MG cells.

		Mean	Std. Deviation	Std. Error Mean	Sig. (2-tailed)	Significant?
Pair 1	U87MG	2319.5000	189.01411	94.50705	.001	Yes
	Vector	3500.0000	216.32383	108.16192		
Pair 2	U87MG	2319.5000	189.01411	94.50705	.000	Yes
	WT	3693.5000	665.02205	332.51103		
Pair 3	U87MG	2319.5000	189.01411	94.50705	.185	No
	C124S	2532.8333	302.52879	151.26439		
Pair 4	U87MG	2319.5000	189.01411	94.50705	.029	Yes
	G129E	3125.0000	367.52279	183.76139		
Pair 5	U87MG	2319.5000	189.01411	94.50705	.014	Yes
	K62R	3095.0000	552.88215	276.44107		
Pair 6	U87MG	2319.5000	189.01411	94.50705	.000	Yes
	Y65C	3413.2500	536.42117	268.21058		
Pair 7	U87MG	2319.5000	189.01411	94.50705	.002	Yes
	K125E	3491.0000	227.37561	113.68780		
Pair 8	U87MG	2319.5000	189.01411	94.50705	.019	Yes
	K125X	2464.0000	277.43107	138.71554		
Pair 9	U87MG	2319.5000	189.01411	94.50705	.027	Yes
	E150Q	2945.5000	42.61455	21.30728		
Pair 10	U87MG	2319.5000	189.01411	94.50705	.001	Yes
	D153N	2498.7500	238.18760	119.09380		
Pair 11	U87MG	2319.5000	189.01411	94.50705	.001	Yes
	D153Y	3602.2500	515.31835	257.65917		
Pair 12	U87MG	2319.5000	189.01411	94.50705	.019	Yes
	N323K	3192.7500	269.48346	134.74173		

Table A.2.4. Independent T-test analysis of G2 cell cycle phase distribution data comparing the G2 phase distribution of each PTEN mutation against that of WT PTEN in U87MG cells.

Manipulated	Mean	Std. Deviation	Std. Error Mean	Sig. (2-tailed)	Significant?
WT	3693.5000	139.25875	69.62938	.000	Yes
C124S	2532.8333	96.31949	48.15975		
WT	3693.5000	139.25875	69.62938	.009	YES
G129E	3125.0000	264.55749	132.27875		
WT	3693.5000	139.25875	69.62938	.001	Yes
K62R	3095.0000	143.67092	71.83546		
WT	3693.5000	139.25875	69.62938	.013	Yes
Y65C	3413.2500	81.53271	40.76636		
WT	3693.5000	139.25875	69.62938	.105	No
K125E	3491.0000	160.44521	80.22261		
WT	3693.5000	139.25875	69.62938	.000	Yes
K125X	2464.0000	121.19406	60.59703		
WT	3693.5000	139.25875	69.62938	.000	Yes
E150Q	2945.5000	154.93977	77.46989		
WT	3693.5000	139.25875	69.62938	.000	Yes
D153N	2498.7500	140.27443	70.13722		
WT	3693.5000	139.25875	69.62938	.449	No
D153Y	3602.2500	177.06567	88.53283		
WT	3693.5000	139.25875	69.62938	.015	Yes
N323K	3192.7500	261.70897	130.85448		

Table A.2.5. Statistical analysis of cell cycle phase distribution data in HCT116 cells. Paired T-tests for G1 cell cycle data comparing the G1 phase distribution results of each PTEN construct against that of the vector transfected HCT116 cells

		Mean	Std. Deviation	Std. Error Mean	Sig. (2-tailed)	Significant?
Pair 1	HCT116	11860.0000	148.14407	74.07204	.330	No
	Vector	11638.5000	245.88547	122.94274		
Pair 2	HCT116	11860.0000	148.14407	74.07204	.006	Yes
	WT	15488.7500	1065.50501	532.75250		
Pair 3	HCT116	11860.0000	148.14407	74.07204	.328	No
	C124S	11766.5000	81.06582	40.53291		
Pair 4	HCT116	11860.0000	148.14407	74.07204	.001	Yes
	G129E	17108.0000	706.24453	353.12226		
Pair 5	HCT116	11860.0000	148.14407	74.07204	.002	Yes
	K62R	9582.0000	424.87018	212.43509		
Pair 6	HCT116	11860.0000	148.14407	74.07204	.000	Yes
	Y65C	14455.0000	54.19717	27.09859		
Pair 7	HCT116	11860.0000	148.14407	74.07204	.053	No
	K125E	12223.5000	199.78906	99.89453		
Pair 8	HCT116	11860.0000	148.14407	74.07204	.002	Yes
	K125X	9460.0000	513.05620	256.52810		
Pair 9	HCT116	11860.0000	148.14407	74.07204	.355	No
	E150Q	12359.0000	953.48134	476.74067		
Pair 10	HCT116	11860.0000	148.14407	74.07204	.012	Yes
	D153N	12560.2500	211.47793	105.73897		
Pair 11	HCT116	11860.0000	148.14407	74.07204	.170	No
	D153Y	12270.7500	389.06844	194.53422		
Pair 12	HCT116	11860.0000	148.14407	74.07204	.012	Yes
	N323K	14892.0000	1146.53216	573.26608		

Table A.2.6. Independent T-test analysis of G1 cell cycle phase distribution data comparing the G1 phase distribution of each PTEN mutation against that of WT PTEN in HCT116 cells.

Manipulated	Mean	Std. Deviation	Std. Error Mean	Sig. (2-tailed)	Significant?
WT	15488.7500	1065.50501	532.75250	.000	Yes
C124S	11766.5000	81.06582	40.53291		
WT	15488.7500	1065.50501	532.75250	.044	Yes
G129E	17108.0000	706.24453	353.12226		
WT	15488.7500	1065.50501	532.75250	.000	Yes
K62R	9582.0000	424.87018	212.43509		
WT	15488.7500	1065.50501	532.75250	.101	No
Y65C	14455.0000	54.19717	27.09859		
WT	15488.7500	1065.50501	532.75250	.001	Yes
K125E	12223.5000	199.78906	99.89453		
WT	15488.7500	1065.50501	532.75250	.000	Yes
K125X	9460.0000	513.05620	256.52810		
WT	15488.7500	1065.50501	532.75250	.005	Yes
E150Q	12359.0000	953.48134	476.74067		
WT	15488.7500	1065.50501	532.75250	.002	Yes
D153N	12560.2500	211.47793	105.73897		
WT	15488.7500	1065.50501	532.75250	.001	Yes
D153Y	12270.7500	389.06844	194.53422		
WT	15488.7500	1065.50501	532.75250	.475	No
N323K	14892.0000	1146.53216	573.26608		

Table A.2.7. Statistical analysis of cell cycle phase distribution data in HCT116 cells. Paired T-tests for G2 cell cycle data comparing the G2 phase distribution results of each PTEN construct against that of the vector transfected HCT116 cells.

		Mean	Std. Deviation	Std. Error Mean	Sig. (2-tailed)	Significant ?
Pair 1	HCT116	3646.2500	180.04513	90.02257	.053	No
	Vector	3493.0000	100.98845	50.49422		
Pair 2	HCT116	3646.2500	180.04513	90.02257	.000	Yes
	WT	1482.0000	126.55434	63.27717		
Pair 3	HCT116	3646.2500	180.04513	90.02257	.341	No
	C124S	3490.0000	130.59862	65.29931		
Pair 4	HCT116	3646.2500	180.04513	90.02257	.227	No
	G129E	3499.5000	152.18738	76.09369		
Pair 5	HCT116	3646.2500	180.04513	90.02257	.001	Yes
	K62R	7062.5000	272.89742	136.44871		
Pair 6	HCT116	3646.2500	180.04513	90.02257	.000	Yes
	Y65C	1481.8750	120.58771	60.29386		
Pair 7	HCT116	3646.2500	180.04513	90.02257	.004	Yes
	K125E	5617.5000	319.63052	159.81526		
Pair 8	HCT116	3646.2500	180.04513	90.02257	.000	Yes
	K125X	5883.7500	123.21898	61.60949		
Pair 9	HCT116	3646.2500	180.04513	90.02257	.001	Yes
	E150Q	6700.5000	301.74327	150.87163		
Pair 10	HCT116	3646.2500	180.04513	90.02257	.001	Yes
	D153N	7233.5000	367.98687	183.99343		
Pair 11	HCT116	3646.2500	180.04513	90.02257	.000	Yes
	D153Y	6518.5000	130.03974	65.01987		
Pair 12	HCT116	3646.2500	180.04513	90.02257	.908	No
	N323K	3669.0000	197.86527	98.93264		

Table A.2.8. Independent T-test analysis of G2 cell cycle phase distribution data comparing the G2 phase distribution of each PTEN mutation against that of WT PTEN in HCT116 cells.

Manipulated	Mean	Std. Deviation	Std. Error Mean	Sig. (2-tailed)	Significant?
WT	1482.0000	126.55434	63.27717	.000	Yes
C124S	3490.0000	130.59862	65.29931		
WT	1482.0000	126.55434	63.27717	.000	Yes
G129E	3499.5000	152.18738	76.09369		
WT	1482.0000	126.55434	63.27717	.000	Yes
K62R	7062.5000	272.89742	136.44871		
WT	1482.0000	126.55434	63.27717	.999	No
Y65C	1481.8750	120.58771	60.29386		
WT	1482.0000	126.55434	63.27717	.000	Yes
K125E	5617.5000	319.63052	159.81526		
WT	1482.0000	126.55434	63.27717	.000	Yes
K125X	5883.7500	123.21898	61.60949		
WT	1482.0000	126.55434	63.27717	.000	Yes
E150Q	6700.5000	301.74327	150.87163		
WT	1482.0000	126.55434	63.27717	.000	Yes
D153N	7233.5000	367.98687	183.99343		
WT	1482.0000	126.55434	63.27717	.000	Yes
D153Y	6518.5000	130.03974	65.01987		
WT	1482.0000	126.55434	63.27717	.000	Yes
N323K	3669.0000	197.86527	98.93264		

Table A.2.9. Statistical analysis of cell cycle phase distribution data in MCF7 cells. Paired T-tests for G1 cell cycle data comparing the G1 phase distribution results of each PTEN construct against that of the vector transfected MCF7 cells.

		Mean	Std. Deviation	Std. Error Mean	Sig. (2-tailed)	Significant?
Pair 1	MCF7	49.0800	.72125	.51000	.694	No
	Vector	50.5450	3.24562	2.29500		
Pair 2	MCF7	49.0800	.72125	.51000	.034	Yes
	WT	75.0000	1.25865	.89000		
Pair 3	MCF7	49.0800	.72125	.51000	.016	Yes
	K62R	61.5100	1.15966	.82000		
Pair 4	MCF7	49.0800[a]	.72125	.51000	.051	No
	Y65C	54.8000[a]	.72125	.51000		
Pair 5	MCF7	49.0800	.72125	.51000	.687	Yes
	C124S	50.2350	2.32638	1.64500		
Pair 6	MCF7	49.0800	.72125	.51000	.223	Yes
	K125E	48.4500	1.04652	.74000		
Pair 7	MCF7	49.0800	.72125	.51000	.289	Yes
	K125X	49.5100	1.01823	.72000		
Pair 8	MCF7	49.0800	.72125	.51000	.581	Yes
	G129E	48.6400	1.52735	1.08000		
Pair 9	MCF7	49.0800	.72125	.51000	.048	Yes
	E150Q	60.3300	.48083	.34000		
Pair 10	MCF7	49.0800	.72125	.51000	.069	Yes
	D153N	60.4700	2.47487	1.75000		
Pair 11	MCF7	49.0800	.72125	.51000	.245	Yes
	D153Y	52.0550	2.42538	1.71500		
Pair 12	MCF7	49.0800	.72125	.51000	.115	Yes
	N323K	56.3650	1.15258	.81500		

Table A.2.10. Independent T-test analysis of G1 cell cycle phase distribution data comparing the G1 phase distribution of each PTEN mutation against that of WT PTEN in MCF7 cells.

Manipulated	Mean	Std. Deviation	Std. Error Mean	Sig. (2-tailed)	Significant?
WT	75.0000	1.25865	.89000	.008	Yes
K62R	61.5100	1.15966	.82000		
WT	75.0000	1.25865	.89000	.003	Yes
Y65C	54.8000	.72125	.51000		
WT	75.0000	1.25865	.89000	.006	Yes
C124S	50.2350	2.32638	1.64500		
WT	75.0000	1.25865	.89000	.002	Yes
K125E	48.4500	1.04652	.74000		
WT	75.0000	1.25865	.89000	.002	Yes
K125X	49.5100	1.01823	.72000		
WT	75.0000	1.25865	.89000	.003	Yes
G129E	48.6400	1.52735	1.08000		
WT	75.0000	1.25865	.89000	.004	Yes
E150Q	60.3300	.48083	.34000		
WT	75.0000	1.25865	.89000	.018	Yes
D153N	60.4700	2.47487	1.75000		
WT	75.0000	1.25865	.89000	.007	Yes
D153Y	52.0550	2.42538	1.71500		
WT	75.0000	1.25865	.89000	.004	Yes
N323K	56.3650	1.15258	.81500		

Table A.2.11. Statistical analysis of cell cycle phase distribution data in MCF7 cells. Paired T-tests for G2 cell cycle data comparing the G2 phase distribution results of each PTEN construct against that of the vector transfected MCF7 breast cancer cells.

		Mean	Std. Deviation	Std. Error Mean	Sig. (2-tailed)	Significant?
Pair 1	MCF7	19.1150	1.33643	.94500	.784	No
	Vector	19.6700	3.56382	2.52000		
Pair 2	MCF7	19.1150	1.33643	.94500	.029	Yes
	WT	9.3850	.70004	.49500		
Pair 3	MCF7	19.1150	1.33643	.94500	.186	No
	K62R	15.3350	.27577	.19500		
Pair 4	MCF7	19.1150	1.33643	.94500	.043	Yes
	Y65C	15.6300	1.66877	1.18000		
Pair 5	MCF7	19.1150	1.33643	.94500	.209	No
	C124S	21.6300	.12728	.09000		
Pair 6	MCF7	19.1150	1.33643	.94500	.064	No
	K125E	10.0150	.03536	.02500		
Pair 7	MCF7	19.1150	1.33643	.94500	.006	Yes
	K125X	10.9450	1.44957	1.02500		
Pair 8	MCF7	19.1150	1.33643	.94500	.171	No
	G129E	21.9450	.23335	.16500		
Pair 9	MCF7	19.1150	1.33643	.94500	.452	No
	E150Q	15.9750	2.48194	1.75500		
Pair 10	MCF7	19.1150	1.33643	.94500	.506	No
	D153N	18.0300	.22627	.16000		
Pair 11	MCF7	19.1150	1.33643	.94500	.910	No
	D153Y	19.2250	2.42538	1.71500		
Pair 12	MCF7	19.1150	1.33643	.94500	.028	Yes
	N323K	21.6050	1.18087	.83500		

Table A.2.12. Independent T-test analysis of G2 cell cycle phase distribution data comparing the G2 phase distribution of each PTEN mutation against that of WT PTEN in MCF7 cells.

Manipulated	Mean	Std. Deviation	Std. Error Mean	Sig. (2-tailed)	Significant?
WT	9.3850	.70004	.49500	.008	Yes
K62R	15.3350	.27577	.19500		
WT	9.3850	.70004	.49500	.040	Yes
Y65C	15.6300	1.66877	1.18000		
WT	9.3850	.70004	.49500	.002	Yes
C124S	21.6300	.12728	.09000		
WT	9.3850	.70004	.49500	.332	No
K125E	10.0150	.03536	.02500		
WT	9.3850	.70004	.49500	.304	No
K125X	10.9450	1.44957	1.02500		
WT	9.3850	.70004	.49500	.002	Yes
G129E	21.9450	.23335	.16500		
WT	9.3850	.70004	.49500	.006	Yes
E150Q	15.9750	2.48194	1.75500		
WT	9.3850	.70004	.49500	.004	Yes
D153N	18.0300	.22627	.16000		
WT	9.3850	.70004	.49500	.031	Yes
D153Y	19.2250	2.42538	1.71500		
WT	9.3850	.70004	.49500	.006	Yes
N323K	21.6050	1.18087	.83500		

REFERENCES

1. Carracedo A, Pandolfi PP: **The PTEN–PI3K pathway: of feedbacks and cross-talks.** *Oncogene* 2008, **27:**5527.
2. Chalhoub N, Baker SJ: **PTEN and the PI3-Kinase Pathway in Cancer.** *Annual review of pathology* 2009, **4:**127-150.
3. Ioffe YJ, Chiappinelli KB, Mutch DG, Zighelboim I, Goodfellow PJ: **Phosphatase and tensin homolog (PTEN) pseudogene expression in endometrial cancer: a conserved regulatory mechanism important in tumorigenesis?** *Gynecologic Oncology* 2012, **124:**340-346.
4. Sun H, Lesche R, Li D-M, Liliental J, Zhang H, Gao J, Gavrilova N, Mueller B, Liu X, Wu H: **PTEN modulates cell cycle progression and cell survival by regulating phosphatidylinositol 3, 4, 5,-trisphosphate and Akt/protein kinase B signaling pathway.** *Proceedings of the National Academy of Sciences* 1999, **96:**6199-6204.
5. Li DM, Sun H: **PTEN/MMAC1/TEP1 suppresses the tumorigenicity and induces G1 cell cycle arrest in human glioblastoma cells.** *Proc Natl Acad Sci U S A* 1998, **95:**15406-15411.
6. Tamura M, Gu J, Takino T, Yamada KM: **Tumor Suppressor PTEN Inhibition of Cell Invasion, Migration, and Growth: Differential Involvement of Focal Adhesion Kinase and p130Cas.** *Cancer Research* 1999, **59:**442-449.
7. Dey N, Crosswell HE, De P, Parsons R, Peng Q, Su JD, Durden DL: **The Protein Phosphatase Activity of PTEN Regulates Src Family Kinases and Controls Glioma Migration.** *Cancer Research* 2008, **68:**1862-1871.
8. Yamada KM, Araki M: **Tumor suppressor PTEN: modulator of cell signaling, growth, migration and apoptosis.** *Journal of cell science* 2001, **114:**2375-2382.
9. Nassif NT, Lobo GP, Wu X, Henderson CJA, Morrison CD, Eng C, Jalaludin B, Segelov E: **PTEN mutations are common in sporadic microsatellite stable colorectal cancer.** *Oncogene* 2004, **23:**617-628.
10. Kapitonov D, Allegood JC, Mitchell C, Hait NC, Almenara JA, Adams JK, Zipkin RE, Dent P, Kordula T, Milstien S, Spiegel S: **Targeting sphingosine kinase 1 inhibits Akt signaling, induces apoptosis, and suppresses growth of human glioblastoma cells and xenografts.** *Cancer Res* 2009, **69:**6915-6923.
11. Zhu L, Wang Z, Lin Y, Chen Z, Liu H, Chen Y, Wang N, Song X: **Sphingosine kinase 1 enhances the invasion and migration of non-small cell lung cancer cells via the AKT pathway.** *Oncol Rep* 2015, **33:**1257-1263.
12. Haddadi N, Lin Y, Travis G, Simpson AM, Nassif NT, McGowan EM: **PTEN/PTENP1: 'Regulating the regulator of RTK-dependent PI3K/Akt signalling', new targets for cancer therapy.** *Mol Cancer* 2018, **17:**37.
13. Song MS, Carracedo A, Salmena L, Song SJ, Egia A, Malumbres M, Pandolfi PP: **Nuclear PTEN Regulates the APC-CDH1 Tumor-Suppressive Complex in a Phosphatase-Independent Manner.** *Cell* 2011, **144:**187-199.
14. Yagoub D, Wilkins MR, Lay AJ, Kaczorowski DC, Hatoum D, Bajan S, Hutvagner G, Lai JH, Wu W, Martiniello-Wilks R: **Sphingosine kinase 1 isoform-specific interactions in breast cancer.** *Molecular Endocrinology* 2014, **28:**1899-1915.
15. Haddadi N, Lin Y, Simpson AM, Nassif NT, McGowan EM: **"Dicing and Splicing" Sphingosine Kinase and Relevance to Cancer.** *Int J Mol Sci* 2017, **18**.
16. Hatoum D, Haddadi N, Lin Y, Nassif NT, McGowan EM: **Mammalian sphingosine kinase (SphK) isoenzymes and isoform expression: challenges for SphK as an oncotarget.** *Oncotarget* 2017, **8:**36898-36929.

17. Li DM, Sun H: **TEP1, encoded by a candidate tumor suppressor locus, is a novel protein tyrosine phosphatase regulated by transforming growth factor beta.** *Cancer Res* 1997, **57:**2124-2129.
18. Steck PA, Pershouse MA, Jasser SA, Yung WK, Lin H, Ligon AH, Langford LA, Baumgard ML, Hattier T, Davis T, et al: **Identification of a candidate tumour suppressor gene, MMAC1, at chromosome 10q23.3 that is mutated in multiple advanced cancers.** *Nat Genet* 1997, **15:**356-362.
19. Hollander MC, Blumenthal GM, Dennis PA: **PTEN loss in the continuum of common cancers, rare syndromes and mouse models.** *Nature Revew Cancer* 2011, **11:**289-301.
20. Li J, Yen C, Liaw D, Podsypanina K, Bose S, Wang SI, Puc J, Miliaresis C, Rodgers L, McCombie R, et al: **PTEN, a putative protein tyrosine phosphatase gene mutated in human brain, breast, and prostate cancer.** *Science* 1997, **275:**1943-1947.
21. Tan MH, Mester JL, Ngeow J, Rybicki LA, Orloff MS, Eng C: **Lifetime cancer risks in individuals with germline PTEN mutations.** *Clin Cancer Res* 2012, **18:**400-407.
22. Boosani CS, Agrawal DK: **PTEN modulators: a patent review.** *Expert Opinion on Therapeutic Patents* 2013, **23:**569-580.
23. Eng C: **PTEN: One Gene, Many Syndromes.** *Human Mutation* 2003, **22:**183-198.
24. Di Cristofano A, Pandolfi PP: **The Multiple Roles of PTEN in Tumor Suppression.** *Cell* 2000, **100:**387-390.
25. Weng L-P, Smith WM, Brown JL, Eng C: **PTEN inhibits insulin-stimulated MEK/MAPK activation and cell growth by blocking IRS-1 phosphorylation and IRS-1/Grb-2/Sos complex formation in a breast cancer model.** *Human Molecular Genetics* 2001, **10:**605-616.
26. Waite KA, Eng C: **Protean PTEN: form and function.** *Am J Hum Genet* 2002, **70:**829-844.
27. Worby CA, Dixon JE: **Pten.** *Annu Rev Biochem* 2014, **83:**641-669.
28. Maehama T, Taylor GS, Dixon JE: **PTEN and myotubularin: novel phosphoinositide phosphatases.** *Annu Rev Biochem* 2001, **70:**247-279.
29. Gerber H-P, McMurtrey A, Kowalski J, Yan M, Keyt BA, Dixit V, Ferrara N: **Vascular Endothelial Growth Factor Regulates Endothelial Cell Survival through the Phosphatidylinositol 3'-Kinase/Akt Signal Transduction Pathway: REQUIREMENT FOR Flk-1/KDR ACTIVATION.** *Journal of Biological Chemistry* 1998, **273:**30336-30343.
30. Ambasta R, Sharma A, Kumar P: **Nanoparticle mediated targeting of VEGFR and cancer stem cells for cancer therapy.** *Vascular Cell* 2011, **3:**1-9.
31. Tibarewal P, Zilidis G, Spinelli L, Schurch N, Maccario H, Gray A, Perera NM, Davidson L, Barton GJ, Leslie NR: **PTEN protein phosphatase activity correlates with control of gene expression and invasion, a tumor-suppressing phenotype, but not with AKT activity.** *Sci Signal* 2012, **5:**ra18.
32. Weng LP, Smith WM, Dahia PL, Ziebold U, Gil E, Lees JA, Eng C: **PTEN suppresses breast cancer cell growth by phosphatase activity-dependent G1 arrest followed by cell death.** *Cancer Res* 1999, **59:**5808-5814.
33. Fang J, Ding M, Yang L, Liu L-Z, Jiang B-H: **PI3K/PTEN/AKT signaling regulates prostate tumor angiogenesis.** *Cellular Signalling* 2007, **19:**2487-2497.
34. Graupera M, Guillermet-Guibert J, Foukas LC, Phng L-K, Cain RJ, Salpekar A, Pearce W, Meek S, Millan J, Cutillas PR, et al: **Angiogenesis selectively requires the p110[agr] isoform of PI3K to control endothelial cell migration.** *Nature* 2008, **453:**662-666.
35. Endersby R, Baker S: **PTEN signaling in brain: neuropathology and tumorigenesis.** *Oncogene* 2008, **27:**5416-5430.
36. Knudson AG, Jr.: **Mutation and cancer: statistical study of retinoblastoma.** *Proc Natl Acad Sci U S A* 1971, **68:**820-823.

37. Salmena L, Carracedo A, Pandolfi PP: **Tenets of PTEN Tumor Suppression.** *Cell* 2008, **133:**403-414.
38. Alimonti A, Carracedo A, Clohessy JG, Trotman LC, Nardella C, Egia A, Salmena L, Sampieri K, Haveman WJ, Brogi E, et al: **Subtle variations in Pten dose determine cancer susceptibility.** *Nat Genet* 2010, **42:**454-458.
39. Mitchell F: **Diabetes: PTEN mutations increase insulin sensitivity and obesity.** *Nat Rev Endocrinol* 2012, **8:**698.
40. Herman GE, Butter E, Enrile B, Pastore M, Prior TW, Sommer A: **Increasing knowledge of PTEN germline mutations: Two additional patients with autism and macrocephaly.** *American Journal of Medical Genetics Part A* 2007, **143:**589-593.
41. Butler MG, Dasouki MJ, Zhou X-P, Talebizadeh Z, Brown M, Takahashi TN, Miles JH, Wang CH, Stratton R, Pilarski R, Eng C: **Subset of individuals with autism spectrum disorders and extreme macrocephaly associated with germline PTEN tumour suppressor gene mutations.** *Journal of Medical Genetics* 2005, **42:**318-321.
42. Kitagishi Y, Wada Y, Matsuda S: **Roles of PI3K/AKT/PTEN pathway in the pathogenesis of parkinson's disease and the neuropsychiatric symptoms.** *International Neuropsychiatric Disease Journal* 2014, **2:**1-12.
43. Yan MH, Wang X, Zhu X: **Mitochondrial defects and oxidative stress in Alzheimer disease and Parkinson disease.** *Free Radical Biology and Medicine* 2013, **62:**90-101.
44. Furnari FB, Lin H, Huang H-JS, Cavenee WK: **Growth suppression of glioma cells by PTEN requires a functional phosphatase catalytic domain.** *Proceedings of the National Academy of Sciences* 1997, **94:**12479-12484.
45. Myers MP, Pass I, Batty IH, Van der Kaay J, Stolarov JP, Hemmings BA, Wigler MH, Downes CP, Tonks NK: **The lipid phosphatase activity of PTEN is critical for its tumor supressor function.** *Proceedings of the National Academy of Sciences* 1998, **95:**13513-13518.
46. Tamura M, Gu J, Matsumoto K, Aota S-i, Parsons R, Yamada KM: **Inhibition of cell migration, spreading, and focal adhesions by tumor suppressor PTEN.** *Science* 1998, **280:**1614-1617.
47. Rodriguez J, Guiteau J, Nazareth L, Reid J, Goss J, Gibbs R, Gingras M-C: **Sequencing the Full-Length of the Phosphatase and Tensin Homolog (PTEN) Gene in Hepatocellular Carcinoma (HCC) Using the 454 GS20 and Illumina GA DNA Sequencing Platforms.** *World Journal of Surgery* 2009, **33:**647-652.
48. Lee J-O, Yang H, Georgescu M-M, Di Cristofano A, Maehama T, Shi Y, Dixon JE, Pandolfi P, Pavletich NP: **Crystal Structure of the PTEN Tumor Suppressor: Implications for Its Phosphoinositide Phosphatase Activity and Membrane Association.** *Cell* 1999, **99:**323-334.
49. Yuvaniyama J, Denu JM, Dixon JE, Saper MA: **Crystal structure of the dual specificity protein phosphatase VHR.** *Science* 1996, **272:**1328-1331.
50. Houslay MD: **Arresting times for PTEN.** *The EMBO Journal* 2011, **30:**2513-2515.
51. Torres J, Pulido R: **The tumor suppressor PTEN is phosphorylated by the protein kinase CK2 at its C terminus implications for PTEN stability to proteasome-mediated degradation.** *Journal of Biological Chemistry* 2001, **276:**993-998.
52. Simpson L, Parsons R: **PTEN: life as a tumor suppressor.** *Experimental cell research* 2001, **264:**29-41.
53. Endersby R, Baker SJ: **PTEN signaling in brain: neuropathology and tumorigenesis.** *Oncogene* 2008, **27:**5416-5430.
54. Song MS, Salmena L, Pandolfi PP: **The functions and regulation of the PTEN tumour suppressor.** *Nat Rev Mol Cell Biol* 2012, **13:**283-296.
55. Downward J: **Mechanisms and consequences of activation of protein kinase B/Akt.** *Current opinion in cell biology* 1998, **10:**262-267.

56. Datta SR, Brunet A, Greenberg ME: **Cellular survival: a play in three Akts.** *Genes & development* 1999, **13:**2905-2927.
57. Hemmings BA, Restuccia DF: **PI3K-PKB/Akt pathway.** *Cold Spring Harb Perspect Biol* 2012, **4:**11189.
58. Dillon LM, Miller TW: **Therapeutic targeting of cancers with loss of PTEN function.** *Curr Drug Targets* 2014, **15:**65-79.
59. Gu J, Tamura M, Pankov R, Danen EH, Takino T, Matsumoto K, Yamada KM: **Shc and FAK differentially regulate cell motility and directionality modulated by PTEN.** *The Journal of cell biology* 1999, **146:**389-404.
60. Milella M, Falcone I, Conciatori F, Cesta Incani U, Del Curatolo A, Inzerilli N, Nuzzo CM, Vaccaro V, Vari S, Cognetti F, Ciuffreda L: **PTEN: Multiple Functions in Human Malignant Tumors.** *Front Oncol* 2015, **5:**24.
61. Park M-J, Kim M-S, Park I-C, Kang H-S, Yoo H, Park SH, Rhee CH, Hong S-I, Lee S-H: **PTEN Suppresses Hyaluronic Acid-induced Matrix Metalloproteinase-9 Expression in U87MG Glioblastoma Cells through Focal Adhesion Kinase Dephosphorylation.** *Cancer Research* 2002, **62:**6318-6322.
62. Besson A, Robbins SM, Wee Yong V: **PTEN/MMAC1/TEP1 in signal transduction and tumorigenesis.** *European Journal of Biochemistry* 1999, **263:**605-611.
63. Preissner KT, Reuning U: **Vitronectin in vascular context: facets of a multitalented matricellular protein.** *Seminars in thrombosis and hemostasis* 2011, **37:**408-424.
64. Felding-Habermann B, Cheresh DA: **Vitronectin and its receptors.** *Current Opinion in Cell Biology* 1993, **5:**864-868.
65. Gassama-Diagne A, Yu W, ter Beest M, Martin-Belmonte F, Kierbel A, Engel J, Mostov K: **Phosphatidylinositol-3,4,5-trisphosphate regulates the formation of the basolateral plasma membrane in epithelial cells.** *Nature Cell Biology* 2006, **8:**963-970.
66. Jiang B-H, Liu L-Z: **PI3K/PTEN Signaling in Angiogenesis and Tumorigenesis.** *Advances in cancer research* 2009, **102:**19-65.
67. Zundel W, Schindler C, Haas-Kogan D, Koong A, Kaper F, Chen E, Gottschalk AR, Ryan HE, Johnson RS, Jefferson AB, et al: **Loss of PTEN facilitates HIF-1-mediated gene expression.** *Genes & Development* 2000, **14:**391-396.
68. Wen S, Stolarov J, Myers MP, Su JD, Wigler MH, Tonks NK, Durden DL: **PTEN controls tumor-induced angiogenesis.** *Proceedings of the National Academy of Sciences* 2001, **98:**4622-4627.
69. Bassi C, Ho J, Srikumar T, Dowling RJO, Gorrini C, Miller SJ, Mak TW, Neel BG, Raught B, Stambolic V: **Nuclear PTEN Controls DNA Repair and Sensitivity to Genotoxic Stress.** *Science* 2013, **341:**395-399.
70. Shen WH, Balajee AS, Wang J, Wu H, Eng C, Pandolfi PP, Yin Y: **Essential Role for Nuclear PTEN in Maintaining Chromosomal Integrity.** *Cell* 2007, **128:**157-170.
71. Chung J-H, Ginn-Pease ME, Eng C: **Phosphatase and Tensin Homologue Deleted on Chromosome 10 (PTEN) Has Nuclear Localization Signal–Like Sequences for Nuclear Import Mediated by Major Vault Protein.** *Cancer Research* 2005, **65:**4108-4116.
72. Planchon SM, Waite KA, Eng C: **The nuclear affairs of PTEN.** *Journal of Cell Science* 2008, **121:**249-253.
73. Trotman LC, Wang X, Alimonti A, Chen Z, Teruya-Feldstein J, Yang H, Pavletich NP, Carver BS, Cordon-Cardo C, Erdjument-Bromage H, et al: **Ubiquitination Regulates PTEN Nuclear Import and Tumor Suppression.** *Cell* 2007, **128:**141-156.
74. Yang JM, Schiapparelli P, Nguyen HN, Igarashi A, Zhang Q, Abbadi S, Amzel LM, Sesaki H, Quinones-Hinojosa A, Iijima M: **Characterization of PTEN mutations in brain cancer reveals that pten mono-ubiquitination promotes protein stability and nuclear localization.** *Oncogene* 2017, **36:**3673-3685.

75. Ming M, He Y-Y: **PTEN: new insights into its regulation and function in skin cancer.** *Journal of Investigative Dermatology* 2009, **129:**2109-2112.
76. Smith JM, Kirk EP, Theodosopoulos G, Marshall GM, Walker J, Rogers M, Field M, Brereton JJ, Marsh DJ: **Germline mutation of the tumour suppressor PTEN in Proteus syndrome.** *J Med Genet* 2002, **39:**937-940.
77. Liaw D, Marsh DJ, Li J, Dahia PL, Wang SI, Zheng Z, Bose S, Call KM, Tsou HC, Peacoke M: **Germline mutations of the PTEN gene in Cowden disease, an inherited breast and thyroid cancer syndrome.** *Nature genetics* 1997, **16:**64-67.
78. Liaw D, Marsh DJ, Li J, Dahia PL, Wang SI, Zheng Z, Bose S, Call KM, Tsou HC, Peacocke M, et al: **Germline mutations of the PTEN gene in Cowden disease, an inherited breast and thyroid cancer syndrome.** *Nat Genet* 1997, **16:**64-67.
79. Mester JL, Moore RA, Eng C: **PTEN germline mutations in patients initially tested for other hereditary cancer syndromes: would use of risk assessment tools reduce genetic testing?** *Oncologist* 2013, **18:**1083-1090.
80. Chen HJ, Romigh T, Sesock K, Eng C: **Characterization of cryptic splicing in germline PTEN intronic variants in Cowden syndrome.** *Hum Mutat* 2017, **38:**1372-1377.
81. Tilot AK, Frazier TW, 2nd, Eng C: **Balancing Proliferation and Connectivity in PTEN-associated Autism Spectrum Disorder.** *Neurotherapeutics* 2015, **12:**609-619.
82. Eng C: **Will the real Cowden syndrome please stand up: revised diagnostic criteria.** *J Med Genet* 2000, **37:**828-830.
83. Marsh DJ, Dahia PL, Coulon V, Zheng Z, Dorion-Bonnet F, Call KM, Little R, Lin AY, Eeles RA, Goldstein AM: **Allelic imbalance, including deletion of PTEN/MMAC1, at the Cowden disease locus on 10q22-23, in hamartomas from patients with cowden syndrome and germline PTEN mutation.** *Genes, Chromosomes and Cancer* 1998, **21:**61-69.
84. Marsh DJ, Dahia PL, Zheng Z, Liaw D, Parsons R, Gorlin RJ, Eng C: **Germline mutations in PTEN are present in Bannayan-Zonana syndrome.** *Nature genetics* 1997, **16:**333-334.
85. Longy M, Coulon V, Duboue B, David A, Larregue M, Eng C, Amati P, Kraimps J-L, Bottani A, Lacombe D: **Mutations of PTEN in patients with Bannayan-Riley-Ruvalcaba phenotype.** *Journal of medical genetics* 1998, **35:**886-889.
86. Zhou X-P, Waite KA, Pilarski R, Hampel H, Fernandez MJ, Bos C, Dasouki M, Feldman GL, Greenberg LA, Ivanovich J: **Germline PTEN promoter mutations and deletions in Cowden/Bannayan-Riley-Ruvalcaba syndrome result in aberrant PTEN protein and dysregulation of the phosphoinositol-3-kinase/Akt pathway.** *The American Journal of Human Genetics* 2003, **73:**404-411.
87. Marsh DJ, Kum JB, Lunetta KL, Bennett MJ, Gorlin RJ, Ahmed SF, Bodurtha J, Crowe C, Curtis MA, Dasouki M, et al: **PTEN mutation spectrum and genotype-phenotype correlations in Bannayan-Riley-Ruvalcaba syndrome suggest a single entity with Cowden syndrome.** *Human Molecular Genetics* 1999, **8:**1461-1472.
88. Biesecker L: **The challenges of Proteus syndrome: diagnosis and management.** *European journal of human genetics* 2006, **14:**1151-1157.
89. Smith JM, Kirk EPE, Theodosopoulos G, Marshall GM, Walker J, Rogers M, Field M, Brereton JJ, Marsh DJ: **Germline mutation of the tumour suppressor PTEN in Proteus syndrome.** *Journal of Medical Genetics* 2002, **39:**937-940.
90. Nelen MR, van Staveren WCG, Peeters EAJ, Ben Hassel M, Gorlin RJ, Hamm H, Lindboe CF, Fryns J-P, Sijmons RH, Woods DG, et al: **Germline Mutations in the PTEN/MMAC1 Gene in Patients With Cowden Disease.** *Human Molecular Genetics* 1997, **6:**1383-1387.

91. Pilarski R, Eng C: **Will the real Cowden syndrome please stand up (again)? Expanding mutational and clinical spectra of the PTEN hamartoma tumour syndrome.** *Journal of Medical Genetics* 2004, **41:**323-326.
92. Hamilton JA, Stewart LMD, Ajayi L, Gray IC, Gray NE, Roberts KG, Watson GJ, Kaisary AV, Snary D: **The expression profile for the tumour suppressor gene PTEN and associated polymorphic markers.** *British Journal of Cancer* 2000, **82:**1671-1676.
93. Zysman MA, Chapman WB, Bapat B: **Considerations when analyzing the methylation status of PTEN tumor suppressor gene.** *The American journal of pathology* 2002, **160:**795-800.
94. Mueller S, Phillips J, Onar-Thomas A, Romero E, Zheng S, Wiencke JK, McBride SM, Cowdrey C, Prados MD, Weiss WA, et al: **PTEN promoter methylation and activation of the PI3K/Akt/mTOR pathway in pediatric gliomas and influence on clinical outcome.** *Neuro-Oncology* 2012, **14:**1146-1152.
95. Poliseno L, Salmena L, Zhang J, Carver B, Haveman WJ, Pandolfi PP: **A coding-independent function of gene and pseudogene mRNAs regulates tumour biology.** *Nature* 2010, **465:**1033-1038.
96. Koul D: **PTEN signaling pathways in glioblastoma.** *Cancer biology & therapy* 2008, **7:**1321-1325.
97. Chiariello E, Roz L, Albarosa R, Magnani I, Finocchiaro G: **PTEN/MMAC1 mutations in primary glioblastomas and short-term cultures of malignant gliomas.** *Oncogene* 1998, **16:**541-545.
98. Duerr EM, Rollbrocker B, Hayashi Y, Peters N, Meyer-Puttlitz B, Louis DN, Schramm J, Wiestler OD, Parsons R, Eng C, von Deimling A: **PTEN mutations in gliomas and glioneuronal tumors.** *Oncogene* 1998, **16:**2259-2264.
99. Liu W, James CD, Frederick L, Alderete BE, Jenkins RB: **PTEN/MMAC1 mutations and EGFR amplification in glioblastomas.** *Cancer Res* 1997, **57:**5254-5257.
100. Teng DH, Hu R, Lin H, Davis T, Iliev D, Frye C, Swedlund B, Hansen KL, Vinson VL, Gumpper KL, et al: **MMAC1/PTEN mutations in primary tumor specimens and tumor cell lines.** *Cancer Res* 1997, **57:**5221-5225.
101. Ittmann MM: **Loss of heterozygosity on chromosomes 10 and 17 in clinically localized prostate carcinoma.** *Prostate* 1996, **28:**275-281.
102. Ittmann M: **Allelic loss on chromosome 10 in prostate adenocarcinoma.** *Cancer Res* 1996, **56:**2143-2147.
103. Cairns P, Okami K, Halachmi S, Halachmi N, Esteller M, Herman JG, Jen J, Isaacs WB, Bova GS, Sidransky D: **Frequent inactivation of PTEN/MMAC1 in primary prostate cancer.** *Cancer Res* 1997, **57:**4997-5000.
104. Suzuki H, Freije D, Nusskern DR, Okami K, Cairns P, Sidransky D, Isaacs WB, Bova GS: **Interfocal heterogeneity of PTEN/MMAC1 gene alterations in multiple metastatic prostate cancer tissues.** *Cancer Res* 1998, **58:**204-209.
105. Feilotter HE, Nagai MA, Boag AH, Eng C, Mulligan LM: **Analysis of PTEN and the 10q23 region in primary prostate carcinomas.** *Oncogene* 1998, **16:**1743-1748.
106. McMenamin ME, Soung P, Perera S, Kaplan I, Loda M, Sellers WR: **Loss of PTEN expression in paraffin-embedded primary prostate cancer correlates with high Gleason score and advanced stage.** *Cancer Res* 1999, **59:**4291-4296.
107. Risinger JI, Hayes AK, Berchuck A, Barrett JC: **PTEN/MMAC1 mutations in endometrial cancers.** *Cancer Res* 1997, **57:**4736-4738.
108. Tashiro H, Blazes MS, Wu R, Cho KR, Bose S, Wang SI, Li J, Parsons R, Ellenson LH: **Mutations in PTEN are frequent in endometrial carcinoma but rare in other common gynecological malignancies.** *Cancer Res* 1997, **57:**3935-3940.

109. Stahl JM, Cheung M, Sharma A, Trivedi NR, Shanmugam S, Robertson GP: **Loss of PTEN promotes tumor development in malignant melanoma.** *Cancer Res* 2003, **63:**2881-2890.
110. Mutter GL, Ince TA, Baak JP, Kust GA, Zhou XP, Eng C: **Molecular identification of latent precancers in histologically normal endometrium.** *Cancer Res* 2001, **61:**4311-4314.
111. Mutter GL, Lin MC, Fitzgerald JT, Kum JB, Baak JP, Lees JA, Weng LP, Eng C: **Altered PTEN expression as a diagnostic marker for the earliest endometrial precancers.** *J Natl Cancer Inst* 2000, **92:**924-930.
112. Bose S, Wang SI, Terry MB, Hibshoosh H, Parsons R: **Allelic loss of chromosome 10q23 is associated with tumor progression in breast carcinomas.** *Oncogene* 1998, **17:**123-127.
113. Rhei E, Kang L, Bogomolniy F, Federici MG, Borgen PI, Boyd J: **Mutation analysis of the putative tumor suppressor gene PTEN/MMAC1 in primary breast carcinomas.** *Cancer Res* 1997, **57:**3657-3659.
114. Perren A, Weng LP, Boag AH, Ziebold U, Thakore K, Dahia PL, Komminoth P, Lees JA, Mulligan LM, Mutter GL, Eng C: **Immunohistochemical evidence of loss of PTEN expression in primary ductal adenocarcinomas of the breast.** *Am J Pathol* 1999, **155:**1253-1260.
115. Wang Y, DiGiovanna JJ, Stern JB, Hornyak TJ, Raffeld M, Khan SG, Oh K-S, Hollander MC, Dennis PA, Kraemer KH: **Evidence of ultraviolet type mutations in xeroderma pigmentosum melanomas.** *Proceedings of the National Academy of Sciences* 2009, **106:**6279-6284.
116. Zhou X-P, Marsh DJ, Hampel H, Mulliken JB, Gimm O, Eng C: **Germline and germline mosaic PTEN mutations associated with a Proteus-like syndrome of hemihypertrophy, lower limb asymmetry, arteriovenous malformations and lipomatosis.** *Human molecular genetics* 2000, **9:**765-768.
117. Cairns P, Evron E, Okami K, Halachmi N, Esteller M, Herman JG, Bose S, Wang SI, Parsons R, Sidransky D: **Point mutation and homozygous deletion of PTEN/MMAC1 in primary bladder cancers.** *Oncogene* 1998, **16:**3215-3218.
118. Okami K, Wu L, Riggins G, Cairns P, Goggins M, Evron E, Halachmi N, Ahrendt SA, Reed AL, Hilgers W, et al: **Analysis of PTEN/MMAC1 Alterations in Aerodigestive Tract Tumors.** *Cancer Research* 1998, **58:**509-511.
119. Wang X, Jiang X: **Post-translational regulation of PTEN.** *Oncogene* 2008, **27:**5454-5463.
120. Freeman DJ, Li AG, Wei G, Li HH, Kertesz N, Lesche R, Whale AD, Martinez-Diaz H, Rozengurt N, Cardiff RD, et al: **PTEN tumor suppressor regulates p53 protein levels and activity through phosphatase-dependent and -independent mechanisms.** *Cancer Cell* 2003, **3:**117-130.
121. Shen YH, Zhang L, Gan Y, Wang X, Wang J, LeMaire SA, Coselli JS, Wang XL: **Up-regulation of PTEN (phosphatase and tensin homolog deleted on chromosome ten) mediates p38 MAPK stress signal-induced inhibition of insulin signaling A cross-talk between stress signaling and insulin signaling in resistin-treated human endothelial cells.** *Journal of Biological Chemistry* 2006, **281:**7727-7736.
122. Bonofiglio D, Gabriele S, Aquila S, Catalano S, Gentile M, Middea E, Giordano F, Ando S: **Estrogen receptor alpha binds to peroxisome proliferator-activated receptor response element and negatively interferes with peroxisome proliferator-activated receptor gamma signaling in breast cancer cells.** *Clin Cancer Res* 2005, **11:**6139-6147.
123. Uygur B, Abramo K, Leikina E, Vary C, Liaw L, Wu WS: **SLUG is a direct transcriptional repressor of PTEN tumor suppressor.** *Prostate* 2015, **75:**907-916.

124. Sulis ML, Parsons R: **PTEN: from pathology to biology.** *Trends Cell Biol* 2003, **13:**478-483.
125. Guil S, Esteller M: **RNA–RNA interactions in gene regulation: the coding and noncoding players.** *Trends Biochem Sci* 2015, **40:**248-256.
126. Stambolic V, MacPherson D, Sas D, Lin Y, Snow B, Jang Y, Benchimol S, Mak TW: **Regulation of PTEN Transcription by p53.** *Molecular Cell* 2001, **8:**317-325.
127. Nakanishi A, Kitagishi Y, Ogura Y, Matsuda S: **The tumor suppressor PTEN interacts with p53 in hereditary cancer (Review).** *Int J Oncol* 2014, **44:**1813-1819.
128. Mayo LD, Donner DB: **The PTEN, Mdm2, p53 tumor suppressor-oncoprotein network.** *Trends Biochem Sci* 2002, **27:**462-467.
129. Virolle T, Adamson ED, Baron V, Birle D, Mercola D, Mustelin T, de Belle I: **The Egr-1 transcription factor directly activates PTEN during irradiation-induced signalling.** *Nature cell biology* 2001, **3:**1124-1128.
130. Moorehead RA, Hojilla CV, De Belle I, Wood GA, Fata JE, Adamson ED, Watson KL, Edwards DR, Khokha R: **Insulin-like growth factor-II regulates PTEN expression in the mammary gland.** *Journal of Biological Chemistry* 2003, **278:**50422-50427.
131. Patel L, Pass I, Coxon P, Downes CP, Smith SA, Macphee CH: **Tumor suppressor and anti-inflammatory actions of PPARγ agonists are mediated via upregulation of PTEN.** *Current Biology* 2001, **11:**764-768.
132. Song L-B, Li J, Liao W-T, Feng Y, Yu C-P, Hu L-J, Kong Q-L, Xu L-H, Zhang X, Liu W-L: **The polycomb group protein Bmi-1 represses the tumor suppressor PTEN and induces epithelial-mesenchymal transition in human nasopharyngeal epithelial cells.** *The Journal of clinical investigation* 2009, **119:**3626.
133. Whelan JT, Forbes SL, Bertrand FE: **CBF-1 (RBP-Jk) binds to the PTEN promoter and regulates PTEN gene expression.** *Cell Cycle* 2007, **6:**80-84.
134. Meng F, Henson R, Lang M, Wehbe H, Maheshwari S, Mendell JT, Jiang J, Schmittgen TD, Patel T: **Involvement of human micro-RNA in growth and response to chemotherapy in human cholangiocarcinoma cell lines.** *Gastroenterology* 2006, **130:**2113-2129.
135. Salmena L, Poliseno L, Tay Y, Kats L, Pandolfi PP: **A ceRNA hypothesis: the Rosetta Stone of a hidden RNA language?** *Cell* 2011, **146:**353-358.
136. Tay Y, Kats L, Salmena L, Weiss D, Tan SM, Ala U, Karreth F, Poliseno L, Provero P, Di Cunto F, et al: **Coding-independent regulation of the tumor suppressor PTEN by competing endogenous mRNAs.** *Cell* 2011, **147:**344-357.
137. Lewis BP, Burge CB, Bartel DP: **Conserved seed pairing, often flanked by adenosines, indicates that thousands of human genes are microRNA targets.** *Cell* 2005, **120:**15-20.
138. Phelps M, Coss C, Wang H, Cook M: **Registered report: Coding-independent regulation of the tumor suppressor PTEN by competing endogenous mRNAs.** *eLife* 2016, **5**.
139. Mohammadi A, Mansoori B, Baradaran B: **The role of microRNAs in colorectal cancer.** *Biomed Pharmacother* 2016, **84:**705-713.
140. Issabekova A, Berillo O, Regnier M, Anatoly I: **Interactions of intergenic microRNAs with mRNAs of genes involved in carcinogenesis.** *Bioinformation* 2012, **8:**513-518.
141. An Y, Furber KL, Ji S: **Pseudogenes regulate parental gene expression via ceRNA network.** *J Cell Mol Med* 2017, **21:**185-192.
142. Dong H, Lei J, Ding L, Wen Y, Ju H, Zhang X: **MicroRNA: function, detection, and bioanalysis.** *Chem Rev* 2013, **113:**6207-6233.
143. He L: **Posttranscriptional regulation of PTEN dosage by noncoding RNAs.** *Sci Signal* 2010, **3:**pe39-45.
144. Poliseno L, Pandolfi PP: **PTEN ceRNA networks in human cancer.** *Methods* 2015, **77-78:**41-50.

145. Tang J, Ning R, Zeng B, Li Y: **Molecular Evolution of PTEN Pseudogenes in Mammals.** *PLoS One* 2016, **11:**e0167851.
146. Shi X, Nie F, Wang Z, Sun M: **Pseudogene-expressed RNAs: a new frontier in cancers.** *Tumor Biology* 2016, **37:**1471-1478.
147. Ambros V: **The evolution of our thinking about microRNAs.** *Nat Med* 2008, **14:**1036-1040.
148. Chen CL, Tseng YW, Wu JC, Chen GY, Lin KC, Hwang SM, Hu YC: **Suppression of hepatocellular carcinoma by baculovirus-mediated expression of long non-coding RNA PTENP1 and MicroRNA regulation.** *Biomaterials* 2015, **44:**71-81.
149. Yu G, Yao W, Gumireddy K, Li A, Wang J, Xiao W, Chen K, Xiao H, Li H, Tang K: **Pseudogene PTENP1 functions as a competing endogenous RNA to suppress clear-cell renal cell carcinoma progression.** *Molecular cancer therapeutics* 2014, **13:**3086-3097.
150. Yao Y, Ma J, Xue Y, Wang P, Li Z, Liu J, Chen L, Xi Z, Teng H, Wang Z, et al: **Knockdown of long non-coding RNA XIST exerts tumor-suppressive functions in human glioblastoma stem cells by up-regulating miR-152.** *Cancer Letters* 2015, **359:**75-86.
151. Li N, Miao Y, Shan Y, Liu B, Li Y, Zhao L, Jia L: **MiR-106b and miR-93 regulate cell progression by suppression of PTEN via PI3K/Akt pathway in breast cancer.** *Cell death & disease* 2017, **8:**e2796.
152. Wu T, Du Y: **LncRNAs: From Basic Research to Medical Application.** *International Journal of Biological Sciences* 2017, **13:**295.
153. Dahia PL, FitzGerald MG, Zhang X, Marsh DJ, Zheng Z, Pietsch T, von Deimling A, Haluska FG, Haber DA, Eng C: **A highly conserved processed PTEN pseudogene is located on chromosome band 9p21.** *Oncogene* 1998, **16:**2403-2406.
154. Fujii GH, Morimoto AM, Berson AE, Bolen JB: **Transcriptional analysis of the PTEN/MMAC1 pseudogene, psiPTEN.** *Oncogene* 1999, **18:**1765-1769.
155. Poliseno L, Salmena L, Riccardi L, Fornari A, Song MS, Hobbs RM, Sportoletti P, Varmeh S, Egia A, Fedele G, et al: **Identification of the miR-106b∼25 MicroRNA Cluster as a Proto-Oncogenic PTEN-Targeting Intron That Cooperates with Its Host Gene MCM7 in Transformation.** *Science signaling* 2010, **3:**ra29-ra29.
156. Poliseno L, Haimovic A, Christos PJ: **Deletion of PTENP1 pseudogene in human melanoma.** *The Journal of investigative dermatology* 2011, **131:**2497.
157. Miller SJ, Lou DY, Seldin DC, Lane WS, Neel BG: **Direct identification of PTEN phosphorylation sites.** *FEBS letters* 2002, **528:**145-153.
158. Mehenni H, Lin-Marq N, Buchet-Poyau K, Reymond A, Collart MA, Picard D, Antonarakis SE: **LKB1 interacts with and phosphorylates PTEN: a functional link between two proteins involved in cancer predisposing syndromes.** *Human molecular genetics* 2005, **14:**2209-2219.
159. Al-Khouri AM, Ma Y, Togo SH, Williams S, Mustelin T: **Cooperative phosphorylation of the tumor suppressor phosphatase and tensin homologue (PTEN) by casein kinases and glycogen synthase kinase 3β.** *Journal of Biological Chemistry* 2005, **280:**35195-35202.
160. Zhang XC, Piccini A, Myers MP, Van Aelst L, Tonks NK: **Functional analysis of the protein phosphatase activity of PTEN.** *Biochem J* 2012, **444:**457-464.
161. Okumura K, Mendoza M, Bachoo RM, DePinho RA, Cavenee WK, Furnari FB: **PCAF modulates PTEN activity.** *Journal of Biological Chemistry* 2006, **281:**26562-26568.
162. Ikenoue T, Inoki K, Zhao B, Guan K-L: **PTEN Acetylation Modulates Its Interaction with PDZ Domain.** *Cancer Research* 2008, **68:**6908-6912.
163. Lee S-R, Yang K-S, Kwon J, Lee C, Jeong W, Rhee SG: **Reversible Inactivation of the Tumor Suppressor PTEN by H2O2.** *Journal of Biological Chemistry* 2002, **277:**20336-20342.

164. Leslie NR, Batty IH, Maccario H, Davidson L, Downes CP: **Understanding PTEN regulation: PIP2, polarity and protein stability.** *Oncogene* 2008, **27:**5464-5476.
165. Bonneau D, Longy M: **Mutations of the human PTEN gene.** *Human Mutation* 2000, **16:**109-122.
166. Furgerson M, Fechheimer M, Furukawa R: **Model Hirano bodies protect against tau-independent and tau-dependent cell death initiated by the amyloid precursor protein intracellular domain.** *PloS one* 2012, **7:**e44996-e44996.
167. Ducrest AL, Amacker M, Lingner J, Nabholz M: **Detection of promoter activity by flow cytometric analysis of GFP reporter expression.** *Nucleic Acids Res* 2002, **30:**e65.
168. Cuyas E, Corominas-Faja B, Joven J, Menendez JA: **Cell cycle regulation by the nutrient-sensing mammalian target of rapamycin (mTOR) pathway.** *Methods Mol Biol* 2014, **1170:**113-144.
169. Persad S, Troussard AA, McPhee TR, Mulholland DJ, Dedhar S: **Tumor suppressor PTEN inhibits nuclear accumulation of beta-catenin and T cell/lymphoid enhancer factor 1-mediated transcriptional activation.** *J Cell Biol* 2001, **153:**1161-1174.
170. Persad S, Attwell S, Gray V, Delcommenne M, Troussard A, Sanghera J, Dedhar S: **Inhibition of integrin-linked kinase (ILK) suppresses activation of protein kinase B/Akt and induces cell cycle arrest and apoptosis of PTEN-mutant prostate cancer cells.** *Proc Natl Acad Sci U S A* 2000, **97:**3207-3212.
171. Cheney IW, Johnson DE, Vaillancourt MT, Avanzini J, Morimoto A, Demers GW, Wills KN, Shabram PW, Bolen JB, Tavtigian SV, Bookstein R: **Suppression of tumorigenicity of glioblastoma cells by adenovirus-mediated MMAC1/PTEN gene transfer.** *Cancer Res* 1998, **58:**2331-2334.
172. Ramaswamy S, Nakamura N, Vazquez F, Batt DB, Perera S, Roberts TM, Sellers WR: **Regulation of G1 progression by the PTEN tumor suppressor protein is linked to inhibition of the phosphatidylinositol 3-kinase/Akt pathway.** *Proc Natl Acad Sci U S A* 1999, **96:**2110-2115.
173. Lu Y, Lin YZ, LaPushin R, Cuevas B, Fang X, Yu SX, Davies MA, Khan H, Furui T, Mao M, et al: **The PTEN/MMAC1/TEP tumor suppressor gene decreases cell growth and induces apoptosis and anoikis in breast cancer cells.** *Oncogene* 1999, **18:**7034-7045.
174. Davies MA, Koul D, Dhesi H, Berman R, McDonnell TJ, McConkey D, Yung WK, Steck PA: **Regulation of Akt/PKB activity, cellular growth, and apoptosis in prostate carcinoma cells by MMAC/PTEN.** *Cancer Res* 1999, **59:**2551-2556.
175. Davies MA, Lu Y, Sano T, Fang X, Tang P, LaPushin R, Koul D, Bookstein R, Stokoe D, Yung WK, et al: **Adenoviral transgene expression of MMAC/PTEN in human glioma cells inhibits Akt activation and induces anoikis.** *Cancer Res* 1998, **58:**5285-5290.
176. Toker A, Newton AC: **Akt/protein kinase B is regulated by autophosphorylation at the hypothetical PDK-2 site.** *J Biol Chem* 2000, **275:**8271-8274.
177. Alessi DR, James SR, Downes CP, Holmes AB, Gaffney PR, Reese CB, Cohen P: **Characterization of a 3-phosphoinositide-dependent protein kinase which phosphorylates and activates protein kinase Bα.** *Current biology* 1997, **7:**261-269.
178. Stokoe D, Stephens LR, Copeland T, Gaffney PR, Reese CB, Painter GF, Holmes AB, McCormick F, Hawkins PT: **Dual role of phosphatidylinositol-3,4,5-trisphosphate in the activation of protein kinase B.** *Science* 1997, **277:**567-570.
179. Cheng ZY, Guo XL, Li SH, Wang SY, Yang XY, Xue F, Wen SP, Pan L: **[The role of PTEN-FAK signaling pathway in metastasis and invasive ability of leukemia cells].** *Zhonghua Xue Ye Xue Za Zhi* 2009, **30:**115-120.
180. Bouali S, Chretien AS, Ramacci C, Rouyer M, Becuwe P, Merlin JL: **PTEN expression controls cellular response to cetuximab by mediating PI3K/AKT and RAS/RAF/MAPK downstream signaling in KRAS wild-type, hormone refractory prostate cancer cells.** *Oncol Rep* 2009, **21:**731-735.

181. Stambolic V, Suzuki A, De La Pompa JL, Brothers GM, Mirtsos C, Sasaki T, Ruland J, Penninger JM, Siderovski DP, Mak TW: **Negative regulation of PKB/Akt-dependent cell survival by the tumor suppressor PTEN.** *Cell* 1998, **95:**29-39.
182. Haas-Kogan D, Shalev N, Wong M, Mills G, Yount G, Stokoe D: **Protein kinase B (PKB/Akt) activity is elevated in glioblastoma cells due to mutation of the tumor suppressor PTEN/MMAC.** *Curr Biol* 1998, **8:**1195-1198.
183. Di Cristofano A, Pandolfi PP: **The multiple roles of PTEN in tumor suppression.** *Cell* 2000, **100:**387-390.
184. Lu XX, Cao LY, Chen X, Xiao J, Zou Y, Chen Q: **PTEN Inhibits Cell Proliferation, Promotes Cell Apoptosis, and Induces Cell Cycle Arrest via Downregulating the PI3K/AKT/hTERT Pathway in Lung Adenocarcinoma A549 Cells.** *Biomed Res Int* 2016, **2016:**2476842.
185. Bruni P, Boccia A, Baldassarre G, Trapasso F, Santoro M, Chiappetta G, Fusco A, Viglietto G: **PTEN expression is reduced in a subset of sporadic thyroid carcinomas: evidence that PTEN-growth suppressing activity in thyroid cancer cells mediated by p27kip1.** *Oncogene* 2000, **19:**3146-3155.
186. Maurice-Duelli A, Ndoye A, Bouali S, Leroux A, Merlin JL: **Enhanced cell growth inhibition following PTEN nonviral gene transfer using polyethylenimine and photochemical internalization in endometrial cancer cells.** *Technol Cancer Res Treat* 2004, **3:**459-465.
187. Weng LP, Brown JL, Eng C: **PTEN coordinates G(1) arrest by down-regulating cyclin D1 via its protein phosphatase activity and up-regulating p27 via its lipid phosphatase activity in a breast cancer model.** *Hum Mol Genet* 2001, **10:**599-604.
188. Wu H, Wang S, Weng D, Xing H, Song X, Zhu T, Xia X, Weng Y, Xu G, Meng L, et al: **Reversal of the malignant phenotype of ovarian cancer A2780 cells through transfection with wild-type PTEN gene.** *Cancer Lett* 2008, **271:**205-214.
189. Davidson L, Maccario H, Perera NM, Yang X, Spinelli L, Tibarewal P, Glancy B, Gray A, Weijer CJ, Downes CP, Leslie NR: **Suppression of cellular proliferation and invasion by the concerted lipid and protein phosphatase activities of PTEN.** *Oncogene* 2010, **29:**687-697.
190. Cantley LC, Neel BG: **New insights into tumor suppression: PTEN suppresses tumor formation by restraining the phosphoinositide 3-kinase/AKT pathway.** *Proc Natl Acad Sci U S A* 1999, **96:**4240-4245.
191. Hill VK, Kim JS, James CD, Waldman T: **Correction of PTEN mutations in glioblastoma cell lines via AAV-mediated gene editing.** *PLoS One* 2017, **12:**e0176683.
192. Vivanco I, Palaskas N, Tran C, Finn SP, Getz G, Kennedy NJ, Jiao J, Rose J, Xie W, Loda M, et al: **Identification of the JNK signaling pathway as a functional target of the tumor suppressor PTEN.** *Cancer Cell* 2007, **11:**555-569.
193. Kim JS, Xu X, Li H, Solomon D, Lane WS, Jin T, Waldman T: **Mechanistic analysis of a DNA damage-induced, PTEN-dependent size checkpoint in human cells.** *Mol Cell Biol* 2011, **31:**2756-2771.
194. Zhang S, Huang W-C, Li P, Guo H, Poh S-B, Brady SW, Xiong Y, Tseng L-M, Li S-H, Ding Z: **Combating trastuzumab resistance by targeting SRC, a common node downstream of multiple resistance pathways.** *Nature medicine* 2011, **17:**461-469.
195. Mounir Z, Krishnamoorthy JL, Robertson GP, Scheuner D, Kaufman RJ, Georgescu MM, Koromilas AE: **Tumor suppression by PTEN requires the activation of the PKR-eIF2alpha phosphorylation pathway.** *Sci Signal* 2009, **2:**ra85.
196. Okumura K, Zhao M, Depinho RA, Furnari FB, Cavenee WK: **Cellular transformation by the MSP58 oncogene is inhibited by its physical interaction with the PTEN tumor suppressor.** *Proc Natl Acad Sci U S A* 2005, **102:**2703-2706.

197. McGowan EM, Alling N, Jackson EA, Yagoub D, Haass NK, Allen JD, Martinello-Wilks R: **Evaluation of cell cycle arrest in estrogen responsive MCF-7 breast cancer cells: pitfalls of the MTS assay.** *PLoS One* 2011, **6:**e20623.
198. Podsypanina K, Ellenson LH, Nemes A, Gu J, Tamura M, Yamada KM, Cordon-Cardo C, Catoretti G, Fisher PE, Parsons R: **Mutation of Pten/Mmac1 in mice causes neoplasia in multiple organ systems.** *Proceedings of the National Academy of Sciences of the United States of America* 1999, **96:**1563-1568.
199. Lobo GP, Waite KA, Planchon SM, Romigh T, Houghton JA, Eng C: **ATP modulates PTEN subcellular localization in multiple cancer cell lines.** *Hum Mol Genet* 2008, **17:**2877-2885.
200. Lobo GP, Waite KA, Planchon SM, Romigh T, Nassif NT, Eng C: **Germline and somatic cancer-associated mutations in the ATP-binding motifs of PTEN influence its subcellular localization and tumor suppressive function.** *Hum Mol Genet* 2009, **18:**2851-2862.
201. He X, Ni Y, Wang Y, Romigh T, Eng C: **Naturally occurring germline and tumor-associated mutations within the ATP-binding motifs of PTEN lead to oxidative damage of DNA associated with decreased nuclear p53.** *Human Molecular Genetics* 2011, **20:**80-89.
202. Costa HA, Leitner MG, Sos ML, Mavrantoni A, Rychkova A, Johnson JR, Newton BW, Yee MC, De La Vega FM, Ford JM, et al: **Discovery and functional characterization of a neomorphic PTEN mutation.** *Proc Natl Acad Sci U S A* 2015, **112:**13976-13981.
203. Georgescu MM, Kirsch KH, Akagi T, Shishido T, Hanafusa H: **The tumor-suppressor activity of PTEN is regulated by its carboxyl-terminal region.** *Proc Natl Acad Sci U S A* 1999, **96:**10182-10187.
204. Han S-Y, Kato H, Kato S, Suzuki T, Shibata H, Ishii S, Shiiba K-i, Matsuno S, Kanamaru R, Ishioka C: **Functional evaluation of PTEN missense mutations using in vitro phosphoinositide phosphatase assay.** *Cancer research* 2000, **60:**3147-3151.
205. Ginn-Pease ME, Eng C: **Increased nuclear phosphatase and tensin homologue deleted on chromosome 10 is associated with G0-G1 in MCF-7 cells.** *Cancer Research* 2003, **63:**282-286.
206. Tsou HC, Ping XL, Xie XX, Gruener AC, Zhang H, Nini R, Swisshelm K, Sybert V, Diamond TM, Sutphen R, Peacocke M: **The genetic basis of Cowden's syndrome: three novel mutations in PTEN/MMAC1/TEP1.** *Hum Genet* 1998, **102:**467-473.
207. Leslie NR, Longy M: **Inherited PTEN mutations and the prediction of phenotype.** *Seminars in Cell & Developmental Biology*.
208. Samuels Y, Ericson K: **Oncogenic PI3K and its role in cancer.** *Curr Opin Oncol* 2006, **18:**77-82.
209. Di Cristofano A, Pesce B, Cordon-Cardo C, Pandolfi PP: **Pten is essential for embryonic development and tumour suppression.** *Nat Genet* 1998, **19:**348-355.
210. Shao J, Washington MK, Saxena R, Sheng H: **Heterozygous disruption of the PTEN promotes intestinal neoplasia in APCmin/+ mouse: roles of osteopontin.** *Carcinogenesis* 2007, **28:**2476-2483.
211. Myers MP, Stolarov JP, Eng C, Li J, Wang SI, Wigler MH, Parsons R, Tonks NK: **P-TEN, the tumor suppressor from human chromosome 10q23, is a dual-specificity phosphatase.** *Proc Natl Acad Sci U S A* 1997, **94:**9052-9057.
212. Caffrey JJ, Darden T, Wenk MR, Shears SB: **Expanding coincident signaling by PTEN through its inositol 1,3,4,5,6-pentakisphosphate 3-phosphatase activity.** *FEBS Lett* 2001, **499:**6-10.
213. Hemmings BA: **Akt signaling: linking membrane events to life and death decisions.** *Science* 1997, **275:**628-630.

214. Downward J: **Mechanisms and consequences of activation of protein kinase B/Akt.** *Curr Opin Cell Biol* 1998, **10:**262-267.
215. Stephens L, Anderson K, Stokoe D, Erdjument-Bromage H, Painter GF, Holmes AB, Gaffney PR, Reese CB, McCormick F, Tempst P, et al: **Protein kinase B kinases that mediate phosphatidylinositol 3,4,5-trisphosphate-dependent activation of protein kinase B.** *Science* 1998, **279:**710-714.
216. Franke TF, Kaplan DR, Cantley LC, Toker A: **Direct regulation of the Akt proto-oncogene product by phosphatidylinositol-3,4-bisphosphate.** *Science* 1997, **275:**665-668.
217. Maehama T: **PTEN: its deregulation and tumorigenesis.** *Biol Pharm Bull* 2007, **30:**1624-1627.
218. Pulkoski-Gross MJ, Donaldson JC, Obeid LM: **Sphingosine-1-phosphate metabolism: A structural perspective.** *Crit Rev Biochem Mol Biol* 2015, **50:**298-313.
219. Maceyka M, Harikumar KB, Milstien S, Spiegel S: **Sphingosine-1-phosphate signaling and its role in disease.** *Trends Cell Biol* 2012, **22:**50-60.
220. Pyne S, Pyne NJ: **New perspectives on the role of sphingosine 1-phosphate in cancer.** *Handb Exp Pharmacol* 2013**:**55-71.
221. Pitson SM: **Regulation of sphingosine kinase and sphingolipid signaling.** *Trends in Biochemical Sciences* 2011, **36:**97-107.
222. Cuvillier O, Pirianov G, Kleuser B, Vanek PG, Coso OA, Gutkind S, Spiegel S: **Suppression of ceramide-mediated programmed cell death by sphingosine-1-phosphate.** *Nature* 1996, **381:**800-803.
223. Gomez-Munoz A, Waggoner DW, O'Brien L, Brindley DN: **Interaction of ceramides, sphingosine, and sphingosine 1-phosphate in regulating DNA synthesis and phospholipase D activity.** *J Biol Chem* 1995, **270:**26318-26325.
224. Pyne S, Pyne NJ: **The differential regulation of cyclic AMP by sphingomyelin-derived lipids and the modulation of sphingolipid-stimulated extracellular signal regulated kinase-2 in airway smooth muscle.** *Biochem J* 1996, **315 (Pt 3):**917-923.
225. Mendelson K, Evans T, Hla T: **Sphingosine 1-phosphate signalling.** *Development* 2014, **141:**5-9.
226. Pyne S, Tolan DG, Conway AM, Pyne N: **Sphingolipids as differential regulators of cellular signalling processes.** *Biochem Soc Trans* 1997, **25:**549-556.
227. Spiegel S, Milstien S: **Sphingosine-1-phosphate: an enigmatic signalling lipid.** *Nat Rev Mol Cell Biol* 2003, **4:**397-407.
228. Maczis M, Milstien S, Spiegel S: **Sphingosine-1-phosphate and estrogen signaling in breast cancer.** *Adv Biol Regul* 2016, **60:**160-165.
229. Sukocheva O, Wadham C: **Role of sphingolipids in oestrogen signalling in breast cancer cells: an update.** *J Endocrinol* 2014, **220:**R25-35.
230. Mastrandrea LD, Sessanna SM, Laychock SG: **Sphingosine kinase activity and sphingosine-1 phosphate production in rat pancreatic islets and INS-1 cells: response to cytokines.** *Diabetes* 2005, **54:**1429-1436.
231. Martin JL, Lin MZ, McGowan EM, Baxter RC: **Potentiation of growth factor signaling by insulin-like growth factor-binding protein-3 in breast epithelial cells requires sphingosine kinase activity.** *J Biol Chem* 2009, **284:**25542-25552.
232. Haass NK, Nassif N, McGowan EM: **Switching the sphingolipid rheostat in the treatment of diabetes and cancer comorbidity from a problem to an advantage.** *Biomed Res Int* 2015, **2015:**165105.
233. Liu H, Sugiura M, Nava VE, Edsall LC, Kono K, Poulton S, Milstien S, Kohama T, Spiegel S: **Molecular cloning and functional characterization of a novel mammalian sphingosine kinase type 2 isoform.** *Journal of Biological Chemistry* 2000, **275:**19513-19520.

234. Alemany R, van Koppen CJ, Danneberg K, Ter Braak M, Meyer Zu Heringdorf D: **Regulation and functional roles of sphingosine kinases.** *Naunyn Schmiedebergs Arch Pharmacol* 2007, **374:**413-428.
235. Pyne NJ, Tonelli F, Lim KG, Long JS, Edwards J, Pyne S: **Sphingosine 1-phosphate signalling in cancer.** *Biochem Soc Trans* 2012, **40:**94-100.
236. Mizugishi K, Yamashita T, Olivera A, Miller GF, Spiegel S, Proia RL: **Essential role for sphingosine kinases in neural and vascular development.** *Mol Cell Biol* 2005, **25:**11113-11121.
237. Michaud J, Kohno M, Proia RL, Hla T: **Normal acute and chronic inflammatory responses in sphingosine kinase 1 knockout mice.** *FEBS Lett* 2006, **580:**4607-4612.
238. Allende ML, Sasaki T, Kawai H, Olivera A, Mi Y, van Echten-Deckert G, Hajdu R, Rosenbach M, Keohane CA, Mandala S, et al: **Mice deficient in sphingosine kinase 1 are rendered lymphopenic by FTY720.** *J Biol Chem* 2004, **279:**52487-52492.
239. Kohama T, Olivera A, Edsall L, Nagiec MM, Dickson R, Spiegel S: **Molecular cloning and functional characterization of murine sphingosine kinase.** *Journal of Biological Chemistry* 1998, **273:**23722-23728.
240. Liu H, Chakravarty D, Maceyka M, Milstien S, Spiegel S: **Sphingosine kinases: a novel family of lipid kinases.** *Prog Nucleic Acid Res Mol Biol* 2002, **71:**493-511.
241. Loveridge C, Tonelli F, Leclercq T, Lim KG, Long JS, Berdyshev E, Tate RJ, Natarajan V, Pitson SM, Pyne NJ: **The sphingosine kinase 1 inhibitor 2-(p-hydroxyanilino)-4-(p-chlorophenyl) thiazole induces proteasomal degradation of sphingosine kinase 1 in mammalian cells.** *Journal of Biological Chemistry* 2010, **285:**38841-38852.
242. Lim KG, Tonelli F, Berdyshev E, Gorshkova I, Leclercq T, Pitson SM, Bittman R, Pyne S, Pyne NJ: **Inhibition kinetics and regulation of sphingosine kinase 1 expression in prostate cancer cells: functional differences between sphingosine kinase 1a and 1b.** *The international journal of biochemistry & cell biology* 2012, **44:**1457-1464.
243. Santos WL, Lynch KR: **Drugging sphingosine kinases.** *ACS Chem Biol* 2015, **10:**225-233.
244. Beloribi-Djefaflia S, Vasseur S, Guillaumond F: **Lipid metabolic reprogramming in cancer cells.** *Oncogenesis* 2016, **5:**e189.
245. Pan Q, Shai O, Lee LJ, Frey BJ, Blencowe BJ: **Deep surveying of alternative splicing complexity in the human transcriptome by high-throughput sequencing.** *Nat Genet* 2008, **40:**1413-1415.
246. Chen J, Weiss WA: **Alternative splicing in cancer: implications for biology and therapy.** *Oncogene* 2015, **34:**1-14.
247. Venables JP, Klinck R, Koh C, Gervais-Bird J, Bramard A, Inkel L, Durand M, Couture S, Froehlich U, Lapointe E, et al: **Cancer-associated regulation of alternative splicing.** *Nat Struct Mol Biol* 2009, **16:**670-676.
248. Xu Q, Lee C: **Discovery of novel splice forms and functional analysis of cancer-specific alternative splicing in human expressed sequences.** *Nucleic Acids Res* 2003, **31:**5635-5643.
249. Hui L, Zhang X, Wu X, Lin Z, Wang Q, Li Y, Hu G: **Identification of alternatively spliced mRNA variants related to cancers by genome-wide ESTs alignment.** *Oncogene* 2004, **23:**3013-3023.
250. Wattenberg BW, Pitson SM, Raben DM: **The sphingosine and diacylglycerol kinase superfamily of signaling kinases: localization as a key to signaling function.** *J Lipid Res* 2006, **47:**1128-1139.
251. Martin JL, de Silva HC, Lin MZ, Scott CD, Baxter RC: **Inhibition of insulin-like growth factor-binding protein-3 signaling through sphingosine kinase-1 sensitizes triple-negative breast cancer cells to EGF receptor blockade.** *Mol Cancer Ther* 2014, **13:**316-328.

252. Sukocheva OA, Wang L, Albanese N, Pitson SM, Vadas MA, Xia P: **Sphingosine kinase transmits estrogen signaling in human breast cancer cells.** *Mol Endocrinol* 2003, **17:**2002-2012.
253. Sukocheva O, Wadham C, Holmes A, Albanese N, Verrier E, Feng F, Bernal A, Derian CK, Ullrich A, Vadas MA, Xia P: **Estrogen transactivates EGFR via the sphingosine 1-phosphate receptor Edg-3: the role of sphingosine kinase-1.** *J Cell Biol* 2006, **173:**301-310.
254. Watson C, Long JS, Orange C, Tannahill CL, Mallon E, McGlynn LM, Pyne S, Pyne NJ, Edwards J: **High expression of sphingosine 1-phosphate receptors, S1P1 and S1P3, sphingosine kinase 1, and extracellular signal-regulated kinase-1/2 is associated with development of tamoxifen resistance in estrogen receptor-positive breast cancer patients.** *Am J Pathol* 2010, **177:**2205-2215.
255. Nava VE, Hobson JP, Murthy S, Milstien S, Spiegel S: **Sphingosine kinase type 1 promotes estrogen-dependent tumorigenesis of breast cancer MCF-7 cells.** *Exp Cell Res* 2002, **281:**115-127.
256. Long JS, Edwards J, Watson C, Tovey S, Mair KM, Schiff R, Natarajan V, Pyne NJ, Pyne S: **Sphingosine kinase 1 induces tolerance to human epidermal growth factor receptor 2 and prevents formation of a migratory phenotype in response to sphingosine 1-phosphate in estrogen receptor-positive breast cancer cells.** *Mol Cell Biol* 2010, **30:**3827-3841.
257. Wang F, Van Brocklyn JR, Edsall L, Nava VE, Spiegel S: **Sphingosine-1-phosphate inhibits motility of human breast cancer cells independently of cell surface receptors.** *Cancer Res* 1999, **59:**6185-6191.
258. Takabe K, Kim RH, Allegood JC, Mitra P, Ramachandran S, Nagahashi M, Harikumar KB, Hait NC, Milstien S, Spiegel S: **Estradiol induces export of sphingosine 1-phosphate from breast cancer cells via ABCC1 and ABCG2.** *J Biol Chem* 2010, **285:**10477-10486.
259. Yagoub D, Wilkins MR, Lay AJ, Kaczorowski DC, Hatoum D, Bajan S, Hutvagner G, Lai JH, Wu W, Martiniello-Wilks R, et al: **Sphingosine kinase 1 isoform-specific interactions in breast cancer.** *Mol Endocrinol* 2014, **28:**1899-1915.
260. Nagahashi M, Ramachandran S, Kim EY, Allegood JC, Rashid OM, Yamada A, Zhao R, Milstien S, Zhou H, Spiegel S, Takabe K: **Sphingosine-1-phosphate produced by sphingosine kinase 1 promotes breast cancer progression by stimulating angiogenesis and lymphangiogenesis.** *Cancer Res* 2012, **72:**726-735.
261. Maiti A, Takabe K, Hait NC: **Metastatic triple-negative breast cancer is dependent on SphKs/S1P signaling for growth and survival.** *Cell Signal* 2017, **32:**85-92.
262. Tsuchida J, Nagahashi M, Takabe K, Wakai T: **Clinical impact of sphingosine-1-phosphate in breast cancer.** *Mediators of Inflammation* 2017 (2017), **2017**.
263. Katsuta E, Yan L, Nagahashi M, Raza A, Sturgill J, Lyon D, Rashid O, Hait N, Takabe K: **Doxorubicin effect is enhanced by sphingosine-1- phosphate signaling antagonist in breast cancer.** *JRS* 2017, **Nov 2017** 202-213.
264. Spiegel S: **Sphingosine-1-Phosphate: A Bridge From Bench To Clinic.** *The FASEB Journal* 2016, **30:**243.241-243.241.
265. Mukhopadhyay P, Ramanathan R, Takabe K: **S1P promotes breast cancer progression by angiogenesis and lymphangiogenesis.** Future Medicine; 2015.
266. Pyne S, Edwards J, Ohotski J, Pyne NJ: **Sphingosine 1-phosphate receptors and sphingosine kinase 1: novel biomarkers for clinical prognosis in breast, prostate, and hematological cancers.** *Front Oncol* 2012, **2:**168.
267. Pchejetski D, Golzio M, Bonhoure E, Calvet C, Doumerc N, Garcia V, Mazerolles C, Rischmann P, Teissie J, Malavaud B, Cuvillier O: **Sphingosine kinase-1 as a chemotherapy sensor in prostate adenocarcinoma cell and mouse models.** *Cancer Res* 2005, **65:**11667-11675.

268. Pchejetski D, Doumerc N, Golzio M, Naymark M, Teissie J, Kohama T, Waxman J, Malavaud B, Cuvillier O: **Chemosensitizing effects of sphingosine kinase-1 inhibition in prostate cancer cell and animal models.** *Mol Cancer Ther* 2008, **7:**1836-1845.
269. Pchejetski D, Bohler T, Stebbing J, Waxman J: **Therapeutic potential of targeting sphingosine kinase 1 in prostate cancer.** *Nat Rev Urol* 2011, **8:**569-678.
270. McNaughton M, Pitman M, Pitson SM, Pyne NJ, Pyne S: **Proteasomal degradation of sphingosine kinase 1 and inhibition of dihydroceramide desaturase by the sphingosine kinase inhibitors, SKi or ABC294640, induces growth arrest in androgen-independent LNCaP-AI prostate cancer cells.** *Oncotarget* 2016, **7:**16663-16675.
271. Malavaud B, Pchejetski D, Mazerolles C, de Paiva GR, Calvet C, Doumerc N, Pitson S, Rischmann P, Cuvillier O: **Sphingosine kinase-1 activity and expression in human prostate cancer resection specimens.** *Eur J Cancer* 2010, **46:**3417-3424.
272. Lim KG, Tonelli F, Berdyshev E, Gorshkova I, Leclercq T, Pitson SM, Bittman R, Pyne S, Pyne NJ: **Inhibition kinetics and regulation of sphingosine kinase 1 expression in prostate cancer cells: functional differences between sphingosine kinase 1a and 1b.** *Int J Biochem Cell Biol* 2012, **44:**1457-1464.
273. Gestaut MM, Antoon JW, Burow ME, Beckman BS: **Inhibition of sphingosine kinase-2 ablates androgen resistant prostate cancer proliferation and survival.** *Pharmacol Rep* 2014, **66:**174-178.
274. Dayon A, Brizuela L, Martin C, Mazerolles C, Pirot N, Doumerc N, Nogueira L, Golzio M, Teissie J, Serre G, et al: **Sphingosine kinase-1 is central to androgen-regulated prostate cancer growth and survival.** *PLoS One* 2009, **4:**e8048.
275. Akao Y, Banno Y, Nakagawa Y, Hasegawa N, Kim TJ, Murate T, Igarashi Y, Nozawa Y: **High expression of sphingosine kinase 1 and S1P receptors in chemotherapy-resistant prostate cancer PC3 cells and their camptothecin-induced up-regulation.** *Biochem Biophys Res Commun* 2006, **342:**1284-1290.
276. Wallington-Beddoe CT, Powell JA, Tong D, Pitson SM, Bradstock KF, Bendall LJ: **Sphingosine kinase 2 promotes acute lymphoblastic leukemia by enhancing MYC expression.** *Cancer Res* 2014, **74:**2803-2815.
277. Xu L, Zhang Y, Gao M, Wang G, Fu Y: **Concurrent targeting Akt and sphingosine kinase 1 by A-674563 in acute myeloid leukemia cells.** *Biochem Biophys Res Commun* 2016, **472:**662-668.
278. Sobue S, Nemoto S, Murakami M, Ito H, Kimura A, Gao S, Furuhata A, Takagi A, Kojima T, Nakamura M, et al: **Implications of sphingosine kinase 1 expression level for the cellular sphingolipid rheostat: relevance as a marker for daunorubicin sensitivity of leukemia cells.** *Int J Hematol* 2008, **87:**266-275.
279. Marfe G, Di Stefano C, Gambacurta A, Ottone T, Martini V, Abruzzese E, Mologni L, Sinibaldi-Salimei P, de Fabritis P, Gambacorti-Passerini C, et al: **Sphingosine kinase 1 overexpression is regulated by signaling through PI3K, AKT2, and mTOR in imatinib-resistant chronic myeloid leukemia cells.** *Exp Hematol* 2011, **39:**653-665 e656.
280. Kennedy AJ, Mathews TP, Kharel Y, Field SD, Moyer ML, East JE, Houck JD, Lynch KR, Macdonald TL: **Development of amidine-based sphingosine kinase 1 nanomolar inhibitors and reduction of sphingosine 1-phosphate in human leukemia cells.** *J Med Chem* 2011, **54:**3524-3548.
281. Zhao Y, Kalari SK, Usatyuk PV, Gorshkova I, He D, Watkins T, Brindley DN, Sun C, Bittman R, Garcia JG, et al: **Intracellular generation of sphingosine 1-phosphate in human lung endothelial cells: role of lipid phosphate phosphatase-1 and sphingosine kinase 1.** *J Biol Chem* 2007, **282:**14165-14177.
282. Wang Q, Li J, Li G, Li Y, Xu C, Li M, Xu G, Fu S: **Prognostic significance of sphingosine kinase 2 expression in non-small cell lung cancer.** *Tumour Biol* 2014, **35:**363-368.

283. Song L, Xiong H, Li J, Liao W, Wang L, Wu J, Li M: **Sphingosine kinase-1 enhances resistance to apoptosis through activation of PI3K/Akt/NF-kappaB pathway in human non-small cell lung cancer.** *Clin Cancer Res* 2011, **17:**1839-1849.
284. Johnson KR, Johnson KY, Crellin HG, Ogretmen B, Boylan AM, Harley RA, Obeid LM: **Immunohistochemical distribution of sphingosine kinase 1 in normal and tumor lung tissue.** *J Histochem Cytochem* 2005, **53:**1159-1166.
285. Aoki H, Aoki M, Katsuta E, Ramanathan R, Idowu MO, Spiegel S, Takabe K: **Host sphingosine kinase 1 worsens pancreatic cancer peritoneal carcinomatosis.** *J Surg Res* 2016, **205:**510-517.
286. Guo YX, Ma YJ, Han L, Wang YJ, Han JA, Zhu Y: **Role of sphingosine 1-phosphate in human pancreatic cancer cells proliferation and migration.** *Int J Clin Exp Med* 2015, **8:**20349-20354.
287. Japtok L, Schmitz EI, Fayyaz S, Kramer S, Hsu LJ, Kleuser B: **Sphingosine 1-phosphate counteracts insulin signaling in pancreatic beta-cells via the sphingosine 1-phosphate receptor subtype 2.** *FASEB J* 2015, **29:**3357-3369.
288. Taguchi Y, Allende ML, Mizukami H, Cook EK, Gavrilova O, Tuymetova G, Clarke BA, Chen W, Olivera A, Proia RL: **Sphingosine-1-phosphate Phosphatase 2 Regulates Pancreatic Islet beta-Cell Endoplasmic Reticulum Stress and Proliferation.** *J Biol Chem* 2016, **291:**12029-12038.
289. Salama MF, Carroll B, Adada M, Pulkoski-Gross M, Hannun YA, Obeid LM: **A novel role of sphingosine kinase-1 in the invasion and angiogenesis of VHL mutant clear cell renal cell carcinoma.** *FASEB J* 2015, **29:**2803-2813.
290. Pyne NJ, Pyne S: **Sphingosine 1-phosphate is a missing link between chronic inflammation and colon cancer.** *Cancer Cell* 2013, **23:**5-7.
291. Liu SQ, Huang JA, Qin MB, Su YJ, Lai MY, Jiang HX, Tang GD: **Sphingosine kinase 1 enhances colon cancer cell proliferation and invasion by upregulating the production of MMP-2/9 and uPA via MAPK pathways.** *Int J Colorectal Dis* 2012, **27:**1569-1578.
292. Kawamori T, Kaneshiro T, Okumura M, Maalouf S, Uflacker A, Bielawski J, Hannun YA, Obeid LM: **Role for sphingosine kinase 1 in colon carcinogenesis.** *FASEB J* 2009, **23:**405-414.
293. Hong G, Baudhuin LM, Xu Y: **Sphingosine-1-phosphate modulates growth and adhesion of ovarian cancer cells.** *FEBS Lett* 1999, **460:**513-518.
294. Lee JW, Ryu JY, Yoon G, Jeon HK, Cho YJ, Choi JJ, Song SY, Do IG, Lee YY, Kim TJ, et al: **Sphingosine kinase 1 as a potential therapeutic target in epithelial ovarian cancer.** *Int J Cancer* 2015, **137:**221-229.
295. Beach JA, Aspuria PJ, Cheon DJ, Lawrenson K, Agadjanian H, Walsh CS, Karlan BY, Orsulic S: **Sphingosine kinase 1 is required for TGF-beta mediated fibroblastto-myofibroblast differentiation in ovarian cancer.** *Oncotarget* 2016, **7:**4167-4182.
296. White MD, Chan L, Antoon JW, Beckman BS: **Targeting ovarian cancer and chemoresistance through selective inhibition of sphingosine kinase-2 with ABC294640.** *Anticancer Res* 2013, **33:**3573-3579.
297. Wang D, Zhao Z, Caperell-Grant A, Yang G, Mok SC, Liu J, Bigsby RM, Xu Y: **S1P differentially regulates migration of human ovarian cancer and human ovarian surface epithelial cells.** *Mol Cancer Ther* 2008, **7:**1993-2002.
298. Zhu W, Jarman KE, Lokman NA, Neubauer HA, Davies LT, Gliddon BL, Taing H, Moretti PAB, Oehler MK, Pitman MR, Pitson SM: **CIB2 negatively regulates oncogenic signaling in ovarian cancer via sphingosine kinase 1.** *Cancer Res* 2017.
299. Quint K, Stiel N, Neureiter D, Schlicker HU, Nimsky C, Ocker M, Strik H, Kolodziej MA: **The role of sphingosine kinase isoforms and receptors S1P1, S1P2, S1P3, and S1P5 in primary, secondary, and recurrent glioblastomas.** *Tumour Biol* 2014, **35:**8979-8989.

300. Bien-Moller S, Lange S, Holm T, Bohm A, Paland H, Kupper J, Herzog S, Weitmann K, Havemann C, Vogelgesang S, et al: **Expression of S1P metabolizing enzymes and receptors correlate with survival time and regulate cell migration in glioblastoma multiforme.** *Oncotarget* 2016, **7:**13031-13046.
301. Zhang H, Li W, Sun S, Yu S, Zhang M, Zou F: **Inhibition of sphingosine kinase 1 suppresses proliferation of glioma cells under hypoxia by attenuating activity of extracellular signal-regulated kinase.** *Cell Prolif* 2012, **45:**167-175.
302. Van Brocklyn JR, Jackson CA, Pearl DK, Kotur MS, Snyder PJ, Prior TW: **Sphingosine kinase-1 expression correlates with poor survival of patients with glioblastoma multiforme: roles of sphingosine kinase isoforms in growth of glioblastoma cell lines.** *J Neuropathol Exp Neurol* 2005, **64:**695-705.
303. Kim HS, Yoon G, Ryu JY, Cho YJ, Choi JJ, Lee YY, Kim TJ, Choi CH, Song SY, Kim BG, et al: **Sphingosine kinase 1 is a reliable prognostic factor and a novel therapeutic target for uterine cervical cancer.** *Oncotarget* 2015, **6:**26746-26756.
304. Cai H, Xie X, Ji L, Ruan X, Zheng Z: **Sphingosine kinase 1: A novel independent prognosis biomarker in hepatocellular carcinoma.** *Oncol Lett* 2017, **13:**2316-2322.
305. Liu H, Zhang CX, Ma Y, He HW, Wang JP, Shao RG: **SphK1 inhibitor SKI II inhibits the proliferation of human hepatoma HepG2 cells via the Wnt5A/beta-catenin signaling pathway.** *Life Sci* 2016, **151:**23-29.
306. Lu Z, Xiao Z, Liu F, Cui M, Li W, Yang Z, Li J, Ye L, Zhang X: **Long non-coding RNA HULC promotes tumor angiogenesis in liver cancer by up-regulating sphingosine kinase 1 (SPHK1).** *Oncotarget* 2016, **7:**241-254.
307. Uranbileg B, Ikeda H, Kurano M, Enooku K, Sato M, Saigusa D, Aoki J, Ishizawa T, Hasegawa K, Kokudo N, Yatomi Y: **Increased mRNA Levels of Sphingosine Kinases and S1P Lyase and Reduced Levels of S1P Were Observed in Hepatocellular Carcinoma in Association with Poorer Differentiation and Earlier Recurrence.** *PLoS One* 2016, **11:**e0149462.
308. Yu X, Zheng H, Chan MT, Wu WK: **HULC: an oncogenic long non-coding RNA in human cancer.** *J Cell Mol Med* 2017, **21:**410-417.
309. Vadas M, Xia P, McCaughan G, Gamble J: **The role of sphingosine kinase 1 in cancer: oncogene or non-oncogene addiction?** *Biochim Biophys Acta* 2008, **1781:**442-447.
310. Pitson SM: **Regulation of sphingosine kinase and sphingolipid signaling.** *Trends Biochem Sci* 2011, **36:**97-107.
311. Nava VE, Lacana E, Poulton S, Liu H, Sugiura M, Kono K, Milstien S, Kohama T, Spiegel S: **Functional characterization of human sphingosine kinase-1.** *FEBS Lett* 2000, **473:**81-84.
312. Liu H, Sugiura M, Nava VE, Edsall LC, Kono K, Poulton S, Milstien S, Kohama T, Spiegel S: **Molecular cloning and functional characterization of a novel mammalian sphingosine kinase type 2 isoform.** *J Biol Chem* 2000, **275:**19513-19520.
313. Melendez AJ, Carlos-Dias E, Gosink M, Allen JM, Takacs L: **Human sphingosine kinase: molecular cloning, functional characterization and tissue distribution.** *Gene* 2000, **251:**19-26.
314. Wang Z, Min X, Xiao SH, Johnstone S, Romanow W, Meininger D, Xu H, Liu J, Dai J, An S, et al: **Molecular basis of sphingosine kinase 1 substrate recognition and catalysis.** *Structure* 2013, **21:**798-809.
315. Pitson SM, D'Andrea R J, Vandeleur L, Moretti PA, Xia P, Gamble JR, Vadas MA, Wattenberg BW: **Human sphingosine kinase: purification, molecular cloning and characterization of the native and recombinant enzymes.** *Biochem J* 2000, **350 Pt 2:**429-441.
316. Taha TA, Hannun YA, Obeid LM: **Sphingosine kinase: biochemical and cellular regulation and role in disease.** *J Biochem Mol Biol* 2006, **39:**113-131.

317. Yokota S, Taniguchi Y, Kihara A, Mitsutake S, Igarashi Y: **Asp177 in C4 domain of mouse sphingosine kinase 1a is important for the sphingosine recognition.** *FEBS Lett* 2004, **578:**106-110.
318. Okada T, Ding G, Sonoda H, Kajimoto T, Haga Y, Khosrowbeygi A, Gao S, Miwa N, Jahangeer S, Nakamura S: **Involvement of N-terminal-extended form of sphingosine kinase 2 in serum-dependent regulation of cell proliferation and apoptosis.** *J Biol Chem* 2005, **280:**36318-36325.
319. Liu H, Toman RE, Goparaju SK, Maceyka M, Nava VE, Sankala H, Payne SG, Bektas M, Ishii I, Chun J, et al: **Sphingosine kinase type 2 is a putative BH3-only protein that induces apoptosis.** *J Biol Chem* 2003, **278:**40330-40336.
320. Billich A, Bornancin F, Devay P, Mechtcheriakova D, Urtz N, Baumruker T: **Phosphorylation of the immunomodulatory drug FTY720 by sphingosine kinases.** *J Biol Chem* 2003, **278:**47408-47415.
321. Maceyka M, Sankala H, Hait NC, Le Stunff H, Liu H, Toman R, Collier C, Zhang M, Satin LS, Merrill AH, Jr., et al: **SphK1 and SphK2, sphingosine kinase isoenzymes with opposing functions in sphingolipid metabolism.** *J Biol Chem* 2005, **280:**37118-37129.
322. Xia P, Gamble JR, Wang L, Pitson SM, Moretti PA, Wattenberg BW, D'Andrea RJ, Vadas MA: **An oncogenic role of sphingosine kinase.** *Curr Biol* 2000, **10:**1527-1530.
323. Sukocheva O, Wadham C, Xia P: **Role of sphingolipids in the cytoplasmic signaling of estrogens.** *Steroids* 2009, **74:**562-567.
324. Pitson SM, Moretti PA, Zebol JR, Lynn HE, Xia P, Vadas MA, Wattenberg BW: **Activation of sphingosine kinase 1 by ERK1/2-mediated phosphorylation.** *EMBO J* 2003, **22:**5491-5500.
325. Takabe K, Paugh SW, Milstien S, Spiegel S: **"Inside-out" signaling of sphingosine-1-phosphate: therapeutic targets.** *Pharmacol Rev* 2008, **60:**181-195.
326. Delon C, Manifava M, Wood E, Thompson D, Krugmann S, Pyne S, Ktistakis NT: **Sphingosine kinase 1 is an intracellular effector of phosphatidic acid.** *J Biol Chem* 2004, **279:**44763-44774.
327. Kobayashi N, Nishi T, Hirata T, Kihara A, Sano T, Igarashi Y, Yamaguchi A: **Sphingosine 1-phosphate is released from the cytosol of rat platelets in a carrier-mediated manner.** *J Lipid Res* 2006, **47:**614-621.
328. Fukuhara S, Simmons S, Kawamura S, Inoue A, Orba Y, Tokudome T, Sunden Y, Arai Y, Moriwaki K, Ishida J, et al: **The sphingosine-1-phosphate transporter Spns2 expressed on endothelial cells regulates lymphocyte trafficking in mice.** *J Clin Invest* 2012, **122:**1416-1426.
329. Nagahashi M, Takabe K, Terracina KP, Soma D, Hirose Y, Kobayashi T, Matsuda Y, Wakai T: **Sphingosine-1-phosphate transporters as targets for cancer therapy.** *Biomed Res Int* 2014, **2014:**651727.
330. Igarashi N, Okada T, Hayashi S, Fujita T, Jahangeer S, Nakamura S: **Sphingosine kinase 2 is a nuclear protein and inhibits DNA synthesis.** *J Biol Chem* 2003, **278:**46832-46839.
331. Hait NC, Allegood J, Maceyka M, Strub GM, Harikumar KB, Singh SK, Luo C, Marmorstein R, Kordula T, Milstien S, Spiegel S: **Regulation of histone acetylation in the nucleus by sphingosine-1-phosphate.** *Science* 2009, **325:**1254-1257.
332. Panneer Selvam S, De Palma RM, Oaks JJ, Oleinik N, Peterson YK, Stahelin RV, Skordalakes E, Ponnusamy S, Garrett-Mayer E, Smith CD, Ogretmen B: **Binding of the sphingolipid S1P to hTERT stabilizes telomerase at the nuclear periphery by allosterically mimicking protein phosphorylation.** *Sci Signal*

2015, **8:**ra58.
333. Adams DR, Pyne S, Pyne NJ: **Sphingosine Kinases: Emerging Structure-Function Insights.** *Trends Biochem Sci* 2016, **41:**395-409.

334. Fukuda Y, Kihara A, Igarashi Y: **Distribution of sphingosine kinase activity in mouse tissues: contribution of SPHK1.** *Biochem Biophys Res Commun* 2003, **309:**155-160.
335. Kharel Y, Lee S, Snyder AH, Sheasley-O'neill S L, Morris MA, Setiady Y, Zhu R, Zigler MA, Burcin TL, Ley K, et al: **Sphingosine kinase 2 is required for modulation of lymphocyte traffic by FTY720.** *J Biol Chem* 2005, **280:**36865-36872.
336. Zemann B, Kinzel B, Muller M, Reuschel R, Mechtcheriakova D, Urtz N, Bornancin F, Baumruker T, Billich A: **Sphingosine kinase type 2 is essential for lymphopenia induced by the immunomodulatory drug FTY720.** *Blood* 2006, **107:**1454-1458.
337. Park SW, Kim M, Kim M, D'Agati VD, Lee HT: **Sphingosine kinase 1 protects against renal ischemia-reperfusion injury in mice by sphingosine-1-phosphate1 receptor activation.** *Kidney Int* 2011, **80:**1315-1327.
338. Gorshkova IA, Wang H, Orbelyan GA, Goya J, Natarajan V, Beiser DG, Vanden Hoek TL, Berdyshev EV: **Inhibition of sphingosine-1-phosphate lyase rescues sphingosine kinase-1-knockout phenotype following murine cardiac arrest.** *Life Sci* 2013, **93:**359-366.
339. Lei M, Shafique A, Shang K, Couttas TA, Zhao H, Don AS, Karl T: **Contextual fear conditioning is enhanced in mice lacking functional sphingosine kinase 2.** *Behav Brain Res* 2017, **333:**9-16.
340. Liu R, Li X, Qiang X, Luo L, Hylemon PB, Jiang Z, Zhang L, Zhou H: **Taurocholate induces Cyclooxygenase-2 expression via the sphingosine 1-phosphate receptor 2 in a human cholangiocarcinoma cell line.** *Journal of Biological Chemistry* 2015, **290:**30988-31002.
341. Liu R, Zhao R, Zhou X, Liang X, Campbell DJ, Zhang X, Zhang L, Shi R, Wang G, Pandak WM: **Conjugated bile acids promote cholangiocarcinoma cell invasive growth through activation of sphingosine 1-phosphate receptor 2.** *Hepatology* 2014, **60:**908-918.
342. Wang Y, Aoki H, Yang J, Peng K, Liu R, Li X, Qiang X, Sun L, Gurley EC, Lai G: **The role of sphingosine 1-phosphate receptor 2 in bile-acid–induced cholangiocyte proliferation and cholestasis-induced liver injury in mice.** *Hepatology* 2017, **65:**2005-2018.
343. Kwong EK, Li X, Hylemon PB, Zhou H: **Sphingosine Kinases/Sphingosine 1-Phosphate Signaling in Hepatic Lipid Metabolism.** *Current Pharmacology Reports* 2017**:**1-8.
344. Nagahashi M, Takabe K, Liu R, Peng K, Wang X, Wang Y, Hait NC, Wang X, Allegood JC, Yamada A, et al: **Conjugated bile acid-activated S1P receptor 2 is a key regulator of sphingosine kinase 2 and hepatic gene expression.** *Hepatology* 2015, **61:**1216-1226.
345. Wang Y, Aoki H, Yang J, Peng K, Liu R, Li X, Qiang X, Sun L, Gurley EC, Lai G, et al: **The role of sphingosine 1-phosphate receptor 2 in bile-acid-induced cholangiocyte proliferation and cholestasis-induced liver injury in mice.** *Hepatology* 2017, **65:**2005-2018.
346. Liang J, Nagahashi M, Kim EY, Harikumar KB, Yamada A, Huang WC, Hait NC, Allegood JC, Price MM, Avni D, et al: **Sphingosine-1-phosphate links persistent STAT3 activation, chronic intestinal inflammation, and development of colitis-associated cancer.** *Cancer Cell* 2013, **23:**107-120.
347. Loveridge C, Tonelli F, Leclercq T, Lim KG, Long JS, Berdyshev E, Tate RJ, Natarajan V, Pitson SM, Pyne NJ, Pyne S: **The sphingosine kinase 1 inhibitor 2-(p-hydroxyanilino)-4-(p-chlorophenyl)thiazole induces proteasomal degradation of sphingosine kinase 1 in mammalian cells.** *J Biol Chem* 2010, **285:**38841-38852.
348. Tonelli F, Lim KG, Loveridge C, Long J, Pitson SM, Tigyi G, Bittman R, Pyne S, Pyne NJ: **FTY720 and (S)-FTY720 vinylphosphonate inhibit sphingosine kinase 1 and promote its proteasomal degradation in human pulmonary artery smooth muscle, breast cancer and androgen-independent prostate cancer cells.** *Cell Signal* 2010, **22:**1536-1542.

349. Kohno M, Momoi M, Oo ML, Paik JH, Lee YM, Venkataraman K, Ai Y, Ristimaki AP, Fyrst H, Sano H, et al: **Intracellular role for sphingosine kinase 1 in intestinal adenoma cell proliferation.** *Mol Cell Biol* 2006, **26:**7211-7223.
350. Venkataraman K, Thangada S, Michaud J, Oo ML, Ai Y, Lee YM, Wu M, Parikh NS, Khan F, Proia RL, Hla T: **Extracellular export of sphingosine kinase-1a contributes to the vascular S1P gradient.** *Biochem J* 2006, **397:**461-471.
351. Sukocheva O, Wang L, Verrier E, Vadas MA, Xia P: **Restoring endocrine response in breast cancer cells by inhibition of the sphingosine kinase-1 signaling pathway.** *Endocrinology* 2009, **150:**4484-4492.
352. Sauer L, Nunes J, Salunkhe V, Skalska L, Kohama T, Cuvillier O, Waxman J, Pchejetski D: **Sphingosine kinase 1 inhibition sensitizes hormone-resistant prostate cancer to docetaxel.** *International journal of cancer* 2009, **125:**2728-2736.
353. Bonhoure E, Pchejetski D, Aouali N, Morjani H, Levade T, Kohama T, Cuvillier O: **Overcoming MDR-associated chemoresistance in HL-60 acute myeloid leukemia cells by targeting shingosine kinase-1.** *Leukemia* 2006, **20:**95.
354. Paugh SW, Paugh BS, Rahmani M, Kapitonov D, Almenara JA, Kordula T, Milstien S, Adams JK, Zipkin RE, Grant S: **A selective sphingosine kinase 1 inhibitor integrates multiple molecular therapeutic targets in human leukemia.** *Blood* 2008, **112:**1382-1391.
355. Price MM, Oskeritzian CA, Falanga YT, Harikumar KB, Allegood JC, Alvarez SE, Conrad D, Ryan JJ, Milstien S, Spiegel S: **A specific sphingosine kinase 1 inhibitor attenuates airway hyperresponsiveness and inflammation in a mast cell-dependent murine model of allergic asthma.** *J Allergy Clin Immunol* 2013, **131:**501-511.e501.
356. Anelli V, Gault CR, Snider AJ, Obeid LM: **Role of sphingosine kinase-1 in paracrine/transcellular angiogenesis and lymphangiogenesis in vitro.** *FASEB J* 2010, **24:**2727-2738.
357. French KJ, Schrecengost RS, Lee BD, Zhuang Y, Smith SN, Eberly JL, Yun JK, Smith CD: **Discovery and evaluation of inhibitors of human sphingosine kinase.** *Cancer research* 2003, **63:**5962-5969.
358. Guillermet-Guibert J, Davenne L, Pchejetski D, Saint-Laurent N, Brizuela L, Guilbeau-Frugier C, Delisle M-B, Cuvillier O, Susini C, Bousquet C: **Targeting the sphingolipid metabolism to defeat pancreatic cancer cell resistance to the chemotherapeutic gemcitabine drug.** *Molecular cancer therapeutics* 2009, **8:**809-820.
359. Gao P, Peterson YK, Smith RA, Smith CD: **Characterization of isoenzyme-selective inhibitors of human sphingosine kinases.** *PLoS One* 2012, **7:**e44543.
360. Antoon JW, White MD, Slaughter EM, Driver JL, Khalili HS, Elliott S, Smith CD, Burow ME, Beckman BS: **Targeting NFκB mediated breast cancer chemoresistance through selective inhibition of sphingosine kinase-2.** *Cancer biology & therapy* 2011, **11:**678-689.
361. Dickson MA, Carvajal RD, Merrill AH, Gonen M, Cane LM, Schwartz GK: **A Phase I Clinical Trial of Safingol in Combination with Cisplatin in Advanced Solid Tumors.** *Clinical cancer research : an official journal of the American Association for Cancer Research* 2011, **17:**2484-2492.
362. French KJ, Zhuang Y, Maines LW, Gao P, Wang W, Beljanski V, Upson JJ, Green CL, Keller SN, Smith CD: **Pharmacology and antitumor activity of ABC294640, a selective inhibitor of sphingosine kinase-2.** *Journal of Pharmacology and Experimental Therapeutics* 2010, **333:**129-139.
363. Coward J, Ambrosini G, Musi E, Truman J-P, Haimovitz-Friedman A, Allegood JC, Wang E, Merrill J, Alfred H, Schwartz GK: **Safingol (L-threo-sphinganine) induces autophagy in solid tumor cells through inhibition of PKC and the PI3-kinase pathway.** *Autophagy* 2009, **5:**184-193.

364. Kunkel GT, Maceyka M, Milstien S, Spiegel S: **Targeting the sphingosine-1-phosphate axis in cancer, inflammation and beyond.** *Nat Rev Drug Discov* 2013, **12:**688-702.
365. Ohta H, Sweeney EA, Masamune A, Yatomi Y, Hakomori S-i, Igarashi Y: **Induction of apoptosis by sphingosine in human leukemic HL-60 cells: a possible endogenous modulator of apoptotic DNA fragmentation occurring during phorbol ester-induced differentiation.** *Cancer Research* 1995, **55:**691-697.
366. Jarvis WD, Fornari FA, Auer KL, Freemerman AJ, Szabo E, Birrer MJ, Johnson CR, Barbour SE, Dent P, Grant S: **Coordinate regulation of stress-and mitogen-activated protein kinases in the apoptotic actions of ceramide and sphingosine.** *Molecular Pharmacology* 1997, **52:**935-947.
367. Sweeney EA, Inokuchi J-i, Igarashi Y: **Inhibition of sphingolipid induced apoptosis by caspase inhibitors indicates that sphingosine acts in an earlier part of the apoptotic pathway than ceramide.** *FEBS letters* 1998, **425:**61-65.
368. Sakakura C, Sweeney EA, Shirahama T, Hakomori S-i: **Suppression of Bcl-2 gene expression by sphingosine in the apoptosis of human leukemic HL-60 cells during phorbol ester-induced terminal differentiation.** *FEBS letters* 1996, **379:**177-180.
369. Klostergaard J, Auzenne E, Leroux E: **Characterization of cytotoxicity induced by sphingolipids in multidrug-resistant leukemia cells.** *Leukemia research* 1998, **22:**1049-1056.
370. Jarvis WD, Frank Jr A, Traylor RS, Martin HA, Kramer LB, Erukulla RK, Bittman R, Grant S: **Induction of apoptosis and potentiation of ceramide-mediated cytotoxicity by sphingoid bases in human myeloid leukemia cells.** *Journal of Biological Chemistry* 1996, **271:**8275-8284.
371. Sawai H, Okazaki T, Domae N: **Sphingosine-induced c-jun expression: differences between sphingosine-and C2-ceramide-mediated signaling pathways.** *FEBS letters* 2002, **524:**103-106.
372. Jendiroba DB, Klostergaard J, Keyhani A, Pagliaro L, Freireich EJ: **Effective cytotoxicity against human leukemias and chemotherapy-resistant leukemia cell lines by N-N-dimethylsphingosine.** *Leukemia research* 2002, **26:**301-310.
373. Endo K, Igarashi Y, Nisar M, Zhou Q, Hakomori S-i: **Cell membrane signaling as target in cancer therapy: inhibitory effect of N, N-dimethyl and N, N, N-trimethyl sphingosine derivatives on in vitro and in vivo growth of human tumor cells in nude mice.** *Cancer research* 1991, **51:**1613-1618.
374. Sweeney EA, SAKAKURA TS, OHTA H, HAKOMORI S-i, IGARASH11 Y: **SPHINGOSINE AND ITS METHYLATED DERIVATIVE IN A VARIETY OF HUMAN CANCER CELL LINES.** *Int J Cancer* 1996, **66:**366.
375. Cuvillier O, Edsall L, Spiegel S: **Involvement of sphingosine in mitochondria-dependent Fas-induced apoptosis of type II Jurkat T cells.** *Journal of Biological Chemistry* 2000, **275:**15691-15700.
376. Cuvillier O, Levade T: **Sphingosine 1-phosphate antagonizes apoptosis of human leukemia cells by inhibiting release of cytochrome c and Smac/DIABLO from mitochondria.** *Blood* 2001, **98:**2828-2836.
377. Shirahama T, Sweeney EA, Sakakura C, Singhal AK, Nishiyama K, Akiyama S-i, Hakomori S-i, Igarashi Y: **In vitro and in vivo induction of apoptosis by sphingosine and N, N-dimethylsphingosine in human epidermoid carcinoma KB-3-1 and its multidrug-resistant cells.** *Clinical Cancer Research* 1997, **3:**257-264.
378. Edsall LC, Cuvillier O, Twitty S, Spiegel S, Milstien S: **Sphingosine kinase expression regulates apoptosis and caspase activation in PC12 cells.** *Journal of neurochemistry* 2001, **76:**1573-1584.

379. Edsall LC, Pirianov GG, Spiegel S: **Involvement of sphingosine 1-phosphate in nerve growth factor-mediated neuronal survival and differentiation.** *Journal of Neuroscience* 1997, **17:**6952-6960.
380. Nava VE, Cuvillier O, Edsall LC, Kimura K, Milstien S, Gelmann EP, Spiegel S: **Sphingosine enhances apoptosis of radiation-resistant prostate cancer cells.** *Cancer Research* 2000, **60:**4468-4474.
381. Wen-Chun H, CHANG H-C, CHUANG L-Y: **Activation of caspase-3-like proteases in apoptosis induced by sphingosine and other long-chain bases in Hep3B hepatoma cells.** *Biochemical Journal* 1999, **338:**161-166.
382. Shida D, Takabe K, Kapitonov D, Milstien S, Spiegel S: **Targeting SphK1 as a new strategy against cancer.** *Current drug targets* 2008, **9:**662-673.
383. Amin HM, Ergin M, Denning MF, Quevedo ME, Alkan S: **Characterization of apoptosis induced by protein kinase C inhibitors and its modulation by the caspase pathway in acute promyelocytic leukaemia.** *British journal of haematology* 2000, **110:**552-562.
384. Chmura SJ, Nodzenski E, Beckett MA, Kufe DW, Quintans J, Weichselbaum RR: **Loss of ceramide production confers resistance to radiation-induced apoptosis.** *Cancer research* 1997, **57:**1270-1275.
385. Sachs CW, Safa AR, Harrison SD, Fine RL: **Partial inhibition of multidrug resistance by safingol is independent of modulation of P-glycoprotein substrate activities and correlated with inhibition of protein kinase C.** *Journal of Biological Chemistry* 1995, **270:**26639-26648.
386. Tavarini S, Colombaioni L, Garcia-Gil M: **Sphingomyelinase metabolites control survival and apoptotic death in SH-SY5Y neuroblastoma cells.** *Neuroscience letters* 2000, **285:**185-188.
387. Pchejetski D, Bohler T, Brizuela L, Sauer L, Doumerc N, Golzio M, Salunkhe V, Teissié J, Malavaud B, Waxman J: **FTY720 (fingolimod) sensitizes prostate cancer cells to radiotherapy by inhibition of sphingosine kinase-1.** *Cancer research* 2010, **70:**8651-8661.
388. Zhang N, Qi Y, Wadham C, Wang L, Warren A, Di W, Xia P: **FTY720 induces necrotic cell death and autophagy in ovarian cancer cells: a protective role of autophagy.** *Autophagy* 2010, **6:**1157-1167.
389. Azuma H, Takahara S, Horie S, Muto S, Otsuki Y, Katsuoka Y: **Induction of apoptosis in human bladder cancer cells in vitro and in vivo caused by FTY720 treatment.** *The Journal of urology* 2003, **169:**2372-2377.
390. Zhang L, Wang H, Zhu J, Ding K, Xu J: **FTY720 reduces migration and invasion of human glioblastoma cell lines via inhibiting the PI3K/AKT/mTOR/p70S6K signaling pathway.** *Tumor Biology* 2014, **35:**10707-10714.
391. Lee TK, Man K, Ho JW, Sun CK, Ng KT, Wang XH, Wong YC, Ng IO, Xu R, Fan ST: **FTY720 induces apoptosis of human hepatoma cell lines through PI3-K-mediated Akt dephosphorylation.** *Carcinogenesis* 2004, **25:**2397-2405.
392. Liu K, Guo TL, Hait NC, Allegood J, Parikh HI, Xu W, Kellogg GE, Grant S, Spiegel S, Zhang S: **Biological characterization of 3-(2-amino-ethyl)-5-[3-(4-butoxyl-phenyl)-propylidene]-thiazolidine-2, 4-dione (K145) as a selective sphingosine kinase-2 inhibitor and anticancer agent.** *PloS one* 2013, **8:**e56471.
393. Zhang Y, Wang Y, Wan Z, Liu S, Cao Y, Zeng Z: **Sphingosine kinase 1 and cancer: a systematic review and meta-analysis.** *PLoS One* 2014, **9:**e90362.
394. Pyne S, Adams DR, Pyne NJ: **Sphingosine 1-phosphate and sphingosine kinases in health and disease: Recent advances.** *Prog Lipid Res* 2016, **62:**93-106.
395. Huang WC, Nagahashi M, Terracina KP, Takabe K: **Emerging Role of Sphingosine-1-phosphate in Inflammation, Cancer, and Lymphangiogenesis.** *Biomolecules* 2013, **3**.

396. Zheng W, Aspelund A, Alitalo K: **Lymphangiogenic factors, mechanisms, and applications.** *J Clin Invest* 2014, **124:**878-887.
397. Pitman MR, Costabile M, Pitson SM: **Recent advances in the development of sphingosine kinase inhibitors.** *Cell Signal* 2016, **28:**1349-1363.
398. PITSON SM, D'ANDREA RJ, VANDELEUR L, MORETTI PA, Pu X, GAMBLE JR, VADAS MA, WATTENBERG BW: **Human sphingosine kinase: purification, molecular cloning and characterization of the native and recombinant enzymes.** *Biochemical Journal* 2000, **350:**429-441.
399. Gyorffy B, Lanczky A, Eklund AC, Denkert C, Budczies J, Li Q, Szallasi Z: **An online survival analysis tool to rapidly assess the effect of 22,277 genes on breast cancer prognosis using microarray data of 1,809 patients.** *Breast Cancer Res Treat* 2010, **123:**725-731.
400. Szasz AM, Lanczky A, Nagy A, Forster S, Hark K, Green JE, Boussioutas A, Busuttil R, Szabo A, Gyorffy B: **Cross-validation of survival associated biomarkers in gastric cancer using transcriptomic data of 1,065 patients.** *Oncotarget* 2016, **7:**49322-49333.
401. Gyorffy B, Surowiak P, Budczies J, Lanczky A: **Online survival analysis software to assess the prognostic value of biomarkers using transcriptomic data in non-small-cell lung cancer.** *PLoS One* 2013, **8:**e82241.
402. Relan V, Morrison L, Parsonson K, Clarke BE, Duhig EE, Windsor MN, Matar KS, Naidoo R, Passmore L, McCaul E, et al: **Phenotypes and karyotypes of human malignant mesothelioma cell lines.** *PLoS One* 2013, **8:**e58132.
403. Kryeziu K, Jungwirth U, Hoda MA, Ferk F, Knasmuller S, Karnthaler-Benbakka C, Kowol CR, Berger W, Heffeter P: **Synergistic anticancer activity of arsenic trioxide with erlotinib is based on inhibition of EGFR-mediated DNA double-strand break repair.** *Mol Cancer Ther* 2013, **12:**1073-1084.
404. Schmitter D, Lauber B, Fagg B, Stahel RA: **Hematopoietic growth factors secreted by seven human pleural mesothelioma cell lines: interleukin-6 production as a common feature.** *Int J Cancer* 1992, **51:**296-301.
405. Wu L, Allo G, John T, Li M, Tagawa T, Opitz I, Anraku M, Yun Z, Pintilie M, Pitcher B, et al: **Patient-Derived Xenograft Establishment from Human Malignant Pleural Mesothelioma.** *Clin Cancer Res* 2017, **23:**1060-1067.
406. Smythe WR, Kaiser LR, Hwang HC, Amin KM, Pilewski JM, Eck SJ, Wilson JM, Albelda SM: **Successful adenovirus-mediated gene transfer in an in vivo model of human malignant mesothelioma.** *Ann Thorac Surg* 1994, **57:**1395-1401.
407. Wu YJ, Parker LM, Binder NE, Beckett MA, Sinard JH, Griffiths CT, Rheinwald JG: **The mesothelial keratins: a new family of cytoskeletal proteins identified in cultured mesothelial cells and nonkeratinizing epithelia.** *Cell* 1982, **31:**693-703.
408. Tinoco I, Jr., Bustamante C: **How RNA folds.** *J Mol Biol* 1999, **293:**271-281.
409. Sim AY, Minary P, Levitt M: **Modeling nucleic acids.** *Curr Opin Struct Biol* 2012, **22:**273-278.
410. Shi Y-Z, Jin L, Wang F-H, Zhu X-L, Tan Z-J: **Predicting 3D structure, flexibility, and stability of RNA hairpins in monovalent and divalent ion solutions.** *Biophysical journal* 2015, **109:**2654-2665.
411. Ding Y, Tang Y, Kwok CK, Zhang Y, Bevilacqua PC, Assmann SM: **In vivo genome-wide profiling of RNA secondary structure reveals novel regulatory features.** *Nature* 2014, **505:**696-700.
412. Mayr C, Bartel DP: **Widespread shortening of 3'UTRs by alternative cleavage and polyadenylation activates oncogenes in cancer cells.** *Cell* 2009, **138:**673-684.
413. Ulitsky I, Shkumatava A, Jan CH, Subtelny AO, Koppstein D, Bell GW, Sive H, Bartel DP: **Extensive alternative polyadenylation during zebrafish development.** *Genome Res* 2012, **22:**2054-2066.

414. Geisberg JV, Moqtaderi Z, Fan X, Ozsolak F, Struhl K: **Global Analysis of mRNA Isoform Half-Lives Reveals Stabilizing and Destabilizing Elements in Yeast.** *Cell* 2014, **156:**812-824.
415. Pchejetski D, Doumerc N, Golzio M, Naymark M, Teissié J, Kohama T, Waxman J, Malavaud B, Cuvillier O: **Chemosensitizing effects of sphingosine kinase-1 inhibition in prostate cancer cell and animal models.** *Molecular cancer therapeutics* 2008, **7:**1836-1845.
416. Paugh SW, Paugh BS, Rahmani M, Kapitonov D, Almenara JA, Kordula T, Milstien S, Adams JK, Zipkin RE, Grant S, Spiegel S: **A selective sphingosine kinase 1 inhibitor integrates multiple molecular therapeutic targets in human leukemia.** *Blood* 2008, **112:**1382-1391.